Molecular and Cellular Investigations Relating to Neuroplasticity in Stroke

JOSHUA WINDERLICH

A thesis submitted for the degree of Doctor of Philosophy

School of Medicine

The University of Adelaide

January 2018

Table of Contents

Declaration

I certify that this work contains no material which has been accepted for the award of any other degree or diploma in my name in any university or other tertiary institution and, to the best of my knowledge and belief, contains no material previously published or written by another person, except where due reference has been made in the text. In addition, I certify that no part of this work will, in the future, be used in a submission in my name for any other degree or diploma in any university or other tertiary institution without the prior approval of the University of Adelaide and where applicable, any partner institution responsible for the joint award of this degree.

The author acknowledges that copyright of published works contained within this thesis resides with the copyright holder(s) of those works.

I give permission for the digital version of my thesis to be made available on the web, via the University's digital research repository, the Library Search and also through web search engines, unless permission has been granted by the University to restrict access for a period of time.

I acknowledge the support I have received for my research through the provision of an Australian Government Research Training Program Scholarship.

Signed:

Date:

Acknowledgments

This thesis and the work contained within wouldn’t exist without the care, guidance and expertise of the many people who have been part of my academic and personal lives over the past five years. I would like to take this opportunity now to offer my thanks to all of you.

Firstly, I would like to recognise the enormous debt of gratitude owed to my supervisors Simon Koblar and Karlea Kremer. Your patient support, guidance and teaching has helped me build my aptitude for research and has encouraged my enthusiasm for science. I am sincerely humbled by your generous gift of time and energy over the past five years.

I would also to thank my many colleagues from the Stroke Research Programme: Maria, Anjali, Chelsea, Austin and Anne, and past members: Fong Chan, Kylie, Martin, Michael, Tom, Wai Khay, Wenru, Xenia, Adam, Bek, Harlene, Mark, Tam and Victoria. Your teamwork and camaraderie in the lab has been enjoyable.

I owe special thanks to Jessica. Your guidance through the world of perineuronal nets formed the scaffold for much of my thesis and your friendship whilst in Cambridge did a lot to make me feel at home. Thanks also to the other colleagues I met in Cambridge for showing me around and relinquishing bench space.

Mum and Dad, thanks for your support and wise council. It goes without saying that none of this would be possible without your backing. Thanks also for providing me with a home to come back to and food in the fridge. Thanks to Sam and Noah for being brothers and thanks to Grandma, Nan and Pop for always checking in to see how the research is going.

Amie, having you with me throughout my studies has been incredible. Thanks for being there for me through stressful times and in the exciting times. Most of all, thanks for all the fun along the way.

Final thanks go to the animals that unknowingly gave their lives to generate the data used in this thesis, and to hopefully improve the care available to stroke victims.

Abstract

Stroke is a leading cause of death and the leading cause of adult neurological disability in Australia. The interventions currently available for the management of stroke include intravenous thrombolysis, thombectomy, decompressive hemicraniectomy, antithrombotic therapy, stroke unit care and rehabilitation. The aims of these interventions are to reduce the amount of damage caused by stroke and to support recovery. Currently, there is no method to reverse the damage caused by stroke. The pattern of functional recovery following stroke reveals a critical period of enhanced neuroplasticity. This period is a candidate therapeutic target for post-stroke neurological repair, either by increasing the degree of neuroplasticity that occurs or by extending the duration of enhancement. Experimental interventions that promise to enhance post-stroke neuroplasticity are being investigated. There is extensive evidence that functional recovery can be improved through interruption of endogenous inhibitory mechanisms, which include perineuronal nets (PNNs) and Nogo signalling. Chapter one outlines a review of the literature concerning the pathophysiology of ischaemic stroke, evidence in support of enhanced post-stroke neuroplasticity and evidence in support of potential therapies that target post-stroke neuroplasticity. This review forms the basis for the body of work described in this thesis.

Cell-based therapy is one potential way of enhancing recovery from ischaemic stroke. Stem cell transplantation following stroke has resulted in functional improvements in pre-clinical studies. The mechanism of action underlying this effect is unclear, though it is thought to be through the paracrine secretion of neurotrophic cytokines and not through replacement of lost tissue. Intriguingly, both direct intracerebral transplantation and intravascular transplantation are efficacious. For transplanted stem cells to enter the brain from circulation, they must cross the blood-brain barrier (BBB). While this has been shown to occur, the mechanism through which stem cells cross the BBB has not been fully elucidated. Chapter two demonstrates that human dental pulp stem cells (DPSC) can increase BBB permeability through the expression of vascular endothelial growth factor. DPSC conditioned medium caused an increase in permeability of an in vitro model of the BBB and this effect was reversed by blocking the VEGF receptor. These results support the further investigation of intravascular DPSC administration as a treatment for ischaemic stroke.

One of the hypothetical mechanisms of action for cell-based therapy is the interruption of PNNs. These are a specialised form of dense ECM within the adult brain and spinal cord that form part of an endogenous system for the inhibition of neuroplasticity. Digestion of PNNs through administration of a bacterial enzyme has been shown to improve outcomes following neurological insults, including stroke. Chapter three demonstrates that DPSC express soluble products that digest PNNs. Application of DPSC conditioned media to *in vitro* PNN models and brain slices resulted in decreased staining of PNNs. Additionally, DPSC were shown to express active matrix metalloproteinase-2, which digested aggrecan, one of the main PNN components. These results suggest that interruption of PNNs may be a mechanism through which cell-based therapy enhances recovery in the setting of ischaemic stroke.

As PNNs are a target for future stroke therapies, it is important to understand the endogenous response of PNNs to stroke. There is evidence in the literature that PNNs are temporarily downregulated after stroke. Numerous studies have demonstrated the temporary downregulation of PNNs after stroke through general staining for the carbohydrate components of PNNs and some of the protein components. However, PNNs are not homogeneous throughout the central nervous system and variations in their composition affect their ability to inhibit neuroplasticity. The response of PNNs to stroke has not yet been fully described. Chapter four addresses this by characterising the expression profile of several PNN components in a mouse stroke model. Following photochemical infarction, there was a temporary decrease in staining of cartilage link protein-1, aggrecan and WFA-binding glycans in the cortex. This effect was more pronounced in the region of the cortex contralateral to the lesion. Additionally, 4-O-sulfated chondroitin, which is the most inhibitory PNN-associated carbohydrate component, was temporarily enriched in the ischaemic border zone. This pattern of regulation may underlie the post-stroke critical period enhanced neuroplasticity.

The development of new stroke treatment strategies targeting neuroplasticity is dependent on preclinical in vivo studies. To ensure that pre-clinical studies are mutually comparable, there is a need for a standardised protocol for modelling human stroke. The requirements of this model are that it be reproducible, technically accessible, it must minimise animal suffering and it must accurately model chronic stroke in humans. Many studies use young animals, which recover rapidly and more completely from ischaemic stroke. This is not appropriate for testing stroke therapies for humans as stroke risk is correlated with age. Additionally, middle cerebral artery occlusion is still considered the gold standard for modelling stroke. This is biologically accurate, but is technically difficult, results in variable infarcts and is associated with relatively high mortality and suffering. Chapter five outlines a preliminary study towards the development of a standardised protocol for chronic stroke in aged mice. A photochemical induction method was used, which resulted in reproducible, targeted lesions that were detectable by MRI. This method produced detectable dysfunction of the affected limb at early time points only. These results suggest that further optimisation needs to be done in developing a standardised model of chronic stroke.

Chapter 1: Introduction

1.1: Stroke

Brain tissue is highly energetic, dependent on oxidative phosphorylation for energy and has limited collateral circulation. Because of this, the brain is susceptible to damage following loss of perfusion. A stroke occurs when a decrease in perfusion is severe enough to result in a permanent lesion[1]. The two main subtypes of stroke are cerebral ischemia, which accounts for 87% of all stroke cases and haemorrhagic stroke, which accounts for 13% of stroke[2]. Ischaemic stroke can be further divided into large vessel and lacunar infarcts. The latter occur within white matter and present as typical clinical syndromes, though many may be silent infarcts. Lacunar infarcts have been identified in approximately 15% of patients presenting with first stroke[3]. While ischaemic stroke is more common, the 30-day mortality rate associated with it is only 11-15%, as compared with 37% for haemorrhagic stroke[4]. Because of this, many people live for years with chronic cognitive and sensory-motor disability as a consequence of ischaemic stroke[5].

Ischaemic stroke refers to a permanent cerebral lesion resulting from the occlusion of a cerebral artery. This occlusion may be the result of local atherosclerotic plaque rupture and thrombosis or the result of an embolism generated distally[6]. The most common sites for ischaemic stroke are the branches of the middle cerebral arteries (MCA)[7]. The symptoms and signs of an ischaemic stroke are directly related to the vascular territory involved and the function of the brain region that it serves. Most ischaemic lesions have cortical involvement with obvious impairment to sensory, motor and cognitive faculties[8].

The acute pathophysiology of a cerebral infarct is characterised by the ischaemic cascade. An initial drop in perfusion causes failure of ion pumps, loss of membrane potential and subsequent uncontrolled depolarisation. The activation of voltage-gated ion channels causes the inappropriate release of excitatory neurotransmitters, including glutamate. Due to continued energetic failure, glutamate reuptake is also inhibited. This results in an accumulation of glutamate within the synaptic cleft. Glutamate excitotoxicity causes an uncontrolled cytoplasmic influx of electrolytes[9,10]. Inappropriate glutamate receptor activation also directly causes reactive oxygen species (ROS) production, resulting in damage to surrounding tissue[11]. Increased cytoplasmic osmotic pressure leads to cytotoxic oedema and cell lysis[12]. Tissue necrosis leads to ROS production, causing further cell death and delayed inflammation.

Ischaemic damage begins at the infarct core, which represents tissue supplied exclusively by the occluded vessel. The ischaemic core is surrounded by a penumbra of poorly perfused but viable tissue[13,14]. Untreated, the penumbra may continue to transform into ischaemic tissue due to ongoing excitotoxicity, ROS production and inflammation. The rate of penumbral transformation is highly variable between individuals and is mainly dependent on the degree of collateral circulation available to support penumbral tissue[15]. Additionally, factors such as comorbid metabolic disease and acute hyperglycaemia increase penumbral transformation rate[16], while pre-stroke physical activity is protective against rapid infarct growth[17]. Typically, penumbral transformation within the acute phase of stroke is rapid, with a loss of approximately 1.9 million neurons per minute[18]. Significant penumbral transformation occurs within the first 4 hours[19], however penumbral tissue has been detected up to 24 hours after an occlusion in rodents[20]. Furthermore, measurement of penumbral volume in humans by perfusion/diffusion weighted MRI mismatch has demonstrated that in some patients, the penumbra may persist up to 48 hours post-stroke. This is an important concept because it suggests that some patients may respond favourably to delayed reperfusion. Reperfusion may be brought about either by intervention or endogenous thrombolysis. Spontaneous endogenous reperfusion may take hours to days and most salvageable tissue will not survive this amount of time[21].

A major therapeutic target for current stroke therapies is acute reperfusion. Current evidence-based management includes antithrombotic medication, stroke unit care, decompressive hemicraniectomy, thrombectomy and intravenous thrombolysis[22–24]. Further to this, primary prevention of stroke guided by modifiable risk factors is a significant clinical target[25]. In particular, smoking cessation, blood pressure control, management of dyslipidaemia and glycaemic control prevent stroke in part by promoting vascular endothelial function. The efficacy of these treatments and management strategies lies in attenuating the damage cause by stroke and in preventing the occurrence of future stroke.

The main limitation of stroke treatment is that intravenous thrombolysis and thombectomy are only effective when provided before complete infarction has occurred. Intravenous thrombolysis also carries a significant risk of haemorrhage[26]. As a result, intravenous thrombolysis is only indicated for patients who can receive it within 4.5 hours of symptomatic onset[27] and thrombectomy has only shown efficacy when received within the first 24 hours[28]. Despite the removal of barriers to care and reductions in time-to-treat, many patients are still not eligible for reperfusion[29]. There is a need for new ways to treat stroke in the sub-acute and chronic phases.

One mode for potential stroke treatment is neuroprotection, a paradigm that has attracted extensive research over the last four decades. While the conventional ways of managing acute stroke focus on salvaging penumbral tissue by establishing reperfusion, neuroprotective strategies target the biochemical processes that underlie the ischaemic cascade. One of the main targets of neuroprotection is glutamate excitotoxicity. Animal studies have identified a plethora of treatments that improve outcomes by blocking NMDA receptors[30–34], inhibiting glutamate indirectly[35] or by providing magnesium to encourage NMDA inactivation[36]. Similarly, targeting apoptotic signalling through calcium channel blockade has demonstrated promising preclinical results[37]. The third major target of neuroprotection is the ROS produced downstream of excitotoxicity; several ROS scavengers have demonstrated efficacy in animal stroke models[38,39].

Despite the positive results of animal studies, neuroprotective agents have not demonstrated efficacy in phase 3 clinical trials and thus none have been translated[40]. It is important to understand the reasons for this failure in translation when considering potential stroke treatments of other modalities. One reason is that the animal models used in pre-clinical studies did not appropriately model stroke in humans. For example, due to cost and time limitations, drugs were often tested in young and otherwise healthy animals. However, we know that in humans the risk of stroke increases with age and often occurs in the context of significant comorbidities. Another factor is that stroke models often create discreet and standardised lesions, which is important because it means that small effect sizes can be detected with reasonable sample sizes. However, in humans, stroke is a highly heterogeneous syndrome and clinical trials are therefore unable to detect such small benefits. A third putative cause for failure in translation is that animal stroke models were treated in the hyper-acute phase of stroke pathogenesis, whereas humans enrolled in clinical trials often experienced a delay[41]. This is important because the mechanism of neuroprotection relies on the salvaging of penumbral tissue and is therefore subject to similar time constraints as reperfusion therapies. One conclusion that may be drawn from this is that hypothetical neuroprotective strategies may be used as an adjuvant to improve the efficacy of reperfusion therapies but are unlikely to extend the treatment window of stroke.

In the wake of extensive research into neuroprotection, we are still left with a dearth of interventions for sub-acute or chronic stroke. Therefore, another possible approach to filling the need for new stroke treatments is to target adult neuroplasticity.

1.2: Neuroplasticity

1.2.1: Overview of neuroplasticity

Cognition and behaviour are emergent properties of the immensely complex network of the brain. While development clearly provides a scaffold and many innate circuits for primal behaviours and reflexes, complex behaviours and the circuits that create them must be built and refined in an experience-dependant way. Neuroplasticity describes the changes in anatomy and electrophysiology that underlie learning in the brain.

While the concept of neuroplasticity was first explored by Ramón y Cajal[42], the idea that physical changes to brain structure underlie learning gained traction with Hebb's postulate in the mid-twentieth century. Prior to this, it was widely held that the adult human brain was anatomically static. Hebb's postulate states that the weights of connections between neurons are increased when one neuron is involved in causing an action potential in another[43]. This model is summarised by the adage *'neurons that fire together, wire together'*. Repetitive communication between neurons in this manner results in the evolution of coherent networks. Improvements of this model led to the development of predictive models of neuroplasticity and *in silico* simulation of neural networks[44,45].

Neuroplasticity is achieved by creating new synapses and changing the weights of existing synapses. One of the main mechanisms for learning and memory is long term potentiation (LTP), a process whereby the weights of existing synapses are altered. When synchronous action potentials occur in two synapsed glutaminergic neurons, N-methyl-D-aspartate (NMDA) receptors in the postsynaptic membrane become activated. This increases the sensitivity of the post-synaptic neuron to depolarisation of the presynaptic neuron. Repeated transmission through a synapse over time results in translocation of glutamate receptors to the post-synaptic membrane, resulting in a long-term increase in synaptic strength[28, see 29].

The anatomic changes underlying neuroplasticity are axonal sprouting, dendritic arborisation and synaptogenesis. These processes allow for the creation of experience-dependent network traces. Synapses that remain unused decay, while those that frequently transmit signals are reinforced by

LTP. Neurogenesis allows for the introduction of new nodes into existing networks. This process predominantly occurs during development, although some adult neurogenesis has been observed, particularly in the hippocampus[48] and subventricular zone.

The degree of neuroplasticity in mammalian brains is variable. Childhood is spanned by critical periods, which are times during which the brain is highly plastic and easily reorganises in response to environmental stimuli. This is the time during which children learn language, learn to recognize objects, learn how to walk and generally adapt to interact with their environment. The timing of critical periods varies for different systems. For example, the critical period for language ends sometime between 5 years of age and puberty[49], whereas the visual critical period ends at approximately 30 months of age[50]. If the required environmental stimulation is not received during the critical period for a skill, then that skill may never be fully acquired. This was demonstrated in the famous study by Hubel and Wiesel, which showed that monocular deprivation in infant cats for the duration of the critical period resulted in permanent monocular blindness[51].

Neuroplasticity in the adult human brain has been measured in response to several types of environmental stimulation. Structural changes can be seen on magnetic resonance imaging (MRI) following the acquisition of new skills, including juggling, ballet, Morse code and learning a second language[52–55]. Importantly, the changes were detected in brain regions responsible for the new skill. More recent investigations using functional MRI and tractography have demonstrated increased axon density in correlation with skill acquisition[56,57].

The degree of neuroplasticity available can be influenced by environmental factors. In animals, stress causes a reversible reduction in the length of hippocampal dendrites and a consequent reduction in the number of synapses they form[58,59]. This causes a temporary impediment to learning during protracted periods of stress. Conversely, voluntary aerobic exercise enhances learning and neuroplasticity[60,61].

1.2.2: Post-Stroke Neuroplasticity

A parallel can be drawn between the timing of behavioural recovery after stroke and critical periods in children. In the months following stroke, skill reacquisition occurs rapidly. While rehabilitation may result in improvements years after a stroke, evidence suggests that most skill reacquisition occurs within the first six months[62–64]. This period of active neuroplasticity is a promising target for new stroke treatments (Figure 1).

It has long been observed that many stroke patients will undergo a period of spontaneous functional recovery [65]. It may be argued that this recovery is the result of normal training effects, independent of the stroke. However, the EXCITE stroke trial presented compelling evidence that the timing of rehabilitation influences the total amount of recovery achieved after 24 months. Patients who received rehabilitation from 0-6 months achieved greater recovery than those who received the same rehabilitation after a three-month delay[66]. One important caveat to this is that the AVERT trial determined that high-dose rehabilitation within the first 24 hours of a stroke resulted in poorer functional outcomes and no reduction in mortality when compared with conventional practices[67]. This study raised concerns that very early high-dose rehabilitation may be harmful, especially in patients with haemorrhagic stroke. While plausible mechanisms may be advanced to explain this effect, it seems unlikely to be related to neuroplasticity.

Additionally, data from rodent stroke models has demonstrated accelerated learning in tasks involving the unaffected forepaw[68]. This suggests that following an ischaemic insult, distant areas of the brain may also experience an increase in neuroplasticity. Another interpretation is that midline-crossing fibres originating from the infarcted cortex convey functional plasticity to the ipsilesional forepaw. The way to differentiate these would be to assess neuroplasticity in a more distant area, such as the ipsilesional hindpaw, or to assess neuroplasticity in a different modality than that controlled by the lesioned cortex, such as fear conditioning.

An interesting outcome of the research into heterogeneous regions of neuroplasticity following stroke is that compensation through neuroplasticity in the contralesional hemisphere paradoxically results in poorer functional outcomes[69]. In one study, stroke patients with increased conduction from the affected leg to the ipsilateral (non-stroke) motor cortex were shown to have poorer control of both limbs[70]. The authors offered that this effect may be due to the generation of uncoordinated and conflicting flexor-extensor signals in the non-lesioned cortex, which may occur due to lack of inhibition from the damaged cortex. Another hypothesis is that alternative ipsilateral motor pathways are more active following more severe damage to primary motor pathways, and that secondary pathways only partially compensate for this damage[71]. The clinical implication of this is that if contralesional neuroplasticity is inherently maladaptive, then treatment models targeting neuroplasticity will need account for this. For example, targeted approaches to increasing neuroplasticity may be possible.

Evidence for post-stroke structural neuroplasticity comes largely from rodent studies. Ischaemic injury increases the rate of hippocampal neurogenesis and some newly generated neurons differentiate and integrate within the brain[72]. Furthermore, stroke results in a temporary period of dendritic outgrowth in the contralesional cortex[73] and a consequent increase in synaptogenesis[74,75]. This is likely to be caused by an upregulation of growth-promoting neurotrophic factors, including brain-derived neurotrophic factor (BDNF)[76], basic fibroblast growth factor (bFGF)[77–79] and growth-associated protein 43 (GAP43)[75,80]. Another possible cause for post-stroke neuroplasticity is the degradation of neurite-outgrowth inhibitory components of the brain extracellular matrix (ECM) (Figure 1).

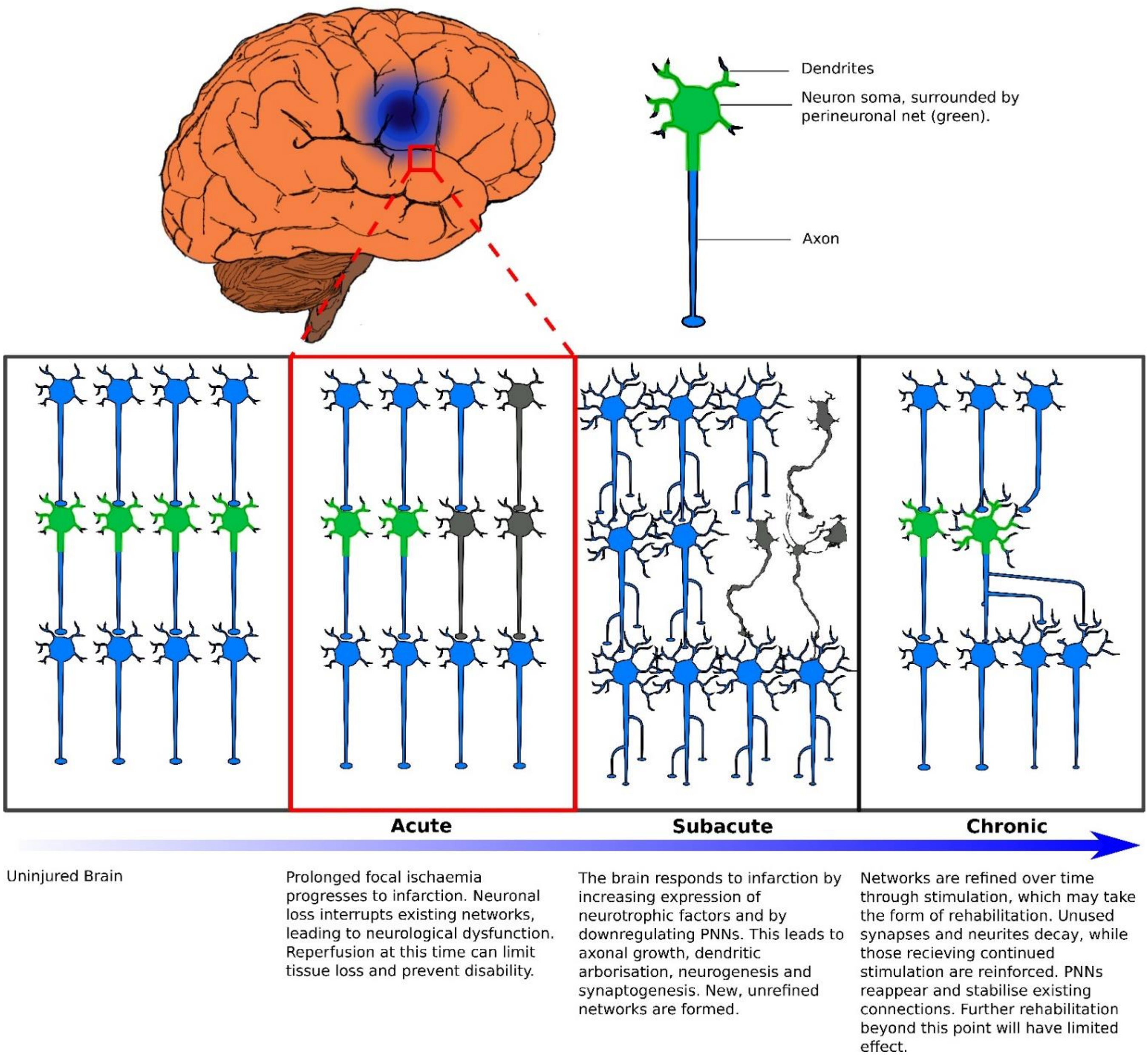

Figure 1: *Underlying recovery from ischaemic stroke is a period of enhanced neuroplasticity. Neuroanatomic reorganisation occurs downstream of neurotrophic factor upregulation and perineuronal net downregulation. Rehabilitation has its greatest effect during this time and only limited recovery of function is possible beyond it.*

1.3: CNS Inhibitors of Neuroplasticity

Compared with those of infants and children, adult brains are relatively resistant to extensive reorganisation. As a result, adults who suffer ischaemic damage or other CNS insults recover to a much lesser extent than children[81]. Several mechanisms have been identified that are responsible for the non-permissive nature of the adult brain to neuroplasticity. The two major systems addressed in this review are the neuron-associated perineuronal nets (PNNs) and the oligodendrocyte-associated Nogo proteins (Figure 2). Other mechanisms that are not evaluated here include negative axonal guidance through semaphorin-plexin interactions and the glial inhibitors of neuroplasticity – myelin associated glycoprotein (MAG) and oligodendrocyte myelin protein (OMgp).

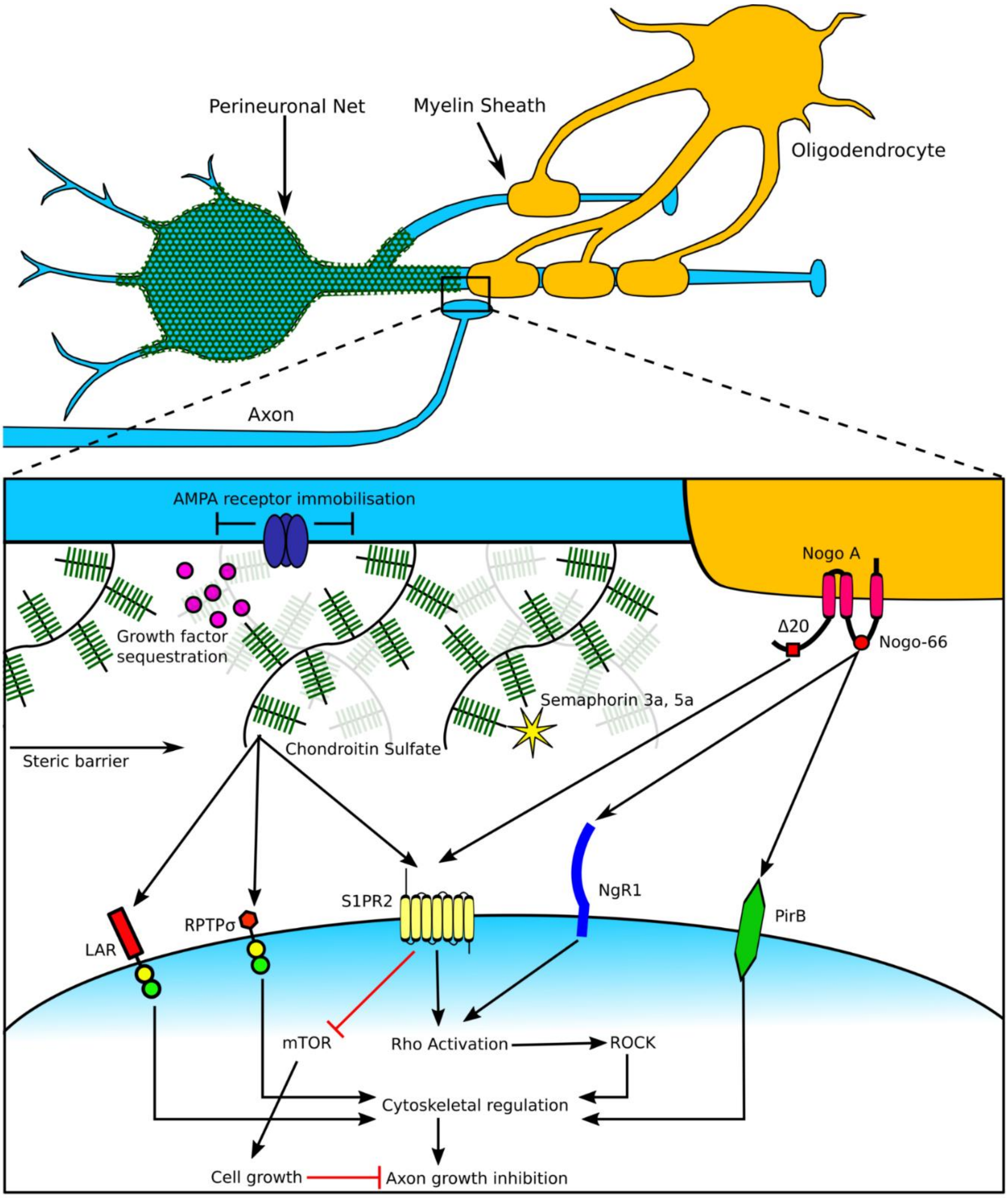

Figure 2: *Two major mechanisms for inhibition of neuroplasticity within the central nervous system are perineuronal nets and the Nogo pathway. Perineuronal nets inhibit plasticity through steric hindrance, growth factor sequestration, receptor immobilisation, presentation of semaphorins and interactions with the neuronal receptors S1PR2, Receptor type protein tyrosine phosphatase (RPTP)σ and LAR. The Nogo proteins are expressed intracellularly and on the membranes of oligodendrocytes, which form the myelin sheaths surrounding axons. Nogo acts through interactions with the neuronal receptors S1PR2, NgR1 and PirB. Both systems converge on cytoskeletal reorganisation, leading to axon repulsion and growth cone collapse.*

1.3.1: Perineuronal Nets

1.3.1.1: Overview of perineuronal nets

PNNs are complex reticular structures surrounding the soma and proximal neurites of subpopulations of neurons in the brain and spinal cord (Figure 3). These structures were first described by Camillo Golgi, who saw them as an extracellular counterpart to the Golgi apparatus[82]. Early hypotheses were that PNNs represented a branching mesh of axon terminals, that they were a component of the blood-brain barrier and that they were staining artefacts[82,83]. PNNs are now understood to be a specialised type of ECM, which has principal functions in development and in regulating adult neuroplasticity.

Microscopically, PNNs appear as a scale-like mesh of dense ECM surrounding neuronal cell membranes and interrupted by axonal and glial contacts[84]. PNNs are predominantly distributed around parvalbumin-expressing GABAergic interneurons and few pyramidal cells of the primary motor and sensory cortices, the hippocampus and purkinje neurons of the cerebellar cortex[85–88].

At a molecular level, PNNs are composed of chains of hyaluronan (HA), which are tethered to neuronal cell membranes by hyaluonan synthase (HAS). Chondroitin sulfate proteoglycans (CSPGs) including aggrecan, versican, brevican and neurocan are bound by cartilage link protein (Crtl-1) or brain link protein (Bral-1) at their N-termini. These link proteins are in turn bound to HA. Tenascin R (Tn-R) binds the C-termini of up to three CSPG molecules[89,90]. The relative amounts of each CSPG varies in different locations within the CNS[91]. CSPGs themselves are composed of a core protein covalently bound to glycosaminoglycan (GAG) side chains[92], which are responsible for much of the biological function of PNNs[93]. In particular, GAG sulfation state is related to function, with 4-O-sulfation (C4S) producing inhibition to neurite outgrowth[94] and 6-O-sulfation (C6S) stimulating neurite outgrowth[95,96].

One of the chief observations that has led to the current understanding of the function of PNNs is the coincidence of PNN maturation and the termination of critical periods[84,97]. The components of PNNs are not assembled concurrently, but rather sequentially. At birth, primordial PNNs are composed only of HA and resemble loose ECM. The ECM does not condense into mature PNNs until aggrecan, TN-R and link proteins are expressed, which in mice occurs 6-21 days postnatal[98,99]. Another observation is that PNN expression in songbirds correlates with the critical period for song learning in age-limited species[100] and with seasonal periods of song learning in species that learn new songs in maturity[101]. As PNNs mature, their ratio of C6S:C4S also changes. Primordial PNNs present high levels of the permissive C6S, which is replaced by the inhibitory C4S in maturity[95,102]. This strongly suggests that PNNs are one of the molecular mechanisms responsible for limiting adult neuroplasticity.

For PNN maturation to take place, specific external stimulation must occur during the critical periods. In mice, whisker trimming results in sensory deprivation of the barrel cortices. If whiskers are trimmed for the duration of the critical period, then mature PNNs fail to develop in the affected barrel cortex[99]. Restoration of sensory input after critical period termination is not sufficient to stimulate maturation of PNNs[103]. Likewise, depriving juvenile songbirds of a tutor delays the development of PNNs in the brain regions responsible for song[100]. It is unclear how this reconciles with the classical understanding that neuroplasticity is limited after critical period termination despite sensory deprivation[51]. It is likely that redundant mechanisms are responsible for limiting critical periods, so perhaps PNN attenuation in sensory deprivation is not sufficient to extend critical period plasticity indefinitely.The mechanisms of action by which PNNs cause inhibition of neuroplasticity have not been fully elucidated, though four main hypotheses exist. 1) By surrounding the soma and proximal neurites, PNNs form a barrier to new synaptic contacts being made[104,105]. 2) PNNs inhibit neurite outgrowth through receptor interactions. CS itself has an affinity for receptor protein tyrosine phosphatase σ (RPTPσ)[106], leukocyte common antigen-related phosphatase (LAR)[107] and Nogo receptor 1 (NgR1)[108]. Moreover, PNNs have an association with other inhibitory molecules[109]. Notably, the chemorepulsive axon guidance molecules semaphorin 3A[110,111] and semaphorin 5A[112] colocalise with PNNs and appear to form an active component. 3) PNNs sequester growth-promoting molecules, including laminin[113] and heparin binding growth factors, preventing their activity[109]. 4) PNNs regulate the mobility of glutamate receptors, which in turn regulates excitatory activity and synaptic plasticity[114] (Figure 2).

It is unclear why inhibition of plasticity around the subpopulation of neurons associated with PNNs is sufficient to control functional neuroplasticity. The two possibilities are 1) PNNs surround enough neurons to affect global neuroplasticity or 2) The neurons associated with PNNs are somehow specialised to act as gatekeepers to neuroplasticity. Whichever hypothesis best explains the effect, the empirical findings that link PNNs with inhibition of neuroplasticity stand to suggest that the neurons associated with PNNs may be a target for stroke therapy.

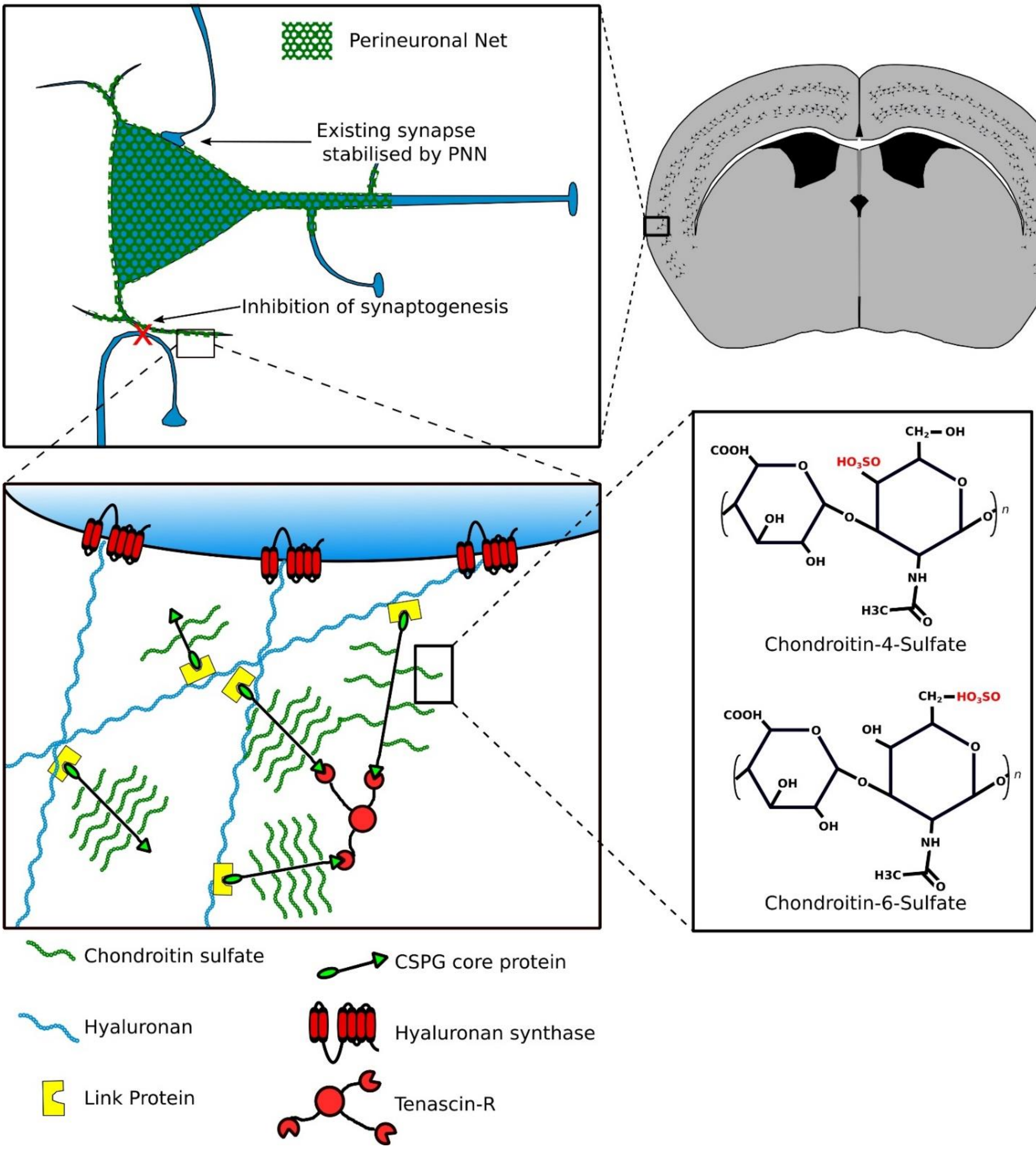

Figure 3: *Perineuronal nets ensheath subsets of neurons in the mammalian brain, predominantly the parvalbumin-expressing GABAergic interneurons. At a microscopic level, PNNs surround the soma, proximal dendrites and axon initial segments, with discontinuities over postsynaptic membrane regions. At a molecular level, PNNs are a lattice of glycosaminoglycans (GAG). Long chains of hyaluronan are bound to neuronal membranes by hyaluronan synthase. Chrondroitin sulfate proteoglycans (CSPGs) are bound to hyaluronan through interactions with cartilage link protein and are stabilised through interactions with tenascin-R. The sulfation state of the CSPG side chains determines the inhibitory activity of PNNs. C6S is permissive to neuroplasticity while C4S is inhibitory.*

1.3.1.2: Disruption of Perineuronal Nets Enhances Neuroplasticity

Disruption of PNNs in mature animals results in a degree of neuroplasticity reminiscent of the critical periods. One way of disrupting PNNs is with direct administration of the bacterial enzyme ABC chondroitinase (chABC), which digests GAG chains in both PNNs and loose ECM. In adult animals who were deprived of visual sensation during the critical period, treatment with chABC re-establishes ocular dominance plasticity and leads to normal development of visual acuity with neuroanatomic correlates[115,116].

Administration of chABC in rodent models of spinal cord injury (SCI) results in extension of axons[117] from the transected spinal cord and significant functional recovery[118–121]. This is relevant because the spinal cord presents the same inhibition to neurite outgrowth as the brain. Notably, optimum recovery was demonstrated when treatment was followed with task-specific rehabilitation[118]. PNN disruption creates a period of enhanced neuroplasticity and Hebbian mechanisms are required to guide it.

Transgenic mice with abnormal PNNs also present with increased adult neuroplasticity. The link protein Crtl-1 is a critical component of PNNs[122]. Animals deficient in link proteins Crtl-1 and Bral2 present with globally attenuated PNNs and extended critical periods, spinal cord plasticity and rapid compensation following vestibular deafferentation[123,124]. Mice deficient in aggrecan likewise present without mature PNNs and while one may hypothesize that this would extend critical periods, such studies have not been published to date. However, mice deficient in RPTPσ, a receptor for CS, show increased axonogenesis following SCI[106,125].

Disruption of PNNs has demonstrated efficacy in the treatment of ischaemic stroke in preclinical studies. Recovery of sensory-motor function has been obtained by treatment with chABC in the spinal cord[126,127] and the ipsilesional cortex[128,129]. The neuroanatomical correlates of this enhanced functional plasticity include growth of midline-crossing axons from the contralateral homotopic region[126] and branching of neurites in the region surrounding the infarct[127]. Disinhibition of neuroplasticity with chABC also had the effect of protecting distant brain regions from delayed secondary damage following ischaemic stroke[129]. The mechanism for this is unclear, but it may be that denervated distant regions are able to be salvaged by forming new synapses with unaffected regions.

Another important concept is that combining chABC treatment with rehabilitation has a synergistic effect on functional recovery and neuroanatomical plasticity. In two recent studies, rat models of focal motor cortex stroke were treated with perilesional[128] or intrathecal[127] injections of chABC, which was combined with a rehabilitation schedule. In the first study, task-specific rehabilitation was provided concurrently with chABC as training in a skilled reach behaviour test. This combination resulted in significant improvement in performance of the behaviour test[128]. The second study compared the effect of combining intrathecal chABC with early task-specific rehabilitation, with late rehabilitation and with no rehabilitation. While all treatment arms resulted in significant improvement in skilled reach performance, the delayed rehabilitation schedule was superior[127]. This is consistent with the hypothesis that chABC treatment opens a window for plasticity that must be guided by Hebbian mechanisms.

1.3.1.3: Endogenous Regulation of Perineuronal Nets

The structure and composition of PNNs in the mature CNS is not static, but varies in response to external factors that are known to stimulate neuroplasticity. Examples of stimuli that trigger neuroplasticity are neurological insult, exposure to novel sensory stimulation and exercise. The co-variation of PNN expression and neuroplasticity in these situations suggests a role for PNN regulation in facilitating learning and skill acquisition in the adult brain.

One model of adult neuroplasticity is the recovery of postural reflexes following vestibular deafferentation. In animal models, unilateral ablation of the vestibular apparatus has been shown to result in a loss of proprioception that can be measured as postural dysfunction. Recovery of postural reflexes over time has been shown to result from compensatory neuroanatomic reorganisation, including axonogenesis, synaptic plasticity[130] and neurogenesis[131] within the vestibular nuclei. One study in mice has demonstrated that wisteria floribuna agglutinin (WFA)-staining PNNs were downregulated in both vestibular nuclei and this effect was correlated with structural remodelling as well as functional recovery[124].

Voluntary aerobic exercise has also been demonstrated to enhance adult neuroplasticity. An extensive systematic review on the effect of exercise on post-stroke neuroplasticity indicated that exercise enhanced functional neuroplasticity through synaptic and dendritic plasticity[132]. A more recent study not included in the systematic review showed that voluntary exercise in rats resulted in a decrease in expression of WFA-staining PNNs in the hippocampus[133]. As the hippocampus is involved in memory consolidation, this suggests that PNN downregulation may be a mechanism through which exercise stimulates neuroplasticity.

As discussed in section 1.2.1, deprivation of visual stimulation during the critical period results in persistent blindness[51]. A study in rats has shown that providing novel sensory input through environmental enrichment stimulated neuroplasticity in the visual cortex, resulting in recovery of visual acuity[134]. Furthermore, it was shown that WFA-stained PNNs were also downregulated in the visual cortex. This has two important implications: 1) A degree of neuroplasticity previously not thought to occur in adulthood can be achieved through environmental stimulation and 2) PNN downregulation may underlie part of this effect.

It has also become apparent that modifications to PNNs are an important characteristic of stroke pathogenesis and recovery. Immediately following stroke, the ischaemic, perilesional and associated distant brain regions showed a decrease in WFA staining, lectican core proteins and link proteins[135–139] along with a loss of the reticular organisation of PNNs in those areas[137,140]. At the same time, human brain tissue showed an increase in hyaluronan staining up to 37 days post-stroke, which is thought to be related to increased turnover of hyaluronan in the brain ECM[141]. These alterations in PNN expression return to baseline by around 30 days post-stroke[135] in animals, and may remain months after stroke in humans[140]. These data suggest that the period of enhanced plasticity experienced after stroke is related to the alteration of PNNs and plasticity, both in areas surrounding the stroke and distant contralesional regions. A summary of these studies can be found in Figure 4.

Many studies did not report on PNN expression in the contralesional hemisphere and some used the contralesional hemisphere as a control[136,137]. This is flawed because it assumes that stroke does not influence PNN regulation in regions unrelated to the infarct. Of the studies that did address the contralesional cortex, one found a decrease in WFA staining 24 hours post-infarct, but not aggrecan or brevican[135], whereas another found no change in contralesional WFA staining at this time point[139]. In these studies, contralesional PNNs were identified only by their CSPG components (WFA staining, aggrecan and brevican). To date, PNN alteration in the contralesional hemisphere more than 24 hours post-infarct has not been reported.

Interestingly, post-stroke changes in the structure and distribution of PNNs are influenced by concurrent environmental stimulation. Two studies have demonstrated that post-stroke downregulation of PNNs was further enhanced by housing rats in enriched environments. Quattromani et.al.[142] showed that enriched housing resulted in significantly reduced PNNs throughout the ipsilesional hemisphere but not the contralesional hemisphere at seven days post-infarction. Madinier et.al.[142] demonstrated an association between enriched housing and PNN downregulation throughout the ipsilesional cortex 63 days post-infarction. This indicates that environmental enrichment not only caused a greater degree of PNN downregulation, but also extended the period of PNN downregulation beyond what was seen in studies without environmental enrichment. Both studies were appropriately controlled with sham stroke animals as opposed to controlling with the contralesional hemisphere. However, only aggrecan was assessed as a PNN marker, meaning that changes in expression of other PNN components were not measured.

These results suggest that the interrelationship between PNNs, environmental stimulation and neuroplasticity is such that endogenous PNN modulation is dependent on environmental stimulation and artificial degradation of PNNs requires environmental stimulation to cause functional neuroplasticity. As such, any stroke therapy targeting PNNs should involve a period of task-specific rehabilitation.

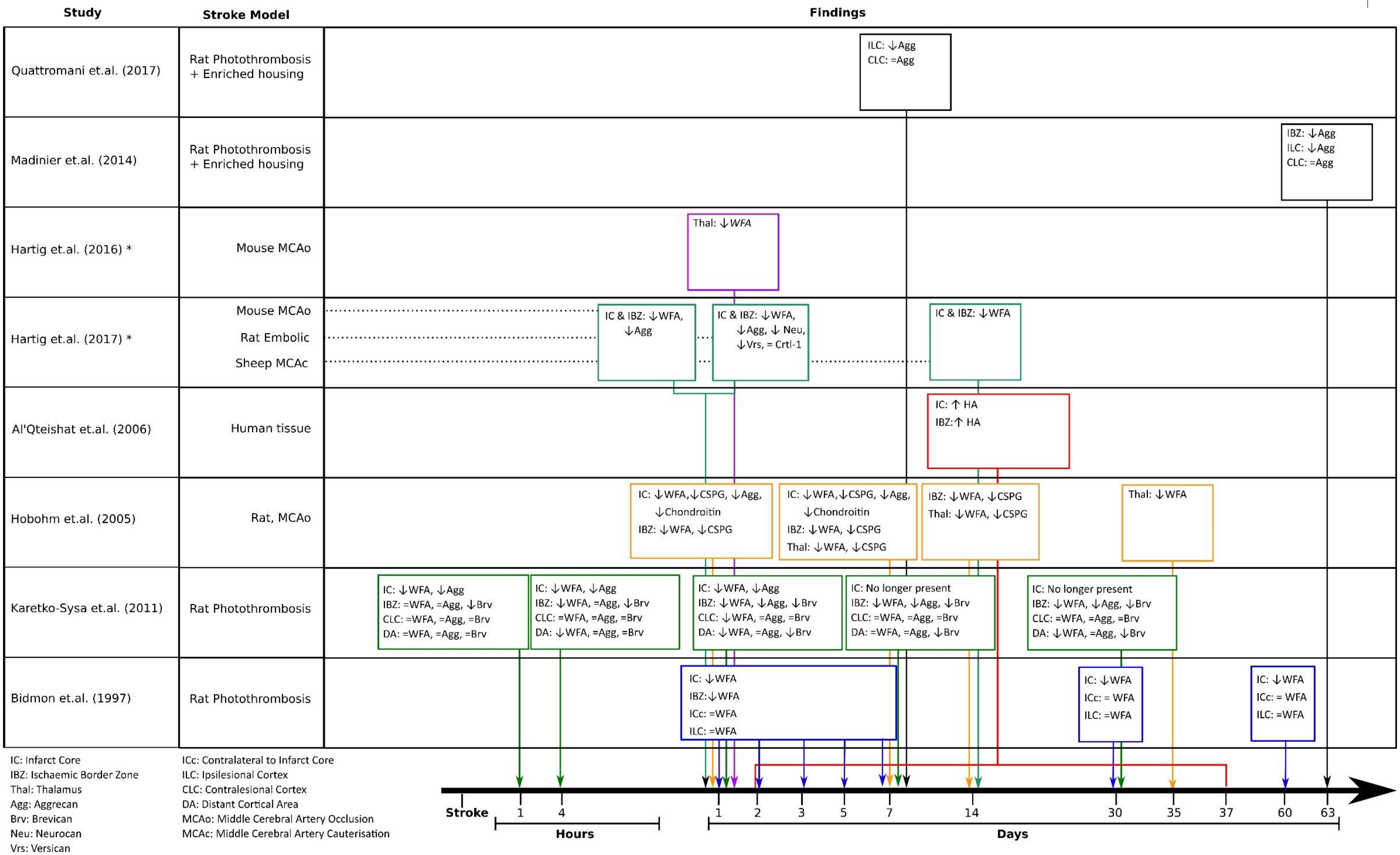

Study
Stroke Model
Findings
Quattromani et.al. (2017)
Rat Photothrombosis + Enriched housing
ILC: ↓Agg
CLC: =Agg
Madinier et.al. (2014)
Rat Photothrombosis + Enriched housing
IBZ: ↓Agg
ILC: ↓Agg
CLC: =Agg
Hartig et.al. (2016) *
Mouse MCAo
Thal: ↓WFA
Hartig et.al. (2017) *
Mouse MCAo
Rat Embolic
Sheep MCAc
IC & IBZ: ↓WFA, ↓Agg
IC & IBZ: ↓WFA, ↓Agg, ↓ Neu, ↓Vrs, = Crtl-1
IC & IBZ: ↓WFA
Al'Qteishat et.al. (2006)
Human tissue
IC: ↑ HA
IBZ:↑ HA
Hobohm et.al. (2005)
Rat, MCAo
IC: ↓WFA,↓CSPG, ↓Agg, ↓Chondroitin
IBZ: ↓WFA, ↓CSPG
IC: ↓WFA,↓CSPG, ↓Agg, ↓Chondroitin
IBZ: ↓WFA, ↓CSPG
Thal: ↓WFA, ↓CSPG
IBZ: ↓WFA, ↓CSPG
Thal: ↓WFA, ↓CSPG
Thal: ↓WFA
Karetko-Sysa et.al. (2011)
Rat Photothrombosis
IC: ↓WFA, ↓Agg
IBZ: =WFA, =Agg, ↓Brv
CLC: =WFA, =Agg, =Brv
DA: =WFA, =Agg, =Brv
IC: ↓WFA, ↓Agg
IBZ: ↓WFA, =Agg, ↓Brv
CLC: =WFA, =Agg, =Brv
DA: ↓WFA, =Agg, =Brv
IC: ↓WFA, ↓Agg
IBZ: ↓WFA, ↓Agg, ↓Brv
CLC: ↓WFA, =Agg, =Brv
DA: ↓WFA, =Agg, ↓Brv
IC: No longer present
IBZ: ↓WFA, ↓Agg, ↓Brv
CLC: =WFA, =Agg, =Brv
DA: =WFA, =Agg, ↓Brv
IC: No longer present
IBZ: ↓WFA, ↓Agg, ↓Brv
CLC: =WFA, =Agg, =Brv
DA: ↓WFA, =Agg, ↓Brv
Bidmon et.al. (1997)
Rat Photothrombosis
IC: ↓WFA
IBZ:↓WFA
ICc: =WFA
ILC: =WFA
IC: ↓WFA
ICc: = WFA
ILC: =WFA
IC: ↓WFA
ICc: = WFA
ILC: =WFA
Stroke
1
4
Hours
1
2
3
5
7
14
30
35
37
60
63
Days
IC: Infarct Core
IBZ: Ischaemic Border Zone
Thal: Thalamus
Agg: Aggrecan
Brv: Brevican
Neu: Neurocan
Vrs: Versican
ICc: Contralateral to Infarct Core
ILC: Ipsilesional Cortex
CLC: Contralesional Cortex
DA: Distant Cortical Area
MCAo: Middle Cerebral Artery Occlusion
MCAc: Middle Cerebral Artery Cauterisation

Figure 4: *A summary of the studies that investigate the post-stroke regulation of PNN components. Results reported from studies indicated by * were qualitative. ↑ indicates a reported increase in expression, ↓ indicates a reported decrease in expression, = indicates no change in reported expression.*

1.3.2: Nogo

1.3.2.1: Overview of Nogo Signalling

The Nogo proteins are myelin-associated inhibitors of neurite outgrowth that play a key role in regulating adult neuroplasticity. The therapeutic potential of targeting the neurite outgrowth inhibitory activity of Nogo was first explored in relation to its role in recovery from SCI. Treatment with anti-Nogo-Antibodies and Nogo receptor antagonists produces improved locomotor recovery and growth of transected axons following experimental models of SCI[143–145].

There are three Nogo isomers, and of these, Nogo-A is the most well-characterised. Nogo-A is a transmembrane protein with two extracellular active domains: Nogo-66 and Nogo-A-Δ20. Nogo-66 is a 66-amino acid loop towards the C terminal of Nogo A that is also conserved in Nogo-B and -C. Nogo-A-Δ20 is located towards the N-terminal and is specific to Nogo-A (Figure 2).

In the adult brain, Nogo-A is primarily expressed by dorsal root ganglion neurons[146], oligodendrocytes[147] and immature neurons in the dentate gyrus[148]. The majority of Nogo-A is intracellular and associated with the endoplasmic reticulum[149–152], though it is also located in the paracellular layer of the myelin sheath[147]. During development, Nogo-A is expressed by postmitotic neurons in the cortex, cerebellum and spinal cord[147]. This early expression pattern is thought to reflect a role in guiding the migration of neuroblasts in the developing CNS.

The neurite outgrowth inhibitory activity of Nogo-A is mediated by three neuronal receptors: Nogo Receptor 1 (NgR1), Sphingosine-1 Phosphate Receptor-2 (S1PR2)[153] and Paired Immunoglobulin-like Receptor B (PirB) (Figure 2). NgR1 and PirB are activated by the common active domain Nogo-66[146,154] and by PNN-associated CSPGs[108]. S1PR2 is a G protein-coupled receptor that is specific to the Nogo-A isomer[153]. The activation of NgR1 and S1PR2 converges on the RhoA/ROCK signalling pathway, which inhibits neurite outgrowth through cytoskeletal reorganisation[155]. Nogo-A-Δ20 has also been shown to decrease expression of mTOR, which is known to regulate cellular growth [156,157].

1.3.2.2: Nogo Antagonism Promotes Neuroplasticity

Inhibition of Nogo-A activity has been achieved in experimental stroke models by several mechanisms. The earliest and most extensively characterised of these is IN-1[158], a monoclonal antibody with affinity for the Nogo-A-Δ20 domain that inhibits the action of S1PR2 but not NgR1[159]. Other immunotherapeutic agents include 11C7[144] and 7B12[160], which are Nogo-A specific monoclonal antibodies and 7E11, a monoclonal antibody against NgR1[161]. A soluble protein antagonist of the NgR1 receptor, NgR(310)Ecto-Fc, has been demonstrated to exhibit similar plasticity-promoting effects to monoclonal antibodies[162]. Disruption of the Nogo signalling mechanism has also been achieved in transgenic animals deficient in NgR1 and NogoA/B[162].

The efficacy of anti-Nogo therapy has been tested on a broad variety of functional deficits in animal models. Significant improvements in skilled sensory-motor function have been reported in animals treated with IN-1, 11C7, NgR(310)Ecto-Fc and 7B12 following experimental stroke[160,162–165]. Animals receiving IN-1, NgR(310)Ecto-Fc and animals deficient in NogoA/B or NgR1 recovered coordination more rapidly and to a greater extent than control animals[162]. Anti-Nogo-A and anti-NgR1 immunotherapy also resulted in improved recovery of spatial memory[166] and reversed visuospatial neglect[167].

Nogo pathway inhibition promotes an enhancement of neuroplasticity in sensory-motor and cognitive systems. Several studies have reported that animals exhibiting improved functional recovery after anti-Nogo treatment also presented with an increase in the number of axons crossing from the homotopic cortex contralateral to the lesion and supplying the denervated corticospinal and rubrospinal tracts[160,162–165,167,168]. The responsibility of these newly generated axons for functional recovery was strongly supported by Brenneman et.al. [167], who demonstrated that corpus callosotomy reversed improvements made in hemispatial neglect due to anti-Nogo treatment. Furthermore, the excellent study by Wahl et.al. [165] described the development of two models for the inducible, selective blockade of midline-crossing axons. Blockade of these fibres temporarily reversed the improvements in sensory-motor function in animals treated with IN-1.

In addition to axonogenesis, anti-Nogo treatment in animal models of stroke has demonstrated an increase in dendritic tree complexity in the contralesional homotopic cortex[169] and somatotopic reorganisation of midline-crossing axons terminating in the pons[170]. This suggests that the novel neurite outgrowth caused by anti-Nogo treatment is directed and functionally relevant.

As anti-NogoA antibody treatment improves recovery of spatial memory following stroke, hippocampal plasticity was hypothesized as a possible mechanism[166]. Moreover, NgR1 activation has been shown to inhibit neural stem cell proliferation in the subgranular zone and S1PR2 activation increases migration of neuroblasts in the rostral migratory stream[171]. However, treatment with 11C7 following stroke does not result in any change in neuronal proliferation in the subgranular zone, accumulation of new neurons in the granule cell layer[148] or any change in the mobilisation or migration speed of subventricular zone neuroblasts[172].These data suggest that enhancement of neuroanatomical plasticity in the hippocampus is not a mechanism by which anti-Nogo therapy produces its effect.

It has emerged that the timing of treatment relative to the stroke and relative to adjunct rehabilitation is vital to achieving enhanced functional recovery. Anti-Nogo-A therapy has a broad therapeutic window. Efficacy has been demonstrated when administration takes place immediately[169] after stroke, and at various time points up to nine weeks post-stroke[162,164]. This suggests the potential to extend the limited therapeutic window for stroke.

The addition of a rehabilitation schedule to treatment involving anti-Nogo-A therapy has been shown to improve recovery beyond either treatment alone[165]. However, this effect was only produced when rehabilitation was provided after anti-Nogo-A therapy. Following a photothrombotic infarction, rats that received anti-Nogo-A therapy followed two weeks later by intensive task-specific forepaw training performed better than those without rehabilitation or those undergoing rehabilitation concurrently with treatment. Furthermore, the group of rats that received concurrent rehabilitation and treatment performed worse than animals receiving no treatment. On histology, the authors reported that rats in both treatment schedules showed enhanced axon growth, but the rats in the simultaneous treatment schedule showed an increase in aberrant branching and overgrowth of axons beyond the grey/white matter boundary. Similar results have been seen in the treatment of experimental spinal cord injury with anti-Nogo-A therapy[173]. This suggests that anti-Nogo-A treatment causes disinhibition of neuroplasticity, which in the context of specific and intentional rehabilitation leads to functional reorganisation of neuronal networks, but in the absence of rehabilitation results in detrimental, disorganised restructuring. This is an important concept that should be considered in the design of clinical trials of anti-Nogo-A treatment for ischaemic stroke.

The remarkable improvements seen in the anti-Nogo treatment of CNS lesions in animal models have not yet been translated into human therapy. Phase I clinical trials have demonstrated the safety of anti-Nogo-A monoclonal antibodies in the treatment of SCI and amyotrophic lateral sclerosis(ALS)[174]. Following the determination that intrathecal delivery of the anti-Nogo-A monoclonal antibody ATI-355 is safe in humans, a phase II trial with a placebo control is currently being planned by the Schwab group. A phase II clinical trial of ozanezumab, another anti-Nogo-A monoclonal antibody, failed to demonstrate efficacy for ALS, suggesting that the Nogo system is not a therapeutic target for this disease[175]. There are currently no clinical trials for anti-Nogo-A therapy in stroke.

1.4: Stem Cells

Stem cells are multipotent or pluripotent populations of undifferentiated cells that have the capacity to regenerate themselves and to differentiate into mature cell types in response to environmental cues[176]. In development, blastocysts divide into three main embryonic lineages that eventually give rise to all adult tissues; the ectoderm, mesoderm and endoderm. In addition to adult somatic cells, embryonic stem cells also give rise to specialised populations of adult stem cells, which serve a maintenance function in replacing aged and damaged tissues. As a result, there are many populations of multipotent adult progenitor cell, which can be distinguished by their differentiation potential. Mesenchymal stem cells reside in niches throughout the body and can give rise to many tissue types including bone, muscle, adipose, neurons and glia[177]. Haematopoietic stem cells reside in bone marrow and differentiate into the cellular components of blood[178]. Neural stem cells, which can give rise to neurons, astrocytes and oligodendrocytes are more limited and can be found mainly within two regions – the subventricular zone and the subgranular zone[179]. Other examples include intestinal mucosal stem cells, epithelial stem cells, endothelial stem cells and dental pulp stem cells (DPSC). Most organs have a stem cell population maintaining them.

Stem cells can also be derived artificially from somatic cells. The novel induction of stem cell properties in adult somatic cells was first described in the landmark study by Okita et.al. (2007)[180]. This study demonstrated that fibroblasts could be transformed into highly proliferative, pluripotent cells through retroviral transduction with embryonic transcription factors (oct 3|4, sox-2, c-myc and klf-4). Induced pluripotent stem cells (iPSC) are antigenically compatible with the donor and are similar to embryonic stem cells in their differentiation potential.

1.4.1: Cell-Based Therapy

The ability of stem cells to proliferate and repopulate damaged tissues lead to the paradigm of cell-based therapy. This field has its origins in the transplantation of haematopoietic stem cells by E.D. Thomas in the 1950's[181,182]. Transplantation of allogeneic haematopoietic stem cells from bone marrow is now routinely carried out to replace cells following full-body irradiation for leukaemia. Cell-based therapy has since been investigated as a potential treatment option in a number of neurological conditions that result from tissue loss, including traumatic brain injury, spinal cord injury and degenerative diseases such as Alzheimer's and Parkinson's.

Cell-based therapy has also been extensively investigated as a potential treatment option for ischaemic stroke. The application of cell-based therapy has been tested in numerous pre-clinical stroke studies[183,184]. Significant improvement in cognitive and sensorimotor function has been demonstrated in animal stroke models through performance in tasks specific to the neurological damage caused. Efficacy has been demonstrated following administration of several types of stem cell, including mesenchymal stem cells (MSC)[185], haematopoietic stem cells[186], iPSC[187,188] and DPSC[189] among others. While these results are promising, several issues still need to be considered with regards to optimising cell-based therapy for ischaemic stroke. These include factors relating to the type of stem cell used, the source, the administration route, the timing of transplantation and combination with other interventions, such as rehabilitation.

The optimism gained from these animal studies should be tempered with caution, a lesson learned in the field of cell-based therapy for Parkinson's disease. Following the success of foetal ventral mesencephalic neuron transplantation in animal models of Parkinson's disease[190,191], a small phase 1 clinical trial was conducted and several of the subjects experienced significant improvement in their Parkinson's symptoms[192]. This led to two larger double-blind placebo controlled clinical trials. In an outcome reminiscent of the failed translation of neuroprotective therapies, the results from both of these trials indicated that foetal ventral mesencephalic stem cell transplantation was not efficacious for Parkinson's disease in humans. Moreover, the treatment was associated with significant adverse events[193,194]. Therefore, success in preclinical studies of stem cell therapy in stroke does not guarantee success in translation.

Cells used in therapy may be pluripotent, such as embryonic stem cells and iPSC, or multipotent progenitor cells. While the rapid proliferation and unlimited differentiation potential of pluripotent cells may seem ideal, these same properties lead to an increased risk of tumorigenicity. The high proliferation rate, myc expression[195] and telomerase activity[196] of embryonic stem cells causes genomic instability[197,198]. As a result, transplantation of embryonic stem cells into animal models characteristically results in teratoma formation[199,200] and may result in malignancy[201]. The use of iPSC likewise results in an increased risk of tumour formation. Other than a rapid proliferation rate, iPSCs also necessarily overexpress the oncogene c-Myc[180], sustain mutagenesis during viral transduction[202,203] and retain accumulated genomic damage from their existence as somatic cells[204]. While there are no reported cases of tumour formation in humans following pluripotent stem cell transplantation, at least one person has developed brain tumours derived from transplanted foetal neural stem cells[196]. Conversely, adult multipotent stem cells carry a lower risk[205]. The other advantage to these is that they can be derived from an autologous source, which eliminates the risk of immune reactivity. Adult multipotent stem cells have been transplanted into humans in numerous studies without cell-related adverse events[206–222]. Therefore, these are a more appropriate cell type for therapeutic use.

Another option is to transplant with pre-differentiated neurons produced ex-vivo. One advantage to this method is that these cells are post-mitotic and are therefore have negligible risk of tumour formation. The other advantage is that the neuronal fate of transplanted cells is guaranteed, as opposed to stem cell transplantations lead predominantly to astrocytic differentiation[189,223–225], which may reduce efficacy. One study demonstrated 30% transplant cell survival and greatly enhanced functional outcomes following transplantation of pre-differentiated GABAergic neurons[225]. The authors suggest this may be due to the regulatory role of GABA in neuroplasticity.

Donor age may also impact the efficacy of cell-based therapy. While stem cells are present throughout life, extensive proliferation and accumulated damage effects their stem-like properties. For example, the differentiation potential of mesenchymal stem cells sourced from adipose[226] and bone marrow[227] is reduced in advancing age, with fewer cells able to differentiate into mature chondrocytes or osteoblasts. This inability of aged mesenchymal stem cells to adequately replace osteoblast populations has been hypothesised as a reason for the reduction of bone mineral density with advancing age[228]. Furthermore, the *in vitro* proliferation rate of mesenchymal stem cells decreases with donor age[227,229]. This has implications for cell-based therapy as autologous therapy requires *in vitro* expansion prior to implantation, and slowed proliferation may result in delayed treatment. As a result, cells sourced from younger donors may provide superior outcomes. One recent pre-clinical study has demonstrated that a rat stroke model treated with human mesenchymal stem cells from younger donors achieved superior functional outcomes in behaviour testing than when treated with cells from older donors[185].

Delivery of cells to the site of action has been achieved by direct intracerebral transplantation and via intravascular routes. Intracerebral transplantation ensures that cells are delivered directly to the brain, giving them the greatest chance of exhibiting an effect. However, this route is highly invasive and carries a high risk of serious adverse events[230,231]. Furthermore, the migratory potential of cells transplanted directly into the brain is limited by glial scar formation[225], a limitation that presumably would not be shared by intravascular transplantation. Stem cells migrate towards the chemokine SDF-1, which is highly expressed in the post-stroke brain. In addition to this, stem cells transplanted via an intravascular route can transmigrate the blood-brain barrier[232–234]. Therefore, administration of stem cells through an intravascular route results in engraftment at the site of action and causes enhanced functional recovery[232]. A recent study has suggested that an intravenous route may be superior to an intra-arterial route, as intra-arterial administration resulted in increased inflammatory damage and poorer outcomes in functional behaviour testing[186].

One of the advantages of cell-based therapy is that it promises to extend the treatment window for stroke. Pre-clinical trials have shown efficacy when treatment is provided up to two weeks[235] after the ischaemic event, though a systematic review has determined that early administration results in greater efficacy[183]. A study using a mouse model of ischaemic stroke determined that the greatest engraftment rates were achieved from intra-arterial transplantation at three days[235]. While it is unclear how this would translate to human studies, it is noteworthy that cells transplanted at two earlier timepoints had poorer engraftment rates. This suggests that factors relating to the evolution of ischaemic stroke influence transplanted cells, and this will need to be addressed to optimise cell-based stroke therapy in humans. The authors suggest that this relates to increased VCAM-1 expression, though this was also upregulated at earlier time points. Other possible explanations for this effect are that acute inflammation at earlier timepoints is damaging to transplanted cells, that blood-brain barrier permeability is maximised at day three[236](discussed further in section 1.5) and that peri-infarct expression of the chemokine SDF-1 also peaks at day three[183].

There is also evidence that like anti-Nogo and PNN-targeted therapy, the combination of stem cell transplantation and rehabilitation is synergistic, or at least additive[237]. The optimum timing schedule for stem cell and rehabilitation combination therapy has not been investigated to date. Given that cell-based therapy may act in part by stimulating neuroplasticity (discussed in section 1.4.4), it is likely that it also requires guidance through Hebbian mechanisms to achieve maximum efficacy.

At least 23 early-phase clinical trials of cell-based therapy for ischaemic stroke have been conducted so far, with a combined sample size of 672 patients[206–222,230,231,238–241]. Of these, nine included control groups and the rest were either phase I or pilot studies. The majority (16) used cells from an autologous source, including MSC derived from bone marrow, haematopoietic stem cells and peripheral blood stem cells. Cells derived from exogenous sources included fetal stem cells, neuronal stem cells, multipotent progenitor cells and modified mesenchymal stem cells. One early study attempted to use cells derived from porcine foetus, though this was aborted after serious adverse events were reported[238]. Transplantation routes used in these experiments included intracerebral (8), subarachnoid (1) intravenous (9) and intra-arterial (5), with one study testing both intravenous and intra-arterial. The main outcome from these studies was that cell-based therapy was generally safe and well-tolerated, with the majority of adverse events being related to the transplantation procedure and not the cells. Despite the many clinical trials that have been published, the positive results seen in preclinical studies have not been replicated unequivocally in human clinical trials. Some of the possible reasons for this are that human stroke is more heterogeneous than animal stroke models, that measuring functional outcomes in humans is more complex than standardised behaviour testing in animals, and that the majority of these studies had small sample sizes without control groups. A recent systematic review suggested that there is a need for a phase 3 clinical trial to determine whether cell-based therapy for ischaemic stroke is efficacious in humans, as this is difficult to infer from phase 2 trials only[242].

1.4.2: Dental Pulp Stem Cells

First described by Gronthos et.al. (2000), DPSC are a heterogeneous population of highly proliferative, multipotent cells residing in perivascular niches within adult teeth [243]. DPSC are similar to MSC in terms of their differentiation potential and are thought to be of a neuroectodermal origin and a subpopulation of DPSC have been shown to derive from Schwann cells during development[244]. The most likely functions of adult DPSC are to repair nerve and vascular tissue and to replenish odontoblast populations for maintenance of dentine in teeth. DPSC seem to be present throughout life as long as dental pulp remains intact[245].

DPSC have been studied extensively both *in vivo* and *in vitro*, and have been shown to be rapidly expandable and multipotent. Aside from their odontoblastic potential, DPSC have been demonstrated to differentiate into neurons, adipocytes, myocytes, chondrocytes[246,247] and retinal photoreceptor-like cells[248]. Under the appropriate conditions, DPSC are capable of forming neurospheres, which contain cells expressing various neuronal and glial antigens[249]. Furthermore, neurons produced through differentiation of DPSC are functionally active, with detectable action potentials and ion channels[246].

Molecular characterisation of undifferentiated DPSC has revealed that they express surface antigens and other markers also associated with other types of stem cell. Cluster of differentiation (CD) markers and others can be used to identify populations of multipotent stem cells[177]. As DPSC are a heterogeneous population, no single set of markers has been identified to distinguish DPSC from other stem cell types. Furthermore, different subpopulations of DPSC with distinct stem-like characteristics have been shown to express different surface antigens[250]. In general, DPSC have been shown to express the mesenchymal stem cell markers CD105, CD73, CD90, CD44 and STRO-1, and to not express the negative MSC selection markers CD45, CD34, CD14 or HLA-DR[248,251–253]. DPSC have also been shown to express the stem cell transcription factors OCT-4 and NANOG[254–256]. The significance of this is that the expression profile of DPSC demonstrates that they are phenotypically similar to other adult multipotent cell types. This is also experimentally relevant as it means that DPSC and sub-populations can be isolated from primary cultures using techniques such as magnetic- and fluorescence-activated cell-sorting.

DPSC express cytokines and receptor molecules that may render them useful in cell-based therapies. Molecular studies have determined that DPSC express the growth factors insulin-like growth factor-1, insulin-like growth factor-binding protein-6 and vascular endothelial growth factor[234], the immunomodulatory cytokines interleukin-10, tumour necrosis factor (TNF)-α and TNF-β[257] and the chemotactic factor stromal-derived factor-1 (SDF-1)[258]. Furthermore, DPSC express chemokine receptor CXCR4, thus enabling them to migrate along SDF-1 concentration gradients[259]. These characteristics relate to the hypothetical mechanisms of action of cell-based therapy, which are discussed further in section 1.4.3.

Their multipotentiality, clinical accessibility, presence in older patients and *in vitro* expandability make DPSC a promising candidate source for cell-based therapy. DPSC, like other adult stem cells, also have an advantage over pluripotent stem cells such as iPSC or those derived from embryos in that they are less likely to be tumorigenic. Specifically, immortalised DPSC do not form tumours when transplanted into immunocompromised animals[260]. As a result, DPSC have been investigated in pre-clinical studies as a therapeutic option for a broad range of disorders including bone defects[261,262], liver cirrhosis[263] and Parkinson's disease[264].

Of relevance to this review, DPSC have also been investigated as a treatment option to enhance recovery following ischaemic stroke. Direct intracerebral transplantation of human DPSC in a rat model of ischaemic stroke resulted significant enhancement in performance of behaviour tests. This effect was underpinned by a low survival rate of transplanted cells, but surviving cells migrated towards the ischaemic border zone and differentiated predominantly towards a glial phenotype[189].

Administration of a DPSC side population in a rat stroke model[265] and administration of DPSC from human deciduous teeth in a mouse model of neonatal hypoxia ischaemia[266] have shown similar results. Interestingly, administration of DPSC conditioned media alone was sufficient to significantly enhance recovery through stimulation of endogenous neuroplasticity[267] and neuroprotection[266]. The effect of a one-time dose of conditioned medium is presumably attenuated as compared with cell transplantation, which would provide prolonged administration of the active components. Transplanted cells survive at least four weeks in the host brain[189,225], though it is likely that they survive much longer. This suggests that at least part of the efficacy of DPSC therapy in stroke is due to soluble factors expressed by the cells. A recent study has reproduced the results showing enhancement of recovery in a rat model of focal infarct and also demonstrated that DPSC were more efficacious than marrow-derived MSC[268]. Therefore, DPSC are a promising cell type that should continue to be investigated as an option for cell-based therapy in ischaemic stroke.

1.4.3: Mechanism of Action

The mechanism of action of cell-based stroke therapy was originally thought to be replacement of lost tissue by neural differentiation and integration into surviving circuits. However, the low engraftment rates of transplanted stem cells and the even lower rates of neuronal differentiation suggest that other mechanisms are likely[189,269]. The predominant model is the bystander effect, which suggests that transplanted stem cells stimulate endogenous repair machinery through paracrine signalling[269]. The specific mechanisms involved in the bystander effect include neuroprotection, immunomodulation, angiogenesis, biobridge formation and neuroplasticity[270,271], which is the main concept explored in this review.

Neuroplasticity occurs through neuroanatomical and electrophysiological changes including axonogenesis, dendritic arborisation and long-term potentiation (discussed in section 1.2). There is compelling evidence from animal studies that transplantation of stem cells enhances these aspects of neuroplasticity. An example of this is from Arthur *et.al.*[258], who demonstrated that injection of human DPSC into chick embryos resulted in aberrant branching of peripheral nerve axons, suggesting that they exerted an effect through axonal guidance. In another study, a rat stroke model demonstrated enhanced branching of cortical dendrites and increased midline-crossing axons following engraftment with human neural stem cells[272]. This neuroanatomic reorganisation was correlated with significant improvement in behaviour test performance. A similar effect was shown in a rat model of neonatal hypoxia-ischaemia, wherein human neural stem cell engraftment caused significant ipsilesional axonal branching and improved functional outcomes[273]. Finally, cell-based therapy can also enhance the electrophysiological substrate of neuroplasticity. Transplantation of human MSC into mice following hippocampal insult partially restored hippocampal long-term potentiation and synaptic transmission as measured by brain slice microelectrode array[274]. This effect was also correlated with improved performance in maze tests, which implied an enhancement of spatial memory. Thus, cell-based therapy has been shown to enhance three primary components of neuroplasticity: axonogenesis, dendritic arborisation and long-term potentiation.

The hypothesis that cell-based therapy enhances performance in behaviour tests through neuroplasticity should be self-evident, as any change behaviour is necessarily precipitated by underlying neuroanatomical reorganisation. A more important question is *how* cell-based therapy stimulates neuroplasticity. The hypothetical mechanism through which stem cells enhance neuroplasticity includes the expression of neurotrophic factors. For example, MSC secrete brain-derived neurotrophic factor (BDNF), glial-derived neurotrophic factor (GDNF) and nerve growth factor (NGF)[275–277]. BDNF stimulates branching of axon terminals and promotes the differentiation and maturation of endogenous neural stem cells[278,279]. NGF causes axonal branching and dendritic arborisation, while expression of glial-derived neurotrophic factor (GDNF) causes axonal extension[280]. Furthermore, over-expression of BDNF and GDNF in MSC increases their efficacy in rodent stroke models[281,282].

More direct evidence for the role of cytokines in stem cell-induced neuroplasticity is found through knock-down or receptor inhibition studies. Antagonism of the SDF-1 receptor CXCR-4 inhibits the axon-guidance effect of DPSC on peripheral nerves[258]. Likewise, transgenic neural stem cells deficient in BDNF were shown through behaviour testing to have an attenuated efficacy in a rat model of traumatic brain injury[283] and vascular endothelial growth factor (VEGF) inhibition was shown to prevent dendrite branching and enhancement of axon transport by NSC[272]. Both neuroplasticity and the interactions that occur in cell-based therapy are highly complex. Thus, it is likely that these cytokines represent a number of redundant systems through which cell-based therapy enhances functional outcomes.

1.5: The Blood-Brain Barrier

As the gatekeeper to the brain parenchyma, the blood-brain barrier (BBB) plays a significant role in the development of new stroke therapies. Firstly, the BBB is affected by ischaemic stroke and its activity underlies the processes of damage and repair. Secondly, any treatment administered by an intravascular route must be able to cross the BBB to gain access to the CNS. The remainder of this review will address these concepts.

The BBB refers to the specialised structure of the neurovascular unit. Anatomically, the BBB is composed of a layer of endothelial cells surrounded by basement membrane, pericytes and astrocyte processes (Figure 5). Unlike other capillaries, the endothelial layer of the BBB is continuous and joined by tight junctions[284,285]. The main function of the BBB is to segregate the environment of the brain parenchyma from peripheral circulation. The extracellular environment of the CNS needs to maintain a balance of ions and neurotransmitters to maintain normal neuronal function. Without the BBB, the CNS would be contaminated by humoral analogues of neurotransmitters, which perform different functions in the periphery. In general, the BBB is selectively impermeable to large, polar molecules[286]. Various sources estimate the maximum size for passive diffusion across the BBB to range from 180 Da[287] to 800 Da[288]. However, the BBB is not a passive filter. It actively transports substances between circulation and the CNS parenchyma through transcytosis[289]. In addition, passage across the BBB may be facilitated by a global increase in permeability between BBB endothelial cells[290].

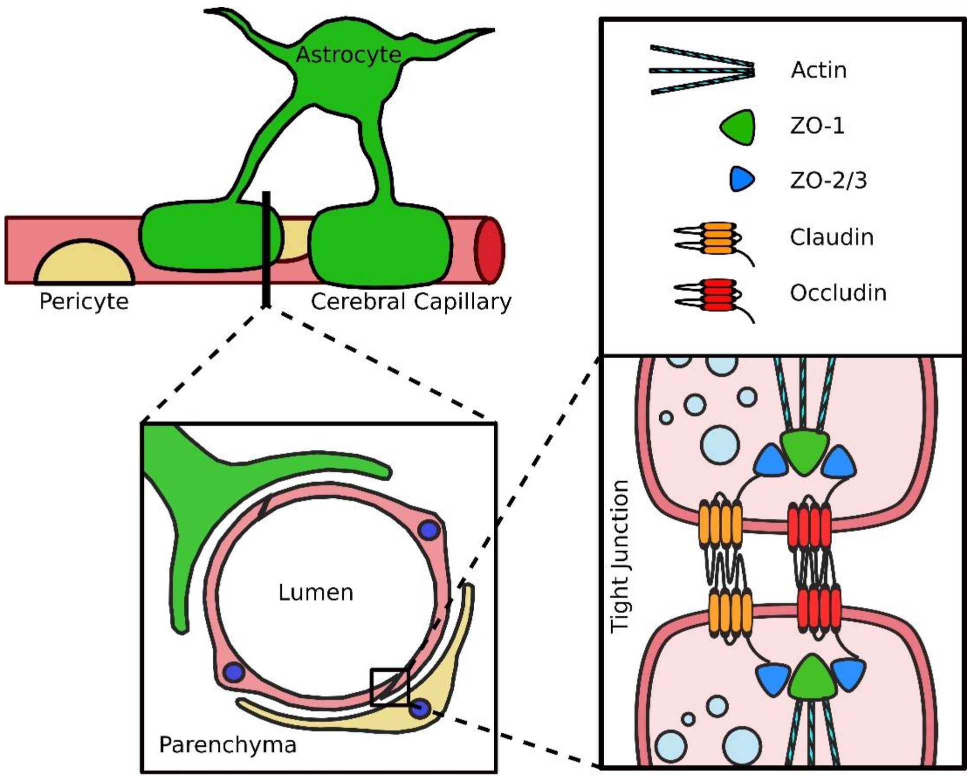

Figure 5: *A diagram of the cellular and molecular structure of the blood-brain barrier. Characteristic features include the close association between endothelial cells, pericytes and astrocytes, presence of tight junctions and transcytotic vesicles. Tight junctions anchor to cytoskeletal components and join the edges of adjacent endothelial cells.*

1.5.1: Structure and Function

One of the defining features of the BBB is the presence of tight junctions at the interface between adjacent endothelial cells. Microscopically, tight junctions appear as focally fused segments of endothelial cell membranes occurring in regions of overlap. At a molecular level, the tight junction complex consists of the cytoplasmic protein zonula occludens (ZO)-1, which binds to ZO2, ZO3 and cytoskeletal actin filaments. The transmembrane proteins occludin and claudin are anchored to ZO1, while their transmembrane domains bind to their counterparts on adjacent endothelial cells[287] (Figure 5). Imaging of these proteins in brain endothelial sections reveals a characteristic honeycomb appearance. Interestingly, when brain microvascular endothelial cells have been cultured *in vitro*, occludin relocalised to the cytoplasm, whereas claudin remained at the cell membrane[291,292].

An important cellular component of the BBB is the pericyte, which provides structural support for the endothelium as well as playing a role in regulating perfusion. Pericytes contain contractile elements in a similar arrangement to smooth muscle tissue[293,294], which relates to two important functions: 1) Pericytes relax to dilate capillaries in response to neuronal stimulation and 2) Pericytes contract to restrict flow in ischaemia.

Due to the close association between astrocyte processes and brain microvascular endothelial cells, it has long been hypothesised that astrocytes are involved in the induction of BBB characteristics in endothelial cells[295,296]. It has been demonstrated *in vitro* that co-culture with astrocytes induces BBB morphology in endothelial cells, including the expression of the tight junction proteins occludin and claudin[297]. Furthermore, endothelial monolayers exposed to astrocytes present a measurable increase in transcellular resistance[298]. This effect has also been produced by exposing endothelial cell cultures to astrocyte conditioned media[299]. Thus, the induction of a BBB phenotype in endothelial cells is likely to be the result of a soluble factor produced by astrocytes. Some candidate factors include glial-derived neurotrophic factor, basic fibroblast growth factor and angiopoietin[300].

Numerous studies have employed *in vitro* models for studying BBB permeability with regards to substances of interest[301–303]. Early models used a monolayer of brain microvascular endothelial cells adhered to a porous substrate, however it was found that endothelial cells lost their tight junctions when outside of the brain[302]. Due to the astrocyte induction hypothesis, subsequent models have used a bilayered co-culture of astrocytes and endothelial cells. Electron microscopy of these more complete BBB models has shown that astrocyte processes extend through the porous substrate to contact endothelial cells[302]. This resembles the structure of the BBB *in vivo*.

1.5.2: Response to Infarction

Increased BBB permeability occurs following most types of CNS injury and is usually associated with oedema. Following ischaemic stroke, there is a well-characterised biphasic increase in BBB permeability[304,305]. This activity is the result of two separate processes involving the BBB. The initial peak of permeability is a result of ischaemic damage, while the second peak is the result of repair processes[236].

The first peak in BBB permeability occurs at approximately 24 hours post-infarct and is the direct result of ischaemic damage to cerebral blood vessels as well as an endothelial response to inflammation. Inflammatory states are thought to increase BBB permeability through changes in tight junction regulation. Exposure to the proinflammatory cytokines interferon γ, interleukin 1b and tumour necrosis factor α has been shown to cause tight junction dysregulation in an *in vitro* model[306]. Furthermore, ZO3 expression has been shown to become disordered in response to inflammation associated with autoimmune encephalitis[307].

The second wave of BBB permeability, which occurs approximately 72 hours after infarction, is associated with angiogenesis. The oedema that characterises the initial peak in permeability is generally absent during the second peak. This time point is also characterised by an upregulation of members of the vascular endothelial growth factor family, which act both to stimulate angiogenesis and to increase BBB permeability[236]. An important early study by Zhang et.al. used a rodent stroke model to demonstrate that administration of VEGFa one hour post-infarct increased oedema and tissue damage, whereas administration at 48 hours post-infarct improved functional outcomes and was not associated with oedema[308]. This supports the hypothesis that the second wave of BBB permeability is not related to oedema or further tissue damage.

A recent MRI study in humans has challenged the current paradigm of biphasic BBB regulation in ischaemic stroke[309]. This study recruited 42 patients and used dynamic contrast-enhanced MRI to measure BBB permeability within the infarct and the contralateral homotopic region. It was found that BBB permeability was elevated at all time points up to 90 hours post-stroke. However, this was not a longitudinal study as each patient was imaged at a single time point and so continuous data were not available. Furthermore, baseline BBB permeability was obtained by imaging the contralateral hemisphere, which assumes that infarct doesn't affect BBB integrity in distant brain regions.

1.5.3: Implications for Cell-Based Therapy

The BBB represents a potential barrier to intravascular cell-based stroke therapy, as any treatment product introduced into the vascular compartment must cross the BBB to access its therapeutic target. This issue has been tackled extensively in the development of centrally-acting pharmaceuticals. Several previous studies have demonstrated that MSC transplanted intravascularly can enter the brain parenchyma from circulation, however the mechanism underlying that effect has not been well-characterised[209,232,233,310]. One aspect that will influence this is the increase in BBB permeability that occurs after stroke. This may be one of the underlying reasons that early post-stroke transplantation has resulted in superior outcomes in animal studies of cell-based therapy.

However, stem cells have been shown to migrate from circulation into the brain even when transplanted at much later time points when the BBB is no longer as permeable[235,311]. Therefore, it is likely that stem cells mediate entry to the brain parenchyma through their interactions with the cerebral endothelium.

In a study by Rosenblum et.al.[235], MSC were transplanted into mice via an intra-arterial injection at various time points from six hours to 14 days after a hypoxia-ischaemia model of stroke. The results demonstrated that while MSC crossed the BBB at all time points, maximum engraftment occurred following transplantation at day three. The authors hypothesised that this related to an increase in diapedesis through expression of vascular cell adhesion molecule-1 (VCAM-1). However, VCAM-1 was shown to also be strongly upregulated at all time points. Therefore, an alternative hypothesis is that transplantation three days post-stroke resulted in maximum engraftment due to coincident endogenous enhancement of BBB permeability.

While intravascular delivery of cell-based therapy for stroke has demonstrated efficacy in pre-clinical studies and stem cells have been shown to cross the BBB, the mechanisms underlying this have not been fully elucidated. Characterisation of this mechanism could inform the optimisation of cell-based therapy for ischaemic stroke.

1.6: Aims and Rationale

The chronic cognitive and sensory-motor disability caused by ischaemic stroke brings vast economic, social and personal costs. Current stroke management can only limit the damage caused by stroke. Due to the limited therapeutic window of recanalization, only a small proportion of patients are treated. There is a need for treatment options that are available to more patients and that can restore lost function after stroke, rather than only limiting damage. One promising treatment modality is cell-based therapy.

Stem cell transplantation following stroke results in improved performance in behaviour testing. This effect is thought to occur due to paracrine signalling rather than tissue replacement. Crucially, transplantation through both direct and intravascular routes has been shown to be efficacious. This is important because intracerebral transplantation is invasive and is more likely to result in adverse events than intravascular transplantation. Transplanted stem cells have been shown to migrate from circulation to the site of injury. The mechanism by which transplanted stem cells are able to migrate across the blood-brain barrier (BBB) is unclear. One hypothesis is that stem cells enhance BBB permeability through the paracrine secretion of VEGF-a. Understanding this mechanism will help to design and optimise cell-based therapy for stroke, as stem cell populations more capable of migrating to the site of injury could be selected.

While many pre-clinical studies have demonstrated the efficacy of stem cell transplantation in stroke, the mechanism of action has not yet been fully elucidated. One hypothesis is that transplanted stem cells interrupt endogenous systems responsible for the inhibition of neuroplasticity. Degradation of PNNs is a likely candidate as PNNs are responsible for inhibition of neuroplasticity in adult mammals. Furthermore, removal of PNNs results in a window of increased neuroplasticity. However, previous studies have demonstrated that PNNs are modified endogenously following stroke. This effect has not yet been fully characterised.

To test these hypotheses, the aims of this thesis are as follows:

1. To test the ability of DPSC to enhance blood-brain barrier permeability and to investigate the mechanism by which this occurs.

2. To investigate the ability of DPSC to alter the expression of PNNs and to identify the expression of enzymes that may be responsible for this effect.

3. To characterise spatial and temporal changes in the distribution of major PNN components following stroke.

4. To develop a standardised model of chronic stroke for the assessment of potential stroke therapies in pre-clinical studies.

1.7: References

1. **Dirnagl U, Iadecola C, Moskowitz M**. Pathobiology of ischaemic stroke: an integrated view. *Trends Neurosci*. 1999;22(9):391–7.

2. **Benjamin EJ, Blaha MJ, Chiuve SE, Cushman M, Das SR, Deo R, et al.** Heart Disease and Stroke Statistics' 2017 Update: A Report from the American Heart Association. Vol. 135, Circulation. 2017. 146-603 p.

3. **Sacco S, Marini C, Totaro R, Russo T, Cerone D, Carolei A**. A population-based study of the incidence and prognosis of lacunar stroke. *Neurology*. 2006;66(9):1335–8.

4. **Xian Y, Holloway RG, Pan W, Peterson ED**. Challenges in assessing hospital-level stroke mortality as a quality measure: comparison of ischemic, intracerebral hemorrhage, and total stroke mortality rates. *Stroke*. 2012;43(6):1687–90.

5. **Norrving B, Kissela B**. The global burden of stroke and need for a continuum of care. *Neurology*. 2013;80(Issue 3, Supplement 2):S5–12.

6. **Woodruff TM, Thundyil J, Tang S-C, Sobey CG, Taylor SM, Arumugam T V**. Pathophysiology, treatment, and animal and cellular models of human ischemic stroke. *Mol Neurodegener*. 2011;6(1):11.

7. **Mohr JP, Lazar RM, Marshall RS**. Middle Cerebral Artery Disease. Fifth Edit. Stroke. Elsevier; 2011. 384-4424 p.

8. **Adams HP, Bendixen BH, Kappelle LJ, Biller J, Love BB, Gordon DL, et al.** Classification of subtype of acute ischemic stroke. Definitions for use in a multicenter clinical trial. TOAST. Trial of Org 10172 in Acute Stroke Treatment. *Stroke*. 1993;24(1):35–41.

9. **Durukan A, Tatlisumak T**. Acute ischemic stroke: overview of major experimental rodent models, pathophysiology, and therapy of focal cerebral ischemia. *Pharmacol Biochem Behav*. 2007;87(1):179–97.

10. **Khatri R, McKinney A, Swenson B, Janardhan V**. Blood–brain barrier, reperfusion injury, and hemorrhagic transformation in acute ischemic stroke. *Neurology*. 2012;

11. **Girouard H, Wang G, Gallo EF, Anrather J, Zhou P, Pickel VM, et al.** NMDA receptor activation increases free radical production through nitric oxide and NOX2. *J Neurosci*. 2009;29(8):2545–52.

12. **Liang D, Bhatta S, Gerzanich V, Simard JM**. Cytotoxic edema: mechanisms of pathological cell swelling. *Neurosurg Focus*. 2007;22(5):E2.

13. **Furlan M, Marchal G, Viader F, Derlon JM, Baron JC**. Spontaneous neurological recovery after stroke and the fate of the ischemic penumbra. *Ann Neurol*. 1996;40(2):216–26.

14. **Astrup J, Siesjo BK, Symon L**. Thresholds in cerebral ischemia - the ischemic penumbra. *Stroke*. 1981;12(6):723–5.

15. **Liebeskind DS**. Collaterals in Acute Stroke: Beyond the Clot. *Neuroimaging Clin N Am*. 2005;15(3):553–73.

16. **Rocha M, Jovin TG**. Fast Versus Slow Progressors of Infarct Growth in Large Vessel Occlusion Stroke: Clinical and Research Implications. *Stroke*. 2017;48(9):2621–7.

17. **Blauenfeldt RA, Hougaard KD, Mouridsen K, Andersen G**. High Prestroke Physical Activity Is Associated with Reduced Infarct Growth in Acute Ischemic Stroke Patients Treated with Intravenous tPA and Randomized to Remote Ischemic Perconditioning. *Cerebrovasc Dis*. 2017;44(1–2):88–95.

18. **Saver JL**. Time Is Brain — Quantified The Growth Function of an Ischemic Stroke. 2006;263–7.

19. **Paciaroni M, Caso V, Agnelli G**. The concept of ischemic penumbra in acute stroke and therapeutic opportunities. *Eur Neurol*. 2009;61(6):321–30.

20. **Hennings LJ, Flores R, Roberson PK, Brown A, Lowery J, Borrelli M, et al.** Persistent penumbra in a rabbit stroke model: incidence and histologic characteristics. *Stroke Res Treat*. 2011;2011:764830.

21. **Molina CA, Montaner J, Abilleira S, Ibarra B, Romero F, Arenillas JF, et al.** Timing of Spontaneous Recanalization and Risk of Hemorrhagic Transformation in Acute Cardioembolic Stroke. *Stroke*. 2001;32(5):1079–84.

22. **Senes S**. How we manage stroke in Australia. *Aust Inst Heal Welf*. 2006;

23. **Campbell BC V, Mitchell PJ, Churilov L, Keshtkaran M, Hong K-S, Kleinig TJ, et al.** Endovascular Thrombectomy for Ischemic Stroke Increases Disability-Free Survival, Quality of Life, and Life Expectancy and Reduces Cost. *Front Neurol*. 2017;8(December):657.

24. **Donnan GA, Fisher M, Macleod M, Davis SM, Royal S, Macleod UKM**. Stroke. *Lancet*. 2008;371.

25. **O'Donnell MJ, Chin SL, Rangarajan S, Xavier D, Liu L, Zhang H, et al.** Global and regional effects of potentially modifiable risk factors associated with acute stroke in 32 countries (INTERSTROKE): a case-control study. *Lancet*. 2016;388(10046):761–75.

26. **Lansberg MG, Thijs VN, Bammer R, Kemp S, Wijman CAC, Marks MP, et al.** Risk factors of symptomatic intracerebral hemorrhage after tPA therapy for acute stroke. *Stroke*. 2007;38(8):2275–8.

27. **Lansberg MG, Bluhmki E, Thijs VN**. Efficacy and safety of tissue plasminogen activator 3 to 4.5 hours after acute ischemic stroke: a metaanalysis. *Stroke*. 2009;40(7):2438–41.

28. **Nogueira RG, Jadhav AP, Haussen DC, Bonafe A, Budzik RF, Bhuva P, et al.** Thrombectomy 6 to 24 Hours after Stroke with a Mismatch between Deficit and Infarct. *N Engl J Med*. 2017;NEJMoa1706442.

29. **Ayromlou H, Soleimanpour H, Farhoudi M, Taheraghdam A, Sadeghi Hokmabadi E, Rajaei Ghafouri R, et al.** Eligibility assessment for intravenous thrombolytic therapy in acute ischemic stroke patients; evaluating barriers for implementation. *Iran Red Crescent Med J*. 2014;16(5):e11284.

30. **Simon R, Shiraishi K**. N-Methyl-D-Aspartate antagonist reduces stroke size and regional glucose metabolism. *Ann Neurol*. 1990;27(6):606–11.

31. **Black MA, Tremblay R, Mealing GA, Durkin JP, Whitfield JF, Morley P**. The desglycinyl metabolite of remacemide hydrochloride is neuroprotective in cultured rat cortical neurons. *J Neurochem*. 1996;66(3):989–95.

32. **Perez-Trepichio AD, Xue M, Ng TC, Majors AW, Furlan AJ, Awad IA, et al.** Sensitivity of magnetic resonance diffusion-weighted imaging and regional relationship between the apparent diffusion coefficient and cerebral blood flow in rat focal cerebral ischemia. *Stroke*. 1995;26(4):667-74; discussion 674-5.

33. **Minematsu K, Fisher M, Li L, Davis MA, Knapp AG, Cotter RE, et al.** Effects of a novel NMDA antagonist on experimental stroke rapidly and quantitatively assessed by diffusion-weighted MRI. *Neurology*. 1993;43(2):397–403.

34. **George CP, Goldberg MP, Choi DW, Steinberg GK**. Dextromethorphan reduces neocortical ischemic neuronal damage in vivo. *Brain Res*. 1988;440(2):375–9.

35. **Scheller DK., De Ryck M, Kolb J, Szathmary S, van Reempts J, Clincke G, et al.** Lubeluzole blocks increases in extracellular glutamate and taurine in the peri-infarct zone in rats. *Eur J Pharmacol*. 1997;338(3):243–51.

36. **Izumi Y, Roussel S, Pinard E, Seylaz J**. Reduction of Infarct Volume by Magnesium after Middle Cerebral Artery Occlusion in Rats. *J Cereb Blood Flow Metab*. 1991;11(6):1025–30.

37. **Silverstein FS, Buchanan K, Hudson C, Johnston M V**. Flunarizine limits hypoxia-ischemia induced morphologic injury in immature rat brain. *Stroke*. 1986;17(3):477–82.

38. **Kuroda S, Tsuchidate R, Smith M-L, Maples KR, Siesjö BK**. Neuroprotective Effects of a Novel Nitrone, NXY-059, after Transient Focal Cerebral Ischemia in the Rat. *J Cereb Blood Flow Metab*. 1999;19(7):778–87.

39. **Shuaib A, Yang Y, Li Q**. Evaluating the Efficacy of Citicoline in Embolic Ischemic Stroke in Rats: Neuroprotective Effects When Used Alone or in Combination with Urokinase. *Exp Neurol*. 2000;161(2):733–9.

40. **Grupke S, Hall J, Dobbs M, Bix GJ, Fraser JF**. Understanding history, and not repeating it. Neuroprotection for acute ischemic stroke: From review to preview. *Clin Neurol Neurosurg*. 2015;129(2015):1–9.

41. **Sutherland BA, Minnerup J, Balami JS, Arba F, Buchan AM, Kleinschnitz C**. Neuroprotection for Ischaemic Stroke: Translation from the Bench to the Bedside. *Int J Stroke*. 2012;7(5):407–18.

42. **Stahnisch FW, Nitsch R**. Santiago Ramón y Cajal's concept of neuronal plasticity: The ambiguity lives on. *Trends Neurosci*. 2002;25(11):589–91.

43. **Hebb DO**. The Organisation of Behaviour. Mahwah: Lawrence Erlbaum Associates, Inc.; 1949.

44. **Sanger TD**. Optimal unsupervised learning in a single-layered linear feedforward network.

Neural Networks. 1989;2:459–73.

45. **Bienenstock EL, Cooper LN, Munro PW**. Theory for the development of neuron selectivity: orientation specificity and binocular interaction in visual cortex. *J Neurosci*. 1982;2(1):32–48.

46. **Huber L, Menzel R**. Structural basis of long-trm potentiation in single dendritic spines. *Nature*. 2004;429(June):761–6.

47. **Lüscher C, Malenka RC**. NMDA receptor-dependent long-term potentiation and long-term depression (LTP/LTD). *Cold Spring Harb Perspect Biol*. 2012;1–15.

48. **Eriksson PS, Perfilieva E, Björk-Eriksson T, Alborn AM, Nordborg C, Peterson DA, et al.** Neurogenesis in the adult human hippocampus. *Nat Med*. 1998;4(11):1313–7.

49. **Hurford J**. The evolution of the critical period for language acquisition. Cognition. 1991.

50. **Vaegan, Taylor D**. Critical period for deprivation amblyopia in children. *Trans Ophthalmol Soc U K*. 1979;99(3):432–9.

51. **Hubel DH, Wiesel TN**. The period of susceptibility to the physiological effects of unilateral eye closure in kittens. *J Physiol*. 1970;206(2):419–36.

52. **Richardson FM, Price CJ**. Structural MRI studies of language function in the undamaged brain. *Brain Struct Funct*. 2009;213(6):511–23.

53. **Busch V, Schuierer G, Bogdahn U, May A**. Changes in grey matter induced by training Newly honed juggling skills show up as a transient feature on a brain-imaging scan . *Nature*. 2004;427:311–2.

54. **Hänggi J, Koeneke S, Bezzola L, Jäncke L**. Structural neuroplasticity in the sensorimotor network of professional female ballet dancers. *Hum Brain Mapp*. 2010;31(8):1196–206.

55. **Schmidt-Wilcke T, Rosengarth K, Luerding R, Bogdahn U, Greenlee MW**. Distinct patterns of functional and structural neuroplasticity associated with learning Morse code. *Neuroimage*. 2010;51(3):1234–41.

56. **Reid LB, Sale M V., Cunnington R, Mattingley JB, Rose SE**. Brain changes following four weeks of unimanual motor training: Evidence from fMRI-guided diffusion MRI tractography. *Hum Brain Mapp*. 2017;38(9):4302–12.

57. **Sale M V., Reid LB, Cocchi L, Pagnozzi AM, Rose SE, Mattingley JB**. Brain changes following four weeks of unimanual motor training: Evidence from behavior, neural stimulation, cortical thickness, and functional MRI. *Hum Brain Mapp*. 2017;38(9):4773–87.

58. **Magariños AM, McEwen BS, Flügge G, Fuchs E**. Chronic psychosocial stress causes apical dendritic atrophy of hippocampal CA3 pyramidal neurons in subordinate tree shrews. *J Neurosci*. 1996;16(10):3534–40.

59. **Kole MHP, Costoli T, Koolhaas JM, Fuchs E**. Bidirectional shift in the cornu ammonis 3 pyramidal dendritic organization following brief stress. *Neuroscience*. 2004;125(2):337–47.

60. **van Praag H, Christie BR, Sejnowski TJ, Gage FH**. Running enhances neurogenesis, learning, and long-term potentiation in mice. *Proc Natl Acad Sci*. 1999;96(23):13427–31.

61. **Perini R, Bortoletto M, Capogrosso M, Fertonani A, Miniussi C**. Acute effects of aerobic exercise promote learning. *Sci Rep*. 2016;6(May):1–8.

62. **Kitago T, Krakauer JW**. Motor learning principles for neurorehabilitation. 1st ed. Vol. 110, Handbook of Clinical Neurology. Elsevier B.V.; 2013. 93-103 p.

63. **Green JB**. Brain Reorganization After Stroke. *Top Stroke Rehabil*. 2003;10(3):1–20.

64. **Dimyan M a, Cohen LG**. Neuroplasticity in the context of motor rehabilitation after stroke. *Nat Rev Neurol*. 2011;7(2):76–85.

65. **Bonita R, Beaglehole R**. Recovery of motor function after stroke. *Stroke*. 1988;19(12):1497–500.

66. **Wolf SL, Thompson PA, Winstein CJ, Miller JP, Blanton SR, Nichols-Larsen DS, et al.** The EXCITE Stroke Trial: Comparing Early and Delayed Constraint-Induced Movement Therapy. *Stroke*. 2010;41(10):2309–15.

67. **Avert T, Collaboration T**. Efficacy and safety of very early mobilisation within 24 h of stroke onset (AVERT): a randomised controlled trial. *Lancet*. 2015;386(9988):46–55.

68. **Hsu JE, Jones TA**. Time-sensitive enhancement of motor learning with the less-affected forelimb after unilateral sensorimotor cortex lesions in rats. *Eur J Neurosci*. 2005;22(8):2069–80.

69. **Schwerin S, Dewald JPA, Haztl M, Jovanovich S, Nickeas M, MacKinnon C**. Ipsilateral versus contralateral cortical motor projections to a shoulder adductor in chronic hemiparetic stroke: Implications for the expression of arm synergies. *Exp Brain Res*. 2008;185(3):509–19.

70. **Madhavan S, Rogers LM, Stinear JW**. A paradox: After stroke, the non-lesioned lower limb motor cortex may be maladaptive. *Eur J Neurosci*. 2010;32(6):1032–9.

71. **Ward NS, Newton JM, Swayne OBC, Lee L, Thompson AJ, Greenwood RJ, et al.** Motor system activation after subcortical stroke depends on corticospinal system integrity. *Brain*. 2006;129(3):809–19.

72. **Sawada M, Sawamoto K**. Mechanisms of neurogenesis in the normal and injured adult brain. *Keio J Med*. 2013;62(1):13–28.

73. **Jones TA, Schallert T**. Overgrowth and pruning of dendrites in adult rats recovering from neocortical damage. *Brain Res*. 1992;581(1):156–60.

74. **Jones TA, Kleim JA, Greenough WT**. Synaptogenesis and dendritic growth in the cortex opposite unilateral sensorimotor cortex damage in adult rats: A quantitative electron microscopic examination. *Brain Res*. 1996;733(1):142–8.

75. **Stroemer RP, Kent TA, Hulsebosch CE**. Neocortical neural sprouting, synaptogenesis, and behavioral recovery after neocortical infarction in rats. *Stroke*. 1995;26(11):2135–44.

76. **Comelli MC, Guidolin D, Seren MS, Zanoni R, Canella R, Rubini R, et al.** Time course, localization and pharmacological modulation of immediate early inducible genes, brain-derived neurotrophic factor and trkB messenger RNAs in the rat brain following photochemical stroke. *Neuroscience*. 1993;55(2):473–90.

77. **Kawamata T, Speliotes EK, Finklestein SP**. The role of polypeptide growth factors in recovery from stroke. *Adv Neurol*. 1997;73:377–82.

78. **Lin TN, Te J, Lee M, Sun GY, Hsu CY**. Induction of basic fibroblast growth factor (bFGF) expression following focal cerebral ischemia. *Brain Res Mol Brain Res*. 1997;49(1–2):255–65.

79. **Rowntree S, Kolb B**. Blockade of basic fibroblast growth factor retards recovery from motor cortex injury in rats. *Eur J Neurosci*. 1997;9(11):2432–41.

80. **Li Y, Jiang N, Powers C, Chopp M**. Neuronal damage and plasticity identified by microtubule-

associated protein 2, growth-associated protein 43, and cyclin D1 immunoreactivity after focal cerebral ischemia in rats. *Stroke*. 1998;29(9):1972-80; discussion 1980-1.

81. **Cooper AN, Anderson V, Hearps S, Greenham M, Ditchfield M, Coleman L, et al.** Trajectories of Motor Recovery in the First Year After Pediatric Arterial Ischemic Stroke. *Pediatrics*. 2017;140(2):e20163870.

82. **Celio MR, Spreafico R, De Biasi S, Vitellaro-Zuccarello L**. Perineuronal nets: past and present. *Trends Neurosci*. 1998;21(12):510–5.

83. **Vitellaro-Zuccarello L, Biasi S, Spreafico R**. One hundred years of Golgi's "perineuronal net": history of a denied structure. *Ital J Neurol Sci*. 1998;19(4):249–53.

84. **Zaremba S, Guimaraes A, Kalb RG, Hockfield S**. Characterization of an activity-dependent, neuronal surface proteoglycan identified with monoclonal antibody Cat-301. *Neuron*. 1989;2(3):1207–19.

85. **Mabuchi M, Murakami S, Taguchi T, Ohtsuka A, Murakami T**. Purkinje cells in the adult cat cerebellar cortex possess a perineuronal net of proteoglycans. *Arch Histol Cytol*. 2001;64(2):203–9.

86. **Seeger G, Brauer K, Härtig W, Brückner G**. Mapping of perineuronal nets in the rat brain stained by colloidal iron hydroxide histochemistry and lectin cytochemistry. *Neuroscience*. 1994;58(2):371–88.

87. **Alpár A, Gärtner U, Härtig W, Brückner G**. Distribution of pyramidal cells associated with perineuronal nets in the neocortex of rat. *Brain Res*. 2006;1120(1):13–22.

88. **Brückner G, Hausen D, Härtig W, Drlicek M, Arendt T, Brauer K, et al.** Cortical areas abundant in extracellular matrix chondroitin sulphate proteoglycans are less affected by cytoskeletal changes in Alzheimer's disease. *Neuroscience*. 1999;92(3):791–805.

89. **Deepa SS, Carulli D, Galtrey C, Rhodes K, Fukuda J, Mikami T, et al.** Composition of perineuronal net extracellular matrix in rat brain: a different disaccharide composition for the net-associated proteoglycans. *J Biol Chem*. 2006;281(26):17789–800.

90. **Siebert JR, Conta Steencken A, Osterhout DJ**. Chondroitin Sulfate Proteoglycans in the Nervous System: Inhibitors to Repair. *Biomed Res Int*. 2014;2014.

91. **Ojima H, Sakai M, Ohyama J**. Molecular heterogeneity of Vicia villosa-recognized perineuronal nets surrounding pyramidal and nonpyramidal neurons in the guinea pig cerebral cortex. *Brain Res*. 1998;786(1–2):274–80.

92. **Yamaguchi Y**. Lecticans: organizers of the brain extracellular matrix. *Cell Mol Life Sci*. 2000;57(2):276–89.

93. **Rhodes KE, Fawcett JW**. Chondroitin sulphate proteoglycans: preventing plasticity or protecting the CNS? *J Anat*. 2004;204(1):33–48.

94. **Wang H, Katagiri Y, McCann TE, Unsworth E, Goldsmith P, Yu Z-X, et al.** Chondroitin-4-sulfation negatively regulates axonal guidance and growth. *J Cell Sci*. 2008;121(18):3083–91.

95. **Miyata S, Komatsu Y, Yoshimura Y, Taya C, Kitagawa H**. Persistent cortical plasticity by upregulation of chondroitin 6-sulfation. *Nat Neurosci*. 2012;15(3):414–22.

96. **Lin R, Rosahl TW, Whiting PJ, Fawcett JW, Kwok JCF**. 6-Sulphated Chondroitins Have a Positive Influence on Axonal Regeneration. Finkelstein DI, editor. *PLoS One*. 2011;6(7):e21499.

97. **Sur M, Frost DO, Hockfield S**. Expression of a surface-associated antigen on Y-cells in the cat lateral geniculate nucleus is regulated by visual experience. *J Neurosci*. 1988;8(3):874–82.

98. **Carulli D, Rhodes KE, Fawcett JW**. Upregulation of Aggrecan , Link Protein 1 , and Hyaluronan Synthases during Formation of Perineuronal Nets in the Rat Cerebellum. 2007;94(August 2006):83–94.

99. **Ueno H, Suemitsu S, Okamoto M, Matsumoto Y, Ishihara T**. Sensory experience-dependent formation of perineuronal nets and expression of Cat-315 immunoreactive components in the mouse somatosensory cortex. *Neuroscience*. 2017;355:161–74.

100. **Balmer TS, Carels VM, Frisch JL, Nick TA**. Modulation of Perineuronal Nets and Parvalbumin with Developmental Song Learning. *J Neurosci*. 2010;29(41):12878–85.

101. **Cornez G, Madison FN, Van der Linden A, Cornil C, Yoder KM, Ball GF, et al.** Perineuronal nets and vocal plasticity in songbirds: A proposed mechanism to explain the difference between closed-ended and open-ended learning. *Dev Neurobiol*. 2017;77(8):975–94.

102. **Kitagawa H, Tsutsumi K, Tone Y, Sugahara K**. Developmental regulation of the sulfation

profile of chondroitin sulfate chains in the chicken embryo brain. *J Biol Chem*. 1997;272(50):31377–81.

103. **McRae PA, Rocco MM, Kelly G, Brumberg JC, Matthews RT**. Sensory deprivation alters aggrecan and perineuronal net expression in the mouse barrel cortex. *J Neurosci*. 2007;27(20):5405–13.

104. **Wang D, Fawcett J**. The perineuronal net and the control of CNS plasticity. *Cell Tissue Res*. 2012;349(1):147–60.

105. **Sorg BA, Berretta S, Blacktop JM, Fawcett JW, Kitagawa H, Kwok JCF, et al.** Casting a Wide Net: Role of Perineuronal Nets in Neural Plasticity. *J Neurosci*. 2016;36(45):11459–68.

106. **Shen Y, Tenney AP, Busch SA, Horn KP, Cuascut FX, Liu K, et al.** PTPsigma is a receptor for chondroitin sulfate proteoglycan, an inhibitor of neural regeneration. *Science*. 2009;326(5952):592–6.

107. **Fisher D, Xing B, Dill J, Li H, Hoang HH, Zhao Z, et al.** LAR is a functional receptor for CSPG axon growth inhibitors. 2011;82(1):145–63.

108. **Dickendesher TL, Baldwin KT, Mironova YA, Koriyama Y, Raiker SJ, Askew KL, et al.** NgR1 and NgR3 are receptors for chondroitin sulfate proteoglycans. *Nat Neurosci*. 2012;15(5):703–12.

109. **Deepa SS, Umehara Y, Higashiyama S, Itoh N, Sugahara K**. Specific molecular interactions of oversulfated chondroitin sulfate E with various heparin-binding growth factors. Implications as a physiological binding partner in the brain and other tissues. *J Biol Chem*. 2002;277(46):43707–16.

110. **Vo T, Carulli D, Ehlert EME, Kwok JCF, Dick G, Mecollari V, et al.** The chemorepulsive axon guidance protein semaphorin3A is a constituent of perineuronal nets in the adult rodent brain. *Mol Cell Neurosci*. 2013;56:186–200.

111. **De Winter F, Kwok JCF, Fawcett JW, Vo TT, Carulli D, Verhaagen J**. The Chemorepulsive Protein Semaphorin 3A and Perineuronal Net-Mediated Plasticity. *Neural Plast*. 2016;2016.

112. **Kantor DB, Chivatakarn O, Peer KL, Oster SF, Inatani M, Hansen MJ, et al.** Semaphorin 5A Is a Bifunctional Axon Guidance Cue Regulated by Heparan and Chondroitin Sulfate Proteoglycans. 2004;44:961–75.

113. **McKeon RJ, Höke A, Silver J**. Injury-induced proteoglycans inhibit the potential for laminin-mediated axon growth on astrocytic scars. *Exp Neurol*. 1995;136(1):32–43.

114. **Frischknecht R, Heine M, Perrais D, Seidenbecher CI, Choquet D, Gundelfinger ED**. Brain extracellular matrix affects AMPA receptor lateral mobility and short-term synaptic plasticity. *Nat Publ Gr*. 2009;12(7):897–904.

115. **Pizzorusso T, Medini P, Berardi N, Chierzi S, Fawcett JW, Maffei L**. Reactivation of Ocular Dominance Plasticity in the Adult Visual Cortex. *Science (80-)*. 2002;298(5596):1248–51.

116. **Pizzorusso T, Medini P, Landi S, Baldini S, Berardi N, Maffei L**. Structural and functional recovery from early monocular deprivation in adult rats. *Proc Natl Acad Sci U S A*. 2006;103(22):8517–22.

117. **Novotna I, Slovinska L, Vanicky I, Cizek M, Radonak J, Cizkova D**. IT Delivery of ChABC Modulates NG2 and Promotes GAP-43 Axonal Regrowth After Spinal Cord Injury. *Cell Mol Neurobiol*. 2011;31(8):1129–39.

118. **García-Alías G, Barkhuysen S, Buckle M, Fawcett JW**. Chondroitinase ABC treatment opens a window of opportunity for task-specific rehabilitation. *Nat Neurosci*. 2009;12(9):1145–51.

119. **Barritt AW, Davies M, Marchand F, Hartley R, Grist J, Yip P, et al.** Chondroitinase ABC Promotes Sprouting of Intact and Injured Spinal Systems after Spinal Cord Injury. *J Neurosci*. 2006;26(42):10856–67.

120. **Lee H, McKeon RJ, Bellamkonda R V**. Sustained delivery of thermostabilized chABC enhances axonal sprouting and functional recovery after spinal cord injury. *Proc Natl Acad Sci U S A*. 2010;107(8):3340–5.

121. **Bradbury EJ, Moon LDF, Popat RJ, King VR, Bennett GS, Patel PN, et al.** Chondroitinase ABC promotes functional recovery after spinal cord injury. *Nature*. 2002;416(6881):636–40.

122. **Kwok JCF, Carulli D, Fawcett JW**. In vitro modeling of perineuronal nets: hyaluronan synthase and link protein are necessary for their formation and integrity. *J Neurochem*. 2010;114(5):1447–59.

123. **Carulli D, Pizzorusso T, Kwok JCF, Putignano E, Poli A, Forostyak S, et al.** Animals lacking link protein have attenuated perineuronal nets and persistent plasticity. *Brain*. 2010;133(Pt 8):2331–47.

124. **Faralli A, Dagna F, Albera A, Bekku Y, Oohashi T, Albera R, et al.** Modifications of perineuronal nets and remodelling of excitatory and inhibitory afferents during vestibular compensation in the adult mouse. *Brain Struct Funct*. 2016;221(6):3193–209.

125. **Fry EJ, Chagnon MJ, López-Vales R, Tremblay ML, David S**. Corticospinal tract regeneration after spinal cord injury in receptor protein tyrosine phosphatase sigma deficient mice. *Glia*. 2010;58(4):423–33.

126. **Soleman S, Yip PK, Duricki D a, Moon LDF**. Delayed treatment with chondroitinase ABC promotes sensorimotor recovery and plasticity after stroke in aged rats. *Brain*. 2012;135(Pt 4):1210–23.

127. **Wiersma AM, Fouad K, Winship IR**. Enhancing spinal plasticity amplifies the benefits of rehabilitative training and improves recovery from stroke. *J Neurosci*. 2017;37(45):0770-17.

128. **Gherardini L, Gennaro M, Pizzorusso T**. Perilesional treatment with chondroitinase ABC and motor training promote functional recovery after stroke in rats. *Cereb Cortex*. 2015;25(1):202–12.

129. **Chen XR, Liao SJ, Ye LX, Gong Q, Ding Q, Zeng JS, et al.** Neuroprotective effect of chondroitinase ABC on primary and secondary brain injury after stroke in hypertensive rats. *Brain Res*. 2014;1543:324–33.

130. **Li H, Dokas LA, Godfrey DA, Rubin AM**. Remodeling of synaptic connections in the deafferented vestibular nuclear complex. *J Vestib Res*. 2003;12(4):167–83.

131. **Dutheil S, Brezun JM, Leonard J, Lacour M, Tighilet B**. Neurogenesis and astrogenesis contribution to recovery of vestibular functions in the adult cat following unilateral vestibular neurectomy: cellular and behavioral evidence. *Neuroscience*. 2009;164(4):1444–56.

132. **Ploughman M, Austin MW, Glynn L, Corbett D**. The Effects of Poststroke Aerobic Exercise on Neuroplasticity: A Systematic Review of Animal and Clinical Studies. *Transl Stroke Res*. 2014;6(1):13–28.

133. **Smith CC, Mauricio R, Nobre L, Marsh B, Wüst RCI, Rossiter HB, et al.** Differential regulation of perineuronal nets in the brain and spinal cord with exercise training. *Brain Res Bull*. 2015;111:20–6.

134. **Sale A, Maya Vetencourt JF, Medini P, Cenni MC, Baroncelli L, De Pasquale R, et al.**

Environmental enrichment in adulthood promotes amblyopia recovery through a reduction of intracortical inhibition. *Nat Neurosci*. 2007;10(6):679–81.

135. **Karetko-Sysa M, Skangiel-Kramska J, Nowicka D**. Disturbance of perineuronal nets in the perilesional area after photothrombosis is not associated with neuronal death. *Exp Neurol*. 2011;231(1):113–26.

136. **Härtig W, Appel S, Suttkus A, Grosche J, Michalski D**. Abolished perineuronal nets and altered parvalbumin-immunoreactivity in the nucleus reticularis thalami of wildtype and 3xTg mice after experimental stroke. *Neuroscience*. 2016;337:66–87.

137. **Härtig W, Mages B, Aleithe S, Nitzsche B, Altmann S, Barthel H, et al.** Damaged Neocortical Perineuronal Nets Due to Experimental Focal Cerebral Ischemia in Mice, Rats and Sheep. *Front Integr Neurosci*. 2017;11(August):1–16.

138. **Hobohm C, Günther A, Grosche J, Rossner S, Schneider D, Brückner G**. Decomposition and long-lasting downregulation of extracellular matrix in perineuronal nets induced by focal cerebral ischemia in rats. *J Neurosci Res*. 2005;80(4):539–48.

139. **Bidmon HJ, Jancsik V, Schleicher A, Hagemann G, Witte OW, Woodhams P, et al.** Structural alterations and changes in cytoskeletal proteins and proteoglycans after focal cortical ischemia. *Neuroscience*. 1997;82(2):397–420.

140. **Quattromani MJ, Pruvost M, Guerreiro C, Backlund F, Englund E, Aspberg A, et al.** Extracellular Matrix Modulation Is Driven by Experience-Dependent Plasticity During Stroke Recovery. *Mol Neurobiol*. 2017;1–18.

141. **Al'Qteishat A, Gaffney J, Krupinski J, Rubio F, West D, Kumar S, et al.** Changes in hyaluronan production and metabolism following ischaemic stroke in man. *Brain*. 2006;129(8):2158–76.

142. **Madinier A, Quattromani MJ, Sjölund C, Ruscher K, Wieloch T**. Enriched housing enhances recovery of limb placement ability and reduces aggrecan-containing perineuronal nets in the rat somatosensory cortex after experimental stroke. *PLoS One*. 2014;9(3).

143. **Li S, Strittmatter SM**. Delayed systemic Nogo-66 receptor antagonist promotes recovery from spinal cord injury. *JNeurosci*. 2003;23(1529–2401 (Electronic)):4219–27.

144. **Liebscher T, Schnell L, Schnell D, Scholl J, Schneider R, Gullo M, et al.** Nogo-A antibody improves regeneration and locomotion of spinal cord-injured rats. *Ann Neurol*.

2005;58(5):706–19.

145. **Merkler D, Metz GA, Raineteau O, Dietz V, Schwab ME, Fouad K**. Locomotor recovery in spinal cord-injured rats treated with an antibody neutralizing the myelin-associated neurite growth inhibitor Nogo-A. *J Neurosci*. 2001;21(10):3665–73.

146. **Gou X, Zhang Q, Xu N, Deng B, Wang H, Xu L, et al.** Spatio-temporal expression of paired immunoglobulin-like receptor-B in the adult mouse brain after focal cerebral ischaemia. *Brain Inj*. 2013;27(11):1311–5.

147. **Huber AB, Weinmann O, Bro C, Oertle T, Schwab ME, Brösamle C, et al.** Patterns of Nogo mRNA and protein expression in the developing and adult rat and after CNS lesions. *J Neurosci*. 2002;22(9):3553–67.

148. **Shepherd DJ, Tsai SY, O'Brien TE, Farrer RG, Kartje GL**. Anti-Nogo-A immunotherapy does not alter hippocampal neurogenesis after stroke in adult rats. *Front Neurosci*. 2016;10(OCT):1–13.

149. **Dodd DA, Niederoest B, Bloechlinger S, Dupuis L, Loeffler JP, Schwab ME**. Nogo-A, -B, and -C are found on the cell surface and interact together in many different cell types. *J Biol Chem*. 2005;280(13):12494–502.

150. **GrandPré T, Nakamura F, Vartanlan T, Strittmatter SM**. Identification of the Nogo inhibitor of axon regeneration as a Reticulon protein. *Nature*. 2000;403(6768):439–44.

151. **Voeltz GK, Prinz WA, Shibata Y, Rist JM, Rapoport TA**. A Class of Membrane Proteins Shaping the Tubular Endoplasmic Reticulum. 2006;573–86.

152. **Wang S, Tukachinsky H, Romano FB, Rapoport TA**. Cooperation of the ER-shaping proteins atlastin, lunapark, and reticulons to generate a tubular membrane network. *Elife*. 2016;5.

153. **Kempf A, Tews B, Arzt ME, Weinmann O, Obermair FJ, Pernet V, et al.** The Sphingolipid Receptor S1PR2 Is a Receptor for Nogo-A Repressing Synaptic Plasticity. Schiavo G, editor. *PLoS Biol*. 2014;12(1):e1001763.

154. **Pignot V, Hein AE, Barske C, Wiessner C, Walmsley AR, Kaupmann K, et al.** Characterization of two novel proteins, NgRH1 and NgRH2, structurally and biochemically homologous to the Nogo-66 receptor. *J Neurochem*. 2003;85(3):717–28.

155. **Joset A, Dodd DA, Halegoua S, Schwab ME**. Pincher-generated Nogo-A endosomes mediate growth cone collapse and retrograde signaling. *J Cell Biol*. 2010;188(2):271–85.

156. **Peng X, Kim J, Zhou Z, Fink DJ, Mata M**. Neuronal Nogo-A regulates glutamate receptor subunit expression in hippocampal neurons. *J Neurochem*. 2011;119(6):1183–93.

157. **Schwab ME, Strittmatter SM**. Nogo limits neural plasticity and recovery from injury. *Curr Opin Neurobiol*. 2014;27:53–60.

158. **Rubin BP, Dusart I, Schwab ME**. A monoclonal antibody (IN-1) which neutralizes neurite growth inhibitory proteins in the rat CNS recognizes antigens localized in CNS myelin. *J Neurocytol*. 1994;23(4):209–17.

159. **Chen MS, Huber AB, van der Haar ME, Frank M, Schnell L, Spillmann AA, et al.** Nogo-A is a myelin-associated neurite outgrowth inhibitor and an antigen for monoclonal antibody IN-1. *Nature*. 2000;403(6768):434–9.

160. **Wiessner C, Bareyre FM, Allegrini PR, Mir AK, Frentzel S, Zurini M, et al.** Anti – Nogo-A Antibody Infusion 24 Hours After Experimental Stroke Improved Behavioral Outcome and Corticospinal Plasticity in Normotensive and Spontaneously Hypertensive Rats. 2003;154–65.

161. **Li W, Walus L, Rabacchi SA, Jirik A, Chang E, Schauer J, et al.** A neutralizing anti-Nogo66 receptor monoclonal antibody reverses inhibition of neurite outgrowth by central nervous system myelin. *J Biol Chem*. 2004;279(42):43780–8.

162. **Lee J-K, Kim J-E, Sivula M, Strittmatter SM**. Nogo receptor antagonism promotes stroke recovery by enhancing axonal plasticity. *J Neurosci*. 2004;24(27):6209–17.

163. **Papadopoulos CM, Tsai SY, Alsbiei T, O'Brien TE, Schwab ME, Kartje GL**. Functional recovery and neuroanatomical plasticity following middle cerebral artery occlusion and IN-1 antibody treatment in the adult rat. *Ann Neurol*. 2002;51(4):433–41.

164. **Shih-Yen T, Papadopoulos CM, Schwab ME, Kartje GL**. Delayed Anti-Nogo-A Therapy Improves Function After Chronic Stroke. 2010;119(Pt 24):5124–36.

165. **Wahl AS, Omlor W, Rubio JC, Chen JL, Zheng H, Schroter A, et al.** Asynchronous therapy restores motor control by rewiring of the rat corticospinal tract after stroke. *Science (80-)*. 2014;344(6189):1250–5.

166. **Gillani RL, Tsai SY, Wallace DG, O'Brien TE, Arhebamen E, Tole M, et al.** Cognitive recovery in the aged rat after stroke and anti-Nogo-A immunotherapy. *Behav Brain Res*. 2010;208(2):415–24.

167. **Brenneman MM, Wagner SJ, Cheatwood JL, Heldt SA, Corwin J V., Reep RL, et al.** Nogo-A inhibition induces recovery from neglect in rats. *Behav Brain Res*. 2008;187(2):262–72.

168. **Kartje GL, Schulz MK, Lopez-Yunez A, Schnell L, Schwab ME**. Corticostriatal plasticity is restricted by myelin-associated neurite growth inhibitors in the adult rat. *Ann Neurol*. 1999;45(6):778–86.

169. **Papadopoulos CM, Tsai SY, Cheatwood JL, Bollnow MR, Kolb BE, Schwab ME, et al.** Dendritic plasticity in the adult rat following middle cerebral artery occlusion and Nogo-A neutralization. *Cereb Cortex*. 2006;16(4):529–36.

170. **Wenk CA, Thallmair M, Kartje GL, Schwab ME**. Increased corticofugal plasticity after unilateral cortical lesions combined with neutralization of the IN-1 antigen in adult rats. *J Comp Neurol*. 1999;410(1):143–57.

171. **Rolando C, Parolisi R, Boda E, Schwab ME, Rossi F, Buffo A**. Distinct roles of Nogo-a and Nogo receptor 1 in the homeostatic regulation of adult neural stem cell function and neuroblast migration. *J Neurosci*. 2012;32(49):17788–99.

172. **Shepherd DJ, Tsai S-Y, Cappucci SP, Wu JY, Farrer RG, Kartje GL**. The Subventricular Zone Response to Stroke Is Not a Therapeutic Target of Anti-Nogo-A Immunotherapy. *J Neuropathol Exp Neurol*. 2017;76(8):683–96.

173. **Chen K, Marsh BC, Cowan M, Al'Joboori YD, Gigout S, Smith CC, et al.** Sequential therapy of anti-Nogo-A antibody treatment and treadmill training leads to cumulative improvements after spinal cord injury in rats. *Exp Neurol*. 2017;292:135–44.

174. **Meininger V, Pradat PF, Corse A, Al-Sarraj S, Brooks BR, Caress JB, et al.** Safety, pharmacokinetic, and functional effects of the Nogo-A monoclonal antibody in amyotrophic lateral sclerosis: A randomized, first-in-human clinical trial. *PLoS One*. 2014;9(5).

175. **Meininger V, Genge A, van den Berg LH, Robberecht W, Ludolph A, Chio A, et al.** Safety and efficacy of ozanezumab in patients with amyotrophic lateral sclerosis: a randomised, double-blind, placebo-controlled, phase 2 trial. *Lancet Neurol*. 2017;16(3):208–16.

176. **Weissman IL, Anderson DJ, Gage F**. Stem and progenitor cells: origins, phenotypes, lineage commitments, and transdifferentiations. *Annu Rev Cell Dev Biol*. 2001;17:387–403.

177. **Uccelli A, Moretta L, Pistoia V**. Mesenchymal stem cells in health and disease. *Nat Rev Immunol*. 2008;8(9):726–36.

178. **Orkin SH, Zon LI**. Hematopoiesis and stem cells: plasticity versus developmental heterogeneity. *Nat Immunol*. 2002;3(4):323–8.

179. **Nogueira AB, Sogayar MC, Colquhoun A, Siqueira SA, Nogueira AB, Marchiori PE, et al.** Existence of a potential neurogenic system in the adult human brain. *J Transl Med*. 2014;12(1):1–33.

180. **Okita K, Ichisaka T, Yamanaka S**. Generation of germline-competent induced pluripotent stem cells. *Nature*. 2007;448(7151):313–7.

181. **Thomas ED, Lochte HL, Lu WC, Ferrebee JW**. Intravenous Infusion of Bone Marrow in Patients Receiving Radiation and Chemotherapy — NEJM. 1957.

182. **Thomas ED, Lochte HL, Cannon JH, Sahler OD, Ferrebee JW**. SUPRALETHAL WHOLE BODY IRRADIATION AND ISOLOGOUS MARROW TRANSPLANTATION IN MAN*†. *J Clin Invest*. 1959;38(10 Pt 1-2):1709–16.

183. **Lees JS, Sena ES, Egan KJ, Antonic A, Koblar SA, Howells DW, et al.** Stem cell-based therapy for experimental stroke: A systematic review and meta-analysis. *Int J Stroke*. 2012;7(7):582–8.

184. **Dharmasaroja P**. Bone marrow-derived mesenchymal stem cells for the treatment of ischemic stroke. *J Clin Neurosci*. 2009;16(1):12–20.

185. **Yamaguchi S, Horie N, Satoh K, Ishikawa T, Mori T, Maeda H, et al.** Age of donor of human mesenchymal stem cells affects structural and functional recovery after cell therapy following ischaemic stroke. *J Cereb Blood Flow Metab*. 2017;

186. **Kasahara Y, Yamahara K, Soma T, Stern DM, Nakagomi T, Matsuyama T, et al.** Transplantation of hematopoietic stem cells: intra-arterial versus intravenous administration impacts stroke outcomes in a murine model. *Transl Res*. 2016;176:69–80.

187. **Oki K, Tatarishvili J, Wood J, Koch P, Wattananit S, Mine Y, et al.** Human-induced pluripotent

stem cells form functional neurons and improve recovery after grafting in stroke-damaged brain. *Stem Cells*. 2012;30(6):1120–33.

188. **Tatarishvili J, Oki K, Monni E, Koch P, Memanishvili T, Buga AM, et al.** Human induced pluripotent stem cells improve recovery in stroke-injured aged rats. *Restor Neurol Neurosci*. 2014;32(4):547–58.

189. **Leong WK, Henshall TL, Arthur A, Kremer KL, Lewis MD, Helps SC, et al.** Human Adult Dental Pulp Stem Cells Enhance Poststroke Functional Recovery Through Non-Neural Replacement Mechanisms. *Stem Cells Transl Med*. 2012;1:177–87.

190. **Dunnett SB, Isacson O, Sirinathsinghji DJS, Clarke DJ, Björklund A**. Striatal grafts in rats with unilateral neostriatal lesions-III. Recovery from dopamine-dependent motor asymmetry and deficits in skilled paw reaching. *Neuroscience*. 1988;24(3):813–20.

191. **Perlow MJ, Freed WJ, Hoffer BJ, Seiger A, Olson L, Wyatt RJ**. Brain grafts reduce motor abnormalities produced by destruction of nigrostriatal dopamine system. *Science*. 1979;204(4393):643–7.

192. **Lindvall O, Brundin P, Widner H, Rehncrona S, Gustavii B, Frackowiak R, et al.** Grafts of fetal dopamine neurons survive and improve motor function in Parkinson's disease. *Science*. 1990;247(4942):574–7.

193. **Freed CR, Greene PE, Breeze RE, Tsai W-Y, DuMouchel W, Kao R, et al.** Transplantation of Embryonic Dopamine Neurons for Severe Parkinson's Disease. *N Engl J Med*. 2001;344(10):710–9.

194. **Olanow CW, Goetz CG, Kordower JH, Stoessl AJ, Sossi V, Brin MF, et al.** A double-blind controlled trial of bilateral fetal nigral transplantation in Parkinson's disease. *Ann Neurol*. 2003;54(3):403–14.

195. **Varlakhanova N V., Cotterman RF, DeVries WN, Morgan J, Donahue LR, Murray S, et al.** myc maintains embryonic stem cell pluripotency and self-renewal. *Differentiation*. 2010;80(1):9–19.

196. **Amariglio N, Hirshberg A, Scheithauer BW, Cohen Y, Loewenthal R, Trakhtenbrot L, et al.** Donor-Derived Brain Tumor Following Neural Stem Cell Transplantation in an Ataxia Telangiectasia Patient. Fischer A, editor. *PLoS Med*. 2009;6(2):e1000029.

197. **Baker DEC, Harrison NJ, Maltby E, Smith K, Moore HD, Shaw PJ, et al.** Adaptation to culture of human embryonic stem cells and oncogenesis in vivo. *Nat Biotechnol*. 2007;25(2):207–15.

198. **Harrison NJ, Baker D, Andrews PW**. Culture adaptation of embryonic stem cells echoes germ cell malignancy. *Int J Androl*. 2007;30(4):275–81.

199. **Thomson JA, Itskovitz-eldor J, Shapiro SS, Waknitz MA, Swiergiel JJ, Marshall VS, et al.** Embryonic Stem Cell Lines Derived from Human Blastocysts. *Adv Sci*. 2009;282(5391):1145–7.

200. **Bjorklund LM, Sanchez-Pernaute R, Chung S, Andersson T, Chen IYC, McNaught KSP, et al.** Embryonic stem cells develop into functional dopaminergic neurons after transplantation in a Parkinson rat model. *Proc Natl Acad Sci*. 2002;99(4):2344–9.

201. **Erdö F, Bührle C, Blunk J, Hoehn M, Xia Y, Fleischmann B, et al.** Host-Dependent Tumorigenesis of Embryonic Stem Cell Transplantation in Experimental Stroke. *J Cereb Blood Flow Metab*. 2003;23(7):780–5.

202. **Moiani A, Paleari Y, Sartori D, Mezzadra R, Miccio A, Cattoglio C, et al.** Lentiviral vector integration in the human genome induces alternative splicing and generates aberrant transcripts. *J Clin Invest*. 2012;122(5):1653–66.

203. **Bokhoven M, Stephen SL, Knight S, Gevers EF, Robinson IC, Takeuchi Y, et al.** Insertional Gene Activation by Lentiviral and Gammaretroviral Vectors. *J Virol*. 2009;83(1):283–94.

204. **Mayshar Y, Ben-David U, Lavon N, Biancotti J-C, Yakir B, Clark AT, et al.** Identification and Classification of Chromosomal Aberrations in Human Induced Pluripotent Stem Cells. *Cell Stem Cell*. 2010;7(4):521–31.

205. **Bernardo ME, Zaffaroni N, Novara F, Cometa AM, Avanzini MA, Moretta A, et al.** Human bone marrow-derived mesenchymal stem cells do not undergo transformation after long-term in vitro culture and do not exhibit telomere maintenance mechanisms. *Cancer Res*. 2007;67(19):9142–9.

206. **Taguchi A, Sakai C, Soma T, Kasahara Y, Stern DM, Kajimoto K, et al.** Intravenous Autologous Bone Marrow Mononuclear Cell Transplantation for Stroke: Phase1/2a Clinical Trial in a Homogeneous Group of Stroke Patients. *Stem Cells Dev*. 2015;24(19):2207–18.

207. **Suárez-Monteagudo C, Hernández-Ramírez P, Álvarez-González L, García-Maeso I, De La Cuétara-Bernal K, Castillo-Díaz L, et al.** Autologous bone marrow stem cell

neurotransplantation in stroke patients. An open study. *Restor Neurol Neurosci*. 2009;27(3):151–61.

208. **Bhasin A, Padma Srivastava M V., Mohanty S, Bhatia R, Kumaran SS, Bose S**. Stem cell therapy: A clinical trial of stroke. *Clin Neurol Neurosurg*. 2013;115(7):1003–8.

209. **Bang OY, Lee JS, Lee PH, Lee G**. Autologous mesenchymal stem cell transplantation in stroke patients. *Ann Neurol*. 2005;57(6):874–82.

210. **Banerjee S, Bentley P, Hamady M, Marley S, Davis J, Shlebak A, et al.** Intra-Arterial Immunoselected CD34+ Stem Cells for Acute Ischemic Stroke. *Stem Cells Transl Med*. 2014;3(11):481–8.

211. **Bhasin A, Srivastava M, Bhatia R, Mohanty S, Kumaran S, Bose S**. Autologous intravenous mononuclear stem cell therapy in chronic ischemic stroke. *J Stem Cells Regen Med*. 2012;8(3):181–9.

212. **Rosado-De-Castro PH, Schmidt FR, Battistella V, Lopes De Souza SA, Gutfilen B, Goldenberg RC, et al.** Biodistribution of bone marrow mononuclear cells after intra-arterial or intravenous transplantation in subacute stroke patients. Vol. 8, Regenerative Medicine. 2013.

213. **Prasad K, Sharma A, Garg A, Mohanty S, Bhatnagar S, Johri S, et al.** Intravenous autologous bone marrow mononuclear stem cell therapy for ischemic stroke: A multicentric, randomized trial. *Stroke*. 2014;45(12):3618–24.

214. **Hess DC, Wechsler LR, Clark WM, Savitz SI, Ford GA, Chiu D, et al.** Safety and efficacy of multipotent adult progenitor cells in acute ischaemic stroke (MASTERS): a randomised, double-blind, placebo-controlled, phase 2 trial. *Lancet Neurol*. 2017;16(5):360–8.

215. **Savitz SI, Misra V, Kasam M, Juneja H, Cox CS, Alderman S, et al.** Intravenous autologous bone marrow mononuclear cells for ischemic stroke. *Ann Neurol*. 2011;70(1):59–69.

216. **Battistella V, de Freitas GR, da Fonseca LMB, Mercante D, Gutfilen B, Goldenberg RC, et al.** Safety of autologous bone marrow mononuclear cell transplantation in patients with nonacute ischemic stroke. *Regen Med*. 2011;6(1):45–52.

217. **Moniche F, Gonzalez A, Gonzalez-Marcos J-R, Carmona M, Pinero P, Espigado I, et al.** Intra-Arterial Bone Marrow Mononuclear Cells in Ischemic Stroke: A Pilot Clinical Trial. *Stroke*. 2012;43(8):2242–4.

218. **Li Z-M, Zhang Z-T, Guo C-J, Geng F-Y, Qiang F, Wang L-X**. Autologous bone marrow mononuclear cell implantation for intracerebral hemorrhage—A prospective clinical observation. *Clin Neurol Neurosurg*. 2013;115(1):72–6.

219. **Prasad K, Mohanty S, Bhatia R, Srixivastava M, Garg A, Srivastava A, et al.** Autologous intravenous bone marrow mononuclear cell therapy for patients with subacute ischaemic stroke: A pilot Study. *Indian J Med Res*. 2012;136(2):221–8.

220. **Honmou O, Houkin K, Matsunaga T, Niitsu Y, Ishiai S, Onodera R, et al.** Intravenous administration of auto serum-expanded autologous mesenchymal stem cells in stroke. *Brain*. 2011;134(6):1790–807.

221. **Ghali AA, Yousef MK, Ragab OA, ElZamarany EA**. Intra-arterial Infusion of Autologous Bone Marrow Mononuclear Stem Cells in Subacute Ischemic Stroke Patients. *Front Neurol*. 2016;7(December):1–8.

222. **Chen DC, Lin SZ, Fan JR, Lin CH, Lee W, Lin CC, et al.** Intracerebral implantation of autologous peripheral blood stem cells in stroke patients: A randomized phase II study. *Cell Transplant*. 2014;23(12):1599–612.

223. **Chen J, Sanberg PR, Li Y, Wang L, Lu M, Willing AE, et al.** Intravenous administration of human umbilical cord blood reduces behavioral deficits after stroke in rats. *Stroke*. 2001;32(11):2682–8.

224. **Takahashi K, Yasuhara T, Shingo T, Muraoka K, Kameda M, Takeuchi A, et al.** Embryonic neural stem cells transplanted in middle cerebral artery occlusion model of rats demonstrated potent therapeutic effects, compared to adult neural stem cells. *Brain Res*. 2008;1234:172–82.

225. **Abeysinghe HCS, Bokhari L, Quigley A, Choolani M, Chan J, Dusting GJ, et al.** Pre-differentiation of human neural stem cells into GABAergic neurons prior to transplant results in greater repopulation of the damaged brain and accelerates functional recovery after transient ischemic stroke. *Stem Cell Res Ther*. 2015;6(1):1–19.

226. **Choudhery MS, Badowski M, Muise A, Pierce J, Harris DT**. Donor age negatively impacts adipose tissue-derived mesenchymal stem cell expansion and differentiation. *J Transl Med*. 2014;12(8):10.1186.

227. **Kretlow JD, Jin Y-Q, Liu W, Zhang W, Hong T-H, Zhou G, et al.** Donor age and cell passage affects differentiation potential of murine bone marrow-derived stem cells. *BMC Cell Biol*. 2008;9(1):60.

228. **D'Ippolito G, Schiller PC, Ricordi C, Roos B a, Howard G a**. Age-related osteogenic potential of mesenchymal stromal stem cells from human vertebral bone marrow. *J Bone Miner Res*. 1999;14(7):1115–22.

229. **Stolzing A, Jones E, McGonagle D, Scutt A**. Age-related changes in human bone marrow-derived mesenchymal stem cells: Consequences for cell therapies. *Mech Ageing Dev*. 2008;129(3):163–73.

230. **Steinberg GK, Kondziolka D, Wechsler LR, Lunsford LD, Coburn ML, Billigen JB, et al.** Clinical outcomes of transplanted modified bone marrow-derived mesenchymal stem cells in stroke: A phase 1/2a study. *Stroke*. 2016;47(7):1817–24.

231. **Kalladka D, Sinden J, Pollock K, Haig C, McLean J, Smith W, et al.** Human neural stem cells in patients with chronic ischaemic stroke (PISCES): a phase 1, first-in-man study. *Lancet*. 2016;388(10046):787–96.

232. **Brenneman M, Sharma S, Harting M, Strong R, Cox CS, Aronowski J, et al.** Autologous bone marrow mononuclear cells enhance recovery after acute ischemic stroke in young and middle-aged rats. *J Cereb Blood Flow Metab*. 2010;30(1):140–9.

233. **Janowski M, Walczak P**. Intravenous route of cell delivery for treatment of neurological disorders: a meta-analysis of preclinical results. *Stem Cells Dev*. 2010;19(1):5–16.

234. **Winderlich JN, Kremer KL, Koblar SA**. Adult human dental pulp stem cells promote blood–brain barrier permeability through vascular endothelial growth factor-a expression. *J Cereb Blood Flow Metab*. 2015;0271678X15608392.

235. **Rosenblum S, Wang N, Smith TN, Pendharkar A V, Chua JY, Birk H, et al.** Timing of intra-arterial neural stem cell transplantation after hypoxia-ischemia influences cell engraftment, survival, and differentiation. *Stroke*. 2012;43(6):1624–31.

236. **Sandoval KE, Witt KA**. Blood-brain barrier tight junction permeability and ischemic stroke. *Neurobiol Dis*. 2008;32(2):200–19.

237. **Sasaki Y, Sasaki M, Kataoka-Sasaki Y, Nakazaki M, Nagahama H, Suzuki J, et al.** Synergic

Effects of Rehabilitation and Intravenous Infusion of Mesenchymal Stem Cells After Stroke in Rats. *Phys Ther*. 2016;96(11):1791–8.

238. **Savitz SI, Dinsmore J, Wu J, Henderson G V., Stieg P, Caplan LR**. Neurotransplantation of fetal porcine cells in patients with basal ganglia infarcts: A preliminary safety and feasibility study. *Cerebrovasc Dis*. 2005;20(2):101–7.

239. **Rabinovich SS, Seledtsov VI, Banul N V, Poveshchenko O V, Senyukov V V, Astrakov S V, et al.** Cell therapy of brain stroke. *Bull Exp Biol Med*. 2005;139(1):126–8.

240. **Kondziolka D, Steinberg GK, Wechsler L, Meltzer CC, Elder E, Gebel J, et al.** Neurotransplantation for patients with subcortical motor stroke: a Phase 2 randomized trial. *J Neurosurg*. 2005;103(1):38–45.

241. **Kondziolka D, Wechsler L, Goldstein S, Meltzer C, Thulborn KR, Gebel J, et al.** Expedited Publication Transplantation of cultured human neuronal cells for. *Neurology*. 2000;565–9.

242. **Nagpal A, Choy FC, Howell S, Hillier S, Chan F, Hamilton-Bruce MA, et al.** Safety and effectiveness of stem cell therapies in early-phase clinical trials in stroke: a systematic review and meta-analysis. *Stem Cell Res Ther*. 2017;8(1):191.

243. **Gronthos S, Mankani M, Brahim J, Robey PG, Shi S**. Postnatal human dental pulp stem cells (DPSCs) in vitro and in vivo. *Proc Natl Acad Sci U S A*. 2000;97(25):13625–30.

244. **Kaukua N, Shahidi MK, Konstantinidou C, Dyachuk V, Kaucka M, Furlan A, et al.** Glial origin of mesenchymal stem cells in a tooth model system. *Nature*. 2014;513(7519):551–4.

245. **Bressan E, Ferroni L, Gardin C, Pinton P, Stellini E, Botticelli D, et al.** Donor age-related biological properties of human dental pulp stem cells change in nanostructured scaffolds. Glod JW, editor. *PLoS One*. 2012;7(11):e49146.

246. **Arthur A, Rychkov G, Shi S, Koblar SA, Gronthos S**. Adult human dental pulp stem cells differentiate toward functionally active neurons under appropriate environmental cues. *Stem Cells*. 2008;26(7):1787–95.

247. **Zhang W, Walboomers XF, Shi S, Fan M, Jansen J a**. Multilineage differentiation potential of stem cells derived from human dental pulp after cryopreservation. *Tissue Eng*. 2006;12(10):2813–23.

248. **Bray AF, Cevallos RR, Gazarian K, Lamas M**. Human dental pulp stem cells respond to cues from the rat retina and differentiate to express the retinal neuronal marker rhodopsin. *Neuroscience*. 2014;280:142–55.

249. **Sasaki R, Aoki S, Yamato M, Uchiyama H, Wada K, Okano T, et al.** Neurosphere generation from dental pulp of adult rat incisor. *Eur J Neurosci*. 2008;27(3):538–48.

250. **Kawashima N**. Characterisation of dental pulp stem cells: A new horizon for tissue regeneration? *Arch Oral Biol*. 2012;57(11):1439–58.

251. **Suchánek J, Visek B, Soukup T, El-Din Mohamed SK, Ivancaková R, Mokrỳ J, et al.** Stem cells from human exfoliated deciduous teeth--isolation, long term cultivation and phenotypical analysis. *Acta Medica (Hradec Kralove)*. 2010;53(2):93–9.

252. **Pivoriūnas A, Surovas A, Borutinskaitė V, Matuzevičius D, Treigytė G, Savickienė J, et al.** Proteomic Analysis of Stromal Cells Derived from the Dental Pulp of Human Exfoliated Deciduous Teeth. *Stem Cells Dev*. 2010;19(7):1081–93.

253. **Lindroos B, Mäenpää K, Ylikomi T, Oja H, Suuronen R, Miettinen S**. Characterisation of human dental stem cells and buccal mucosa fibroblasts. *Biochem Biophys Res Commun*. 2008;368(2):329–35.

254. **Kerkis I, Kerkis A, Dozortsev D, Stukart-Parsons GC, Gomes Massironi SM, Pereira L V., et al.** Isolation and Characterization of a Population of Immature Dental Pulp Stem Cells Expressing OCT-4 and Other Embryonic Stem Cell Markers. *Cells Tissues Organs*. 2006;184(3–4):105–16.

255. **Ishkitiev N, Yaegaki K, Calenic B, Nakahara T, Ishikawa H, Mitiev V, et al.** Deciduous and Permanent Dental Pulp Mesenchymal Cells Acquire Hepatic Morphologic and Functional Features In Vitro. *J Endod*. 2010;36(3):469–74.

256. **Dissanayaka WL, Zhu X, Zhang C, Jin L**. Characterization of dental pulp stem cells isolated from canine premolars. *J Endod*. 2011;37(8):1074–80.

257. **Joo KH, Song JS, Kim S, Lee HS, Jeon M, Kim SO, et al.** Cytokine Expression of Stem Cells Originating from the Apical Complex and Coronal Pulp of Immature Teeth. *J Endod*. 2017;44(1):87–92.e1.

258. **Arthur A, Shi S, Zannettino ACW, Fujii N, Gronthos S, Koblar SA**. Implanted adult human dental pulp stem cells induce endogenous axon guidance. *Stem Cells*. 2009;27(9):2229–37.

259. **Suzuki T, Lee CH, Chen M, Zhao W, Fu SY, Qi JJ, et al.** Induced migration of dental pulp stem cells for in vivo pulp regeneration. *J Dent Res*. 2011;90(8):1013–8.

260. **Wilson R, Urraca N, Skobowiat C, Hope KA, Miravalle L, Chamberlin R, et al.** Assessment of the Tumorigenic Potential of Spontaneously Immortalized and hTERT-Immortalized Cultured Dental Pulp Stem Cells. *Stem Cells Transl Med*. 2015;4(8):905–12.

261. **Yamada Y, Ito K, Nakamura S, Ueda M, Nagasaka T**. Promising cell-based therapy for bone regeneration using stem cells from deciduous teeth, dental pulp, and bone marrow. *Cell Transplant*. 2011;20(7):1003–13.

262. **Zheng Y, Liu Y, Zhang CM, Zhang HY, Li WH, Shi S, et al.** Stem cells from deciduous tooth repair mandibular defect in swine. *J Dent Res*. 2009;88(3):249–54.

263. **Ikeda E, Yagi K, Kojima M, Yagyuu T, Ohshima A, Sobajima S, et al.** Multipotent cells from the human third molar: Feasibility of cell-based therapy for liver disease. *Differentiation*. 2008;76(5):495–505.

264. **Nesti C, Pardini C, Barachini S, D'Alessandro D, Siciliano G, Murri L, et al.** Human dental pulp stem cells protect mouse dopaminergic neurons against MPP+ or rotenone. *Brain Res*. 2011;1367:94–102.

265. **Sugiyama M, Iohara K, Wakita H, Hattori H, Ueda M, Matsushita K, et al.** Dental pulp-derived $CD31^-/CD146^-$ side population stem/progenitor cells enhance recovery of focal cerebral ischemia in rats. *Tissue Eng Part A*. 2011;17(9–10):1303–11.

266. **Yamagata M, Yamamoto A, Kako E, Kaneko N, Matsubara K, Sakai K, et al.** Human dental pulp-derived stem cells protect against hypoxic-ischemic brain injury in neonatal mice. *Stroke*. 2013;44(2):551–4.

267. **Inoue T, Sugiyama M, Hattori H, Wakita H, Wakabayashi T, Ueda M**. Stem Cells from Human Exfoliated Deciduous Tooth-Derived Conditioned Medium Enhance Recovery of Focal Cerebral Ischemia in Rats. *Tissue Eng Part A*. 2012;19:121010064807009.

268. **Song M, Lee J-H, Bae J, Bu Y, Kim E-C**. Human Dental Pulp Stem Cells are more Effective than Human Bone Marrow-Derived Mesenchymal Stem Cells in Cerebral Ischemic Injury. *Cell Transplant*. 2017;26(6):1001–16.

269. **Martino G, Pluchino S**. The therapeutic potential of neural stem cells. *Nat Rev Neurosci*.

2006;7(5):395–406.

270. **Gervois P, Wolfs E, Ratajczak J, Dillen Y, Vangansewinkel T, Hilkens P, et al.** Stem Cell-Based Therapies for Ischemic Stroke: Preclinical Results and the Potential of Imaging-Assisted Evaluation of Donor Cell Fate andMechanisms of Brain Regeneration. *Med Res Rev*. 2016;36(6):1080–126.

271. **Duncan K, Gonzales-Portillo GS, Acosta SA, Kaneko Y, Borlongan C V., Tajiri N**. Stem cell-paved biobridges facilitate stem transplant and host brain cell interactions for stroke therapy. *Brain Res*. 2015;1623:160–5.

272. **Andres RH, Horie N, Slikker W, Keren-Gill H, Zhan K, Sun G, et al.** Human neural stem cells enhance structural plasticity and axonal transport in the ischaemic brain. *Brain*. 2011;134(Pt 6):1777–89.

273. **Daadi MM, Davis AS, Arac A, Li Z, Maag AL, Bhatnagar R, et al.** Human Neural Stem Cell Grafts Modify Microglial Response and Enhance Axonal Sprouting in Neonatal Hypoxic-Ischemic Brain Injury. *Stroke*. 2010;41(3):516–23.

274. **Nivet E, Vignes M, Girard SD, Pierrisnard C, Baril N, Devèze A, et al.** Engraftment of human nasal olfactory stem cells restores neuroplasticity in mice with hippocampal lesions. *J Clin Invest*. 2011;121(7):2808–20.

275. **Giordano A, Galderisi U, Marino IR**. From the laboratory bench to the patient's bedside: an update on clinical trials with mesenchymal stem cells. *J Cell Physiol*. 2007;211(1):27–35.

276. **Kingham PJ, Kolar MK, Novikova LN, Novikov LN, Wiberg M**. Stimulating the Neurotrophic and Angiogenic Properties of Human Adipose-Derived Stem Cells Enhances Nerve Repair. *Stem Cells Dev*. 2014;23(7):741–54.

277. **Lin W, Li M, Li Y, Sun X, Li X, Yang F, et al.** Bone marrow stromal cells promote neurite outgrowth of spinal motor neurons by means of neurotrophic factors in vitro. *Neurol Sci*. 2014;35(3):449–57.

278. **Cohen-Cory S, Fraser SE**. Effects of brain-derived neurotrophic factor on optic axon branching and remodelling in vivo. *Nature*. 1995;378(6553):192–6.

279. **Sanchez AL, Matthews BJ, Meynard MM, Hu B, Javed S, Cohen Cory S**. BDNF increases synapse density in dendrites of developing tectal neurons in vivo. *Development*.

2006;133(13):2477–86.

280. **Madduri S, Papaloïzos M, Gander B**. Synergistic effect of GDNF and NGF on axonal branching and elongation in vitro. *Neurosci Res*. 2009;65(1):88–97.

281. **Kurozumi K, Nakamura K, Tamiya T, Kawano Y, Ishii K, Kobune M, et al.** Mesenchymal stem cells that produce neurotrophic factors reduce ischemic damage in the rat middle cerebral artery occlusion model. *Mol Ther*. 2005;11(1):96–104.

282. **Jeong CH, Kim SM, Lim JY, Ryu CH, Jun JA, Jeun S-S**. Mesenchymal Stem Cells Expressing Brain-Derived Neurotrophic Factor Enhance Endogenous Neurogensis in an Ischemic Stroke Model. *Biomed Res Int*. 2014;2014.

283. **Xiong L-L, Hu Y, Zhang P, Zhang Z, Li L-H, Gao G-D, et al.** Neural Stem Cell Transplantation Promotes Functional Recovery from Traumatic Brain Injury via Brain Derived Neurotrophic Factor-Mediated Neuroplasticity. *Mol Neurobiol*. 2017;

284. **Rubin LL, Staddon JM**. The cell biology of the blood-brain barrier. *Annu Rev Neurosci*. 1999;22(1).

285. **Ballabh P, Braun A, Nedergaard M**. The blood-brain barrier: an overview: structure, regulation, and clinical implications. *Neurobiol Dis*. 2004;16(1):1–13.

286. **Fu X-C, Wang G-P, Shan H-L, Liang W-Q, Gao J-Q**. Predicting blood–brain barrier penetration from molecular weight and number of polar atoms. *Eur J Pharm Biopharm*. 2008;70(2):462–6.

287. **Mitic LL, Anderson JM**. Molecular architecture of tight junctions. *Annu Rev Physiol*. 1998;60:121–42.

288. **Hirohashi T, Terasaki T, Shigetoshi M, Sugiyama Y**. In Vivo and In Vitro Evidence for Nonrestricted Transport of 2’,7’-Bis(2-Carboxyethyl)-5(6)-Carboxyfluorescein Tetraacetoxymethyl Ester at the Blood-Brain Barrier. *J Pharmacol Exp Ther*. 1997;280(2):813–9.

289. **Friden PM, Olson TS, Obar R, Walus LR, Putney SD**. Characterization, receptor mapping and blood-brain barrier transcytosis of antibodies to the human transferrin receptor. *J Pharmacol Exp Ther*. 1996;278(3):1491–8.

290. **Deli MA**. Potential use of tight junction modulators to reversibly open membranous barriers

and improve drug delivery. *Biochim Biophys Acta*. 2009;1788(4):892–910.

291. **Savettieri G, Di Liegro I, Catania C, Licata L, Pitarresi GL, D'Agostino S, et al.** Neurons and ECM regulate occludin localization in brain endothelial cells. *Neuroreport*. 2000;11(5):1081–4.

292. **Andreeva a Y, Krause E, Müller EC, Blasig IE, Utepbergenov DI**. Protein kinase C regulates the phosphorylation and cellular localization of occludin. *J Biol Chem*. 2001;276(42):38480–6.

293. **Shepro D, Morel NM**. Pericyte physiology. *FASEB J*. 1993;7(11):1031–8.

294. **Kelley C, D'Amore P, Hechtman HB, Shepro D**. Vasoactive hormones and cAMP affect pericyte contraction and stress fibres in vitro. *J Muscle Res Cell Motil*. 1988;9(2):184–94.

295. **Haseloff RF, Blasig IE, Bauer H-C**. In Search of the Astrocytic Factor(s) Modulating Blood–Brain Barrier Functions in Brain Capillary Endothelial Cells In Vitro. *Cell Mol Neurobiol*. 2005;25(1):25–39.

296. **Kacem K, Lacombe P, Seylaz J, Bonvento G**. Structural organization of the perivascular astrocyte endfeet and their relationship with the endothelial glucose transporter: a confocal microscopy study. *Glia*. 1998;23(1):1–10.

297. **Janzer RC, Raff MC**. Astrocytes induce blood-brain barrier properties in endothelial cells. *Nature*. 1987;325(6101):253–7.

298. **Arthur FE, Shivers RR, Bowman PD**. Astrocyte-mediated induction of tight junctions in brain capillary endothelium: an efficient in vitro model. *Brain Res*. 1987;433(1):155–9.

299. **Rubin LL, Hall DE, Porter S, Barbu K, Cannon C, Horner HC, et al.** A cell culture model of the blood-brain barrier. *J Cell Biol*. 1991;115(6):1725–35.

300. **Lee S-W, Kim WJ, Choi YK, Song HS, Son MJ, Gelman IH, et al.** SSeCKS regulates angiogenesis and tight junction formation in blood-brain barrier. *Nat Med*. 2003;9(7):900–6.

301. **Niego B, Freeman R, Puschmann TB, Turnley AM, Medcalf RL**. t-PA-specific modulation of a human blood-brain barrier model involves plasmin-mediated activation of the Rho kinase pathway in astrocytes. *Blood*. 2012;119(20):4752–61.

302. **Dehouck M, Mkresse S, Delorme JP, Fruchart J, Cecchelli R**. An Easier, Reproducible, and Mass-Production Method to Study the Blood-Brain Bamer In Vitro. *J Neurochem*. 1990;798–

801.

303. **Lundquist S, Renftel M, Brillault J, Fenart L, Cecchelli R, Dehouck M-P**. Prediction of Drug Transport Through the Blood-Brain Barrier in Vivo: A Comparison Between Two in Vitro Cell Models. *Pharm Res*. 2002;19(7):976–81.

304. **Başkaya MK, Rao a M, Doğan a, Donaldson D, Dempsey RJ**. The biphasic opening of the blood-brain barrier in the cortex and hippocampus after traumatic brain injury in rats. *Neurosci Lett*. 1997;226(1):33–6.

305. **Belayev L, Busto R, Zhao W, Ginsberg MD**. Quantitative evaluation of blood-brain barrier permeability following middle cerebral artery occlusion in rats. *Brain Res*. 1996;739(1–2):88–96.

306. **Vries HE De, Blom-roosemalen CM, Oosten M Van, Boer AG De, Berkel TJC Van, Breimer DD, et al.** The influence of cytokines on the integrity of the blood-brain barrier in vitro. 1996;64:37–43.

307. **Wolburg H, Wolburg-Buchholz K, Kraus J, Rascher-Eggstein G, Liebner S, Hamm S, et al.** Localization of claudin-3 in tight junctions of the blood-brain barrier is selectively lost during experimental autoimmune encephalomyelitis and human glioblastoma multiforme. *Acta Neuropathol*. 2003;105(6):586–92.

308. **Zhang ZG, Zhang L, Jiang Q, Zhang R, Davies K, Powers C, et al.** VEGF enhances angiogenesis and promotes blood-brain barrier leakage in the ischemic brain. *J Clin Invest*. 2000;106(7):829–38.

309. **Merali Z, Huang K, Mikulis D, Silver F, Kassner A**. Evolution of blood-brain-barrier permeability after acute ischemic stroke. *PLoS One*. 2017;12(2):1–11.

310. **Su L, Xu J, Ji BX, Wan SG, Lu CY, Dong HQ, et al.** Autologous peripheral blood stem cell transplantation for severe multiple sclerosis. *Int J Hematol*. 2006;84(3):276–81.

311. **Shen LH, Li Y, Chen J, Zacharek A, Gao Q, Kapke A, et al.** Therapeutic benefit of bone marrow stromal cells administered 1 month after stroke. *J Cereb Blood Flow Metab*. 2007;27(1):6–13.

Chapter 2

Adult human dental pulp stem cells promote blood-brain barrier permeability through vascular endothelial growth factor-a expression

Joshua N Winderlich[1,3]; Karlea L Kremer[1,3]; Simon A Koblar[1,2,3]

1. Stroke Research Programme, School of Medicine, University of Adelaide, South Australia, Australia.

2. Department of Neurology, Queen Elizabeth Hospital, Woodville, South Australia, Australia.

3. Centre for Stem Cell Research, Robinson Institute, Adelaide, South Australia, Australia.

Journal of Cerebral Blood Flow & Metabolism; 2015, doi: 10.1177/0271678X15608392

Statement of Authorship

Title of Paper	Adult human dental pulp stem cells promote blood–brain barrier permeability through vascular endothelial growth factor-a expression
Publication Status	☑ Published ☐ Accepted for Publication ☐ Submitted for Publication ☐ Unpublished and Unsubmitted work written in manuscript style
Publication Details	Winderlich JN, Kremer KL, Koblar SA. Adult human dental pulp stem cells promote blood–brain barrier permeability through vascular endothelial growth factor-a expression. *J Cereb Blood Flow Metab.* SAGE Publications; 2015 Oct 2

Principal Author

Name of Principal Author (Candidate)	Joshua Winderlich		
Contribution to the Paper	Designed study, conducted experimental work, data collection, analysis and compiled manuscript.		
Overall percentage (%)	90		
Certification:	This paper reports on original research I conducted during the period of my Higher Degree by Research candidature and is not subject to any obligations or contractual agreements with a third party that would constrain its inclusion in this thesis. I am the primary author of this paper.		
Signature		Date	15/1/2018

Co-Author Contributions

By signing the Statement of Authorship, each author certifies that:

i. the candidate's stated contribution to the publication is accurate (as detailed above);

ii. permission is granted for the candidate in include the publication in the thesis; and

iii. the sum of all co-author contributions is equal to 100% less the candidate's stated contribution.

Name of Co-Author	Karlea Kremer		
Contribution to the Paper	Guidance during experimental design, aided in data analysis and revision of the manuscript.		
Signature		Date	12/01/2018

Name of Co-Author	Simon Koblar		
Contribution to the Paper	Allocation of funding support, guidance in study design, interpretation of results and revision of manuscript drafts.		
Signature		Date	12/1/18

Original Article

JCBFM

Journal of Cerebral Blood Flow & Metabolism
0(00) 1–11

Reprints and permissions:
sagepub.co.uk/journalsPermissions.nav
DOI: 10.1177/0271678X15608392
jcbfm.sagepub.com
SAGE

Adult human dental pulp stem cells promote blood–brain barrier permeability through vascular endothelial growth factor-a expression

Joshua N Winderlich[1,2], Karlea L Kremer[1,2] and Simon A Koblar[1,2,3]

Abstract

Stem cell therapy is a promising new treatment option for stroke. Intravascular administration of stem cells is a valid approach as stem cells have been shown to transmigrate the blood–brain barrier. The mechanism that causes this effect has not yet been elucidated. We hypothesized that stem cells would mediate localized discontinuities in the blood–brain barrier, which would allow passage into the brain parenchyma. Here, we demonstrate that adult human dental pulp stem cells express a soluble factor that increases permeability across an in vitro model of the blood–brain barrier. This effect was shown to be the result of vascular endothelial growth factor-a. The effect could be amplified by exposing dental pulp stem cell to stromal-derived factor 1, which stimulates vascular endothelial growth factor-a expression. These findings support the use of dental pulp stem cell in therapy for stroke.

Keywords

Dental pulp stem cells, blood–brain barrier, vascular endothelial growth factor, stromal-derived factor 1, in vitro

Received 27 January 2015; Revised 2 June 2015; Accepted 30 June 2015

Introduction

The chronic cognitive and motor–sensory dysfunction resulting from stroke presents a major challenge to healthcare in much of the developed world. As of 2010, there were approximately 33 million people living with the effects of stroke, making stroke responsible for 4% of the total disability-adjusted life years of disease burden.[1] Given the scope of this issue, it is clear that much importance must be placed on developing efficacious treatments to return patients to a healthy and functional state.

Cell-based therapy is emerging as a possible treatment option for stroke.[2] This field of study was sparked by the ability of stem cells to populate areas and replace the function of many divergent tissue types. Transplantation of stem cells provides the potential to extend the post-stroke recovery of function beyond what is possible by endogenous recovery alone. This has been demonstrated over the last decade in animal models.[2–6] However, this effect is not well explained by the tissue replacement model alone. The paracrine secretion of various factors may underlie the functional improvement seen in animal stroke models of cell-based therapy whereby immunomodulation, neuroprotection, neurogenesis, neuroplasticity and angiogenesis are supported and enhanced.[7]

Research into cell-based therapy for stroke has advanced to a point where a number of early phase clinical trials have been undertaken.[8–11] However, several basic questions remain unanswered, with the focus from this study being on how stem cells may transmigrate the blood–brain barrier (BBB) if administered via the vasculature.

[1]Stroke Research Programme, School of Medicine, University of Adelaide, Adelaide, Australia
[2]Centre for Stem Cell Research, Robinson Institute, Adelaide, Australia
[3]Department of Neurology, Queen Elizabeth Hospital, Woodville, Australia

Corresponding author:
Simon A Koblar, School of Medicine, University of Adelaide, Adelaide, SA 5005, Australia.
Email: simon.koblar@adelaide.edu.au

One potential source of stem cells for therapy is dental pulp stem cell (DPSC), which was first described by Gronthos et al.[12] These are a population of highly proliferative, undifferentiated cells residing in perivascular niches within the dental pulp of adult teeth. DPSCs have been demonstrated to have the capacity to differentiate into neurons, adipocytes, myocytes and chondrocytes in vitro.[13–15] Intracerebral (IC) transplantation following stroke in a rat model showed an improvement in functional outcomes.[2]

There are two paradigms for the administration of therapeutic stem cells in stroke research: intravascular (IV) and IC. IC transplantation delivers stem cells directly to the site of damage, which may result in a greater surviving population of viable cells. However, this is a highly invasive procedure and is associated with an increased mortality rate of approximately 10% when administered acutely in rodent stroke models.[2] As such, acute IC transplantation may not be a clinically viable model.

IV administration of stem cells in animal models of stroke has been validated as efficacious. It has even been demonstrated in some studies that small populations of transplanted stem cells can be detected within the brain parenchyma.[5] A likely mechanism for this is that stem cells migrate along a stromal-derived factor-1 (SDF-1) gradient towards the ischaemic border zone via the receptor CXCR4. SDF-1 is upregulated for at least a month following stroke, so the effective window for treatment could hypothetically be extended significantly.[16,17] However, this depends on how stem cells interact with the BBB.

The BBB refers to the specialized structure of the neurovascular unit. The BBB is composed of a continuous layer of endothelial cells, which are surrounded by a basement membrane, pericytes and astrocyte processes. The main function of the BBB is to segregate the environment of the brain parenchyma from peripheral circulation. In general, the BBB is selectively impermeable to large polar molecules and cells.[18]

The mechanisms by which stem cells transmigrate the BBB have not yet been fully characterized. It is possible that IV stem cells administered post-stroke take advantage of existing damage to the BBB to gain access to the therapeutic target. However, even stem cells administered after the usual period of post-stoke BBB opening are able to gain access to the brain parenchyma.[5,19] This study will therefore investigate the possibility that DPSCs are capable of mediating passage through the BBB by causing a temporary opening of the barrier.

There are a number of cytokines known to cause increases in BBB permeability. Notable examples are members of the vascular endothelial growth factor (VEGF) family, including VEGF-a and placental growth factor, both of which are potent permeability factors involved in repair of cerebral circulation following stroke.[20,21] A study by Díaz-Coránguez et al. implicates VEGF-a as one of the mediators of permeability in glioma-induced BBB permeability.[22] VEGF-a acts by causing a downregulation of occludin and claudins, both components of tight junctions.[21] Stem cells, in general, and DPSC, in particular, have been shown to express VEGF-a and stimulate angiogenesis.[23,24]

Therefore, a reasonable explanation for trans-neuroendothelial migration by stem cells is that as circulating transplanted cells pass near ischaemic tissue, they secrete VEGF-a onto adjacent endothelial tissue. VEGF-a binds to VEGFR2 on the surface of endothelial cells, causing downregulation of tight junction proteins and ultimately a local increase in BBB permeability.

Co-cultures of endothelial cells and astrocytes have been used previously to model the BBB, allowing for a highly reproducible experimental construct.[25–28] It has been proposed that (an) unknown factor(s) expressed by astrocytes stimulate the adoption of BBB characteristics in an endothelial monolayer. This type of model has been shown to have a similar permeability profile to the BBB in vivo and also to respond to some permeability-inducing drugs.[26,28,29]

This study aims to develop an in vitro model of the BBB, to investigate the ability of DPSC to mediate BBB permeability and to determine the molecular mechanism underlying this activity.

Materials and methods

Cell culture

Cells were passaged when near 80% confluency. Adherent cells were harvested from plastic surfaces by incubating in trypsin/EDTA (Invitrogen) in phosphate-buffered saline (PBS) and resuspended in the appropriate media for experimental use. Cells were cultured in media described in Table 1.

Human DPSC. DPSCs (Figure 1(c)) were previously isolated from molar teeth extracted during routine dental procedures from otherwise healthy adults. Before use, DPSCs were stored in 10% DMSO (Merck, 10323.4L) in foetal calf serum at a liquid nitrogen storage facility.

Use of human tissue was approved by the University of Adelaide Human Research Ethics Committee (ethics approval number: H-2012-164). This study adheres to guidelines set out in the National Statement of Ethical Conduct in Human Research (2007) and sections 95 and 95 A of the Privacy act (1988). Written, informed consent was given by all human donors.

Table 1. Culture media and supplements for DPSC, BMEC and astrocytes.

Human DPSC		
a-modified Eagle's media		Sigma-Aldrich, St. Louis
FCS	10% (v/v)	Invitrogen
L-Glutamine	2 mM	Invitrogen, 250030081
Penicillin	100 µg/ml	Invitrogen cat#15140122
Streptomycin	100 µg/ml	Invitrogen cat#15140122
L-ascorbic acid 2-phosphate	100 µM	Wako, Richmond, VA
Human BMEC		
M199 medium		Sigma-Aldrich, St. Louis
FCS	16% (v/v)	Invitrogen
Penicillin	100 µg/ml	Invitrogen cat#15140122
Streptomycin	100 µg/ml	Invitrogen cat#15140122
Non-essential amino acids	0.8X	Invitrogen cat#11140050
Sodium pyruvate	0.8 mM	Sigma cat#S8636
Murine astrocytes		
Dulbecco's modified eagle's medium		Sigma-Aldrich, St. Louis
FCS	10% (v/v)	Invitrogen
Penicillin	100 µg/ml	Invitrogen cat#15140122
Streptomycin	100 µg/ml	Invitrogen cat#15140122

BMEC: bone marrow endothelial cell; DPSC: dental pulp stem cell; FCS: Foetal calf serum.

Human bone marrow endothelial cells (BMEC). The BMEC line (Figure 1(b)) was kindly provided by Prof. Andrew Zanettino (SA Pathology), who had previously acquired it from Dr Babette Walker (Weill Medical College of Cornell University).

Murine cerebellar astrocytes. Astrocytes (ATCC, CRL-2541) (Figure 1(a)) were originally obtained from the cerebellum of an eight-day-old mouse and the permanent line was selected following spontaneous transformation.

Preparation of the in vitro BBB model

The luminal surface of an 8 µm pore cell culture insert (BD Falcon TM, 353182) was coated with bovine collagen (Sigma, C4243) at a density of 20 µg/cm^2 and left to dry. On day two, astrocytes were harvested and 1×10^5 cells were seeded onto the underside of the membrane. The astrocytes were allowed to adhere for 4 h. BMECs were harvested and 1×10^5 cells were seeded onto the upper surface of the membrane. Astrocyte medium supplemented with EGF (BD Biosciences, BD356006) and heparin (Sigma, H-0777) at a dilution of 1:333 was added to both compartments; this was done to increase proliferation of the BMEC. On day four, the medium was replaced with unsupplemented astrocyte medium to slow down BMEC proliferation and allow BBB characteristics to form. On day five, the co-culture was confluent and resembled the BBB in terms of permeability (Figure 1(d) and (e)).

Immunocytochemistry

To confirm the presence and regulation of the molecular components of the BBB, a monolayer of endothelial cells was cultured on 12 mm glass coverslips. A selection of these was co-cultured with astrocytes. These were then treated with 100 ng/ml VEGF-a (ebioscience®, 14-8359-80), DPSC-conditioned media or vehicle for 24 h. Additionally, rodent brain sections were obtained for use as a positive control. The slides were fixed in 4% (w/v) PFA (Sigma, P6148) in PBS for 30 min and stored in PBS. Samples were permeabilized by washing with 5% (v/v) TX-100 (Sigma, T8787) in PBS for 5 min, then blocked with 2% (w/v) BSA (Sigma, A7906) and 0.2% (v/v) TX-100 in PBS for 2 h, then washed 3X in PBS. Each slide was incubated overnight with 1:200 rabbit anti-occludin (Abcam, ab31721) in 1% (w/v) BSA, 0.05% (v/v) TX-100 and 0.5% (v/v) normal donkey serum (Sigma, D9663) in PBS (blocking buffer B). The slides were then washed 3X in PBS and once in blocking buffer B before being incubated for 2 h with 1:200 Cy2 anti-rabbit (Jackson ImmunoResearch, 109225008). The coverslips were then washed twice with PBS, inverted and fixed to microscope slides with ProLong® Gold Antifade

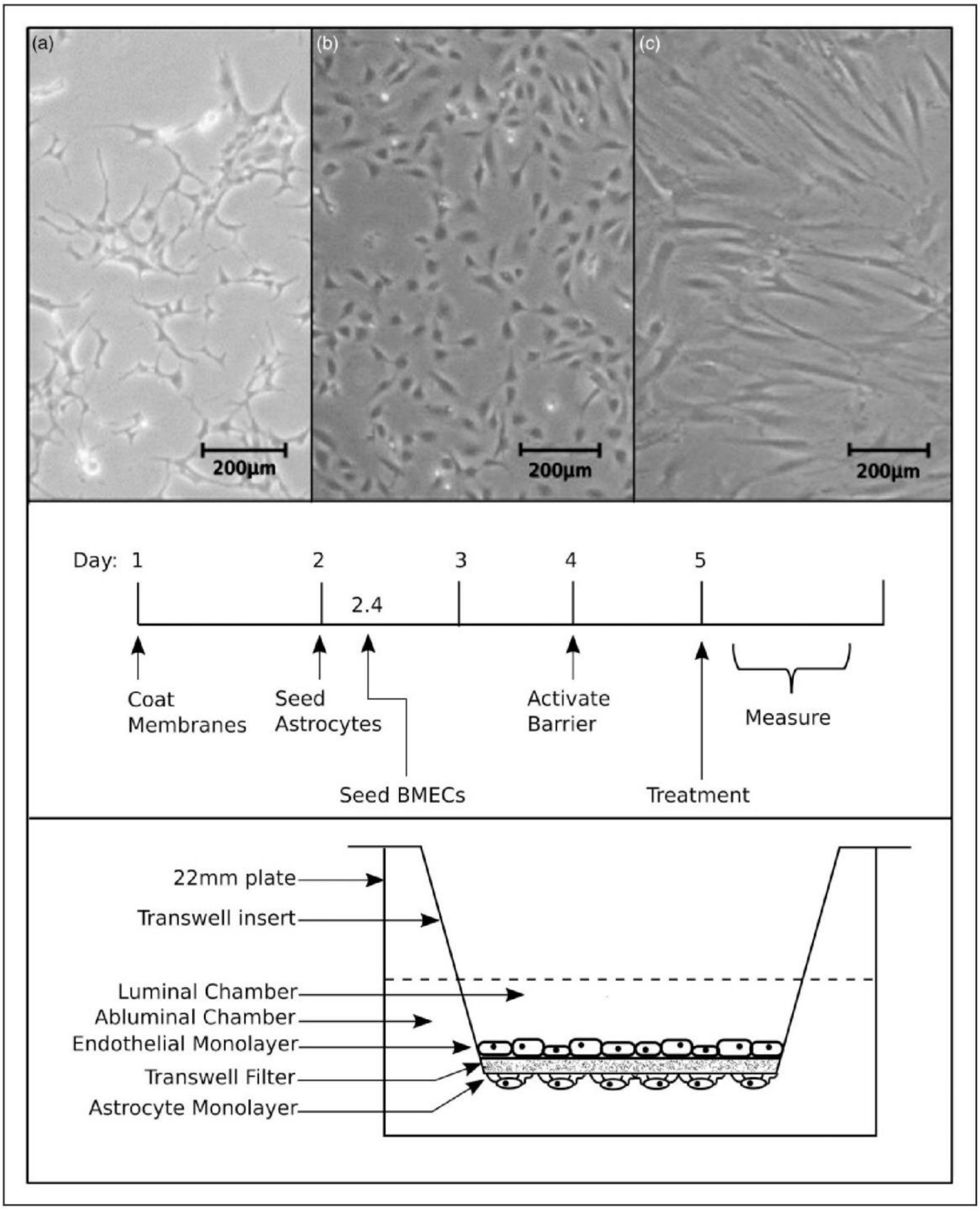

Figure 1. Phase contrast micrographs of astrocytes (a), endothelial cells (b) and DPSC (c). (d) A timeline showing the procedure followed during the preparation of an in vitro BBB. (e) A diagram showing the arrangement of the BBB model ready for testing at day five.

containing DAPI (Life Technologies, P-36931). Capture of micrographs was not subject to blinding; however, images were analysed using a computer algorithm (ImageJ, 1.49C) to prevent human error. Micrographs were taken from areas on each slide containing sufficient cells for statistical analysis.

VEGF-a-induced permeability across different sized markers

In vitro BBB models were prepared as described above. On day five, nine assemblies were incubated with 100 ng/ml VEGF-a for 5.5 h and nine were used as controls. Two microlitres of 5% (w/v) Evan's Blue (EB) (Sigma, E2129) in 12.5% (w/v) BSA (Sigma, A-7906), 2 µl of 5% (w/v) methylene blue (Probing & Structure, C124) or 2 µl of 5% (w/v) bromophenol blue (Sigma, B-8026) in PBS was added to each luminal compartment. After 30 min, the micropore inserts were removed and 2 × 100 µl samples were removed from the abluminal chamber and transferred to a 96-well plate. Absorbance for EB, bromophenol blue and methylene blue was read at 620, 590 and 600 nm, respectively, using a plate reader (BioTek®, Synergy MX).

VEGF-a-induced permeability

BBB models were prepared as described above. Assemblies were incubated with VEGF-a at a concentration between 0 and 100 ng/ml for 5.5 h. Two microlitres EB-BSA was then added to the luminal chamber and the assembly was incubated for a further 30 min. The transwell inserts were then removed and 2 × 100 µl samples were taken from the abluminal chamber and transferred to a 96-well plate. Absorbance was read at a wavelength of 620 nm.

DPSC-conditioned media-induced permeability

DPSCs were cultured in two 75 cm^2 flasks (samples 1 and 2) until they had reached ~80% confluency. Media were changed then harvested after three days and sub-sequently stored at -80°C. In vitro BBB models were prepared as described above. On day five, the assemblies were incubated for 30 min with 1 ml of DPSC-conditioned medium (sample 1 or sample 2) or unconditioned DPSC medium. Each assembly was incubated for 30 min with 2 µl of EB-BSA added to the luminal compartment. The transwell inserts were removed and 2 × 100 µl samples were taken from the abluminal compartments and transferred to a 96-well plate. Absorbance was read at a wavelength of 620 nm.

ELISA

DPSCs were cultured until they reached ~80% confluency. Media were then changed and cells were cultured for a further 72 h. The conditioned media were subsequently aspirated and stored at -80°C. Prior to testing, 4 ml samples were thawed at room temperature and concentrated using Amicon filters (Millipore, UFC801024) and 100 µl samples were set aside for total protein quantitation. ELISAs were conducted using a duoset kit (R&D, DY293B-05) as per the manufacturer's instruction. Samples were tested at serial dilutions between concentrations of 16X and 0.25X and the peak reading within the sensitivity of the assay was taken. Protein quantitation was carried out using a colourimetric protein quantitation kit (Bio-Rad, 500-0006EDU) as per the manufacturer's instruction. The amount of protein sequestered by cells in culture was determined by subtracting total protein in each conditioned medium sample from total protein in unconditioned medium. The VEGF-a concentration determined by ELISA was then standardized to sequestered protein for each sample. This was done to control for cell number.

Pharmacological control of permeability

BBB models were prepared as described above. Assemblies were incubated with either VEGF-a at a concentration of 100 ng/ml (as a positive control) or DPSC-conditioned medium for 5.5 h. Cediranib (life research, S1017), a VEGFR2 antagonist was added immediately prior to treatment at a concentration of 10 µM in DMSO. Three replicates from each treatment group were exposed to DMSO only as a negative control. EB-BSA (2 µl) was added to the luminal compartment and assemblies were incubated a further 30 min. The inserts were removed and 2 × 100 µl samples of media from the abluminal compartment were transferred to a 96-well plate. Absorbance was read at a wavelength of 620 nm.

Statistics

Graphpad Prism (V5.04) was used to calculate all statistics. For the in vitro BBB model, the concentration of dye present in the abluminal chamber was determined by interpolating the absorbance within serial dilutions, results were expressed as percentage of maximum equilibration. One-way ANOVA with a Tukey post hoc test was used to compare grouped data. Dose–response assays were assessed by testing the strength of their linear correlation. Normality was confirmed by calculating quantile–quantile plots with the pooled data from each experiment. Power calculations indicate a minimum sample size of three BBB model systems per group is required to detect a 44% difference between groups to account for a standard deviation of 4.15%, with 80% power and 95% confidence. Parameters for this power calculation were set using data obtained from the initial permeability experiment described above.

Results

Characterization of an in vitro BBB model system

Tight junction modulation is the major physiological mechanism underlying changes in BBB permeability. In order to assess the validity of this in vitro BBB model, immunocytochemistry was used to characterize the mechanisms that underlie modulation of permeability (Figure 2(a) to (d)). The tight junction protein occludin appeared to be upregulated when BMECs were co-cultured with astrocytes. However, this failed to reach statistical significance (Figure 2(e)).

To investigate whether this in vitro model could approximate the permeability characteristics of the BBB, three dyes with different molecular sizes were added to the luminal side of the assembly along with VEGF-a, a known inducer of permeability. As shown (Figure 3(a)), EB-BSA was least able to equilibrate under normal conditions. EB-BSA was also the only marker to increase significantly in equilibration when the in vitro model was treated with VEGF-a. Hence, EB-BSA was used as the marker in all subsequent in vitro BBB experiments.

VEGF-a was shown to mediate an increase in permeability of the in vitro BBB model. To determine whether this is dose dependent, a range of concentrations of VEGF-a were added to the luminal compartment of in vitro BBB models. The relationship between VEGF-a concentration and equilibration was subjected to linear regression analysis. As shown (Figure 3(b)), there was a significant positive correlation between VEGF-a dose and permeability.

DPSC mediates an increase in BBB permeability via VEGF-a expression

Next, this in vitro BBB model was used as a permeability assay to investigate whether soluble factors expressed by DPSC were capable of mediating an

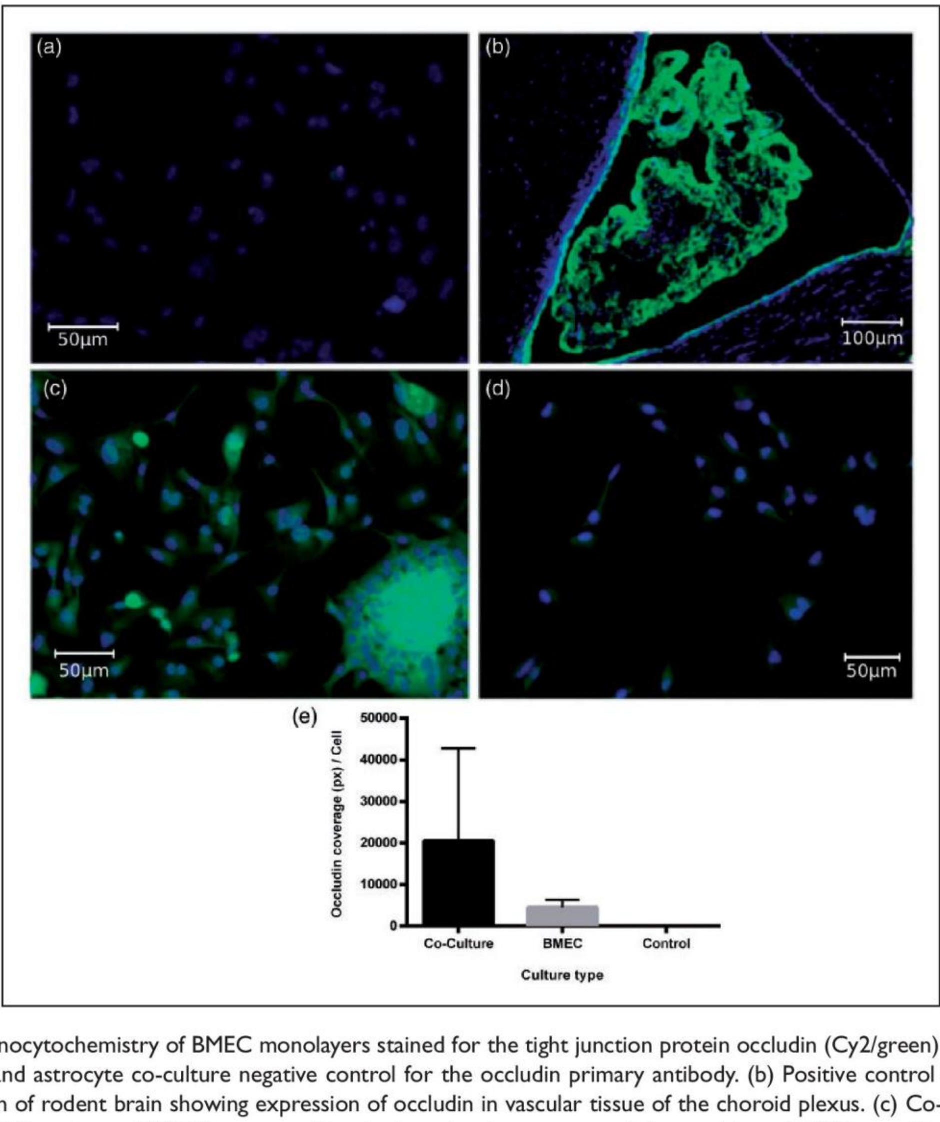

Figure 2. Immunocytochemistry of BMEC monolayers stained for the tight junction protein occludin (Cy2/green) and nuclei (DAPI/blue). (a) BMEC and astrocyte co-culture negative control for the occludin primary antibody. (b) Positive control for the occludin antibody, a section of rodent brain showing expression of occludin in vascular tissue of the choroid plexus. (c) Co-culture of BMECs and astrocytes. (d) Monolayer of BMECs grown without astrocytes. Images a, c and d were taken at 200X magnification, image b was taken at 100X magnification. (e) Quantitation of relative occludin expression for above immunocytochemistry. Error bars depict standard deviation.

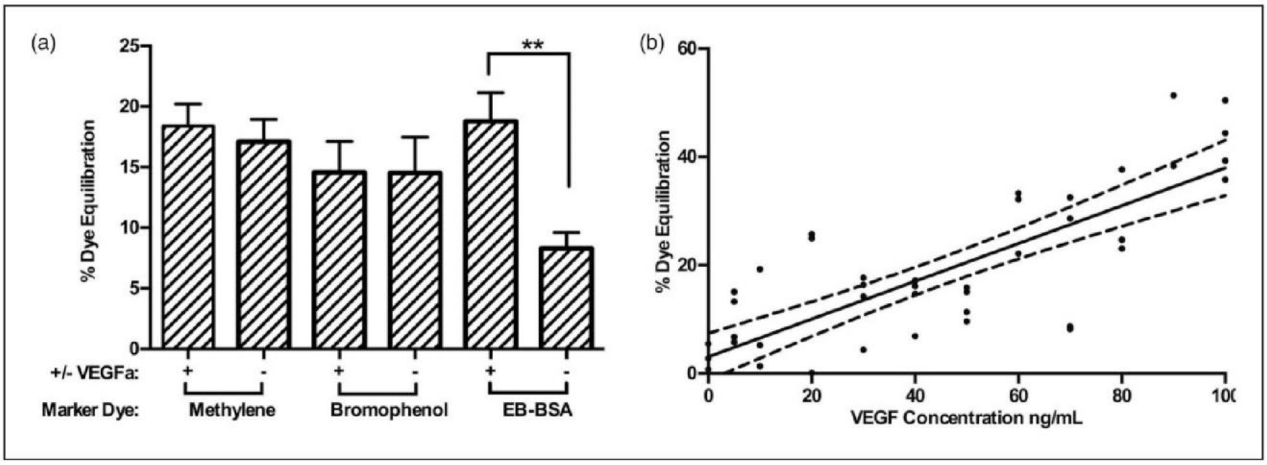

Figure 3. (a) A representation of the percentage of equilibration detected for three markers of different molecular weight with or without 100 ng/ml VEGF-a treatment. Methylene blue = 319 Da, bromophenol blue = 670 Da and EB-BSA = 66,423 Da. For EB-BSA VEGF-a: Control, $P < 0.0001$, $n \geq 5$ experimental replicates per group. Error bars depict standard deviation. (b) The linear association between the concentration of VEGF-a added to the model and the percentage of equilibration. Discontinuous lines show 95% confidence intervals. $P < 0.0001$, $R^2 = 0.64$, $n = 23$ experimental replicates total.

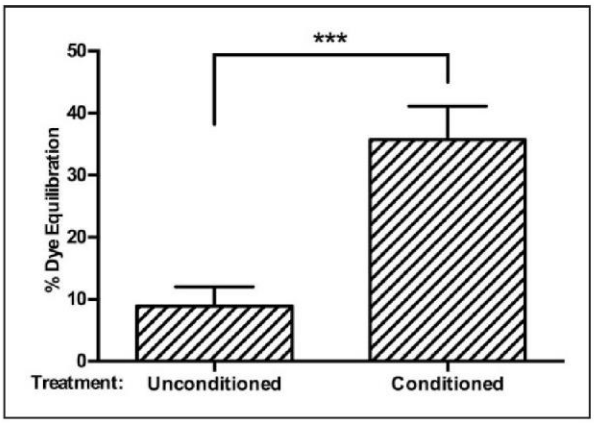

Figure 4. Comparison between the equilibration allowed by barriers treated with DPSC conditioned and identical but unconditioned media. $P = 0.0002$, $n \geq 6$ experimental replicates per group. Error bars depict standard deviation.

increase in permeability. It was found that DPSC-conditioned media caused a statistically significant increase in permeability above unconditioned media (Figure 4).

DPSC-conditioned media caused a significant increase in BBB permeability. To investigate the mechanism by which this downregulation occurred, occludin expression was assessed following treatment with DPSC-conditioned media and VEGF-a. It was shown (Figure 5(a) to (e)) that treatment with both DPSC-conditioned media and VEGF-a caused a similar downregulation in occludin expression in the in vitro BBB and this was found to be statistically significant.

It was necessary to determine whether DPSC expressed VEGF-a in the conditioned media. This was assessed by sandwich ELISA of DPSC-conditioned media. Three samples were taken from each of two separate populations of DPSC. Figure 6(a) demonstrates that VEGF-a was present in the conditioned media at a concentration of 0.33 ng/ml, with a standard error of 0.27 ng/ml. These concentrations have been shown to be biologically relevant.[30]

Next it was investigated whether VEGF-a expression in DPSC-conditioned media was the dominant biological active factor using our in vitro BBB assay. Cediranib, a VEGF-R2 antagonist,[31] was used to block VEGF-a activity. The in vitro BBB was treated with DPSC-conditioned media with or without the addition of cediranib. Recombinant human VEGF-a was used as a positive control. It was found that cediranib significantly attenuated DPSC-mediated BBB permeability by approximately fourfold (Figure 6(b)).

Discussion

In this study the data demonstrate the appropriateness of a previously characterized in vitro model of the BBB for assessing the permeability-mediating potential of soluble stem cell factors in culture medium. Using this model, we have demonstrated that DPSC expresses VEGF-a in biologically significant quantities to mediate an increase in BBB permeability.

The BBB is selectively impermeable to large, polar molecules, though penetration is dependent on a multitude of other factors.[32,33] This is consistent with the findings presented in Figure 3(a), which suggest that the in vitro BBB may be used to assess the ability of substances to diffuse across the BBB. The low level of background penetration may be attributed either

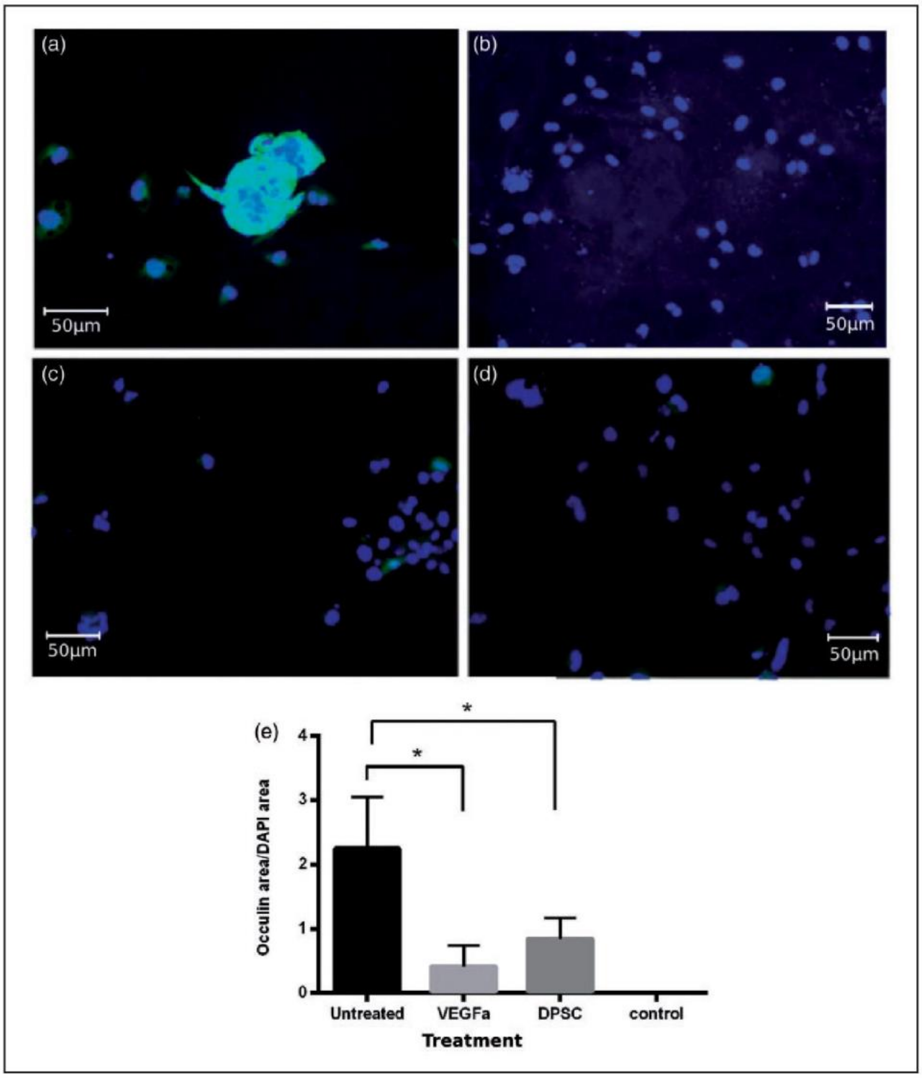

Figure 5. Immunocytochemistry of BMEC monolayers stained for the tight junction protein occludin (Cy2/green) and nuclei (DAPI/blue). (a) Untreated co-culture of BMECs and astrocytes. (b) BMEC and astrocyte co-culture negative control for the occludin primary antibody. (c) Co-culture of BMECs and astrocytes treated with DPSC-conditioned medium. (d) Co-culture of BMECs and astrocytes treated with VEGF-a. The images presented are representative samples from 24 co-cultures examined. Images were taken at 200X magnification. (e) Quantitation of relative occludin expression for above immunocytochemistry. Error bars depict standard deviation.

to perfusion by unbound EB, which has a molecular weight of 960 Da, or to minor discontinuities in the endothelial monolayer. Obviously, molecular size is only one predictor of BBB penetration; other factors include polarity and lipid solubility.[34] This may explain the tendency for methylene blue to equilibrate more readily than bromophenol blue, despite being smaller.

To characterize the molecular mechanisms by which the in vitro BBB may be modulated, occludin expression was studied. Occludin is one of the main components of the tight junction assembly and its expression is therefore characteristic of the BBB.[35] The in vitro BBB was treated with either VEGF-a, DPSC-conditioned media or vehicle and stained for occludin. BMEC grown in co-culture with astrocytes showed greater staining than BMEC grown in isolation. This is consistent with the observation that astrocytes induce and maintain BBB characteristics in BMEC. Co-cultures treated with VEGF-a showed a decrease in expression of occludin. This is consistent with previous studies showing that (i) VEGF-a causes BBB permeability by promoting tight junction dysregulation[21] and (ii) VEGF-a expression is responsible for BBB leakage in the post-ischaemic brain.[20]

It may be noted that in many studies, occludin expression is punctate in appearance and localized at the intersection between endothelial cells. This was not seen in the present study. Localization of occludin to the cell membrane is dependent on phosphorylation by protein kinase C, which appears only to occur in the

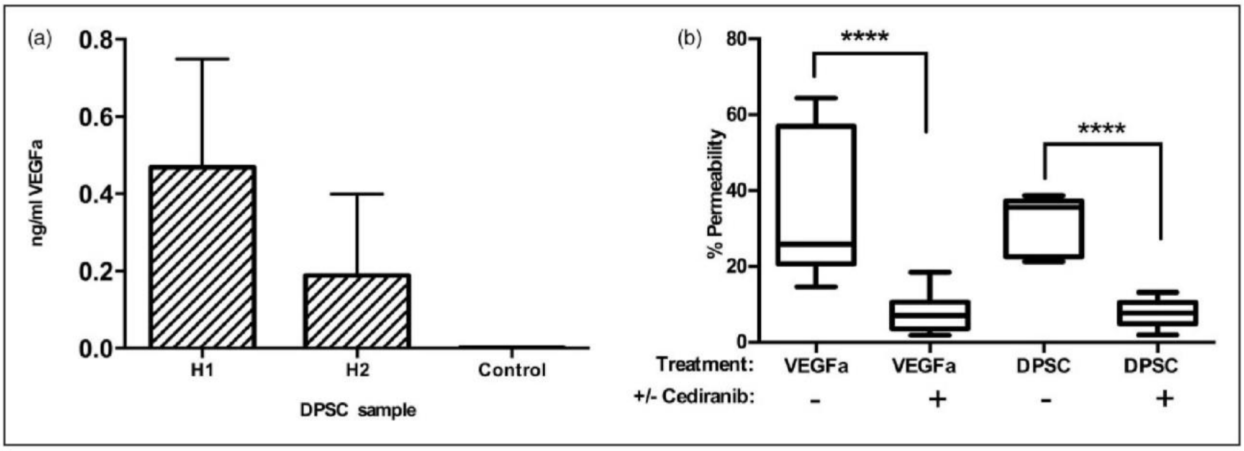

Figure 6. (a) The concentration of VEGF-a detected in DPSC-conditioned media, standardized to total post-culture protein deficit. N = 3 biological replicates per sample. (b) Comparison between in vitro BBB treated with VEGF-a and DPSC-conditioned media, with or without cediranib. N = 9 experimental replicates per group. Error bars depict standard deviation.

presence of the brain extracellular matrix. The cytoplasmic expression of occludin is still an indicator of tight junction regulation.[36,37]

VEGF-a was demonstrated to cause a dose-dependent increase in permeability of the in vitro BBB. This was expected as VEGF-a-mediated BBB permeability is a receptor-mediated response, so incremental increases in VEGF-a concentration should continue to cause increases in permeability until saturation is reached. VEGF-a treatment only took place within a physiologically relevant range and so the dose–response relationship was best described as linear. The correlation between VEGF-a dose and in vitro BBB permeability was moderate. Random error in equilibration was likely due to variance in unmeasured variables such as the final quantity of BMEC adhered to each membrane.

The allocation of individual in vitro BBB assemblies in this exploratory study was not subject to randomization. Operators were also not blinded to the conditions of the experiments. As the factors that contribute to the precision and power of this construct cannot be tested directly, the inclusion of randomization and blinding will improve the strength of conclusions drawn from subsequent investigations.

Occludin expression in response to treatment of the in vitro BBB to DPSC-conditioned media was investigated. The results from this suggest that DPSC expresses soluble factors capable of causing tight junction dysregulation. It was then confirmed that soluble DPSC factors are capable of causing an increase in permeability of the in vitro BBB.

As DPSC caused permeability of the in vitro BBB in a similar manner to VEGF-a, this cytokine was investigated as a major soluble component of the conditioned media from DPSC. VEGF-a was shown by ELISA to be expressed in biologically significant quantities by DPSC, though the amount varied between the two human donors. To determine whether VEGF-a was responsible for inducing permeability, the in vitro BBB was treated with cediranib.[38] Treatment with cediranib significantly attenuated the permeability-inducing effect of DPSC by a factor of four. This suggests that VEGF-a is the major soluble component of DPSC-conditioned media responsible for inducing permeability in the in vitro BBB. These findings are consistent with previous literature implicating VEGF-a in BBB permeability and oedema.[22]

Another possible mechanism to explain neuroendothelial transmigration of stem cells is the interaction between selectins and their endothelial ligands. This is similar to the mechanism involved in leukocyte migration into the parenchyma. Membrane-bound integrins bind to endothelial VCAM-1 and ICAM-1, triggering diapedesis and transmigration. This mechanism was investigated by Rosenblum et al. as an explanation for mesenchymal stem cell migration into the CNS following intra-arterial transplantation.[5] The effects noted by this study may occur downstream of VEGF-a upregulation. VEGF-a has been observed to increase expression of VCAM-1 by vascular endothelial cells,[39] as well as increasing transendothelial migration.[40] It may be the case that trans-neuroendothelial migration of stem cells via selectin–integrin interaction is VEGF-a dependent. In this case, the role of VEGF-a can be considered to be twofold; being both responsible for increasing BBB permeability and stimulating adhesion and transmigration of transplanted stem cells.

Funding

The author(s) disclosed receipt of the following financial support for the research, authorship, and/or publication of this article: The Australian National Health and Medical

Research Council project grant. The Peter Couche Foundation

Declaration of conflicting interests

The author(s) declared no potential conflicts of interest with respect to the research, authorship, and/or publication of this article.

Authors' contributions

JNW was responsible for carrying out all experimental work and data collection in this manuscript, as well as compiling draft versions. KLK was responsible for guidance during design of the experiments described in this manuscript, for aiding in data analysis and for the major revision of content prior to submission. SAK allocated funding support to this project, guided the study design, was responsible for interpretation of results and critically revised drafts of this manuscript. All authors approved this manuscript prior to submission.

References

1. Feigin VL, Forouzanfar MH, Krishnamurthi R, et al. Global and regional burden of stroke during 1990–2010: findings from the Global Burden of Disease Study 2010. *Lancet* 2014; 383: 245–255.
2. Leong WK, Henshall TL, Arthur A, et al. Human adult dental pulp stem cells enhance poststroke functional recovery through non-neural replacement mechanisms. *Stem Cells Transl Med* 2012; 1: 177–187.
3. Lees JS, Sena ES, Egan KJ, et al. Stem cell-based therapy for experimental stroke: a systematic review and meta-analysis. *Int J Stroke* 2012; 7: 582–588.
4. Dharmasaroja P. Bone marrow-derived mesenchymal stem cells for the treatment of ischemic stroke. *J Clin Neurosci* 2009; 16: 12–20.
5. Rosenblum S, Wang N, Smith TN, et al. Timing of intra-arterial neural stem cell transplantation after hypoxia-ischemia influences cell engraftment, survival, and differentiation. *Stroke* 2012; 43: 1624–1631.
6. Li Y and Chopp M. Marrow stromal cell transplantation in stroke and traumatic brain injury. *Neurosci Lett* 2009; 456: 120–123.
7. Martino G and Pluchino S. The therapeutic potential of neural stem cells. *Nat Rev Neurosci* 2006; 7: 395–406.
8. Bang OY, Lee JS, Lee PH, et al. Autologous mesenchymal stem cell transplantation in stroke patients. *Ann Neurol* 2005; 57: 874–882.
9. Giordano A, Galderisi U and Marino IR. From the laboratory bench to the patient's bedside: an update on clinical trials with mesenchymal stem cells. *J Cell Physiol* 2007; 211: 27–35.
10. Kalladka D and Muir KW. Brain repair: cell therapy in stroke. *Stem Cells Cloning* 2014; 7: 31–44.
11. Lemmens R and Steinberg GK. Stem cell therapy for acute cerebral injury: what do we know and what will the future bring? *Curr Opin Neruol* 2013; 26: 617–625.
12. Gronthos S, Mankani M, Brahim J, et al. Postnatal human dental pulp stem cells (DPSCs) in vitro and in vivo. *Proc Natl Acad Sci USA* 2000; 97: 13625–13630.
13. Arthur A, Rychkov G, Shi S, et al. Adult human dental pulp stem cells differentiate toward functionally active neurons under appropriate environmental cues. *Stem Cells* 2008; 26: 1787–1795.
14. Zhang W, Walboomers XF, Shi S, et al. Multilineage differentiation potential of stem cells derived from human dental pulp after cryopreservation. *Tissue Eng* 2006; 12: 2813–2823.
15. Huang GT-J, Gronthos S and Shi S. Mesenchymal stem cells derived from dental tissues vs. those from other sources: their biology and role in regenerative medicine. *J Dent Res* 2009; 88: 792–806.
16. Borlongan CV. Bone marrow stem cell mobilization in stroke: a "bonehead" may be good after all! *Leuk Off J Leuk Soc Am Leuk Res Fund, UK* 2011; 25: 1674–1686.
17. Hill W and Hess D. SDF-1 (CXCL12) is upregulated in the ischemic penumbra following stroke: association with bone marrow cell homing to injury. *Neuropathology* 2004; 63: 84–96.
18. Rubin LL and Staddon JM. The cell biology of the blood-brain barrier. *Annu Rev Neurosci* 1999; 22: 11–28.
19. Shen LH, Li Y, Chen J, et al. Therapeutic benefit of bone marrow stromal cells administered 1 month after stroke. *J Cereb Blood Flow Metab* 2007; 27: 6–13.
20. Sandoval KE and Witt KA. Blood-brain barrier tight junction permeability and ischemic stroke. *Neurobiol Dis* 2008; 32: 200–219.
21. Argaw AT, Gurfein BT, Zhang Y, et al. VEGF-mediated disruption of endothelial CLN-5 promotes blood-brain barrier breakdown. *Proc Natl Acad Sci USA* 2009; 106: 1977–1982.
22. Díaz-Coránguez M, Segovia J, López-Ornelas A, et al. Transmigration of neural stem cells across the blood brain barrier induced by glioma cells. *PLoS One* 2013; 8: e60655.
23. Bronckaers A, Hilkens P, Fanton Y, et al. Angiogenic properties of human dental pulp stem cells. *PLoS One* 2013; 8: e71104.
24. Chopp M and Li Y. Treatment of neural injury with marrow stromal cells. *Lancet Neurol* 2002; 1: 92–100.
25. Niego B, Freeman R, Puschmann TB, et al. t-PA-specific modulation of a human blood-brain barrier model involves plasmin-mediated activation of the Rho kinase pathway in astrocytes. *Blood* 2012; 119: 4752–4761.
26. Dehouck M-P, Jolliet-Riant P, Brée F, et al. Drug transfer across the blood-brain barrier: correlation between in vitro and in vivo models. *J Neurochem* 1992; 58: 1790–1797.
27. Abbott NJ, Hughes CCW, Revest PA, et al. Development and characterisation of a rat brain capillary endothelial culture: towards an in vitro blood-brain barrier. *J Cell Sci* 1992; 37: 23–37.
28. De Vries HE, Blom-roosemalen CM, Van Oosten M, et al. The influence of cytokines on the integrity of the blood-brain barrier in vitro. *J Neuroimmunol* 1996; 64: 37–43.

29. Bicker J, Alves G, Fortuna A, et al. Blood-brain barrier models and their relevance for a successful development of CNS drug delivery systems: a review. *Eur J Pharm Biopharm* 2014; 87: 409–432.
30. Ablonczy Z and Crosson CE. VEGF modulation of retinal pigment epithelium resistance. *Exp Eye Res* 2007; 85: 762–771.
31. Wedge SR, Kendrew J, Hennequin LF, et al. AZD2171: a highly potent, orally bioavailable, vascular endothelial growth factor receptor-2 tyrosine kinase inhibitor for the treatment of cancer. *Cancer Res* 2005; 65: 4389–4400.
32. Mitic LL and Anderson JM. Molecular architecture of tight junctions. *Annu Rev Physiol* 1998; 60: 121–142.
33. Fischer H, Gottschlich R and Seelig A. Blood-brain barrier permeation: molecular parameters governing passive diffusion. *J Membr Biol* 1998; 165: 201–211.
34. Reddy KVR, Reddy V and Loya PC. Molecular aspects of BBB. *Res J Pharm Dos Forms Technol* 2014; 6: 105–109.
35. Ballabh P, Braun A and Nedergaard M. The blood-brain barrier: an overview: structure, regulation, and clinical implications. *Neurobiol Dis* 2004; 16: 1–13.
36. Andreeva AY, Krause E, Müller EC, et al. Protein kinase C regulates the phosphorylation and cellular localization of occludin. *J Biol Chem* 2001; 276: 38480–38486.
37. Savettieri G, Di Liegro I, Catania C, et al. Neurons and ECM regulate occludin localization in brain endothelial cells. *Neuroreport* 2000; 11: 1081–1084.
38. Robertson JD, Botwood NA, Rothenberg ML, et al. Phase III trial of FOLFOX plus bevacizumab or cediranib (AZD2171) as first-line treatment of patients with metastatic colorectal cancer: HORIZON III. *Clin Colorectal Cancer* 2009; 8: 59–60.
39. Kim I, Moon SO, Kim SH, et al. Vascular endothelial growth factor expression of intercellular adhesion molecule 1 (ICAM-1), vascular cell adhesion molecule 1 (VCAM-1), and E-selectin through nuclear factor-kappa B activation in endothelial cells. *J Biol Chem* 2001; 276: 7614–7620.
40. Avraham S, Jiang S, Wang L, et al. VEGF-mediated effects on brain microvascular endothelial tight junctions and transmigration of breast cancer cells across the blood-brain barrier. In: Martin TA and Jiang WG (eds) *Tight junctions in cancer metastasis*. Dordrecht: Springer, 2013.

Chapter 2 Supplementary Discussion

Following publication of this chapter, several points remain to be explored regarding both technical aspects of the study and the clinical implications of its outcomes. Firstly, whilst one of the outcomes of this study was to validate the use of a cross-species co-culture model of the BBB, this facet deserves more explanation. The main conclusion of this paper is that human DPSC can increase permeability across the BBB through a VEGF-dependent mechanism and it was hypothesised that this mechanism would allow DPSC to transmigrate the BBB. One question this raises is whether this VEGF-dependent mechanism manifests as an increase in permeability of existing vessels or as the creation of new cerebral vessels, which are inherently permeable. Whichever mechanism is responsible, it also remains to be discussed that an increase in BBB permeability may also enable the passage of other blood products into the brain parenchyma, which may result in adverse events.

Co-cultures of astrocyte and endothelial cell monolayers are a well-characterised *in vitro* BBB model. This study developed a model using a co-culture of murine astrocytes and human endothelial cells. The main reason for this is that while human endothelial cells are readily accessible, human astrocytes are much more ethically burdensome and difficult to obtain. The BBB is a highly conserved feature[1] and has a similar structure among mammals[2]. We hypothesised that the signalling mechanisms responsible for astrocyte-induced BBB properties in endothelial cells would be similar enough between the two species to allow for sufficient cross-reactivity. While at the time of writing the responsible astrocytic factor has not been determined, we attempted to validate this model empirically. Namely, the co-culture of murine astrocytes with human endothelial cells resulted in an increase in occludin staining (Figure 2). Furthermore, this model was demonstrated to have similar permeability properties to the BBB (Figure 3). Together, these results provide evidence in support of the validity of this cross-species BBB model.

VEGF-a has been shown to increase vessel permeability, but also to stimulate the formation of new vessels. In particular, post-stroke endogenous upregulation of VEGF-a and its receptors is associated with a wave of angiogenesis. These new vessels are more permeable than mature vessels. It is possible that rather than increasing permeability in mature vessels, the VEGF-dependent increase in BBB permeability occurs as a by-product of new vessel formation. It would be possible to address this hypothesis by introducing a condition where endothelial proliferation is inhibited but the other downstream effects of VEGF-a are maintained. For example, raf-1 inhibition would prevent cell cycle stimulation downstream of PCK, while not interacting with the effects of VEGF-a downstream of PI3K. Care must be taken designing such an experiment as at least one raf-1 inhibitor, Sorafenib, also directly blocks VEGFR2[3]. Another hypothesis is that increased permeability in mature vessels is part of the process of angiogenesis that the two possible mechanisms described are components of one single mechanism. Even if DPSC-induced BBB permeability is the result of permeable immature vessels, the outcome of increased BBB permeability remains the same.

The interaction between the peripheral immune system and the brain is highly regulated and was once thought to be completely separate as per the concept of immune privilege. The BBB is largely responsible for limiting access of peripheral immune system components to the brain. If DPSC can transmigrate the BBB by increasing permeability, then this may also allow infiltration of peripheral immune cells. Whether this occurs depends on the duration and extent of BBB ‘opening’. If BBB permeability only increases while in close proximity to transplanted DPSC, then extensive infiltration of other cells is unlikely. However, if DPSC transplantation triggers an extended period of global BBB permeability, then leukocyte infiltration is more likely. This could be determined *in vivo* by measuring the numbers of both DPSC and peripheral immune cells in the brain following intravascular DPSC transplantation. The clinical implication of this are not clear, though neural damage caused by extended exposure to cytotoxic products of immune cells has been linked to several neurodegenerative processes including Alzheimer’s disease, Parkinson’s disease and multiple sclerosis[4]. However, peripheral immune cells already gain access to the brain following stroke[5] and so it is not clear whether any increase in this caused by DPSC transplantation would significantly increase the probability of adverse events. The possibility of exacerbating neural damage by cell-based therapy renders this a critical area for future investigation.

References:

1. **Mayer F, Mayer N, Chinn L, Pinsonneault RL, Kroetz D, Bainton RJ**. Evolutionary Conservation of Vertebrate Blood-Brain Barrier Chemoprotective Mechanisms in Drosophila. *J Neurosci*. 2009;29(11):3538–50.

2. **Rubin LL, Staddon JM**. The cell biology of the blood-brain barrier. *Annu Rev Neurosci*. 1999;22(1).

3. **Wilhelm SM, Carter C, Tang L, Wilkie D, McNabola A, Rong H, et al.** BAY 43-9006 Exhibits Broad Spectrum Oral Antitumor Activity and Targets the RAF / MEK / ERK Pathway and Receptor Tyrosine Kinases Involved in Tumor Progression and Angiogenesis BAY 43-9006 Exhibits Broad Spectrum Oral Antitumor Activity and Targets the Pr. *Cancer Res*. 2004;64(19):7099–109.

4. **Sommer A, Winner B, Prots I**. The Trojan horse - Neuroinflammatory impact of T cells in neurodegenerative diseases. *Mol Neurodegener*. 2017;12(1):1–11.

5. **Jones KA, Maltby S, Plank MW, Kluge M, Nilsson M, Foster PS, et al.** Peripheral immune cells infiltrate into sites of secondary neurodegeneration after ischemic stroke. *Brain Behav Immun*. 2018;67:299–307.

Chapter 3

Title: Adult human dental pulp stem cells express active enzymes capable of digesting perineuronal nets.

Author Names: Joshua N. Winderlich[1] *(corresponding author)*, Karlea L. Kremer[1], Xenia Kaidonis[1], James W. Fawcett[3], Simon A. Koblar[1,2,*] and Jessica Kwok[3,4*].

Laboratory of Origin: Stroke Research Programme

Address: Heart Health Theme, Level 6, SAHMRI, North Terrace, Adelaide SA 5000

Telephone Numbers: 61-400-989-607 (Joshua N. Winderlich); 61-8-8128 4545 (Simon A. Koblar)

Email Addresses:

Joshua N. Winderlich:	joshua.winderlich@student.adelaide.edu.au
Karlea L. Kremer:	karlea.kremer@adelaide.edu.au
Xenia Kaidonis:	x.kaidonis@victorchang.edu.au
James W. Fawcett:	jwf@lists.cam.ac.uk
Simon A. Koblar:	simon.koblar@adelaide.edu.au
Jessica Kwok:	j.kwok@leeds.ac.uk

Author Affiliations:

1) Stroke Research Programme, School of Medicine, University of Adelaide, Adelaide, Australia.

2) Department of Neurology, Queen Elizabeth Hospital, Woodville, Australia

3) John van Geest Centre for Brain Repair, Department of Clinical Neurosciences, University of Cambridge, Cambridge, UK.

4) School of Biomedical Sciences, Faculty of Biological Sciences, University of Leeds, Leeds, UK

*Co-senior authors

Running Title: DPSC digest PNNs

Statement of Authorship

Title of Paper	Adult human dental pulp stem cells express active enzymes capable of digesting perineuronal nets.
Publication Status	☐ Published ☐ Accepted for Publication ☐ Submitted for Publication ☑ Unpublished and Unsubmitted work written in manuscript style
Publication Details	

Principal Author

Name of Principal Author (Candidate)	Joshua Winderlich		
Contribution to the Paper	Study design, experimental work, data analysis, interpretation of results and manuscript production.		
Overall percentage (%)	80		
Certification:	This paper reports on original research I conducted during the period of my Higher Degree by Research candidature and is not subject to any obligations or contractual agreements with a third party that would constrain its inclusion in this thesis. I am the primary author of this paper.		
Signature		Date	15/01/2018

Co-Author Contributions

By signing the Statement of Authorship, each author certifies that:

i. the candidate's stated contribution to the publication is accurate (as detailed above);

ii. permission is granted for the candidate in include the publication in the thesis; and

iii. the sum of all co-author contributions is equal to 100% less the candidate's stated contribution.

Name of Co-Author	Karlea L Kremer		
Contribution to the Paper	Supervision of experimental work, revision of manuscript drafts.		
Signature		Date	12/01/2018

Name of Co-Author	Xenia Kaidonis		
Contribution to the Paper	Revision of manuscript drafts.		
Signature		Date	12/01/18

Please cut and paste additional co-author panels here as required.

Name of Co-Author	James W. Fawcett		
Contribution to the Paper	Allocation of funding support.		
Signature		Date	12/1/2018

Name of Co-Author	Simon A. Koblar		
Contribution to the Paper	Allocation of funding support, supervision of study design, major revision of manuscript drafts.		
Signature		Date	12/1/18

Name of Co-Author	Jessica Kwok		
Contribution to the Paper	Supervision of study design and experimental work, interpretation of results and major revision of manuscript drafts.		
Signature		Date	12/1/2018.

Abstract:

Background: Human dental pulp stem cells (DPSC) are a promising candidate for cell-based therapy following brain injury. DPSC have previously been shown to express the cytokines stromal-derived factor 1 (SDF-1) and vascular endothelial growth factor (VEGF), as well as chemokine receptor type-4 (CXCR4), which allow DPSC to migrate to areas of damage when transplanted into the brain. DPSC also need to express enzymes to facilitate their migration through tissues. Some of the major candidates are members of the enzyme families matrix metalloproteinase (MMP) and a-disintegrin and metalloprotease with thrombospondin motifs (ADAMTS). MMPs and ADAMTSs are capable of degrading the perineuronal net (PNN), a structure important in the control of adult neuroplasticity. To date, the enzymatic profile of DPSC has not yet been fully characterised. The present study aimed to assess the expression of MMPs and ADAMTSs by DPSC and to confirm the biological activity of the expressed enzymes in three *in vitro* settings.

Methods: Enzyme expression was assessed by western blot of DPSC conditioned media. Enzymatic activity was assessed by substrate digestion analysis, gel zymography, *in vitro* brain slice digestion and live-cell digestion assays.

Results: We found DPSC express MMP-1, MMP-2, MMP-7, MMP-8, MMP-9, MMP-13, ADAMTS-4 and ADAMTS-5. DPSC conditioned media was capable of digesting aggrecan, one of the key PNN components. MMP-2 was confirmed to be active by gel-zymography of immunoprecipitated conditioned media samples.

Conclusions: Adult human DPSC express active enzymes capable of degrading PNNs, which may contribute to the efficacy of DPSC transplantation following CNS injury.

Keywords:

Dental pulp stem cells, matrix metalloproteinase, perineuronal net.

Introduction:

Within perivascular niches of adult human teeth reside populations of highly proliferative and multipotent cells of neural crest origin termed dental pulp stem cells (DPSC), first described by Gronthos *et al.* (2000)[1]. We have shown that DPSC populations are present throughout life and maintain their differentiation potential even when isolated from older teeth (unpublished data) These properties, in conjunction with their clinical accessibility and the possibility of auto-transplantation, have made DPSC a promising candidate for cell-based therapy in the field of brain repair.

The initial hypothesis for the mechanism of cell-based therapy was that stem cells transplanted into the damaged brain would replace lost tissue. Several studies have demonstrated the efficacy of DPSC transplantation in animal models of CNS injury[2,3]. In particular, we have observed that following intracerebral transplantation, DPSC will migrate to the ischaemic border zone of an experimental stroke in rats, resulting in significant improvement in functional outcomes[4]. However, only a small population of transplanted cells engraft in the host brain. One of the unsolved puzzles from these investigations is how these small populations contribute to the level of recovery observed.

The current predominant hypothesis is that DPSC enhance functional recovery through the paracrine secretion of soluble products that support endogenous recovery processes. This bystander effect has been attributed to the stimulation of neuroplasticity, angiogenesis, neuroprotection and immunomodulation[5].

We have previously demonstrated that DPSC express VEGFa and SDF-1 at biologically relevant quantities that may influence the way they interact with brain microvascular tissue and migrate to the site of damage[6,7].

Given the ability of DPSC to migrate through the brain parenchyma, it is likely that they would express enzymes capable of degrading the extracellular matrix (ECM) of the brain. One of the key types of ECM component in the brain are the chondroitin sulfate proteoglycans, which are present in the general brain ECM and also assemble into structures called perineuronal nets (PNNs). The PNNs are specialised aggregations of ECM on the surface of sub-populations of neurons, which have been implicated in controlling neural plasticity[8]. The PNNs are distributed as mesh-like structures surrounding primarily inhibitory interneurons of the motor and sensory cortices, the hippocampus and Purkinje neurons of the cerebellar cortex[9]. The molecular structure of the PNNs and the enzymes responsible for their degradation are outlined in figure 1.

Enzymes capable of degrading PNNs include members of the MMP, ADAMTS and hyaluronidase families (figure 1). Healthy dental pulp has been shown to express MMP-1, -2, -13, and -14 at both the RNA and protein level and to produce active MMP-9[10,11] DPSC specifically have been shown to express MMP-1 and MMP-20 during osteogenic differentiation at the levels of RNA and protein synthesis[12,13]. The presence and activity of matrix enzymes produced by DPSC has yet to be fully characterised, particularly in the context of cell-based therapy and enhancement of plasticity.

This study aimed to characterise the expression and activity of enzymes capable of degrading the PNN, which may contribute to the observed functional benefits of DPSC transplantation. These data will contribute towards building a more complete enzymatic profile of DPSC, which may have implications for the use of DPSC in therapy through re-activation of plasticity.

Methods:

DPSC culture:

DPSC (H1-H6) were isolated from healthy donors aged 15-25 years following routine tooth extraction, with human ethics approval from The University of Adelaide. DPSC were cultured in α-modified Eagle's Medium (Sigma, M4526) containing 10mL/L fetal calf serum (FCS), 100U/mL penicillin and 100μg/mL streptomycin (Invitrogen, 15140122) (PS) and 2mmol/L L-glutamine (Invitrogen, 250030081) (DPSC medium). Cells were passaged once 80% confluent.

Conditioned media (CM):

Once DPSC were approximately 80% confluent, cells were washed with PBS and given fresh medium. After 72 hours in culture, the medium was removed and stored at -20^{o}C. Cells were detached and counted using the trypan blue exclusion method to ensure consistency.

HEK cells:

An *in vitro* model of PNNs was used for quick screening. Human embryonic kidney 293T (HEK) cells manipulated to express hyaluronan synthase-3 (HAS3) and cartilage link protein-1 (crtl1) (termed HEK-PNN cells) were used as they produce a dense PNN-like structure[14]. HEK-PNN were cultured in 75cm^2 flasks (Corning) containing 10mL Dulbeco's modified Eagle's medium (Life Technologies, 11995-073) with 10% FCS and PS.

Western blots:

CM samples were concentrated by 10 times using centrifuge filtration columns (Millipore, MILUFC801024). CM samples were loaded into a 4-12% gradient polyacrylamide gel (ThermoFisher, NP0322BOX) and run under reducing conditions. Following transfer, blots were stained with MMP and ADAMTS antibodies (table 1) and visualised by chemiluminescence.

Immunoprecipitation (IP):

CM samples (500µL) were incubated with primary antibodies (table 1) overnight at 4°C on a shaker at 30RPM. Magnetic bead suspensions (Novex, 10004D) were used to sequester immunocomplexes from the solution, as per manufacturer's instructions. Proteins were then eluted using 20µL 0.154mol/L hydrochloric acid, before beads were magnetically separated and the supernatant neutralized with 0.154mol/L sodium hydroxide.

Aggrecan digestion:

Aggrecan (1mg) (Sigma, A1960) was first digested with 1UN of chondroitinase ABC (Sigma, c3667; in 2mL 0.1M ammonium acetate buffer) overnight at 37°C to remove the attached glycosaminoglycans. This was performed to allow MMPs or ADAMTS to act on the core aggrecan protein (figure 1). Aggrecan (1mg) was then added to 200µL of CM and incubated overnight at 37°C on a shaker at 30RPM. Aggrecan fragments were purified by IP using an antibody specific to the aggrecan-G3 domain (table 1). Aggrecan fragments were then separated and detected by Western blot using an aggrecan antibody (table1).

Gel zymography:

CM (15µL) was separated by electrophoresis on a 10% gelatin-polyacrylamide zymography gel (ThermoFisher, EC61752BOX), as per the manufacturer's instructions. Briefly, CM was separated by electrophoresis, the enzyme was then renatured and incubated with enzyme reaction buffer. Active enzyme digests gelatin in situ, leaving the digested area unstained. Following whole-CM zymography, MMP-2 and -8 were purified from CM by IP (table 1) and precipitates were then processed for zymography as above.

Digestion of *in vitro* model of PNNs:

HEK-PNN cells were cultured on glass coverslips until 80% confluent. Media were replaced with 10x CM reconstituted in fresh medium and cells were incubated overnight at 37°C. Fresh medium was used as a control. Live staining of HEK-PNN was then performed with immunocytochemistry (ICC) antibodies described in table 1. Antigen staining intensity and DAPI coverage were quantified algorithmically (Image J version 1.49) using weighted RGB correction.

Brain slice PNN digestion:

Humanely killed mice were scavenged in accordance with The University of Adelaide Animal Ethics Committee requirements. Brains were removed and tissue within 2mm of the coronal suture was sliced into 1mm frontal sections, which were then incubated in CM or unconditioned medium control for 24 hours at 37^oC. Sections were then fixed with 4% paraformaldehyde overnight at 4^oC and snap frozen in Tissue Tek® O.C.T. Due to tissue fragility, digested specimens were sliced at 40µm. Slides were stained with Wisteria *floribunda* agglutinin (WFA), a representative marker of PNNs (table 1) and DAPI.

Statistics:

Graphpad Prism (version 6.05) was used to assess significance, using a one-way ANOVA with Dunnett's multiple comparison test. For the quantitation of HEK-PNN digestion, three experimental repeats were used to detect a 44% difference between groups with a standard deviation of 4.15%, power of 80% and 95% confidence. Assessment was not conducted by a blinded operator.

Results:

DPSC express active enzymes associated with PNN degradation

In order to investigate the enzyme expression profile of DPSC, conditioned media (CM) collected from DPSC culture were interrogated by Western blot (figure 2A). DPSC expressed MMP-1, -2, -7, -8, -9, -13, ADAMTS-4 and ADAMTS-5. No expression of MMP-14, -19 or -20 was observed.

The enzymatic cascades of MMPs and ADAMTS are complex and their activity is tightly controlled. To determine the activity of matrix enzymes expressed by DPSC, the CM was incubated with aggrecan, a core component of PNNs. Following incubation with CM, the digested fragments of aggrecan were immunoprecipitated with an antibody specific to the G3 domain of aggrecan (figure 1B) before being separated by SDS-PAGE electrophoresis. Figure 2B demonstrated that incubation with CM resulted in multiple bands when visualised using an anti-aggrecan antibody. Major digestion products were detected at 42, 31 and 27 kDa, while minor digestion products were detected at 151, 91 and 67 kDa. As fragments were purified by IP using a G3 antibody, these fragments suggest MMP cleavage at multiple sites from the G3 terminus. The band at 244 kDa represents undigested aggrecan backbone protein.

In order to determine the identity of the active matrix-degrading enzymes present in the CM, gelatin zymography was performed (figure 2C). The results from this experiment identified a single band of 72kDa (figure 2). This limits the possibilities to either MMP-2 or MMP-8, which were then isolated by IP and again assessed by zymogram. A band was detected following IP of MMP-2 but not MMP-8 (figure 2C).

Enzymes in DPSC CM degrade the PNN

The above results suggested the presence of active matrix-degrading enzymes in DPSC CM. To assess whether this enzymatic activity was sufficient to degrade the PNN, we tested the activity in two models: 1) an *in vitro* model of the PNN (Kwok *et al*., 2010) and 2) murine coronal cortical.

The cells expressing PNNs in the *in vitro* model were digested with CM for 12 hours. The cells were then stained with WFA and antibodies specific to aggrecan and Crtl1. CM digestion resulted in a significant decrease in WFA staining but no change was detected in aggrecan or Crtl1 (figure 3A-D).

To provide a more complete model of brain matrices, fresh murine coronal cortical tissue sections were digested with DPSC CM. The results showed that WFA staining was reduced upon incubation with DPSC CM (Figure 3E-F). This reduction was not limited to the PNN structure, but extended to the general brain matrix.

Discussion:

We aimed to provide a more complete profile of the enzymes expressed by DPSC. The results demonstrated that DPSC express active soluble enzymes capable of digesting core CSPG protein, one of which was identified as MMP-2. The activity of soluble enzymes expressed by DPSC was shown to be sufficient to digest the PNN both in the *in vitro* HEK cell model and on adult murine coronal cortical tissue slices.

In order to navigate through the ECM after transplantation, DPSC must be equipped with ECM degrading enzymes. To determine which relevant enzymes were expressed by DPSC, a shortlist of enzymes of interest was compiled and assessed for their presence in the CM by Western blot. The results corroborate previous studies demonstrating the expression of MMP-1, -2, -13 and -9[10,11]. In addition, we have demonstrated the expression of MMP-7, -8, ADAMTS-4 and -5. We did not observe the expression of MMP-14 as previously reported by Zheng et al. (2009)[11]. This is unsurprising as MMP-14 is membrane-bound and therefore not expected to be present in CM.

The proteolytic activity of CM was further demonstrated by aggrecan digestion. Results from Western blot showed multiple bands of digestion products, indicating the activity of one or more aggrecan-degrading enzymes in the CM. As aggrecan is a major component of PNNs, these results imply that DPSC may be able to degrade PNNs through the expression of a soluble enzyme.

To identify the enzymes responsible for the detected proteolytic activity, CM was assessed by gelatin zymography. This is relevant because western blot cannot determine whether enzymes have been degraded or whether they are present in an inactive state. Gelatin is a common substrate for the relevant enzymes and their ability to degrade gelatin reflects their ability to degrade PNN components. Gelatin was degraded in a single band at 72 kDa. Of the enzymes detected Western blot, only MMP2 and MMP8 corresponded to this molecular weight. Despite being a similar weight, ADAMTS-5 was not considered as it does not exhibit gelatinolytic activity[15]. CM samples were then purified by IP for MMP-2 and MMP-8 and the resulting protein was again analysed by zymography. Only MMP-2 was able to demonstrate gelatinolytic activity.

It is unlikely that MMP2 is the only active matrix enzyme present in CM, primarily because MMP2 must be activated by other enzymes, such as MMP-1, -3, -7 or -16[16]. It is possible that other MMPs are present in lower concentrations and that these activate MMP2. Gusman *et al.* (2002)[10] identified active MMP-9 expressed in dental pulp, however this was not detected in our investigations. The likely reason for this is that Gusman *et al* (2002)[10] studied dental pulp under inflammatory conditions. It is possible that certain environmental cues are necessary to stimulate the expression of different MMPs by DPSC. The other possibility is that some active MMPs are blocked by tissue inhibitors of metalloproteinase (TIMPs), which the present study did not assess.

The presence and detectable activity of matrix enzymes in CM does not demonstrate that this activity is sufficient to facilitate degradation of brain extracellular matrices. By using HEK-PNN cells, which express a PNN-like structure, we demonstrated that DPSC CM significantly reduced chondroitin sulfate staining on the surface of the cells. However, protein components of PNNs (aggrecan and Crtl1) did not change. The lack of aggrecanase activity is likely due to steric hindrance presented by chondroitin sulfate surrounding the aggrecan core protein. HEK-PNN cells have been previously validated as a human PNN model as they express the key PNN components Crtl-1, aggrecan, hyaluronan and HAS3 in a dense structure morphologically similar to human PNNs[14].

MMP activity was further confirmed on murine coronal cortical tissue sections, which are often used as a model of human PNNs as these structures are highly conserved among many animal species[17–19]. Following 24 hours of digestion in CM, there was an appreciable decrease in WFA staining, which strongly suggests that DPSC express soluble enzymes capable of degrading PNNs and brain matrices. We would contend that this may underlie the migratory ability of DPSC when transplanted into the rodent brain[4].

Condensation of CSPGs into PNNs towards the end of development restricts plasticity in the CNS. Enzymatic digestion of chondroitin sulfate in PNNs reactivates plasticity[8]. In this paper we have demonstrated the ability of DPSC to express enzymes capable of degrading CSPGs. This raises the hypothesis that our findings may underlie therapeutic efficacy of DPSC transplantation observed in animal models of CNS injury[2–4].

Another important implication of these results is that transplantation of DPSC may destabilise existing synapses. The role of PNNs in the adult brain appears to be stabilisation of synapses in network traces for vital lifelong behaviours, skills and memories. For example, the appearance of PNNs after the critical period for speech development is thought to stabilise the neural networks that encode language, so that the skill of language production and interpretation is maintained for life, regardless of ongoing reinforcement. Fear conditioning is another learned behaviour thought to be stabilised by PNNs. An important recent study has demonstrated that enzymatic degradation of PNNs in adult rats erased a long-term conditioned fear response[20]. This suggests that DPSC may also have a destabilising effect on PNN-protected skills and memories. If this is the case, treatment with DPSC may require the addition of interventions to reinforce those skills, behaviours or memories affected by PNN degradation.

Conclusions:

The present study demonstrates for the first time that adult human DPSC express active enzymes that are capable of degrading PNNs. DPSC CM was shown to degrade an in-vitro model of PNNs and to digest aggrecan, a major component of PNNs. Western blot analysis of DPSC CM revealed the expression MMP-1, -2, -13 and -9, ADAMTS-4 and ADAMTS-5. Zymography was used to identify MMP2 in its active form. These findings may underlie the migratory ability of DPSC as well as their possible efficacy in the context of stem cell transplantation following CNS injury.

Abbreviations:

CNS (central nervous system)

DPSC (dental pulp stem cells)

SDF1 (stromal-derived factor 1)

VEGF (vascular endothelial growth factor)

CXCR4 (chemokine receptor type-4)

MMP (matrix metalloproteinase)

ADAMTS (a disintegrin and metalloprotease with thrombospondin motifs)

PNN (perineuronal net)

FCS (fetal calf serum)

PS (penicillin and streptomycin)

CM (conditioned medium)

HAS3 (hyaluronan synthase 3)

Crtl1 (cartillage link protein 1)

ICC (immunocytochemistry)

IHC (immunohistochemistry)

IP (immunoprecipitation)

WFA (Wisteria floribunda agglutinin)

TIMPs (Tissue inhibitors of metalloproteinases)

Declarations:

Funding:

Funding for this study was provided by the Wings for Life Foundation, the European Research Council, the Peter Couche foundation and the University of Adelaide Discipline of Medicine. The funding bodies had no role in study design, data collection, data analysis, interpretation of data or in writing the manuscript.

Ethics Approval and consent to participate:

Human dental pulp stem cells were obtained with ethics approval from the University of Adelaide. Humanely killed mice were scavenged in accordance with The University of Adelaide Animal Ethics Committee requirements.

Consent for publication:

Not applicable.

Availability of data and material:

The datasets generated during this study can be accessed from the figshare repository at the address https://figshare.com/s/765cbb70c0e9ba7fb58a and https://figshare.com/s/05649011e271ef91f15e.

Competing interests:

The authors declare that they have no competing interests.

Author's contributions:

JW conducted all experimental work, data collection and draft composition. KLK contributed to experimental design, data analysis and major revision. XK contributed to data analysis and major revision. JWF contributed to study conception and review of results. SAK contributed to study conception, interpretation of data and major review. JK contributed to study design, data interpretation and major revision. All authors approve publication of this paper.

Figure legends:

Table 1: Antibodies listed were used for western blotting (WB), immunoprecipitation (IP), immunocytochemistry (ICC) and immunohistochemistry (IHC).

Primary antibodies			
Detected component	**Product details**	**Use**	**Dilution**
MMP1	R&D Systems, MAB901	WB	1:500
MMP2	R&D Systems, MAB 902	IP, WB	1:500, 1:200 IP
MMP7	R&D Systems, MAB9071	WB	1:500
MMP8	Abcam, AB81286	IP, WB	1:1000, 1:200 IP
MMP9	Abcam, AB38898	WB	1:1000
MMP13	Abcam, AB39012	WB	1:3000
MMP14	Abcam, AB51074	WB	1:2000
MMP19	Novus, NB600-1518	WB	1:1000
MMP20	Thermo Scientific, Pa5-13188	WB	1:1000
ADAMTS-4	Thermo Scientific, PA1-1750	WB	1:1000
ADAMTS-5	Abcam, ab41037	WB	1:1000
Aggrecan	Millipore, ab1031	ICC, IHC, WB	1:400D1, 1:200(IP)
Aggrecan G3 domain	Thermo Scientific, PA1-1745	ICC, WB, IP	1:400, 1:200(IP)
WFA	Sigma, L1516-2MG	ICC, IHC	1:150
Cartilage link protein	R&D Systems, AF2608	ICC	1:400
Secondary antibodies			
Conjugate	**Product details**	**Antibody**	**Dilution**
Alexa 488	ThermoFisher, S-11223	Streptavidin	1:500
Alexa 568	ThermoFisher, A-11079	Anti-goat	1:500
Alexa 555	ThermoFisher, A-21424	Anti-mouse	1:500
Alexa 488	ThermoFisher A-21204	Anti-mouse	1:500
Alexa 488	ThermoFisher A-21441	Anti-rabbit	1:500

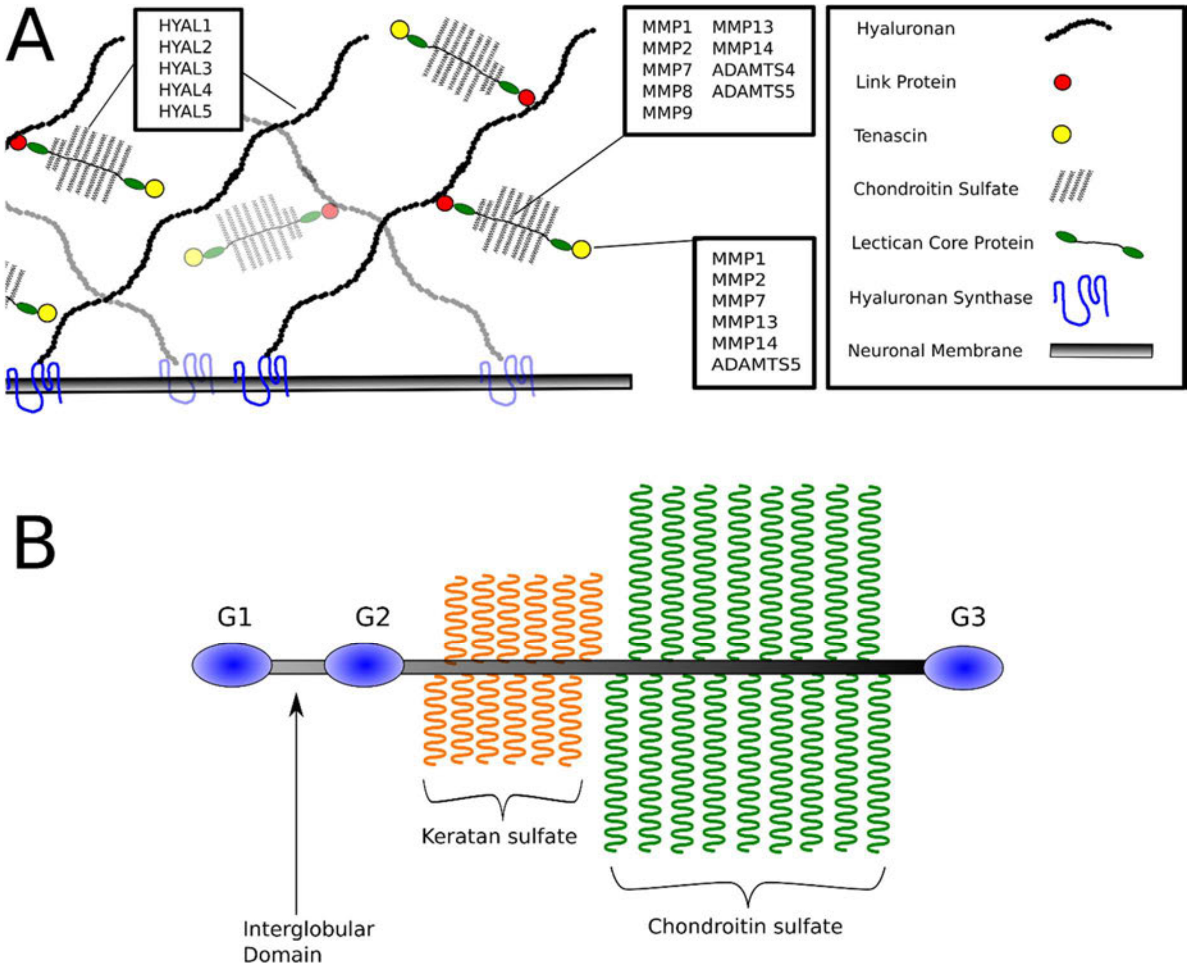

Figure 1: A) PNNs are a dense matrix composed of hyaluronan (HA), which is tethered to neuronal cell membranes by hyaluronan synthase (HAS). Chondroitin sulfate proteoglycans (CSPGs) are bound to HA by cartilage link protein 1 (Crtl-1) or brain link protein 1 (Bral-1). Members of the MMP and ADAMTS families of enzymes are capable of degrading the protein components of the PNN, while chondroitin sulfate and hyaluronan are degraded by members of the hyaluonidase family (HYAL). Adapted from Wang & Fawcett (2012)[21]. B) A schematic showing aggrecan, a widely expressed member of the CSPG family of ECM molecules. Glycosaminoglycan (GAG) chains (chondroitin sulfaste and keratin sulfate) are bound to a protein backbone, which is divided into three globular domains (G1-3), an interglobular domain and a glycosylated region[22].

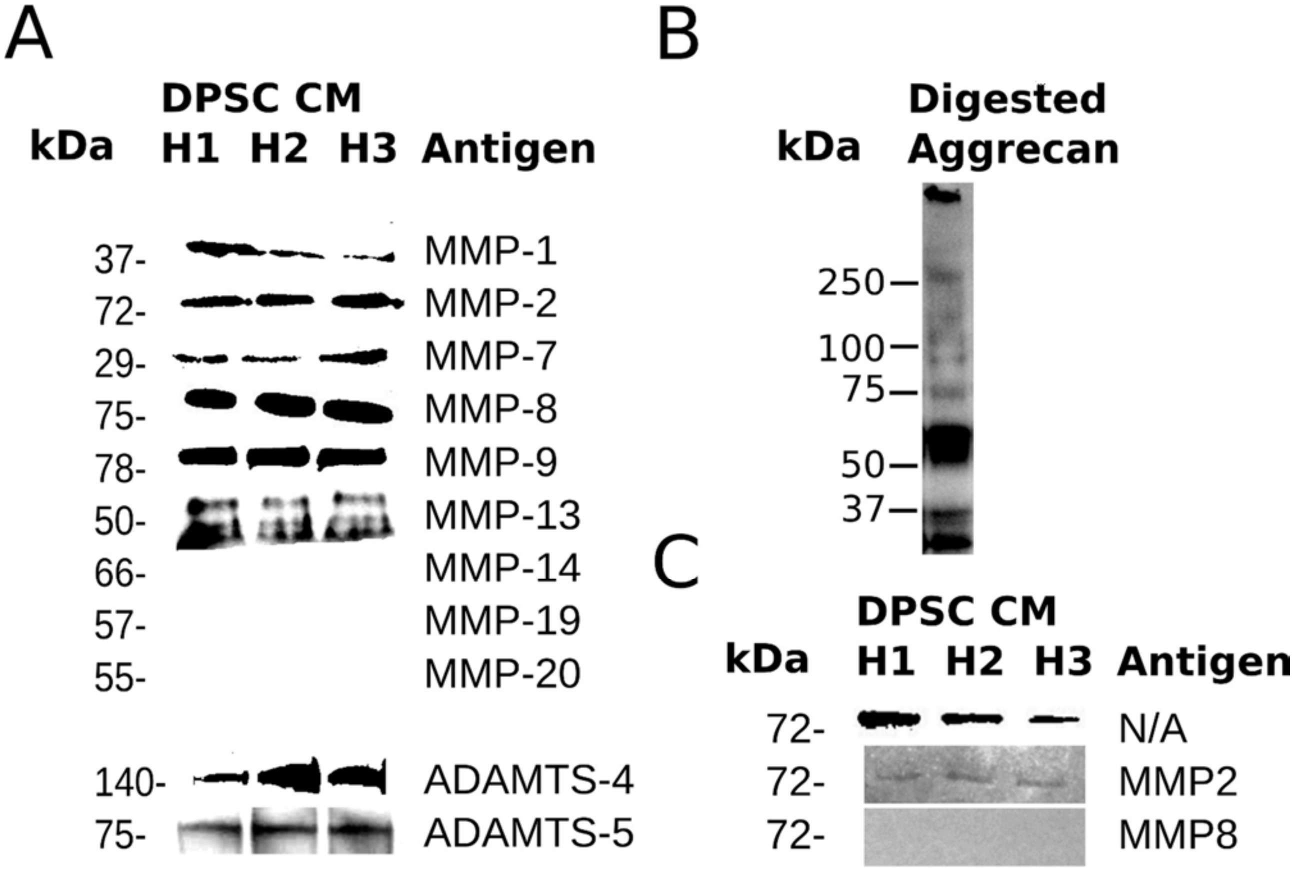

Figure 2: Expression of MMPs in the DPSC CM. A) MMP-1, -2, -7, -8, -9, -13 and ADAMTS-4 and -5 were expressed by the three independent DPSC populations (H1-H3; n=3). B) Representative image of aggrecan digested by the CM (n=9 replicates). C) Zymography was used to demonstrate enzyme activity in whole CM and CM immunoprecipitated MMP-2 (n=3).

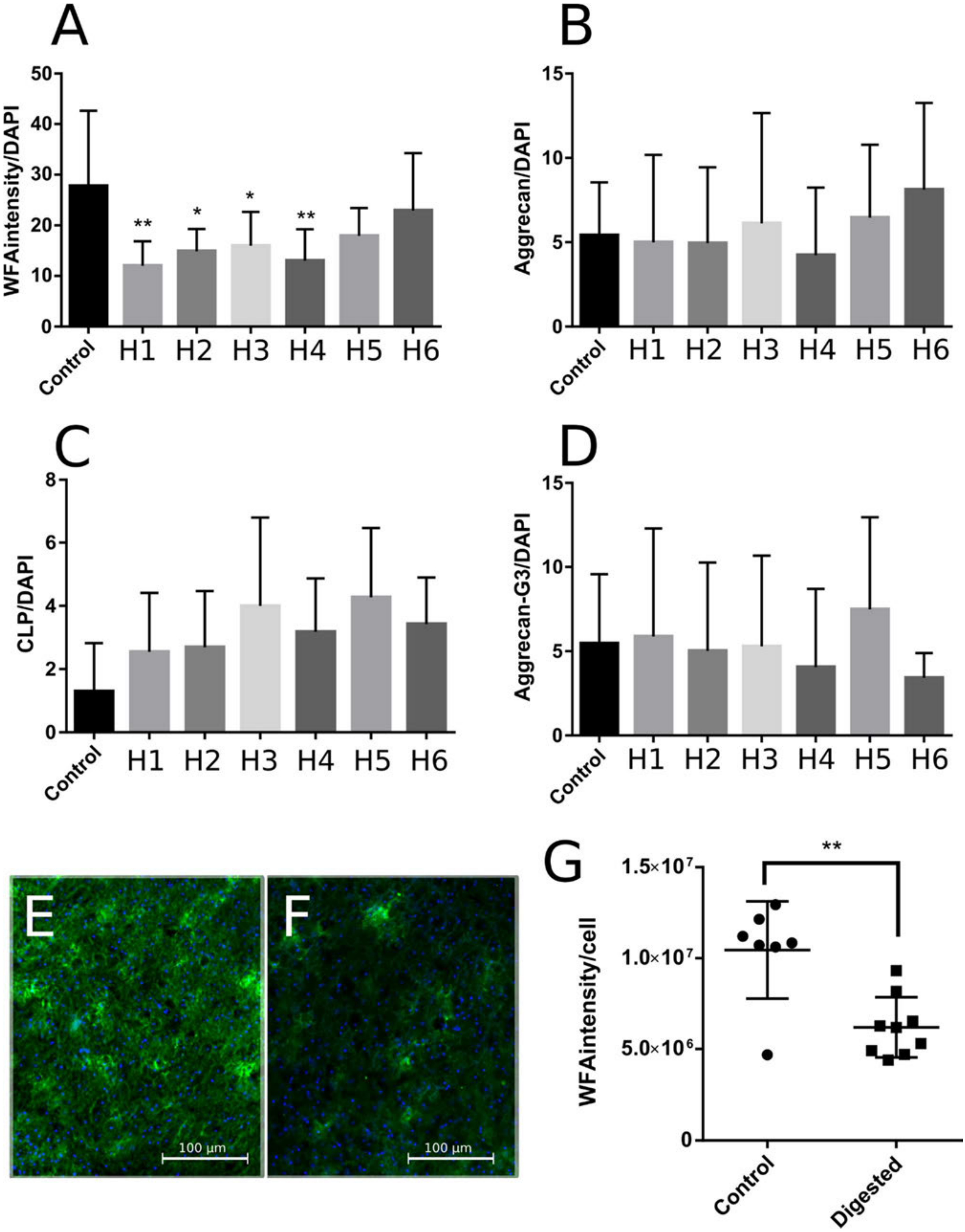

Figure 3: A-D provide a quantification of ICC of HEK-PNN cells digested in CM. N=3 for each DPSC sample (H1-H6). E-F are representative examples from n=9 experimental replicates of murine coronal cortical sections undergone immunohistochemistry showing WFA (green) counterstained with DAPI (blue) following digestion with control medium (E) or CM (F). n=9 experimental replicates. G quantifies the staining intensity of WFA on brain slice sections following digestion with control medium or CM (n=3).

References

1. **Gronthos S, Mankani M, Brahim J, Robey PG, Shi S**. Postnatal human dental pulp stem cells (DPSCs) in vitro and in vivo. *Proc Natl Acad Sci U S A*. 2000;97(25):13625–30.

2. **Sakai K, Yamamoto A, Matsubara K, Nakamura S, Naruse M, Yamagata M, et al.** Human dental pulp-derived stem cells promote locomotor recovery after complete transection of the rat spinal cord by multiple neuro-regenerative mechanisms. *J Clin Invest*. 2012;122(1):80–90.

3. **Sugiyama M, Iohara K, Wakita H, Hattori H, Ueda M, Matsushita K, et al.** Dental Pulp-Derived CD31 $^{-}$ /CD146 $^{-}$ Side Population Stem/Progenitor Cells Enhance Recovery of Focal Cerebral Ischemia in Rats. *Tissue Eng Part A*. 2011;17(9–10):1303–11.

4. **Leong WK, Henshall TL, Arthur A, Kremer KL, Lewis MD, Helps SC, et al.** Human Adult Dental Pulp Stem Cells Enhance Poststroke Functional Recovery Through Non-Neural Replacement Mechanisms. *Stem Cells Transl Med*. 2012;1:177–87.

5. **Leong WK, Lewis MD, Koblar SA**. Concise review: Preclinical studies on human cell-based therapy in rodent ischemic stroke models: where are we now after a decade? *Stem Cells*. 2013;31(6):1040–3.

6. **Arthur A, Shi S, Zannettino ACW, Fujii N, Gronthos S, Koblar SA**. Implanted adult human dental pulp stem cells induce endogenous axon guidance. *Stem Cells*. 2009;27(9):2229–37.

7. **Winderlich JN, Kremer KL, Koblar SA**. Adult human dental pulp stem cells promote blood–brain barrier permeability through vascular endothelial growth factor-a expression. *J Cereb Blood Flow Metab*. 2015;0271678X15608392.

8. **Carulli D, Pizzorusso T, Kwok JCF, Putignano E, Poli A, Forostyak S, et al.** Animals lacking link protein have attenuated perineuronal nets and persistent plasticity. *Brain*. 2010;133(Pt 8):2331–47.

9. **Vo T, Carulli D, Ehlert EME, Kwok JCF, Dick G, Mecollari V, et al.** The chemorepulsive axon guidance protein semaphorin3A is a constituent of perineuronal nets in the adult rodent brain. *Mol Cell Neurosci*. 2013;56:186–200.

10. **Gusman H, Santana RB, Zehnder M**. Matrix metalloproteinase levels and gelatinolytic activity in clinically healthy and inflamed human dental pulps. *Eur J Oral Sci*. 2002;110(5):353–7.

11. **Zheng L, Amano K, Iohara K, Ito M, Imabayashi K, Into T, et al.** Matrix metalloproteinase-3 accelerates wound healing following dental pulp injury. *Am J Pathol*. 2009;175(5):1905–14.

12. **Iohara K, Nakashima M, Ito M, Ishikawa M, Nakasima A, Akamine A**. Dentin Regeneration by Dental Pulp Stem Cell Therapy with Recombinant Human Bone Morphogenetic Protein 2. *J Dent Res*. 2004;83(8):590–5.

13. **Liu J, Jin T, Chang S, Ritchie HH, Smith AJ, Clarkson BH**. Matrix and TGF-β-related gene expression during human dental pulp stem cell (DPSC) mineralization. *Vitr Cell Dev Biol - Anim*. 2007;43(3–4):120–8.

14. **Kwok JCF, Carulli D, Fawcett JW**. In vitro modeling of perineuronal nets: hyaluronan synthase and link protein are necessary for their formation and integrity. *J Neurochem*. 2010;114(5):1447–59.

15. **Tortorella MD, Liu R-Q, Burn T, Newton RC, Arner E**. Characterization of human aggrecanase 2 (ADAM-TS5): substrate specificity studies and comparison with aggrecanase 1 (ADAM-TS4). *Matrix Biol*. 2002;21(6):499–511.

16. **Chandler S, Miller K., Clements J., Lury J, Corkill D, Anthony DC., et al.** Matrix metalloproteinases, tumor necrosis factor and multiple sclerosis: an overview. *J Neuroimmunol*. 1997;72(2):155–61.

17. **Dutheil S, Brezun JM, Leonard J, Lacour M, Tighilet B**. Neurogenesis and astrogenesis contribution to recovery of vestibular functions in the adult cat following unilateral vestibular neurectomy: cellular and behavioral evidence. *Neuroscience*. 2009;164(4):1444–56.

18. **Ueno H, Suemitsu S, Okamoto M, Matsumoto Y, Ishihara T**. Sensory experience-dependent formation of perineuronal nets and expression of Cat-315 immunoreactive components in the mouse somatosensory cortex. *Neuroscience*. 2017;355:161–74.

19. **Cornez G, Madison FN, Van der Linden A, Cornil C, Yoder KM, Ball GF, et al.** Perineuronal nets and vocal plasticity in songbirds: A proposed mechanism to explain the difference between closed-ended and open-ended learning. *Dev Neurobiol*. 2017;77(8):975–94.

20. **Thompson EH, Lensjø KK, Wigestrand MB, Malthe-Sørenssen A, Hafting T, Fyhn M**. Removal of perineuronal nets disrupts recall of a remote fear memory. *Proc Natl Acad Sci*. 2017;201713530.

21. **Wang D, Fawcett J**. The perineuronal net and the control of CNS plasticity. *Cell Tissue Res*. 2012;349(1):147–60.

22. **Yamaguchi Y**. Lecticans: organizers of the brain extracellular matrix. *Cell Mol Life Sci*. 2000;57(2):276–89.

Chapter 4

Title: Spatial and temporal modifications in the expression of perineuronal net components following photochemical stroke in a mouse model.

Authors: Joshua N. Winderlich *(corresponding author)*, Xenia Kaidonis, Karlea L. Kremer, Jessica Kwok and Simon A. Koblar

Laboratory of Origin: Stroke Research Programme

Address: Heart Health Theme, Level 6, SAHMRI, North Terrace, Adelaide SA 5000

Telephone Numbers: 61-400-989-607 (Joshua N. Winderlich); 61-8-8128 4545 (Simon A. Koblar)

Email Addresses:

Joshua N. Winderlich:	joshua.winderlich@student.adelaide.edu.au
Karlea L. Kremer:	karlea.kremer@adelaide.edu.au
Xenia Kaidonis:	x.kaidonis@victorchang.edu.au
Jessica Kwok:	j.kwok@leeds.ac.uk
Simon A. Koblar:	simon.koblar@adelaide.edu.au

Statement of Authorship

Title of Paper	Spatial and temporal modifications in the expression of perineuronal net components following photochemical stroke in a mouse model.
Publication Status	☐ Published ☐ Accepted for Publication ☐ Submitted for Publication ☑ Unpublished and Unsubmitted work written in manuscript style
Publication Details	

Principal Author

Name of Principal Author (Candidate)	Joshua Winderlich
Contribution to the Paper	Study design, experimental work, data collection, interpretation of results and manuscript production.
Overall percentage (%)	70
Certification:	This paper reports on original research I conducted during the period of my Higher Degree by Research candidature and is not subject to any obligations or contractual agreements with a third party that would constrain its inclusion in this thesis. I am the primary author of this paper.
Signature	Date 15/1/2018

Co-Author Contributions

By signing the Statement of Authorship, each author certifies that:

i. the candidate's stated contribution to the publication is accurate (as detailed above);

ii. permission is granted for the candidate in include the publication in the thesis; and

iii. the sum of all co-author contributions is equal to 100% less the candidate's stated contribution.

Name of Co-Author	Xenia Kaidonis
Contribution to the Paper	Experimental work, data collection and revision of manuscript draft.
Signature	Date 12/01/18

Name of Co-Author	Karlea Kremer
Contribution to the Paper	Supervision of experimental work, major revision of manuscript.
Signature	Date 12/01/2018

Please cut and paste additional co-author panels here as required.

Name of Co-Author	Jessica Kwok
Contribution to the Paper	Advised on study design and interpretation of results.
Signature	Date 12/1/18

Name of Co-Author	Simon Koblar
Contribution to the Paper	Allocation of funding support, guidance in study design, interpretation of results and major revision of manuscript drafts.
Signature	Date 12/1/18

Abstract:

Perineuronal nets (PNNs) are specialised regions of condensed extracellular matrix surrounding neuronal cell bodies and proximal processes. The main function of PNNs is to inhibit neuronal reorganisation in adult brains. Ischaemic stroke causes the loss of large numbers of neurons that cannot be fully regenerated, resulting in chronic cognitive and motor/sensory disturbances. The months following stroke are characterised by a limited period of enhanced capacity for neuronal reorganisation and functional recovery. There is limited evidence that this effect is the result of a downregulation of PNN components. The present study aimed to characterise endogenous changes in the expression of key components of PNNs in an experimental model of stroke. Mice were subject to photochemical ischaemia prior to being euthanized at regular intervals up to nine weeks post-stroke. Expression of WFA-binding glycans, aggrecan, chondroitin 4-sulfate (CSA), hyaluronan, cartilage link protein and tenascin-R was assessed in different cortical locations by immunohistochemistry. The results demonstrated that stroke is immediately followed by a downregulation of PNNs in the area contralateral to the lesion and an upregulation of CSA in the ischaemic border zone. WFA and aggrecan staining then increased gradually towards baseline, while CSA staining decreased towards baseline. These results are consistent with the hypothesis that post-stroke enhancement of neuroplasticity is facilitated by temporary endogenous modulation of PNNs.

Introduction

Perineuronal nets (PNNs) are specialised regions of extracellular matrix that predominantly surround the soma and proximal processes of inhibitory interneurons in the cortex, basal nuclei and the spinal cord (Karetko & Skangiel-Kramska 2009; Galtrey et al. 2008). Microscopically, PNNs appear as a mesh surrounding the soma and proximal processes of neurons, interrupted by sites of axonal and glial contact.

At a molecular level, PNNs are composed of hyaluronan (HA) chains tethered to neurons by hyaluronan synthase. Chondroitin sulfate proteoglycans (CSPGs) are bound to HA at their N-termini by cartilage link protein (Crtl1) or brain link protein. Tenascins provide further stability to PNNs by each binding up to three CSPGs at their C-termini (Wang & Fawcett 2012; Yamaguchi 2000).

The physiological function of PNNs is thought to be associated with the inhibition of synaptogenesis and the stabilisation of existing synapses in the adult CNS. The first clue pertaining to the function of PNNs lies in the timing of their appearance during development. This time also marks the termination of a period of enhanced neuroplasticity during which all basic motor and sensory skills must be acquired, termed critical periods (Carulli et al. 2007).

Further evidence for the role of PNNs in inhibiting adult neuroplasticity is demonstrated in animal models. Transgenic mice lacking Crtl1 do not develop mature PNNs and show an extension of the ocular dominance critical period into adulthood as well as spontaneous axonal sprouting into lesioned areas (Carulli et al. 2010). Disruption of PNNs has been achieved in adult animals by treatment with ABC chondroitinase, which digests HA and the glycosaminoglycan (GAG) chains of CSPGs. García-Alías et.al. (2009) showed that treatment with chABC in conjunction with rehabilitation resulted in functional recovery in a rat model of cervical spinal cord injury.

The presence of PNNs alone is not a sufficient predictor of inhibition of neuroplasticity, but rather their specific composition appears to play a significant role in determining function. The sulfation states of GAGs in particular seem to determine their activity. Prior to the termination of critical periods, primordial PNNs contain a high proportion of chondroitin 6-sulfate (CSC) as compared with chondroitin 4-sulfate (CSA) (Carulli et al. 2010). Coinciding with the decrease in plasticity following critical periods, the ratio of CSA:CSC increases (Miyata et al. 2012). Additionally, Miyata and Kitagawa (2012) demonstrated that transgenic animals maintaining a low CSA:CSC ratio show significant delay in the termination of ocular dominance critical periods. This suggests that the presence of PNNs enriched with CSA inhibits neuroplasticity, while those enriched with CSC allow plasticity.

The postulated mechanisms by which PNNs exert their inhibitory effect include the formation of a physical barrier to new synapse formation by occupying areas of neuronal membrane, that PNN components are directly inhibitory against axonal outgrowth and that PNNs sequester and present inhibitory axon guidance molecules (Vo et al. 2013; Apostolova et al. 2006). The role of CSA in PNN activity is likely structural as transgenic mice that maintain a high proportion of CSC fail to develop condensed PNNs (Miyata et al. 2012).

The role of PNNs in the regulation of adult neuroplasticity makes them an attractive therapeutic target for the treatment of ischaemic stroke. The mechanisms of action for all extant stroke therapies rely on minimising the extent of ischaemic damage. Modulation of PNNs may enhance neuroplasticity. In combination with rehabilitation, PNN disruption may allow patients to compensate with existing brain tissue and recover lost function beyond what can be achieved with rehabilitation alone. However, in order to develop this type of therapy, the function of PNNs in the context of ischaemic stroke must first be understood.

There is evidence that PNNs are modified in response to external stimuli. Loss of sensory input and environmental enrichment both cause a decrease in expression of PNNs in specific areas of cortex (McRae et al. 2007; Sale et al. 2007), while damaging stimuli cause a more complex response. The development of a glial scar surrounding the borders of a mature ischaemic lesion has been well-characterised (Hobohm et al. 2005). The components of a glial scar bear a marked resemblance to those of PNNs and perform the same inhibitory function (Harris et al. 2009). However, occurring concurrently with the increase in expression of PNN components in the glial scar, Hobohm et al. (2005) showed a decrease in PNN expression in areas distal to the infarct. This study posited that the loss of PNNs may underlie post-stroke loss of function, however the current understanding of the inhibitory functions of PNNs suggests that this response to stroke may be part of a mechanism to regain function. Similarly, Harris et al. (2009) showed that CSPGs associated with both PNNs and extracellular matrix (ECM) were upregulated in the glial scar surrounding a traumatic brain injury, but downregulated in the distal ipsilateral regions. These findings were corroborated by Karetko-Sysa et.al. (2011), who showed a decrease in PNN density following cortical photothrombosis in rats.

Endogenous modification of PNNs may underlie the observation that stroke patients experience a temporary period of enhanced neuroplasticity. Spontaneous recovery of cognitive and motor-sensory function occurs rapidly in the first few months following a stroke and plateaus thereafter. For example, most recovery from visuospatial neglect occurs within the first 12-14 weeks (Nijboer et al. 2013), recovery of upper limb motor deficits occurs within nine weeks (Jørgensen et al. 1995) and the majority of spontaneous recovery of language function occurs within six weeks (Pedersen et al. 1995). Task-specific rehabilitation can produce further recovery (Tombari et al. 2004), but any abilities that remain lost beyond this initial period do not demonstrate further spontaneous recovery without intervention and are often lost in perpetuity.

Furthermore, Hsu et al. (2005) demonstrated that a unilateral stroke enhanced learning in the contralateral hemisphere in rats. This time course for stroke recovery suggests a *critical period* of enhanced plasticity. Given the function of PNNs and their known propensity to alter in response to changing environmental stimuli, it is possible that post-stroke enhanced neuroplasticity is accommodated by either a global decrease in PNN density or a shift towards a low CSA:CSC ratio.

The literature demonstrates that following focal cerebral injury, inhibitory ECM components are upregulated in the glial scar and downregulated in distal areas. Numerous studies have assessed the expression of different markers of PNNs, including WFA-binding glycans and CSPG core proteins. These studies have used different methods of inducing a focal lesion and have noted a decrease in PNNs up to 14 days after the insult. This study aims to characterise changes in the spatial expression of the major components of PNNs and sulfation of GAGs following stroke and to detect trends in their expression levels over time. This information can be used to inform the design of therapies that target PNNs to improve the functional outcomes of stroke.

Methods

Mice:

Male C57BL6 mice aged six months were obtained through the University of Adelaide Laboratory Animal Services. Approval was granted by the University of Adelaide animal ethics committee (M-2013-166).

Determination of handedness:

Handedness in mouse populations varies with approximately 50% preferring either paw. Handedness was determined for each mouse prior to induction of photochemical ischaemia by using a skilled reaching assembly previously described by Whishaw et al. (1990). Briefly, a small chamber was constructed from opaque acrylic plastic with a transparent window at the front containing a 10mm aperture through which the mice could reach and grasp for pellets of food. The aperture was small enough that only one paw could be used at a time. Mice were fasted overnight prior to testing and then given 20 pellets consecutively. The paw used to grasp the most pellets was recorded as the preferred paw.

Photochemical stroke model:

Ischemic stroke was modeled using the photochemical method described by (Watson et al. 1985). Rose Bengal dye (Sigma, R3877) was prepared fresh as needed at 10mg/mL in normal saline and then filtered through a 0.45um filter (minisart, Sartorius). Mice were administered Rose Bengal solution via an intraperitoneal injection at a dose of 100mg/kg. Ten minutes was allowed for the dye to perfuse into systemic circulation. The mice were anaesthetised with isoflurane in a sealed induction box, then secured in a stereotaxic frame while a maintenance dose of isoflurane was provided via a nose cone. A sagittal incision was made from the interparietal bone to the mid-orbital point to expose the cranium. The stereotaxic frame was used to locate the point 1.5mm lateral to bregma on the side contralateral to the preferred paw. This point lies over the primary motor region for the dominant forepaw. A 500-570nm cold light source at 240 lumens was directed through a 2.5mm aperture centered on the point located. The light source was removed after ten minutes. Mice in the sham stroke group were subject to the same surgical procedure and the same dose of Rose Bengal, but the light source was never switched on. Allocation of mice to stroke or sham group was randomized by computer.

After the procedure, the scalp incision was sutured and treated with topical mupirocin (Bactroban®, GSK). An epidermal injection of 50µl 0.5% bupivacaine hydrochloride was administered at the site of the incision to prevent discomfort. The mice were allowed to recover in a dark, heated box and were given enriched feed. The well-being of the mice was assessed three times daily for the first week post-surgery and daily thereafter until recovery was complete.

Tissue preparation:

A total of 15 mice were humanely killed by deep anaesthesia with isoflurane at one, three, five, seven or nine weeks post-stroke (Figure 1B). Allocation of mice to different time cohorts was not randomized. A longitudinal incision was made from the manubrium to the umbilicus, then the ribs were cut bilaterally at the mid-clavicular line and the diaphragm was removed to expose the mediastinum. A small incision was made in the right ventricle of the heart, while PBS was infused into the left ventrical at constant pressure. When exsanguination was complete, a 4^{o}C solution of 4% paraformaldehyde (PFA) in normal saline was infused into the left ventrical.

The brain was then removed and placed in a solution of 4% PFA in normal saline for 24 hours. The PFA solution was then removed by washing the brain in normal saline three times for 30 seconds. The brain was placed in a solution of 30% sucrose in normal saline for 24 hours to cryopreserve the tissue for sectioning. Brains were sliced into 1mm coronal sections and then snap frozen in O.C.T. compound (Tissue Tek®) for cryosectioning.

Immunohistochemistry:

Slides containing brain sections were washed in 0.03% Triton-X 100 (Sigma, T8787) in phosphate buffered saline (PBS) (washing buffer) three times for five minutes each. Slides were then blocked with 3% normal horse serum in washing buffer (blocking buffer) for one hour at room temperature. Slides being probed for CSA underwent an additional blocking step with 0.1mg/mL unconjugated affinity purified F(ab) fragment anti-mouse IgG in PBS for 30 minutes. After blocking, the slides were incubated with primary antibodies in blocking buffer overnight at 4^{o}C. Control slides were incubated in blocking buffer without primary antibodies. The slides were returned to room temperature over 30 minutes, then washed three times for five minutes each in washing buffer. Secondary antibodies in blocking buffer were applied and slides were incubated at room temperature for two hours. The slides were incubated with DAPI (1x, ThermoFisher, D1306) in blocking buffer for five minutes, then washed three times for five minutes each in washing buffer. Coverslips were applied to the slides with gold antifade mounting medium (ProLong®, ThermoFisher, P36930).

Primary antibodies were chosen to detect chondroitin sulfate A (1:100, United Bio Research, CAC-NU-07-001), aggrecan (1:100, Millipore, AB1031), Cartilage link protein 1 (Crtl1) (1:200, Abcam, ab181997), wisteria floribunda agglutinin (WFA)-binding glycans (1:100, Sigma, L1516-2MG), hyalauronan (1:100, United Bio Research, HKD-BC41) and tenascin-R (1:100, Abcam, ab198863). Secondary antibodies were alexa 488 anti-mouse, Cy3 anti rabbit and strepavidin-conjugated alexa 548.

Microscopy:

Panoramic micrographs of each brain slice were taken at 40x magnification. Microscopy was conducted with a Nikon® Eclipse Ni-E microscope and micrographs were captured using a Nikon® DS-Qi2 camera. Exposure time and excitation intensity were set using staining control slides and were kept constant for each antibody combination.

Quantitation and statistics:

Quantitation of micrograph data was done using ImageJ (version 1.49, NIH). Coronal brain section micrographs were divided into sections representing the infarct core, the ischaemic border zone (IBZ), the ipsilateral hemisphere and the equivalent areas in the contralateral hemisphere. The infarct core was outlined manually and was defined by the border of the acellular region. The IBZ was defined as an area 1.5 times as large as the infarct core, beginning at the outer edge of the cortex. The cortex was defined as the rest of the cortex not included in the infarct core or IBZ. The equivalent areas on the contralateral hemisphere were identified by transposing a horizontally mirrored version of the selection mask onto the unaffected hemisphere. These areas are outlined in Figure 1A.

DAPI staining was used to determine a cell count within each area of the brain slices. Mask thresholds and particle parameters were kept constant for all images. Staining intensity for each of the PNN components was determined within each area of the brain slices. While outcome assessment was mainly algorithmic, this was not conducted by a blinded operator.

Statistical analyses were carried out using Prism (version 7.02, Graphpad). Comparisons between the control group and post-stroke time points were assessed by two-way ANOVA with a Tukey post-hoc test.

Results:

Histological outcomes of photochemical ischaemia:

A total of 15 mice were used in this study. The original project design called for the confirmation of stroke induction by observing circling behavior and limb paresis, however the majority of mice did not display obvious signs of stroke. Therefore, all mice were included in the study and presence of an infarct was confirmed later by histology.

Characteristic changes were seen in DAPI staining of cortical tissue from all mice that underwent photochemical ischaemia. Tissue corresponding to the area of illumination became anuclear by seven days post-infarct. The ischemic core was replaced by a cavity 21 days post-infarct and showed some contraction when compared to earlier samples. From 35 days onward, the lesions had contracted significantly and were surrounded by scar tissue that was denser than the surrounding parenchyma. These changes are evident in Figures 2-7.

Changes in the spatial expression of PNN components:

The expression of total PNNs following photochemical ischaemia was visualised using WFA lectin histochemistry (Figure 2). In the sham stroke group, WFA-binding GAGs were strongly expressed in two cortical layers. Staining morphology revealed punctate PNNs surrounding soma and short neurite segments on a background of diffuse staining consistent with loose ECM. One week following photochemical ischaemia, individual PNNs were no longer visible in either cortex. Dense staining was seen within the infarct, but this did not suggest expression surrounding cells with neuronal morphology and appeared to be associated with necrotic debris. By three weeks a region of dense WFA staining was visible in the perilesional region. From five weeks onwards, PNNs appeared first in areas distant to the infarct. By week nine, normal PNN distribution was seen throughout the cortex.

Aggrecan is the most ubiquitous CSPG component of PNNs. Immunohistochemistry was conducted to visualise the response of aggrecan to photochemical ischaemia (Figure 3). In the sham group, aggrecan was strongly expressed in two cortical layers, which is similar to the staining pattern of WFA. Dense, punctate regions of aggrecan surrounded the soma and proximal processes of cells with a neuronal appearance in these cortical regions. Following stroke, aggrecan-containing PNNs were completely abolished in both cortices and diffuse staining was also reduced. There was some dense staining with non-neuronal morphology within the lesion that was not consistent with PNNs. Aggrecan-containing PNNs were visible again from week five post-stroke, being denser in the contralesional cortex. By nine weeks post-stroke, aggrecan-containing PNNs of normal morphology were plentiful in both hemispheres, but appeared sparser in the region surrounding the infarct.

CSA is the type of CSPG GAG sidechain most inhibitory to neurite outgrowth and synaptic plasticity. Immunohistochemistry was used to assess CSA expression following photochemical ischaemia (Figure 4). Compared with WFA and aggrecan, CSA staining was diffuse and did not demonstrate a punctate, neuronal morphology. One week after photochemical ischaemia, CSA expression was more intense in the IBZ and was still diffuse. By three weeks post-stroke hyperintense perilesional staining had taken on a spiculated appearance, with expression suggesting projections radiating out from the infarct. Over the course of the study, CSA staining intensity in the IBZ decreased towards baseline.

Crtl1 is a critical component of PNNs that links CSPGs with their hyaluronan scaffold. Immunohistochemistry was used to investigate Crtl1 expression following photochemical ischaemia (Figure 5). In the sham group, Crtl1 staining was seen throughout the cortical layers. Dense Crtl1 staining surrounded soma, but there was no visible staining of neurites. Crtl1-containing PNNs were abolished in weeks 1-3, with some nonspecific staining within the lesion boundary. At five weeks post-stroke, PNNs containing Crtl1 were apparent in the contralesional hemisphere, but were still absent in the ipsilesional hemisphere. At nine weeks post-stroke, Crtl1 staining revealed only sparse PNNs visible in the ipsilesional hemisphere.

Tenascin-R is a stabilising component of PNNs that binds the C-termini of CSPGs. Immunohistochemistry was used to characterise changes in Tenascin-R expression following photochemical ischaemia (Figure 6). In the sham group, tenascin-R staining was diffuse and did not reveal a characteristic PNN morphology. Staining intensity appeared to be globally upregulated in weeks 1-3 post-stroke. From week five onwards, Tenascin-R staining intensity was indistinguishable from baseline and no change in morphology was seen.

Chains of hyaluronan anchor to neuronal cell membranes and form scaffolds for the other PNN components. Hyaluronan binding protein was used to visualise changes in hyaluronan expression following photochemical ischaemia (Figure 7). In tissue from the sham group, hyaluronan staining was diffuse and was not specifically associated with soma or neurites. No change in staining intensity or morphology was seen in weeks 1-3 post-stroke. In one sample, hyaluronan staining intensity in the perilesional region appeared to increase at five weeks, but this was not consistent. Staining in weeks 7-9 post-stroke was indistinguishable from the sham group.

Quantitation of Immunohistochemistry

Two-way ANOVA demonstrated a significant decrease in aggrecan staining in the area contralateral to the ischaemic core and IBZ at early post-stroke time points, as compared with the control group. This was followed by an increase in aggrecan staining at later time points. CSA staining intensity was significantly increased in the IBZ of early post-stroke mice (Figure 8).

Discussion:

This study aimed to characterise changes in the expression of key PNN components following an experimental model of focal ischaemic stroke in mice. The results indicate that following stroke, there is an acute and temporary decrease in the expression of Crtl1, aggrecan and other WFA-binding glycans in the area contralateral to the ischaemic core. Whilst no significant increase in aggrecan or WFA binding glycans was detected in the IBZ, there was a marked enrichment of CSA in this area. Over the course of observation, WFA binding glycans and aggrecan increased towards baseline levels. CSA expression in the IBZ decreased towards baseline. This study did not identify any change in the expression of hyaluronan, or TNR.

WFA binds GAG chains associated with ECM and is commonly used as a marker for PNNs. This stain does not enable interrogation of the specific composition of PNNs, but provides an overview of PNN density. Global WFA staining appeared to diminish one week post-stroke as compared with the control group and morphologically characteristic PNNs were almost completely abolished (figure 2). Statistical analysis of quantitation determined that diminished WFA staining at week one was only significant in the areas contralateral to the ischaemic core and IBZ (Figure 8), though there was a tendency towards this change in all areas. Over time, WFA staining increased towards baseline. In sham group tissue, PNNs surrounded the soma and proximal neurites of cells in two distinct cortical layers, which is consistent with previous descriptions of PNN distribution (Karetko-Sysa et.al. 2011; Karetko & Skangiel-Kramska 2009). These findings suggest a temporary decrease in the expression of PNNs after ischaemic stroke, which may be more pronounced in the contralesional homotopic region.

Aggrecan core protein is the most ubiquitously expressed of the CSPGs, which comprise the major functional components of PNNs. Expression of aggrecan decreased during weeks 1-3 post-stroke (figure 3). Interestingly, most of the reduction in aggrecan expression was seen in the area contralateral to the infarct core and IBZ (Figure 8). This is consistent with previous findings that demonstrated a decrease in cortical expression of aggrecan following photochemical infarction (Karetko-Sysa et al. 2011) and focal traumatic brain injury (Harris et al. 2009), which shares a similar pathophysiological course with ischaemic stroke. The gradual return to baseline expression levels of aggrecan is also consistent with these previous findings, though our results suggest that this occurs over a period of nine weeks as opposed to the 14-30 days. Possible reasons for this discrepancy are species differences and differences in lesion methodology. Harris et al. (2009) investigated aggrecan in a rat model, while Karetko-Sysa et al. (2011) used a variation of the photochemical ischaemia protocol with a smaller aperture and a longer illumination time. Given that aggrecan is a widely expressed member of the family of CSPGs that are essential components of PNNs, our results suggest that cerebral ischaemia is followed by an acute, temporary decrease in cortical PNN density contralateral to the lesion.

CSA is the main neurite-outgrowth inhibitory GAG component of PNNs and a low CSA:CSC ratio is associated with increased neuroplasticity (Carulli et al. 2010; Miyata et al. 2012). Cortical expression of CSA in the sham group showed a similar pattern to WFA, though at higher magnification CSA staining surrounding soma was more diffuse and did not have an obvious branching morphology (Figure 4). This is similar to the appearance of CSA expression in the brains of adult rats (Foscarin et al. 2017). Following stroke, a marked enrichment of CSA was detected in the IBZ (Figure 8). In weeks 1-3 post-stroke, distinct regions of CSA associated with soma were no longer visible in either cortex, though this effect was not robust enough to be detected by quantitation. CSA enrichment in the IBZ decreased towards baseline over the course of the study. As CSA is inhibitory to neurite outgrowth, its enrichment in the IBZ may represent a component of glial scars. These structures develop in the regions surrounding infarcts and are inhibitors of neurite outgrowth containing some of the same CPSGs as PNNs (McKeon et al. 1999; Harris et al. 2009). This hypothesis could be tested by assessing colocalization of CSA and glial fibrillary acidic protein (GFAP) in the IBZ following stroke, as GFAP is a marker of gliosis. Previous studies have also demonstrated an enrichment of CSC and 4,6-O-CS (CSE) in the glial scar following TBI (Gilbert et al. 2005). It is likely that as in the developing brain, the ratio of these CS subtypes may underlie the inhibitory capacity of the glial scar.

Crtl1 is a critical component of PNNs and its expression appears to trigger PNN formation in development (Kwok et al. 2010; Carulli et al. 2010). Results from immunohistochemistry of sham stroke mouse brains show pan-cortical expression of Crtl1 (Figure 5). Dense regions of staining surrounded soma but did not appear to surround dendrites. These formations were obliterated following stroke and returned first in the contralesional hemisphere after 5 weeks. Punctate Crtl1 staining in the region surrounding the stroke was visible after nine weeks, but did not appear as intense as the contralesional cortex. These changes in expression were a qualitative impression only as the staining method was not sufficiently robust to demonstrate the effect quantitatively.. These results reflect an effect demonstrated by Carulli et al. (2010), who showed that sensory deprivation of mice caused a reversible decrease in Crtl1 expression. In the present study, ipsilesional reduction of Crtl1 may be caused by deafferentation of brain regions that received inputs from the infarcted region.

TN-R facilitates cross-linking of lecticans, which stabilises PNNs. Its expression forms a major step in the maturation of PNNs in development (Guntinas-Lichius et al. 2005). Results from immunohistochemistry did not demonstrate a change in TN-R following photochemical infarction (Figures 6,8). As TN-R has an affinity for CSPG core proteins, it was expected that TN-R staining would follow the same post-stroke pattern of attenuation as aggrecan. One reason this was not seen may be that its association with loose ECM masked changes in its expression within PNNs. This hypothesis is consistent with the diffuse staining pattern of TN-R (Figure 6).

Hyaluronan is the major structural component of PNNs. It is attached to neuronal cell membranes through hyaluronan synthases and provides a loose scaffold onto which CSPGs can bind and organise into a dense lattice. Staining intensity appeared to increase following stroke, particularly in the IBZ (Figure 7), though this did not reach statistical significance (Figure 8). Earlier findings also showed that hyaluronan expression was upregulated following stroke, though these results were obtained through western blot rather than immunohistochemistry (Al Qteishat et al. 2006). One reason that significant changes in hyaluronan-containing PNNs were not detected is that hyaluronan staining was very diffuse and did not clearly localize to PNNs (Figure 7). Staining for hyaluronan synthases instead may provide better imaging for quantitation as these proteins localise to cell membranes (Al Qteishat et al. 2006). Additionally, changes in PNNs may occur independently of hyaluronan as this is not an active contributor to neurite outgrowth inhibition. Hyaluronan alone is not sufficient for functional PNNs and it has been shown to be present in inactive PNN precursors (Kwok et al. 2010; Carulli et al. 2007).

The ability of this study to resolve smaller changes in the expression of hyaluronan, Crtl1 and TNR could be improved with a larger sample size at early time points. To provide adequate data for analysis by ANOVA, data were grouped into control, weeks 1-3, weeks 5-7 and week 9. While this provided a robust analysis of long-term trends, it also meant a loss of temporal resolution.

It has been observed that stroke patients experience a temporary increase in neuroplasticity that conveys the potential for rapid functional recovery (Bonita & Beaglehole 1988; see Murphy & Corbett 2009; Dimyan & Cohen 2011 for review). The main function of PNNs is to inhibit neuroplasticity and artificial removal of PNNs results in a period of increased neuroplasticity like that seen in juveniles prior to the termination of critical periods (Soleman et al. 2012; Carulli et al. 2007; García-Alías et al. 2009). The present study demonstrated a temporary downregulation of aggrecan and other WFA-binding components of PNNs. Therefore, a likely hypothesis is that the period of increased plasticity that accompanies recovery from ischaemic stroke is the result of a decrease in the expression of these components. In particular, the marked reduction in aggrecan expression in the contralateral hemisphere may represent a mechanism to compensate for lost cortical regions by relocating their function to their contralateral equivalent. This phenomenon of function relocation has been observed in functional MRI studies of stroke patients (Carey et al. 2002; Abo et al. 2001; Staudt 2002). Furthermore, artificial disruption of PNNs after stroke has been shown to increase branching from the contralesional hemisphere (Soleman et al. 2012). The role of endogenous PNN alteration in cortical function relocation remains to be investigated.

This study characterised spatial and temporal changes in the expression of PNN components following focal ischaemic stroke in mice. Specifically, staining for WFA binding glycans and aggrecan underwent modifications consistent with decreased inhibition to neuronal plasticity. These changes may underlie a mechanism for a temporary post-stroke enhancement of neuroplasticity. Future research into potential stroke therapies should focus on extending the post-stroke period of enhanced neuroplasticity. This may be achieved by artificially enhancing the endogenous post-stroke reduction in PNN density observed here. Current methods for achieving this include digestion with ABC chondroitinase (Soleman et al. 2012; García-Alías et al. 2009) or members of the matrix metalloproteinase family (our unpublished results). This strategy has the potential to improve the potential for recovery of neurological function following stroke.

Figure Legends

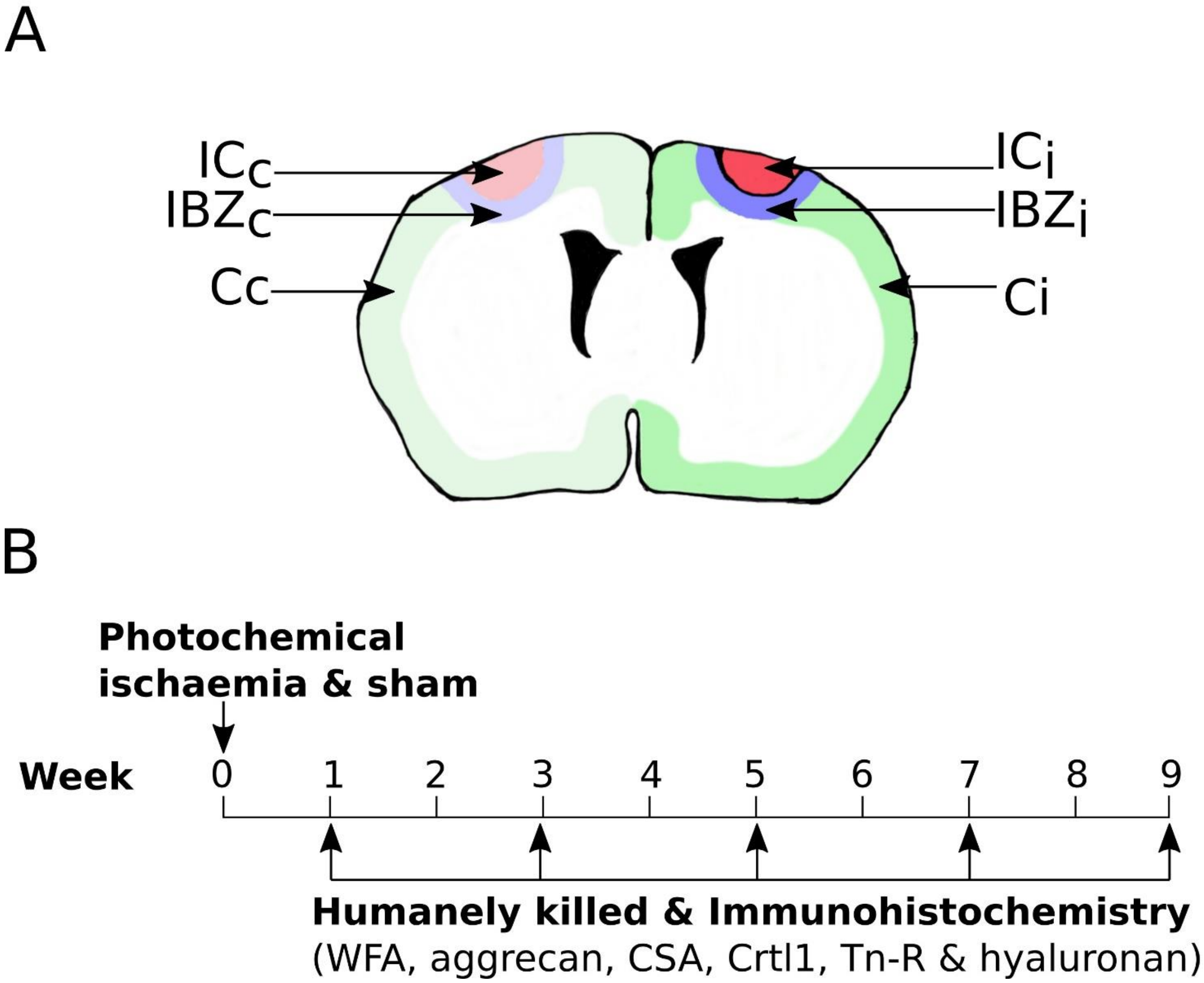

Figure 1: A) Coronal brain sections were divided into areas for quantitation and analysis. ICc is the area contralateral to the infarct core, IBZc is the area contralateral to the ischaemic border zone, Cc is the contralateral cortex, ICi is the infarct core, IBZ is the ischaemic border zone and Ci is the ipsilateral cortex. As the infarct core is acellular, this area was left out of analysis. B) Experimental timeline. Mice were humanely killed 1, 3, 5, 7 and 9 weeks after photochemical ischaemia or sham surgery. Brains were then sectioned and stained for PNN components.

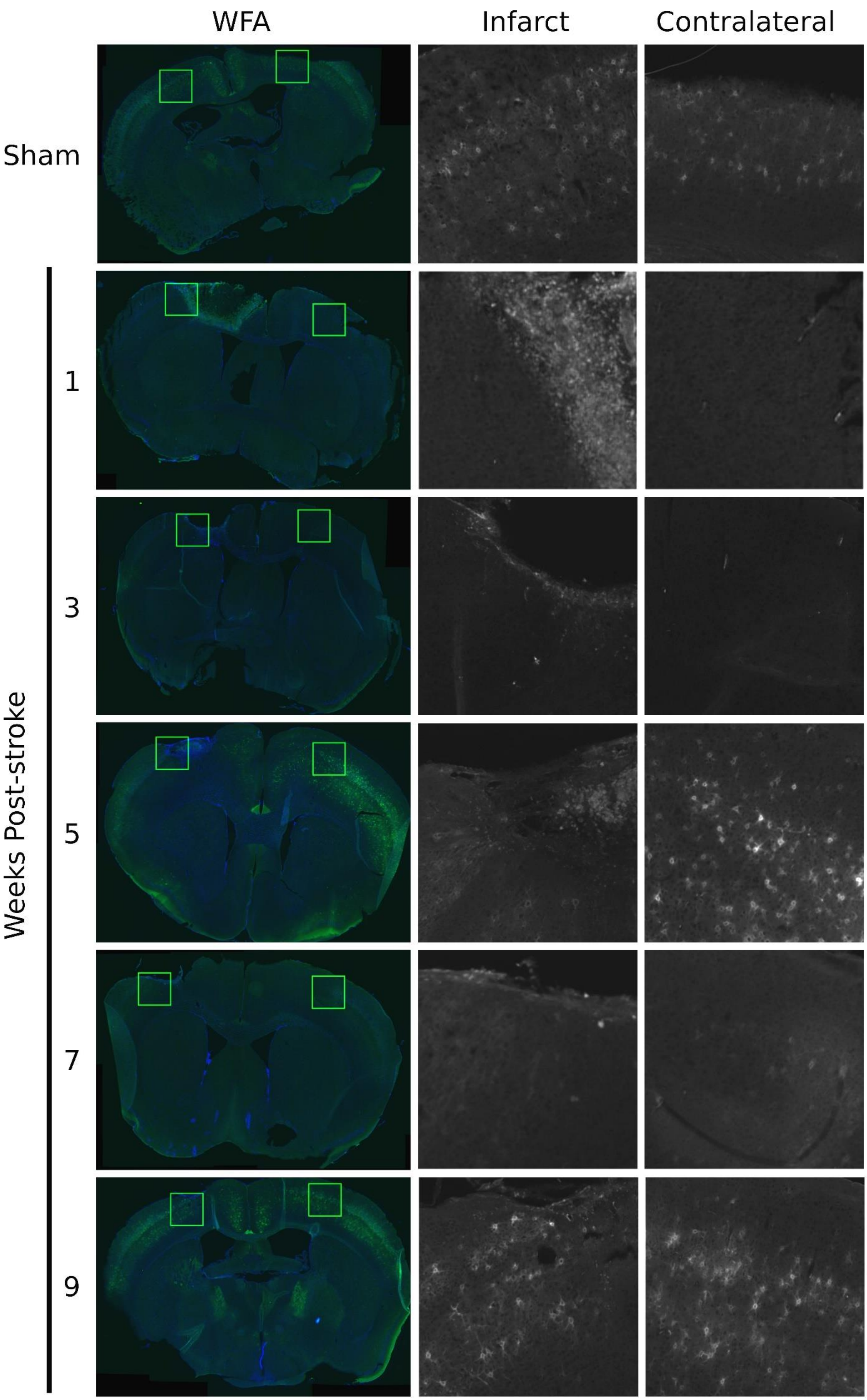
WFA
Infarct
Contralateral
Sham
Weeks Post-stroke
1
3
5
7
9

Figure 2: Distribution of total PNNs following photochemical ischaemia. PNNs were detected through their WFA-binding lectin component (green) and nuclei were detected with DAPI (blue). Photochemical lesions are located on the left of each section. Higher power magnifications of WFA staining of the infarct and the contralateral cortex are displayed in greyscale to improve visual contrast. The locations of the higher-power magnification images are indicated by green boxes in the low-power counterstained images. Images are representative of n=5 in the sham group, n=3 at week 1, n=1 at week 3, n=3 at week 5, n=3 at week 7 and n=6 at week 9.

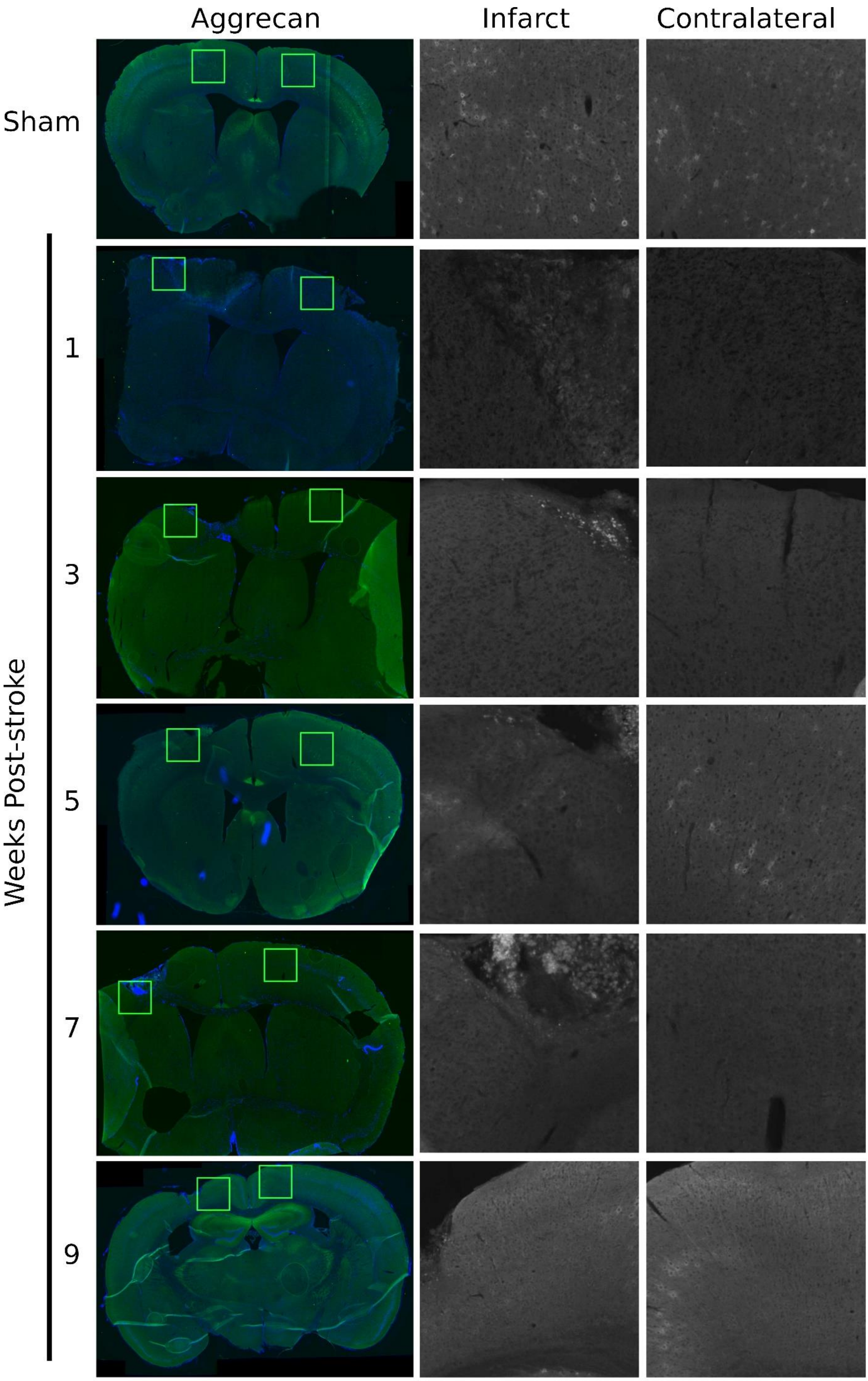
Aggrecan
Infarct
Contralateral
Sham
Weeks Post-stroke
1
3
5
7
9

Figure 3: Response of aggrecan core-protein expression to photochemical ischaemia. Immunofluorescence staining shows aggrecan (green) and DAPI (blue). Photochemical lesions are located on the left of each section. Higher power magnifications of aggrecan staining of the infarct and the contralateral cortex are displayed in greyscale to improve visual contrast. The locations of the higher-power magnification images are indicated by green boxes in the low-power counterstained images.. Images are representative of n=5 in the sham group, n=3 at week 1, n=1 at week 3, n=3 at week 5, n=3 at week 7 and n=6 at week 9.

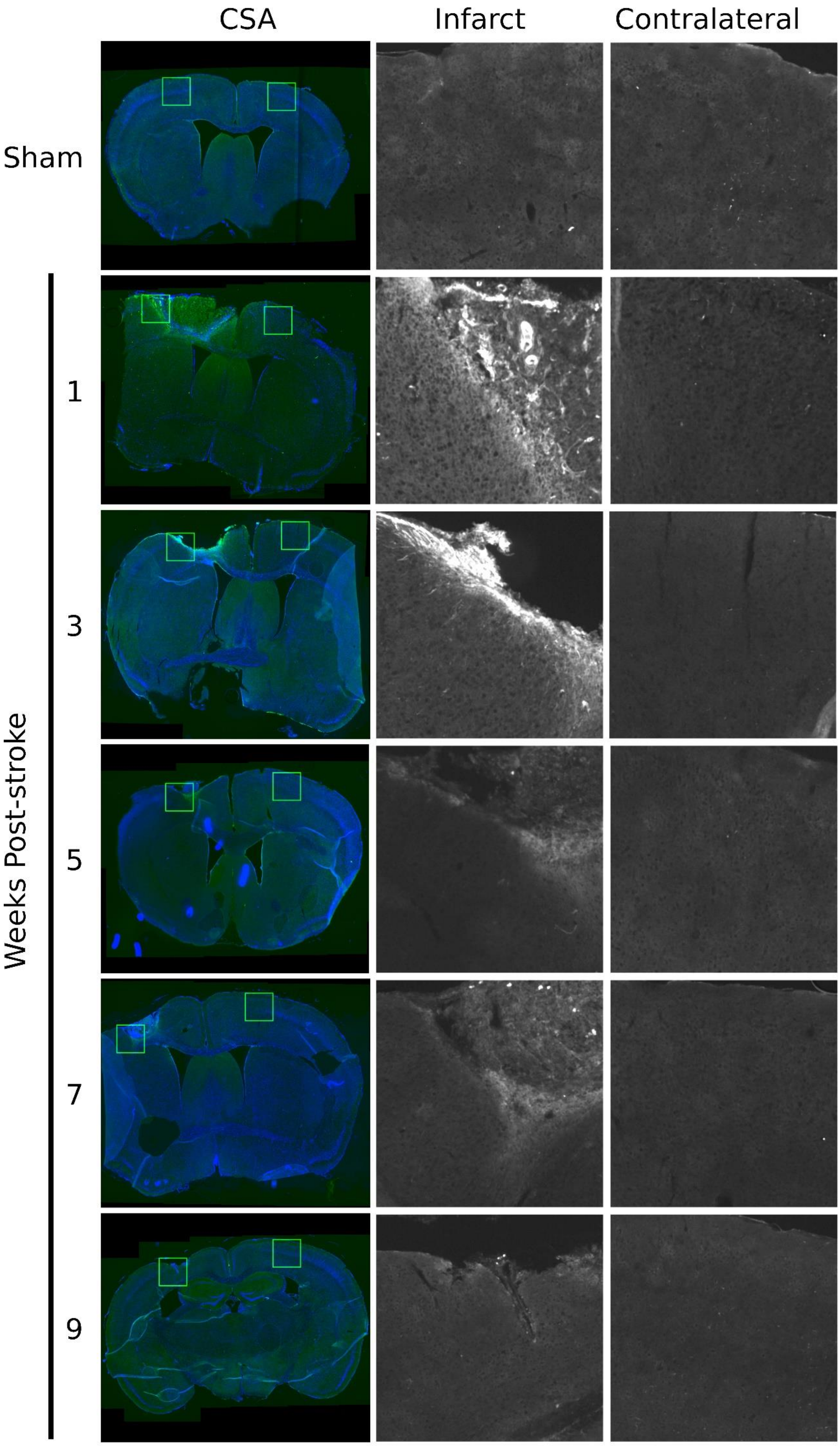
CSA
Infarct
Contralateral
Sham
Weeks Post-stroke
1
3
5
7
9

Figure 4: Expression of 4-O-sulfated chondroitin (CSA) following photochemical ischaemia. Immunofluorescence staining shows CSA (green) and DAPI (blue). Photochemical lesions are located on the left of each section. Higher power magnifications of CSA staining of the infarct and the contralateral cortex are displayed in greyscale to improve visual contrast. The locations of the higher-power magnification images are indicated by green boxes in the low-power counterstained images.. Images are representative of n=5 in the sham group, n=3 at week 1, n=1 at week 3, n=3 at week 5, n=3 at week 7 and n=6 at week 9.

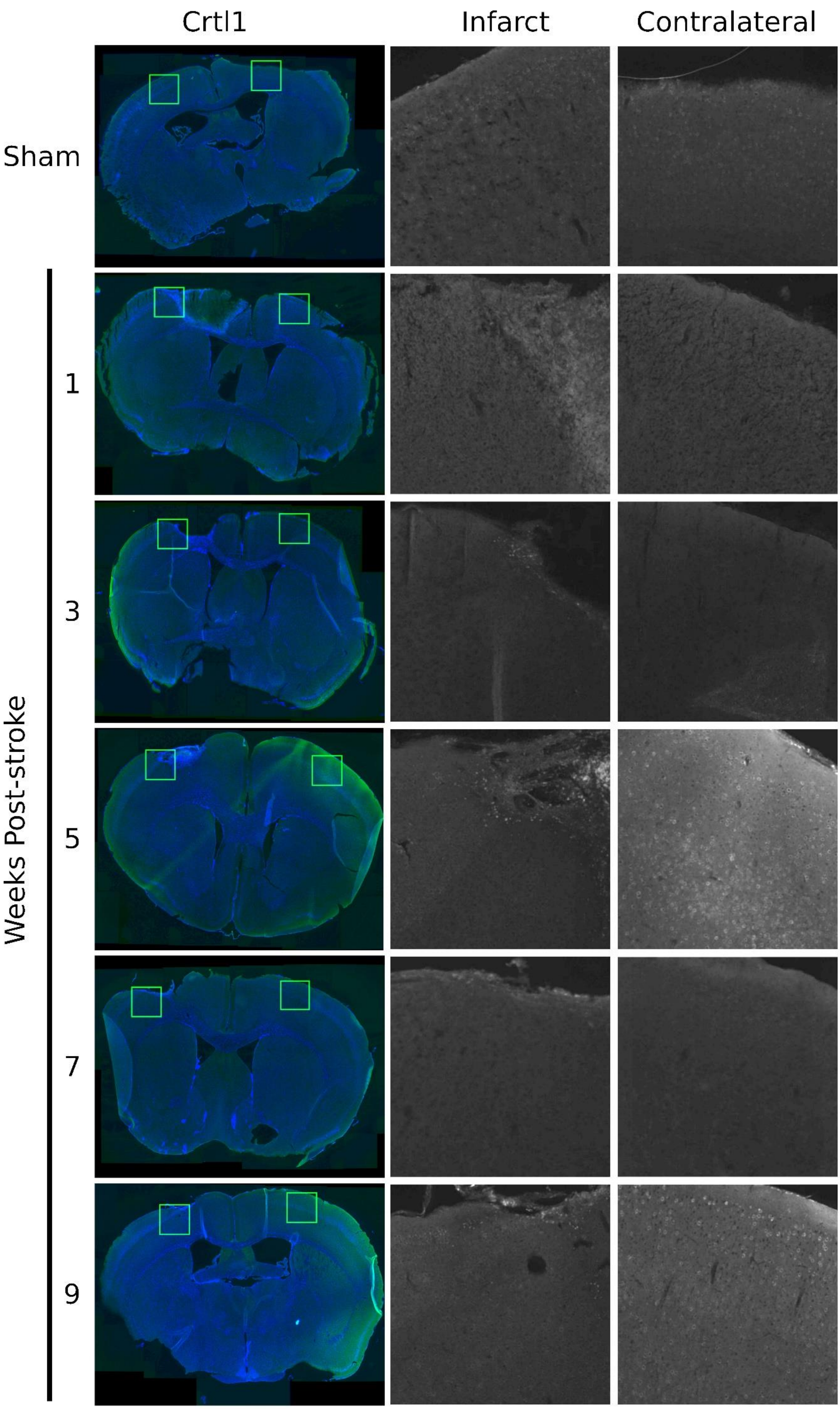
Crtl1
Infarct
Contralateral
Sham
Weeks Post-stroke
1
3
5
7
9

Figure 5: Expression of Crtl1 following photochemical ischaemia. Immunofluorescence staining shows Crtl1 (green) and DAPI (blue). Photochemical lesions are located on the left of each section.
Higher power magnifications of Crtl1 staining of the infarct and the contralateral cortex are displayed in greyscale to improve visual contrast. The locations of the higher-power magnification images are indicated by green boxes in the low-power counterstained images.. Images are representative of n=5 in the sham group, n=3 at week 1, n=1 at week 3, n=3 at week 5, n=3 at week 7 and n=6 at week 9.

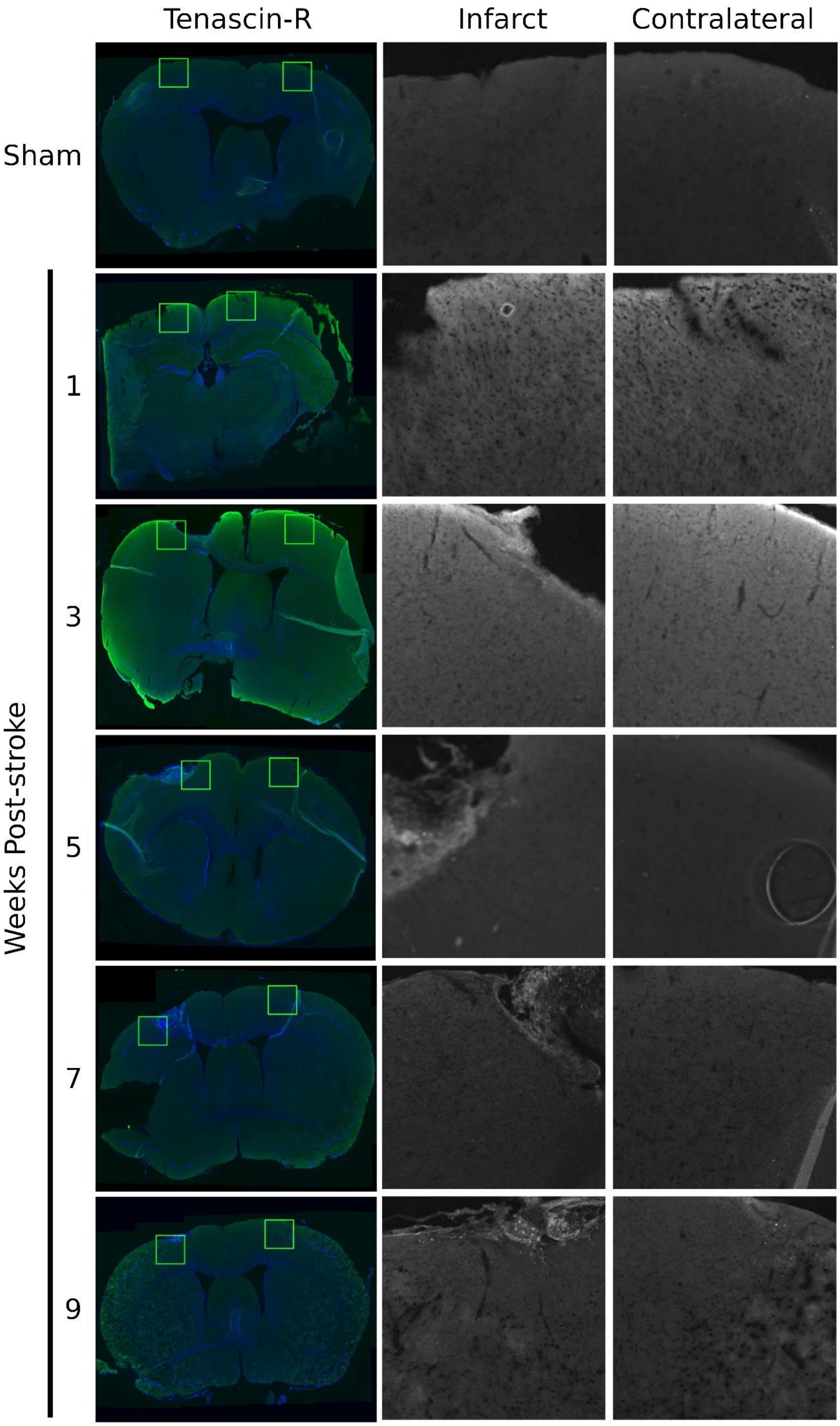
Tenascin-R
Infarct
Contralateral
Sham
Weeks Post-stroke
1
3
5
7
9

Figure 6: Expression of Tenascin-R following photochemical ischaemia. Immunofluorescence staining shows Tenascin-R (green) and DAPI (blue). Photochemical lesions are located on the left of each section. Higher power magnifications of Tenascin-R staining of the infarct and the contralateral cortex are displayed in greyscale to improve visual contrast. The locations of the higher-power magnification images are indicated by green boxes in the low-power counterstained images.. Images are representative of n=5 in the sham group, n=2 at week 1, n=1 at week 3, n=3 at week 5, n=3 at week 7 and n=6 at week 9.

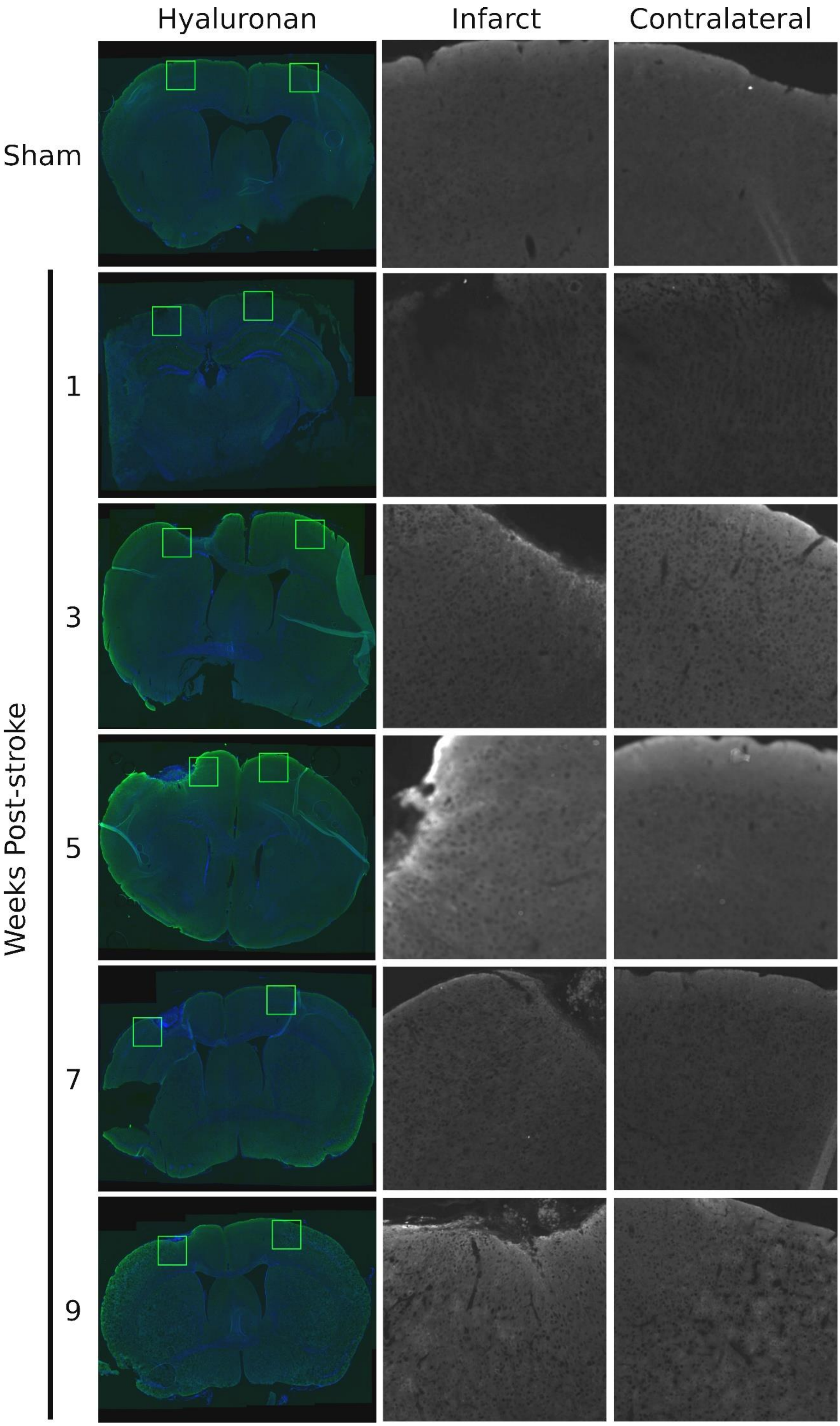
Hyaluronan
Infarct
Contralateral
Sham
Weeks Post-stroke
1
3
5
7
9

Figure 7: Expression of hyaluronan following photochemical ischaemia. Immunofluorescence staining shows hyaluronan (green) and DAPI (blue). Photochemical lesions are located on the left of each section.
Higher power magnifications of hyaluronan staining of the infarct and the contralateral cortex are displayed in greyscale to improve visual contrast. The locations of the higher-power magnification images are indicated by green boxes in the low-power counterstained images.. Images are representative of n=5 in the sham group, n=2 at week 1, n=1 at week 3, n=3 at week 5, n=3 at week 7 and n=6 at week 9.

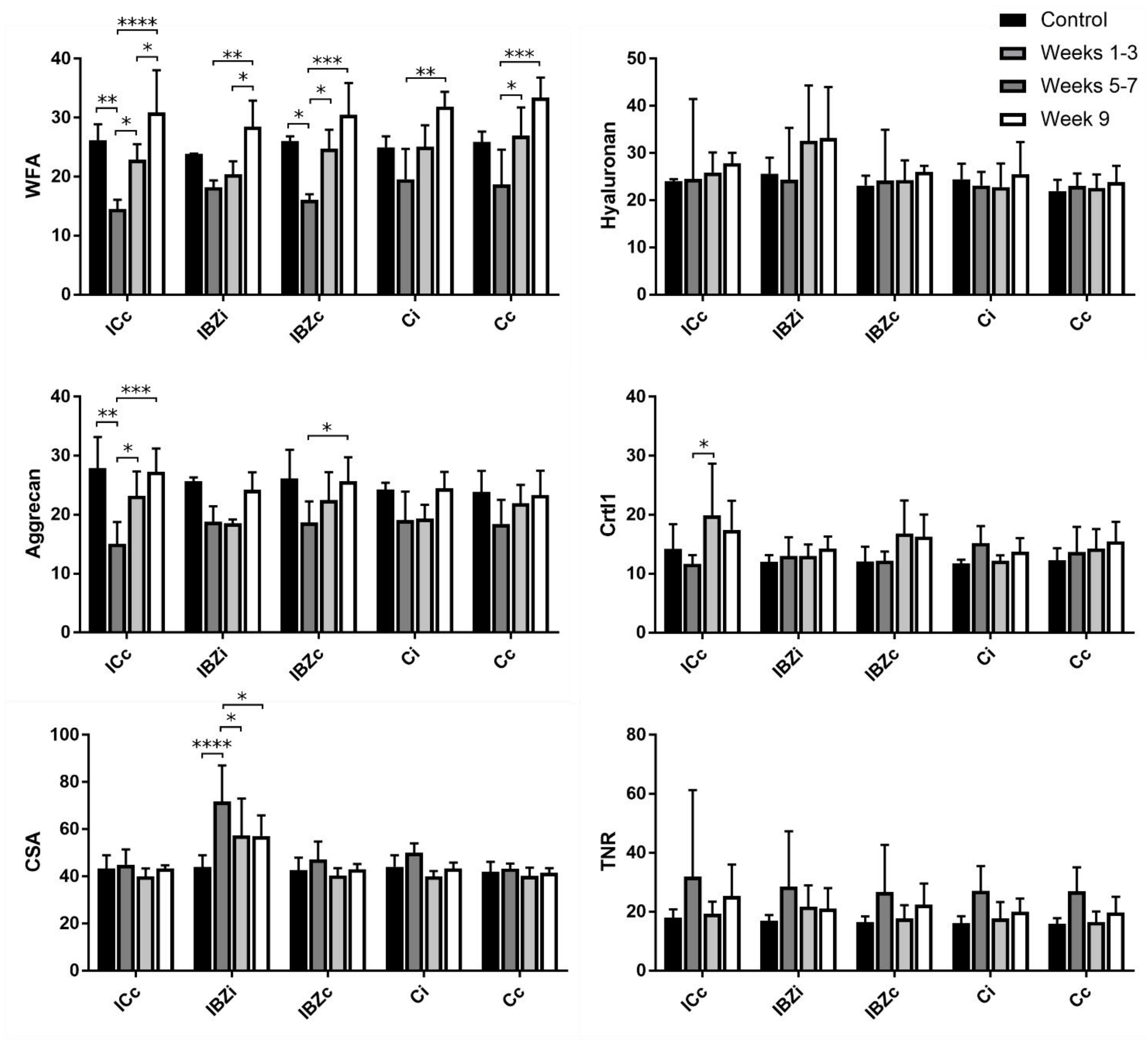

Figure 8: Immunohistochemical staining intensity for each PNN component (y-axes) was quantified in the five locations specified (x-axes) in three time periods post-stroke. Data were expressed as mean ± standard deviation of n≥11 samples. Significance was determined by one-way ANOVA. * $p < 0.05$, ** $p<0.01$.

Abbreviations:

PNN	Perineuronal Net
WFA	Wisteria Floribunda Agglutinin
CSA	Chondroitin Sulfate A	Chondroitin 4-sulfate
HA	Hyaluronan
CSPG	Chondroitin Sulfate Proteoglycan
GAG	Glycosaminoglycan
CSC	Chondroitin Sulfate C	Chondroitin 6-sulfate
CSE	Chondroitin Sulfate E	Chondroitin 4,6-sulfate
ECM	Extracellular Matrix
PFA	Paraformaldehyde
IBZ	Ischaemic Border Zone
TNR	Tenascin-R

References

Abo, M. et al., 2001. Functional recovery after brain lesion--contralateral neuromodulation: an fMRI study. *Neuroreport*, 12(7), pp.1543–1547.

Apostolova, I., Irintchev, A. & Schachner, M., 2006. Tenascin-R restricts posttraumatic remodeling of motoneuron innervation and functional recovery after spinal cord injury in adult mice. *The Journal of neuroscience : the official journal of the Society for Neuroscience*, 26(30), pp.7849–7859.

Bonita, R. & Beaglehole, R., 1988. Recovery of motor function after stroke. *Stroke*, 19(12), pp.1497–1500.

Carey, J.R. et al., 2002. Analysis of fMRI and finger tracking training in subjects with chronic stroke. *Brain*, 125(4), pp.773–788.

Carulli, D. et al., 2010. Animals lacking link protein have attenuated perineuronal nets and persistent plasticity. *Brain : a journal of neurology*, 133(Pt 8), pp.2331–47.

Carulli, D., Rhodes, K.E. & Fawcett, J.W., 2007. Upregulation of Aggrecan , Link Protein 1 , and Hyaluronan Synthases during Formation of Perineuronal Nets in the Rat Cerebellum. , 94(August 2006), pp.83–94.

Dimyan, M. a & Cohen, L.G., 2011. Neuroplasticity in the context of motor rehabilitation after stroke. *Nature reviews. Neurology*, 7(2), pp.76–85.

Foscarin, S. et al., 2017. Brain ageing changes proteoglycan sulfation, rendering perineuronal nets more inhibitory. Aging, 9(6), pp.1607–1622.

Galtrey, C.M. et al., 2008. Distribution and synthesis of extracellular matrix proteoglycans, hyaluronan, link proteins and tenascin-R in the rat spinal cord. *The European journal of neuroscience*, 27(6), pp.1373–90.

García-Alías, G. et al., 2009. Chondroitinase ABC treatment opens a window of opportunity for task-specific rehabilitation. *Nature neuroscience*, 12(9), pp.1145–51.

Gilbert, R.J. et al., 2005. CS-4,6 is differentially upregulated in glial scar and is a potent inhibitor of neurite extension. Molecular and Cellular Neuroscience, 29(4), pp.545–558.

Guntinas-Lichius, O. et al., 2005. Opposite impacts of tenascin-C and tenascin-R deficiency in mice on the functional outcome of facial nerve repair. *European Journal of Neuroscience*, 22(9), pp.2171–2179.

Harris, N.G. et al., 2009. Traumatic brain injury results in disparate regions of chondroitin sulfate proteoglycan expression that are temporally limited. *Journal of neuroscience research*, 87(13), pp.2937–50.

Hobohm, C. et al., 2005. Decomposition and long-lasting downregulation of extracellular matrix in perineuronal nets induced by focal cerebral ischemia in rats. *Journal of neuroscience research*, 80(4), pp.539–48.

Hsu, J.E. & Jones, T.A., 2005. Time-sensitive enhancement of motor learning with the less-affected forelimb after unilateral sensorimotor cortex lesions in rats. *The European journal of neuroscience*, 22(8), pp.2069–80.

Jørgensen, H.S. et al., 1995. Outcome and time course of recovery in stroke. Part II: Time course of recovery. The copenhagen stroke study. *Archives of Physical Medicine and Rehabilitation*, 76(5), pp.406–412.

Karetko-Sysa, M., Skangiel-Kramska, J. & Nowicka, D., 2011. Disturbance of perineuronal nets in the perilesional area after photothrombosis is not associated with neuronal death. *Experimental neurology*, 231(1), pp.113–26.

Karetko, M. & Skangiel-Kramska, J., 2009. Diverse functions of perineuronal nets. *Acta neurobiologiae experimentalis*, 69(4), pp.564–77.

Kwok, J.C.F., Carulli, D. & Fawcett, J.W., 2010. In vitro modeling of perineuronal nets: hyaluronan synthase and link protein are necessary for their formation and integrity. *Journal of neurochemistry*, 114(5), pp.1447–59.

McKeon, R.J., Jurynec, M.J. & Buck, C.R., 1999. The Chondroitin Sulfate Proteoglycans Neurocan and Phosphacan Are Expressed by Reactive Astrocytes in the Chronic CNS Glial Scar. Journal of Neuroscience , 19(24), pp.10778–10788.

McRae, P.A. et al., 2007. Sensory deprivation alters aggrecan and perineuronal net expression in the mouse barrel cortex. *The Journal of neuroscience : the official journal of the Society for Neuroscience*, 27(20), pp.5405–13.

Miyata, S. et al., 2012. Persistent cortical plasticity by upregulation of chondroitin 6-sulfation. *Nature Neuroscience*, 15(3), pp.414–422.

Murphy, T.H. & Corbett, D., 2009. Plasticity during stroke recovery: from synapse to behaviour. *Nature reviews. Neuroscience*, 10(12), pp.861–872.

Nijboer, T.C.W., Kollen, B.J. & Kwakkel, G., 2013. Time course of visuospatial neglect early after stroke: A longitudinal cohort study. *Cortex*, 49(8), pp.2021–2027.

Pedersen, P.M. et al., 1995. Aphasia in acute stroke: Incidence, determinants, and recovery. *Annals of Neurology*, 38(4), pp.659–666.

Al Qteishat, A. et al., 2006. Hyaluronan expression following middle cerebral artery occlusion in the rat. *NeuroReport*, 17(11), pp.1111–1114.

Sale, A. et al., 2007. Environmental enrichment in adulthood promotes amblyopia recovery through a reduction of intracortical inhibition. *Nature neuroscience*, 10(6), pp.679–81.

Soleman, S. et al., 2012. Delayed treatment with chondroitinase ABC promotes sensorimotor recovery and plasticity after stroke in aged rats. *Brain: a journal of neurology*, 135(Pt 4), pp.1210–23.

Staudt, M., 2002. Two types of ipsilateral reorganization in congenital hemiparesis: A TMS and fMRI study. *Brain*, 125(10), pp.2222–2237.

Tombari, D. et al., 2004. A longitudinal fMRI study: in recovering and then in clinically stable sub-cortical stroke patients. *NeuroImage*, 23(3), pp.827–839.

Vo, T. et al., 2013. The chemorepulsive axon guidance protein semaphorin3A is a constituent of perineuronal nets in the adult rodent brain. *Molecular and Cellular Neuroscience*, 56, pp.186–200.

Wang, D. & Fawcett, J., 2012. The perineuronal net and the control of CNS plasticity. *Cell and tissue research*, 349(1), pp.147–60.

Watson, B.D. et al., 1985. Induction of reproducible brain infarction by photochemically initiated thrombosis. *Annals of Neurology*, 17(5), pp.497–504.

Whishaw, I.Q. & Pellis, S.M., 1990. The structure of skilled forelimb reaching in the rat: A proximally driven movement with a single distal rotatory component. *Behavioural Brain Research*, 41(1), pp.49–59.

Yamaguchi, Y., 2000. Lecticans: organizers of the brain extracellular matrix. *Cellular and molecular life sciences: CMLS*, 57(2), pp.276–89.

Chapter 4 Supplement 1

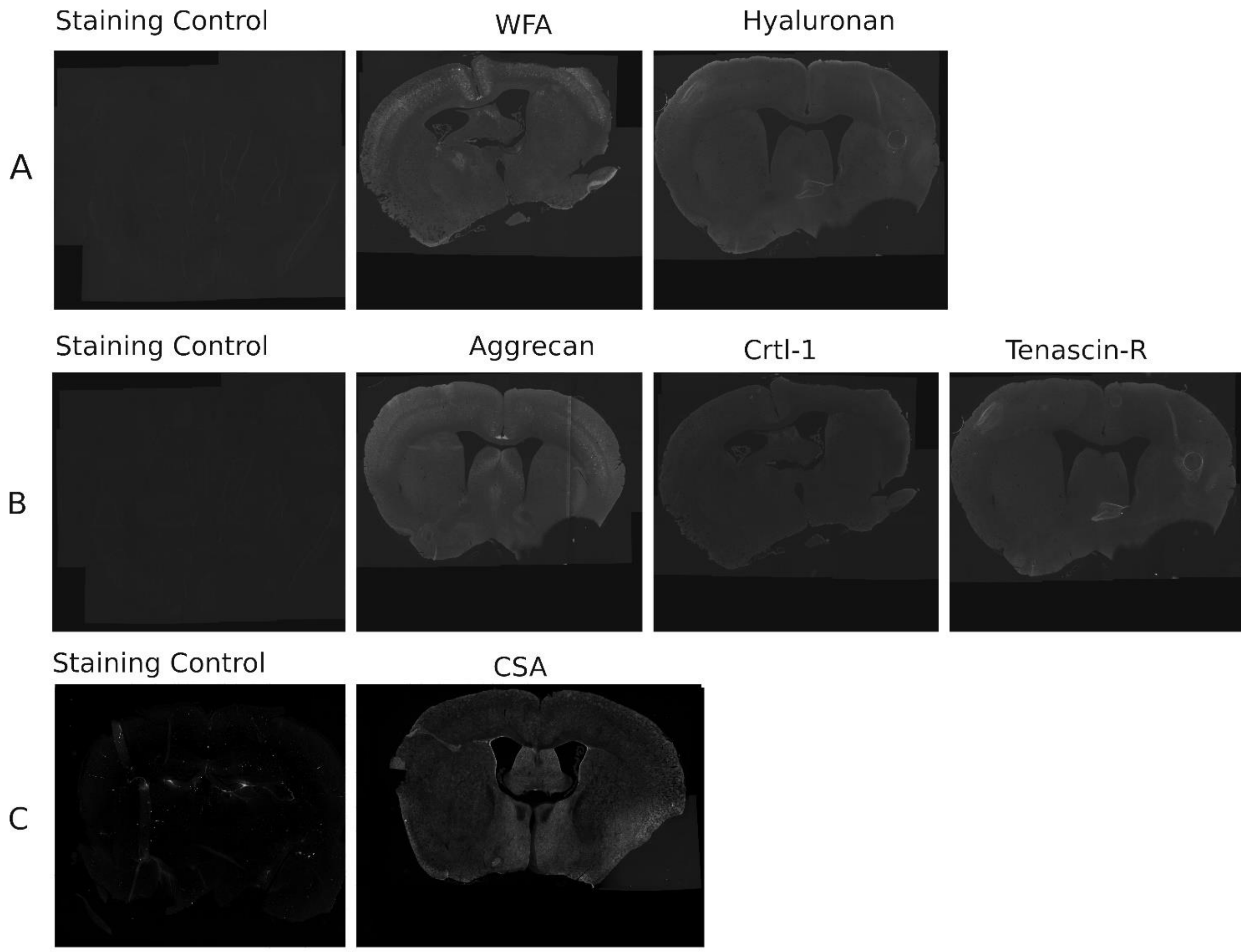

Supplementary figure 1: Nonspecific staining was controlled for by omitting the primary antibodies or binding proteins from the protocol. A) Alexa 458-Streptavidin only was used to control for biotinylated WFA and hyaluronan binding protein stains. B) Cy3 anti-rabbit only was used to control for Aggrecan, Crtl-1 and tenascin-R staining. C) Alexa 488 anti-mouse only was used to control for CSA staining. All micrograph capture parameters and image processing steps were kept constant between stains and controls.

Chapter 4 Supplement 2

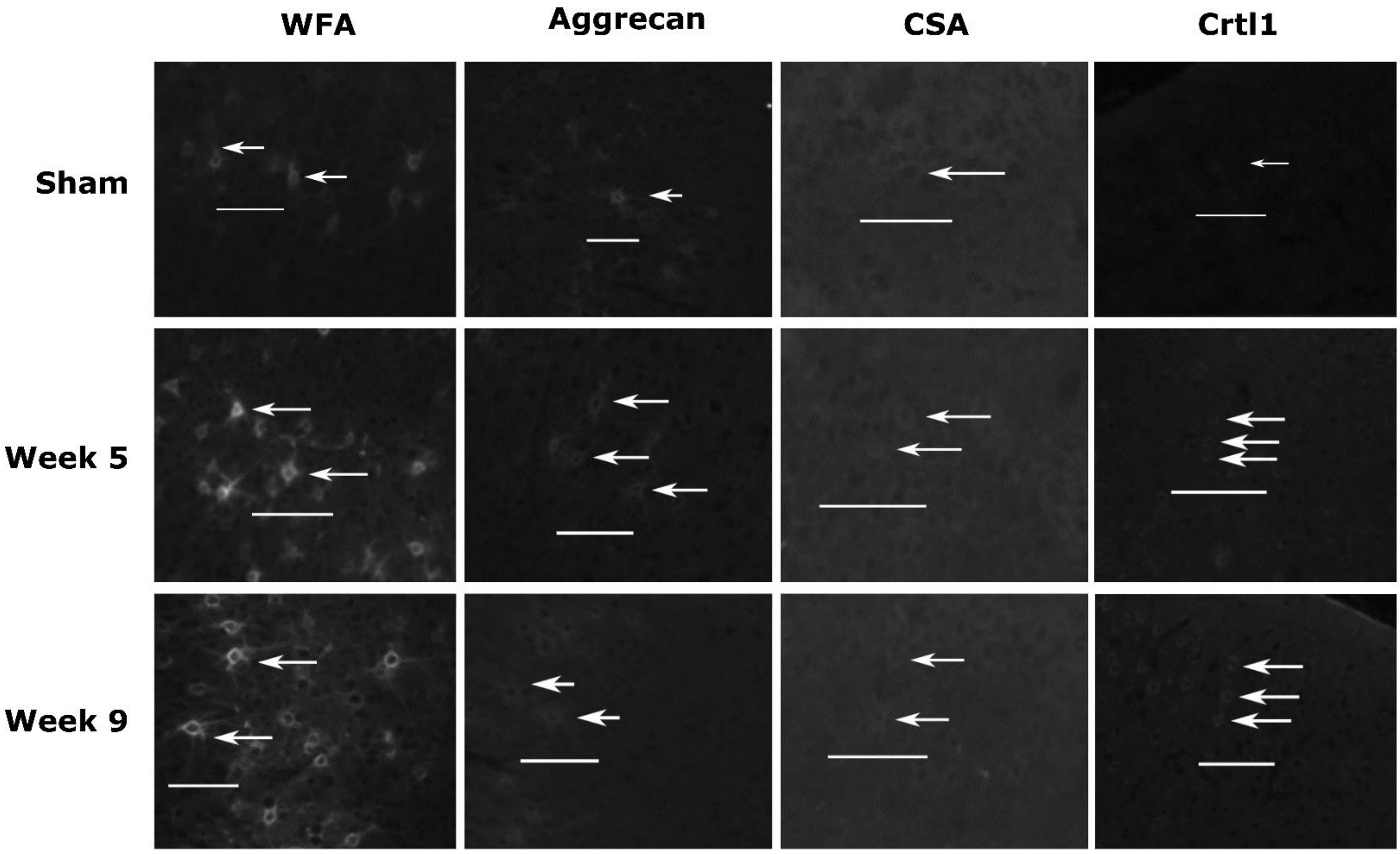

Supplementary figure 2: Higher magnification images from figures 2-5 demonstrating staining morphology of PNN components around individual cells at selected timepoints. WFA and aggrecan staining was concentrated around soma and short segments of cell processes. CSA staining was more diffuse, but also appeared more intense around soma and processes. Crtl-1 staining surrounded soma but did not appear to surround processes. Hyaluronan and Tenascin-R staining examples are not shown as these were diffuse and did not appear to condense around cells. Scale bars represent 100µm in each image.

Chapter 5

Title: Development of a standardised protocol for modelling chronic stroke in mice.

Author Names: Joshua N. Winderlich, Xenia Kaidonis, Karlea L. Kremer, Simon A. Koblar

Laboratory of Origin: Stroke Research Programme

Address: Heart Health Theme, Level 6, SAHMRI, North Terrace, Adelaide SA 5000

Telephone Numbers: 61-400-989-607 (Joshua N. Winderlich); 61-8-8128 4545 (Simon A. Koblar)

Email Addresses:

Joshua N. Winderlich:	joshua.winderlich@student.adelaide.edu.au
Xenia Kaidonis:	x.kaidonis@victorchang.edu.au
Karlea L. Kremer:	karlea.kremer@adelaide.edu.au
Simon A. Koblar:	simon.koblar@adelaide.edu.au

Statement of Authorship

Title of Paper	Development of a standardised protocol for modelling chronic stroke in mice.
Publication Status	☐ Published ☐ Accepted for Publication ☐ Submitted for Publication ☑ Unpublished and Unsubmitted w ork w ritten in manuscript style
Publication Details	

Principal Author

Name of Principal Author (Candidate)	Joshua Winderlich
Contribution to the Paper	Study design, experimental work, data collection, interpretation of results and manuscript production.
Overall percentage (%)	70
Certification:	This paper reports on original research I conducted during the period of my Higher Degree by Research candidature and is not subject to any obligations or contractual agreements with a third party that would constrain its inclusion in this thesis. I am the primary author of this paper.
Signature	Date 15/1/2018

Co-Author Contributions

By signing the Statement of Authorship, each author certifies that:

i. the candidate's stated contribution to the publication is accurate (as detailed above);

ii. permission is granted for the candidate in include the publication in the thesis; and

iii. the sum of all co-author contributions is equal to 100% less the candidate's stated contribution.

Name of Co-Author	Xenia Kaidonis
Contribution to the Paper	Study design, experimental work and manuscript revision.
Signature	Date 12/01/18

Name of Co-Author	Karlea Kremer
Contribution to the Paper	Supervised study design and experimental work, manuscript revision.
Signature	Date 12/01/2018

Name of Co-Author	Simon Koblar		
Contribution to the Paper	Guidance of study design, allocation of resources and manuscript revision.		
Signature		Date	12/1/18

Abstract

Ischaemic stroke lacks a medical intervention to restore lost cognitive and sensory motor function in the chronic phase of recovery. To investigate potential interventions that may fill this gap in treatment, a protocol must be designed to produce a model of stroke that is reproducible, technically accessible and that accurately models the chronic phase of stroke in humans. In this study, a photochemical protocol was used to create ischaemic lesions in aged mice. The resultant lesions were imaged at regular intervals using MRI and histology, which together demonstrated that the patterns of organisation following photochemical infarction mimic the pathophysiological course in ischaemic stroke. Behaviour testing showed a marked decline in the function of the targeted forepaw up to two weeks following photochemical infarction, but failed to detect the long-term functional deficits that are required in a model of chronic stroke. Future optimisation of this protocol will contribute to the development of treatments for the unmet need of overcoming chronic disability caused by ischaemic stroke.

Introduction

Ischaemic stroke is an increasingly common cause of long-term intellectual and sensory-motor disability. Approximately 1.8% of the Australian population reports to have suffered a previous stroke and of these, 35% report suffering chronic disability as a result[1]. Current medical interventions for stroke include intravenous thrombolysis[2], endovascular thrombectomy[3,4], decompressive hemicraniectomy[5], stroke unit care[6] and prophylactic anticoagulation[7,8]. The mechanisms for these interventions are biased towards the acute period of stroke pathophysiology and act with a view to limit the extent of damage caused by ischaemia and prevent future stroke events from occurring. While primary and secondary prevention should be the focus, there is a dearth of active biological agents to overcome the chronic disability caused by stroke.

The ability to recover lost function following stroke appears to be temporarily enhanced by endogenous mechanisms[9,10]. The goal of stroke research should be to enhance the extent of recovery following stroke. Methods of achieving improvements in long-term outcomes for stroke patients will need to focus on either reversing the neuro-anatomical damage caused by the stroke or by modifying the surviving brain to better compensate for damage. Potential treatment modalities that have been explored to date include transplantation of stem or progenitor cells[11–14], which is thought to act through bystander effects[15], and enhancement of neuroplasticity through a combination of interruption of inhibitory mechanisms, such as the perineuronal net[16], semaphorin[17] and Nogo systems[18–20], and rehabilitation.

In order to fully investigate these potential treatment modalities, we require a highly reproducible, pathophysiologically accurate and technically straightforward model of chronic ischaemic stroke. Common methods of stroke induction in animals include middle cerebral artery (MCA) occlusion (MCAo), endothelin-1 vasoconstriction, microembolus injection, and photochemical ischaemia.

Up to this point, the gold-standard model for ischaemic stroke has been MCAo in rodents[21]. This model involves gaining access to the MCA via the internal carotid artery, then temporarily occluding the origin of the MCA. Reperfusion occurs instantly when the occlusion is removed, as opposed to the gradual reperfusion that occurs following endogenous clot lysis. This arguably makes MCAo a more accurate model of intravascular thrombectomy than it is of untreated stroke or stroke treated with intravenous thrombolysis. MCAo is a highly invasive and intricate procedure analogous to human microvascular surgery. Small differences in technique and vascular anatomy can result in both inter- and intra-operator variation in stroke size, lesion location, behavioural outcomes and well-being of the animals used[22]. Other factors that affect the suitability of this technique include the potential for spontaneous subarachnoid haemorrhage[23] and dysphagia resulting from ligation of the external carotid artery[24].

The endothelin-1 stroke model involves infusion of endothelin-1, a potent vasoconstrictor, into the MCA. This results in the formation of ischaemic lesions of highly variable size and location anywhere within the vascular territory of the MCA[25]. Due to the high outcome variability, this model more accurately models the variation seen in human stroke and is useful in studying the effect of infarct size and location on outcomes. However, this high degree of variation may be responsible for masking signals in treatment studies. For example, Abeysinghe et al (2015) failed to detect improvement in lesion size or behaviour following a neuroprotective intervention in endothelin-1 MCA stroke rats, which may have been due to a conspicuously large variation in lesion volume.

Another related model creates uniform lesions by applying endothelin-1 to the brain surface or injecting it into the cortex[26].This method creates localised and well-controlled lesions, however these are not strictly representative of spontaneous stroke in humans. As endothelin-1 is a vasoconstrictor, this model produces little post-stroke oedema, an important component of stroke pathophysiology[27]. Additionally, endothelin-1 has neuronal and glial receptors that appear to cause effects unrelated to ischaemic stroke[28–30].

Embolism is a common causal event of human stroke, and the arterial introduction of microemboli closely resembles this in terms of pathophysiology. This method involves the injection of emboli ranging between 50 and 400µm into the MCA or internal carotid artery. These emboli lodge, depending on their size, into the MCA, its major branches or smaller arteries[31,32]. Introduction of macrospheres into the MCA results in an infarct that is similar to the filament MCAo model[33]. As these emboli are not removed, this results in permanent occlusion and infarcts of highly variable size,location and clinical outcome. Variations of this protocol use fibrin-based emboli to induce thrombosis in cerebral vessels, more closely approximating stroke in humans[34]. One setting where this type of model is highly appropriate is in the study of thrombosis and thrombectomy, as the emboli behave in a similar way to endogenous thromboemboli[35].

Photochemical ischaemia is a highly consistent and streamlined method for producing ischaemic lesions in mice. This protocol involves intraperitoneal injection of Rose Bengal, a photosensitive pigment, followed by illumination of the cranial area overlying the required lesion space[36,37]. The advantages of this method are that it produces localised and targetable lesions, is technically straightforward, has little inter-operator variation in lesion size or position and is associated with lower rates of mortality than other stroke models [see 38,39 for review]. As this model does not involve the occlusion of large cerebral blood vessels, the pathophysiological properties of the lesion differ from others in certain aspects. This model does not create an extensive region of penumbra as it is the terminal vessels that are occluded. Variants of the photochemical ischaemia protocol using ring illumination or targeted illumination of the MCA can be used to simulate a penumbra[40,41]. This should only be a consideration for studies that attempt to characterise acute stroke therapies, but should not affect the results of studies aimed at recovery of disability in chronic stroke.

The incidence of stroke and stroke risk factors in humans increases with age, however many models of stroke use juvenile animals[42]. Not only is this less likely to provide a model that is representative of stroke in humans, younger animals also have a greater capacity for recovery following stroke, which may mask the outcomes of interventional studies[43]. Therefore, animal studies of therapies targeted at stroke in adult humans should use animals that have at least been approximately age-matched. Mice reach sexual maturity at 5-10 weeks of age and have an average lifespan of approximately two years[44]. Therefore, experimental stroke induction in mice should ideally take place in mice above the age of 12 months. However, obtaining aged animals can be cost-prohibitive. To avoid masking of results by spontaneous recovery, non-juvenile animals should be used. One study has validated a chronic MCAo stroke model in six-month old rats[45], and another has characterised acute MCAo in rats aged 56 weeks[46]. Here, we will investigate using mice at six months of age.

While the focus of this study is on developing a standard model of stroke, it is important to recognise that stroke in humans does not conform to a standard. Indeed, stroke varies in terms of lesion size, location, the number of foci and clinical outcomes. However, early preclinical studies rely on controlling these factors to accurately measure treatment response and establish causality. While a model of stroke may be conceived to better model the variability seen in human stroke, this would vastly increase the sample size required to detect a given effect size. For example, the production of highly uniform focal motor lesions would allow for uniformity in the measurement of behavioural outcomes, whereas a more variable model would necessitate measurement of less-specific clinical outcomes that may be more prone to statistical noise. Therefore, a standardised model of stroke with low variability in lesion parameters fits the purpose of testing early pre-clinical interventions for stroke.

This paper aims to characterise a stroke model appropriate for assessing the efficacy of therapies targeted at the chronic phase of ischaemic stroke recovery. Stroke will be induced in the forepaw primary motor cortex of six-month-old mice by the photochemical method. In order to evaluate the applicability of this model to future chronic stroke studies, mice will undergo behaviour testing for nine weeks following photochemical infarction. Mice will be humanely killed for histological analysis and MRI at regular time points over the duration of the study. It is expected that the mice will undergo a certain degree of spontaneous recovery over the course of observation. To establish a chronic stroke model, both the structural changes and behavioural deficits associated with the stroke must be detectable at later time points.

Methods

Mice

Male C57BL6 mice aged six months were sourced from the University of Adelaide Laboratory Animal Services. Approval for all surgical procedures and behaviour assessment was granted by the University of Adelaide animal ethics committee (M-2013-166). Mice were housed in the University of Adelaide animal facility in enriched cages on a 12 hour light/dark cycle. Mice were given free access to food and water, except nights before behaviour testing when food was withheld.

Photochemical stroke model

Stroke induction was executed using a variant of the photochemical stroke model described by Watson *et. al.*[36]. Rose Bengal dye (10mg/mL; Sigma, R3877) was dissolved in normal saline, agitated and then filtered through a 0.45 micron filter (minisart, Sartorius). The Rose Bengal solution was administered to mice via intraperitoneal (IP) injection at a dose of 100mg/Kg. Mice were anaesthetised with 3% isoflurane in a sealed induction chamber, then switched to a maintenance dose of 2% isoflurane via a nose cone. A saggital incision was made from the interparietal bone to mid-orbital point and the scalp was retracted bilaterally to expose the cranium. A stereotaxic frame was used to secure the mice and locate a point 1.5mm lateral to bregma on the side contralateral to handedness, as determined by the skilled reaching test. This location represents the surface anatomy corresponding to the area of cortex responsible for forepaw motor control on the dominant side. Ten minutes was allowed for the IP rose bengal solution to distribute into systemic circulation prior to illumination. A 500-570nm cold light source at an intensity of 240 lumens was directed through a 2.5mm aperture centred on the desired lesion location. A housing was designed and printed to provide the aperture and couple the light source to the stereotaxic frame. The light source was removed after a ten-minute exposure period. Mice allocated to the sham stroke group underwent the procedure described above, but with the light intensity kept at zero lumens. Allocation of mice to stroke or sham group was randomised by computer.

The scalp incision was closed and treated with mupirocin to prevent infection (Bactroban, GSK). Bupivacaine hydrochloride (0.5%, GSK) was provided as a 50µL epidermal injection to reduce suffering during recovery. Isoflurane was removed and mice were allowed to regain consciousness in a dark, warmed box and were provided with enriched feed. Mice were assessed three times daily for clinical signs of morbidity for the first week following surgery and daily thereafter until the clinical score reached zero.

Behaviour testing

Forepaw sensory motor function was assessed by the ladder rung and skilled reach behaviour tests. Mice were trained in both activities daily for one week prior to induction of photochemical ischaemia (Figure 1C).

Baseline scores were recorded on the final day of training. As food pellets were used as a reward, mice were fasted overnight prior to training and prior to testing days. Conduct of the behaviour tests was unblinded, but assessment of the behaviour tests was conducted by a blinded operator.

Ladder rung

Mice were required to cross a 45cm long horizontal ladder with rungs spaced one centimetre apart. A mirror was placed behind the ladder and along its length at an angle of 10° to the apparatus so that both the near and far limbs could be viewed from one side (Figure 1A). For each trial, mice were required to cross the ladder three times in succession. Each attempt was recorded with a video camera and foot faults were evaluated while viewing footage at a decreased frame rate.

Foot fault scoring was conducted using the method described by Metz and Whishaw[47]. Every step for each forepaw was categorised as being either a total miss [0], deep slip [1], slight slip [2], replacement [3], correction [4], partial placement [5] or correct placement [6]. The parameters used for comparison were the average score per step of the stroke-affected limb and the unaffected limb. Comparisons were made between affected and unaffected limb scores at each time point.

Skilled reach and determination of handedness

Forepaw motor function was assessed in mice using a skilled reaching assembly first described by Whishaw *et. al.*[48]. Mice were placed in a small, dark chamber 72mm wide, 200mm tall and 78mm deep constructed of opaque acrylic plastic. The front of the chamber was transparent and contained a 10mm wide aperture in the centre. Mice were required to reach through the aperture and retrieve pellets of pasta located on a ledge 10mm high and 10mm from the aperture. Pellets aligned with either edge of the aperture could only be reached with the contralateral forepaw.

During the week of daily training for this task, mice were presented with 20 pellets in both the left and right positions. The mice progressed from initially using both forepaws to settling on a retrieval strategy that used only the dominant forepaw.

During assessment, mice were presented with 20 pellets in succession in the location contralateral to their dominant forepaw. Retrieval attempts were categorised into successes, failures with pellet contact and failures without pellet contact. Invalid retrieval strategies were not recorded. These included attempts to reach the pellet with the non-dominant forepaw or the tongue.

Tissue preparation

Mice were humanely killed with 5% isoflurane in a sealed induction box at one, three, five, seven or nine weeks post-stroke (Figure 1C). An incision was made from the manubrium to the umbilicus, then the ribs were cut bilaterally at the mid-clavicular line and the diaphragm was cut to expose the mediastinum. A small incision was made in the right ventricle of the heart, while PBS was infused into the left ventricle at a constant rate. Once all blood was displaced, 4% paraformaldehyde (PFA) in normal saline at 4^{o}C was infused into the left ventricle.

The brain was carefully removed and fixed in a solution of 4% PFA in normal saline for 24 hours at 4^{o}C. The brain was washed in normal saline three time for 30 seconds each, then cryoprotected in a solution of 30% sucrose in normal saline for 24 hours at 4^{o}C before being returned to normal saline for MRI scans.

Brains were sliced into 1mm coronal sections and then snap frozen in O.C.T compound (Tissue Tek). Tissue blocks were then cryosectioned to a depth of 30 microns. Haematoxylin and eosin staining was carried out by standard protocols. Histological analysis was not conducted by a blinded operator.

Magnetic resonance imaging

Brains were placed in 15mL falcon tubes filled completely with normal saline to ensure no air bubbles were present. A modified transfer pipette was used to prevent movement of the brain during imaging. T1-weighted MRI was conducted using a 1.05T small animal MR machine (Bruker, ICON Compact MRI) (echo time = 12ms, repetition time = 45ms, flip angle = 30^{o}). Images were taken in the frontal plane and slices were separated by 0.5mm. Data were collected using Paravision 6 (Bruker) and post-processing was conducted using ITK-SNAP (version 3.3.0)[49]. MRI assessment was not conducted by a blinded operator.

Statistics:

All calculations were performed using Prism (Graphpad, version 7.02). With regards to behaviour test data, differences between the sham and stroke groups for each time point, and between time points for each group, were tested by two-way ANOVA with Sidak's correction for multiple comparisons.
A total of 19 mice were analysed by MRI and 21 were analysed by histology. For the ladder rung behaviour test, six stroke and four sham mice were analysed at each time point. For the skilled reach behaviour test, 12 mice from each group were analysed at each time point. This sample size was chosen to detect an effect size of 25% in behaviour testing with 95% confidence, given a standard deviation of 20% and a power of 80%.

Results

Photochemical infarction did not cause measurable chronic sensory-motor deficits

To characterise the long-term neurological deficit caused by photochemical infarction, a total of 24 mice were subject to behaviour testing. The location of the lesion in this model corresponded to the area of primary motor cortex associated with control of forepaw function. Therefore, the affected limbs of mice in the stroke group experienced a relative decrease in limb placement score in the ladder rung test from 5.329 ± 0.228 to 4.412 ± 0.459 one week post-stroke ($p < 0.0001$) (Figure 2A). The difference in ladder rung scores of the affected limbs relative to the unaffected limbs between the stroke and sham group at one week post-stroke was 0.13 ± 0.04 ($p = 0.02$). This indicates a pronounced asymmetry in forelimb sensory-motor function acutely following induction of photochemical ischaemia. Mice recovered rapidly, with scores not significantly different from baseline achieved by week three. No significant difference in ladder rung score between the affected and unaffected forepaws was observed at any time points later than week three. Mice in the sham group did not exhibit any difference in skilled reaching with either forepaw (Figure 2B).

The skilled reaching behaviour test was used to further assess sensory-motor deficits in the affected forepaw (Figure 2C). After five days of training, mice had a pellet retrieval success rate of 0.47 ± 0.15. One week post-stroke, mice in the stroke group had a lower success rate than the control group, though this may have been a chance event as it did not reach significance. No significant difference was observed between groups at any other time point.

Histological analysis

To analyse the tissue-level characteristics and long-term progression of this stroke model, brain sections were taken from mice at regular intervals following induction of photochemical ischaemia and imaged with H&E staining ($n \geq 2$ per timepoint). Sections for histology were taken from the midpoint of the lesions that were visible in the stroke group mice (Figure 3A) and from the corresponding region in the sham group.

A well-demarcated lesion was visible at seven days post-stroke(Figure 4A). This early lesion was characterised by a border of macrophage-like cells at the perimeter of a necrotic core containing caseating eosinophillic debris and sparse picnotic nuclei. At three weeks post-stroke, the infarct core had completely necrosed and was eliminated during processing, leaving behind an indentation in the cortex. The size of the lesion had partly contracted and its peripheral surface was bordered by a layer of elongated cells consistent with a glial scar. By five weeks post-stroke the outer layer of elongated cells had thickened and the lesion had contracted further. At seven weeks post-stroke the lesion had contracted and flattened out considerably. A number of haemosiderin-laden macrophages were bordering the infarct. At nine weeks post-stroke the outer scar layer had thickened and a greater number of haemosiderin-laden macrophages were present. Over time, the area represented by the infarct decreased considerably (Figure 4B).

Photochemical infarction creates lesions detectable by MRI

MRI was used to evaluate the presence, size and location of photochemical infarcts without sacrificing tissue (Figure 3B,C). Hyperintense regions corresponding with the location of visible cortical lesions were seen only in the brains of mice taken one week post-stroke. The mean volume of the three lesions detected by MRI at one-week post-stroke was 9.22mm^3 (SD=3.51mm), or 1.8% of total brain volume. Lesions detected by MRI were at the location targeted by the protocol.

Despite having lesions that were visually apparent (Figure 3A) and detectable on later histology (Figure 4A), none of the MRI results from mice at later time points showed any evidence of an infarct. None of the mice from the sham group showed evidence of infarct at any time point.

Discussion

This study provides preliminary investigations of a potential standard protocol for producing an *in vivo* model of chronic stroke in aged mice. The data demonstrate that the photochemical infarction protocol creates a reproducible cortical lesion, as has been demonstrated previously with similar protocols[36,37]. The lesions produced were apparent visually and were able to be measured by MRI, which would allow multiple analyses for individual mice without sacrificing for histology. This model of infarct also showed a typical pattern of organisation on analysis by histology. Behaviour testing of animals demonstrated a decline in sensory-motor function of the forepaw targeted by the photochemical stroke, but only in the acute phase of stroke recovery.

This study demonstrated acute, but not chronic sensory-motor deficits in the function of the targeted forepaw. Figure 2A shows that this experimental model of stroke resulted in a significant reduction in performance in the ladder rung task and that spontaneous recovery of this function occurred within three weeks. No significant change in performance was detected by the skilled reach behaviour test. This was surprising as it was expected that the isolation of the affected forepaw in this protocol would provide a more sensitive test of function.

Functional improvement is the most important goal for potential stroke therapies and therefore a relevant experimental model of chronic stroke must demonstrate long-term functional deficits. The photochemical stroke model described here did not produce chronic functional deficits that could be detected by the ladder rung or skilled reach behaviour tests. There were a number of limitations to our study, which will inform future studies.

The most likely reason that the mice were able to achieve near-total recovery so quickly is that the lesion size was too small. Future development of this model should create a larger lesion by varying aperture size and illumination time. In previous studies, aperture size varied from 1.5mm[50] to 4.5mm[18,51], and larger apertures consequently resulted in larger lesions. Likewise, illumination times of 5[52], 10[53], 15[18,51] and 20[50] minutes have all been used to produce lesions in similar models. It is unclear whether varying illumination time within this range influences experimental outcomes. This study used an aperture of 2.5mm and a 10 minute illumination time as we found larger apertures resulted in higher mortality, while smaller apertures did not produce measurable behavioural deficits. Future development of this model should test the effects of aperture size and illumination time on functional outcomes.

Notably, the skilled reach behaviour test did not detect any decline in function. Previous studies have demonstrated this test to be an effective test of function in stroke models [9,19,54–56]. These studies took place in rats and infarction was induced by MCAo[19,54], endothelin-1[9] and photochemical infarction[55,56]. However, Alaverdashvili *et al*[57] determined that the skilled reach test was not able to detect chronic dysfunction in rats following photochemical infarction. Likewise, Clarkson *et. al.*[58] determined that the skilled reach test was only able to detect dysfunction up to seven days following photochemical infarction in mice. As a result, it is possible that the skilled reach test is not an appropriate method for measuring chronic dysfunction following photochemical infarction in mice.

Another limitation of the skilled reach test is that there may have been a training effect, which could mask chronic dysfunction. While not statistically significant, pellet retrieval success rates in both the sham and stroke groups appeared to trend upwards over the course of the study (Figure 2C). This may indicate that performance in this task had not reached a stable state prior to photochemical infarction. This issue could be addressed by increasing the time allowed for training prior to photochemical infarction. The five day training schedule used in this study was suggested in the original description of the skilled reach test in mice[59], though at least one subsequent study has increased this time to 14 days[58].

Another likely reason that this study did not detect chronic disability is the low sample size. Twelve mice were used in each group at each time point in the skilled reach test, which was calculated to detect differences in function of 25% with a standard deviation of 20%, confidence of 95% and power of 80%. Only six stroke group mice were used per time point in the ladder rung test. It is possible that smaller differences in performance of these tests were missed. Increasing the sample size to 29 per group would allow the tests to resolve changes in performance as low as 15%.

A standard protocol for stroke must produce a lesion that is consistent in volume and location. To address this, preliminary MRI investigations were undertaken to image lesions at regular intervals following induction of photochemical infarction. Lesions were measurable, but only in the brains of mice humanely killed one week post-stroke. The results demonstrated that at this time point, mean lesion size was $9.22mm^3$ and these lesions were located at the target area. This builds on earlier studies of the progression of photochemical stroke, which have demonstrated that hyperintense lesions are detectable on T2- and diffusion-weighted MRI as early as 90 minutes after illumination and as late as seven days[60,61].

To ensure technical consistency, previous protocols have used a quality control process whereby a certain proportion of animals are removed from the study early so that lesion consistency can be confirmed using imaging techniques such as tetrazolium chloride or cresyl violet staining[37]. This results in loss of precious tissue samples and represents an area where animal numbers may be reduced with respect to ethical considerations. A previous study suggested that MRI is as sensitive as these other techniques for quality control of MCAo infarcts in rats[62], which would support our results. As it is only necessary to confirm the presence and consistency of photochemical lesions once after induction, the inability of the present protocol to resolve lesions at later time points is not detrimental. These results are only preliminary as MRI studies were limited and were not conducted in live animals. However, these results do suggest that use of MRI to confirm photochemical infarct in mice may prevent the need to sacrifice tissue for quality control.

It was expected that lesions imaged in the chronic phase would appear as hypointense regions as seen in human stroke[63], but this was not demonstrated. One reason that MRI failed to detect infarcts at later time points is that only T1-weighted imaging was used. T2- or diffusion-weighted MRI may be more appropriate for showing regions of enhancement at later timepoints[64]. Gross structural abnormalities including cavitations and perilesional distortions should still be detectable by T1-weighted imaging. However, histological data demonstrated that the lesions contracted over time (Figure 4B). The lesion shown in Figure 3B,C representing a brain at week one post-stroke had a depth of 1.25mm when measured on histology, whereas the brain imaged at week three measured 0.53mm deep. The MRI protocol captured 0.5mm slices in the transverse axis, so older lesions fell below the minimum detectable volume at this resolution. Use of a higher resolution MRI protocol may have been able to image lesions at later time points.

Another limitation is the choice of animal used in this study. The evolution of human stroke is influenced by the anatomy of the brain, cerebral circulation and cranium. There is no ideal animal model for human stroke as the human brain is a much larger and more complex structure than any animal brain. Despite being by far the most common animal model of stroke[43], mouse brains are more unlike humans' in terms of size and complexity than are other mammals. Indeed, MCAo in mice has produced more variation in lesion sizes than has MCAo in rats [see 29 for review]. Larger, gyrencephalic animals such as sheep or non-human primates may provide a more appropriate model for human stroke as they are closer in anatomy. However, these animals are more expensive to use and require a higher degree of ethical justification. A balance may be found in using larger animals, such as rats or sheep.

Following ischaemic stroke, the brain undergoes a well-defined organisation and resolution process that is unique amongst other tissues. The histologic data presented in Figure 4 demonstrate that this chronic stroke protocol produced a lesion that underwent a similar evolution to other well-recognised stroke models, such as MCAo[65]. The lesion was initially large and showed evidence of inflammatory processes with extensive macrophage infiltration bordering the infarct. The necrotic debris was cleared to leave a cavity and a wall of elongated cells and extracellular matrix formed around the infarct. Over the course of the study, lesion size decreased markedly, with the resolved scar at week nine barely visible (Figure 4A,B). These results suggest that the methods produce an accurate model of chronic ischaemic stroke at a tissue level.

It should be noted that in human stroke, lesions also occur within subcortical regions and in particular often have white matter involvement. The present study aimed to produce a focal lesion within the motor cortex as a way of reducing variability in outcome measurement. As a result, this model does not address such sub-cortical damage. While this is not problematic for the study of many potential stroke treatments, it would not be appropriate for any treatment where the proposed mechanism lies specifically in white matter or basal ganglia repair. For example, this model would not be suitable for the study of treatments for multi-infarct parkinsonism.

Medical interventions currently available for the treatment of stroke are limited to attenuating the ischaemic damage that occurs during the acute phase of stroke pathogenesis. In order to develop new therapeutic options for stroke, an appropriate *in vivo* model is required. This study presented preliminary investigations towards the development of a standard protocol for an experimental model of chronic stroke that is highly reproducible, technically straightforward and biologically relevant. The protocol described here produced consistent lesions, was technically straightforward and caused less morbidity than other protocols.

Future development of this model should investigate the use of larger apertures and longer illumination times to generate larger infarcts. This will ensure that the cortical target is more likely to be completely within the infarcted area and therefore more likely to manifest the desired functional deficits. A larger infarct size will also improve measurement by MRI at later time points. An increase in lesion volume would likely increase morbidity and unintentional mortality, but it appears that this is necessary to better approximate ischaemic stroke in humans. T2- and diffusion-weighted MRI techniques should be employed early to confirm infarction and to detect long-term changes following stroke. A larger sample should be analysed by this method. Stroke volume should be determined in live animals, as the goal of MRI in this case is to confirm infarct without sacrificing animals for that purpose. The protocol should also be tested in rats, as these may be a more appropriate model animal model for human stroke. Finally, a larger battery of behaviour tests should be employed to determine the best method of detecting chronic neurologic disability following stroke in rodents.

This study represented a starting point for the development of a standard protocol for a model of chronic stroke in aged mice. Further development of this protocol will enable more efficient assessment of new therapies for stroke that act in the chronic phase of stroke recovery, an area that currently lacks acceptable intervention.

Figures

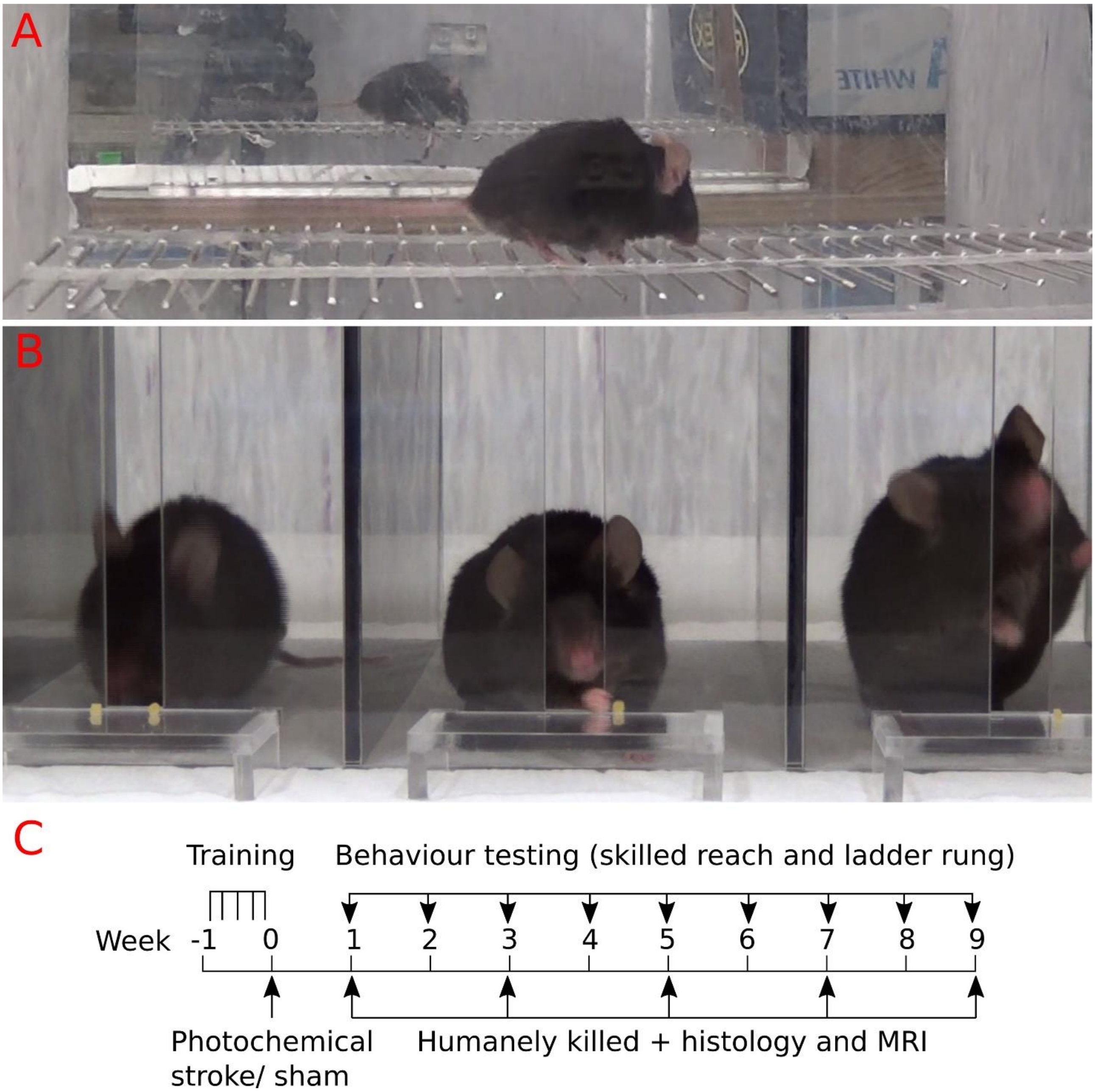

Figure 1: Post-stroke forepaw sensory-motor dysfunction was assessed with behaviour tests. A) Foot faults were scored for both the affected (near) and unaffected (far) forepaws as mice traversed a horizontal ladder. Relative dysfunction of the affected forepaw compared with the unaffected forepaw was recorded over time. B) Mice were placed in a feeding apparatus where they were trained to retrieve pellets from a platform through an aperture. Handedness was determined by presenting mice with pellets in both left and right positions concurrently (right). Function was assessed by counting retrieval attempts for the dominant/stroke-affected forepaw (middle). C) Experimental timeline. Mice were trained in behaviour tests for five consecutive days prior to induction of photochemical stroke. Behaviour testing took place weekly following stroke and mice were humanely killed one, three, five, seven and nine weeks post-stroke.

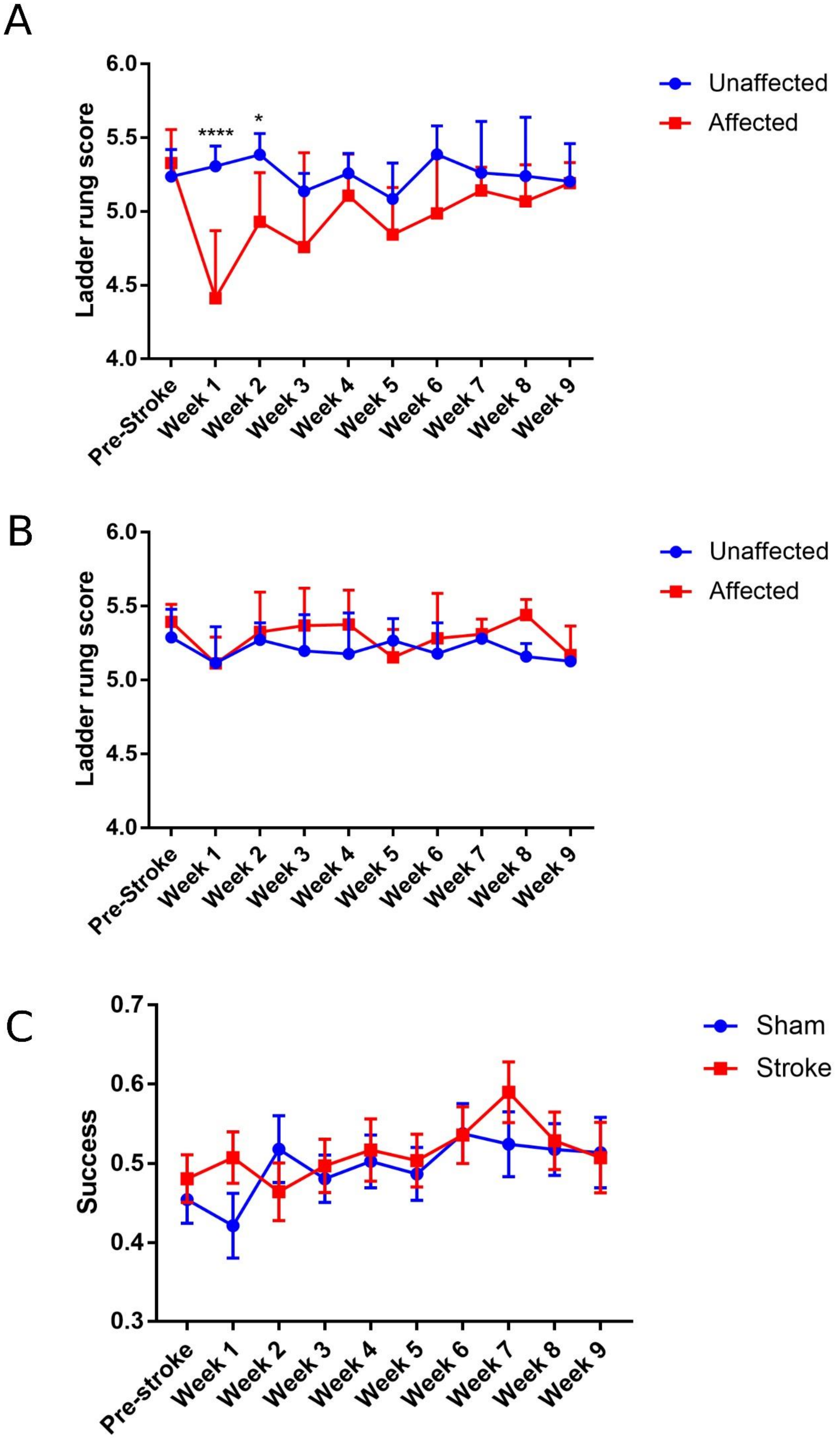
A
Ladder rung score
6.0
5.5
5.0
4.5
4.0
****
*
Pre-Stroke
Week 1
Week 2
Week 3
Week 4
Week 5
Week 6
Week 7
Week 8
Week 9
Unaffected
Affected
B
Ladder rung score
6.0
5.5
5.0
4.5
4.0
Pre-Stroke
Week 1
Week 2
Week 3
Week 4
Week 5
Week 6
Week 7
Week 8
Week 9
Unaffected
Affected
C
Success
0.7
0.6
0.5
0.4
0.3
Pre-stroke
Week 1
Week 2
Week 3
Week 4
Week 5
Week 6
Week 7
Week 8
Week 9
Sham
Stroke

Figure 2: Analysis of behaviour testing. Ladder rung and skilled reaching behaviour tests were conducted to evaluate forepaw sensory-motor function prior to induction of photochemical ischaemia and at seven day intervals up to nine weeks post-stroke. A) analysis of ladder rung testing in stroke group mice. Dots indicate mean ladder rung score. Error bars indicate SD, * indicates $p<0.05$. N = 6 experimental repeats at each time point. B) Analysis of ladder rung testing in sham surgery mice. Dots indicate mean ladder rung score. Error bars indicate SD, * indicates $p<0.05$. n = 4 experimental repeats at each time point. C) Analysis of skilled reaching behaviour test. Dots indicate mean successful pellet retrievals as a proportion of total attempts. Error bars represent SEM. $n \geq 12$ repeats per group at each time point.

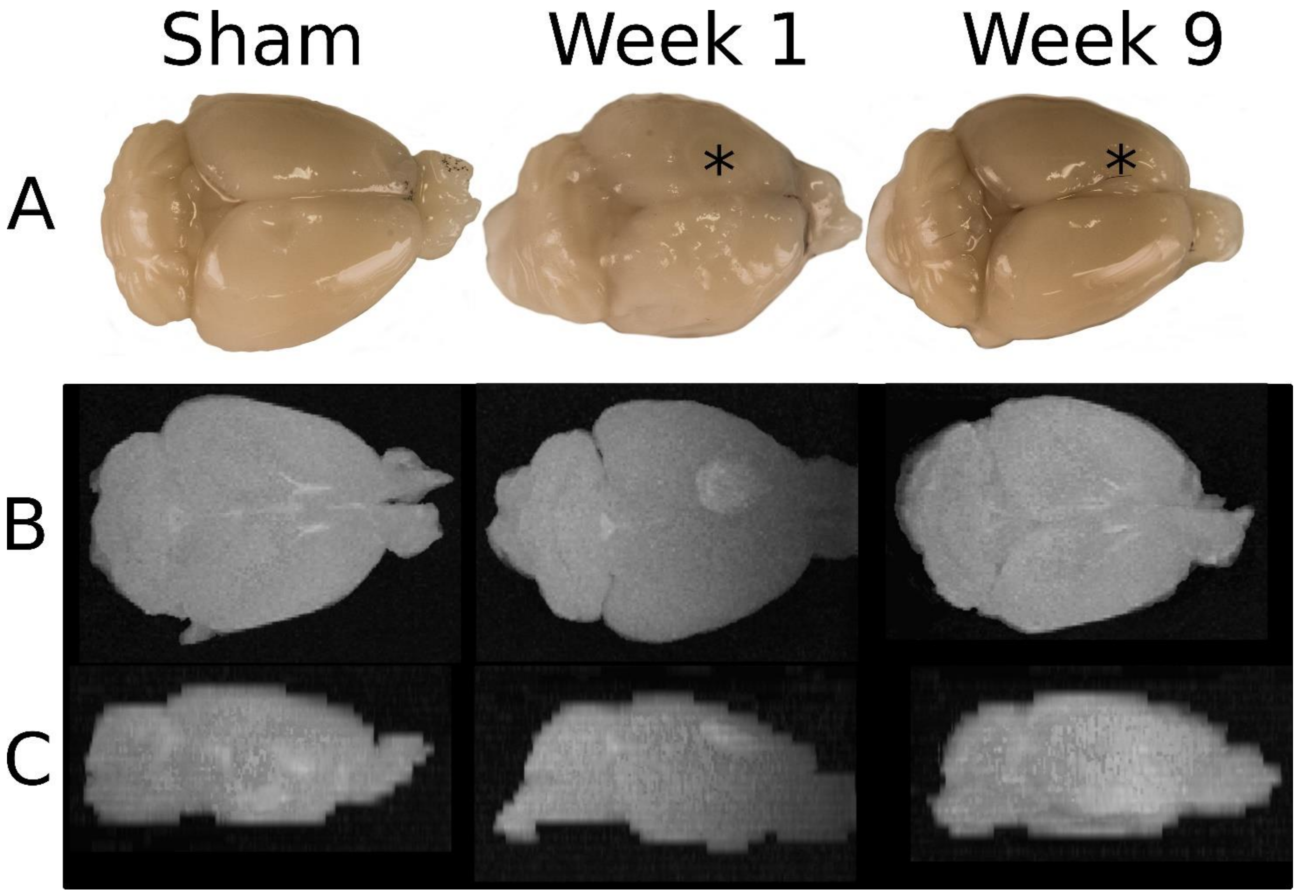

Figure 3: A) Photographs were taken of the dorsal aspects of brains from mice in the sham group, one week post-stroke and nine weeks post stroke. Lesion site is indicated by *. B) Transverse and C) lateral composite images of MRI sections of brains from mice in the sham group, one week post stroke and nine weeks post-stroke. Images in each group correspond to the same mouse. Representative MR images shown of n=3 brains at week one, n=1 brain at weeks three, five and seven, n=6 brains at week 9 and n=7 sham brains.

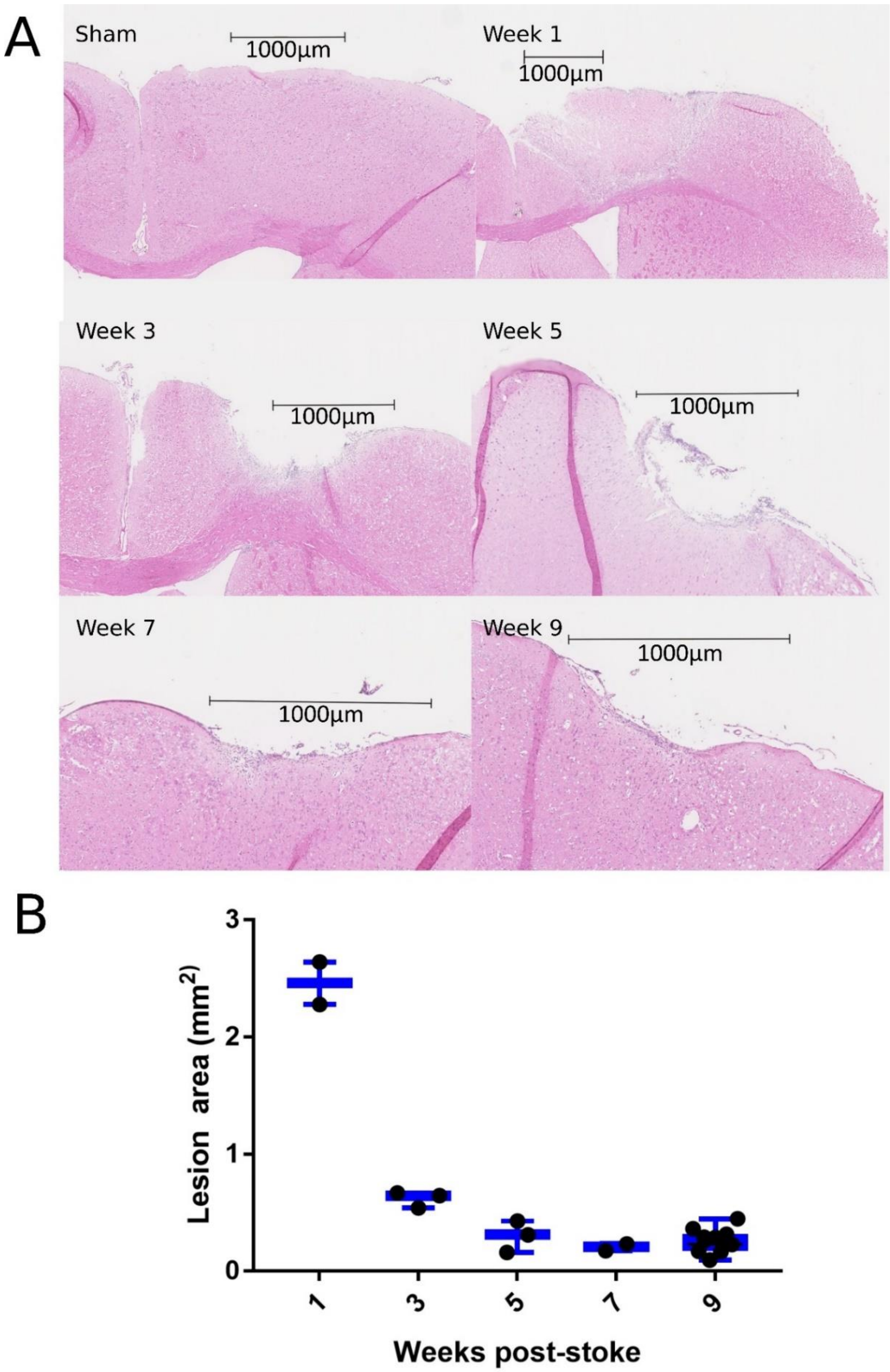

Figure 4: A) Mouse brain sections were gathered at regular intervals up to nine weeks post-stroke. These were examined histologically with haematoxylin and eosin staining. Images shown are representative of n=21 brains. B) Data points represent the infarcted area on histological sections, bold lines indicate mean and error bars indicate range.

References

1. **Australian Bureau of Statisics**. Profiles of Disability, Australia. 2012.
2. **Bertog SC, Grunwald IQ, Kühn AL, Franke J, Hofmann I, Sievert H**. Acute Stroke Intervention. *Urgent Interv Ther*. 2014;313(14):286–301.
3. **Campbell BCV, Mitchell PJ, Kleinig TJ, Dewey HM, Churilov L, Yassi N, et al.** Endovascular Therapy for Ischemic Stroke with Perfusion-Imaging Selection. *N Engl J Med*. 2015;372(11):1009–18.
4. **Meurer WJ, Barth BE, Gaddis G, Vilke GM, Lam SHF**. Rapid Systematic Review: Intra-Arterial Thrombectomy (???Clot Retrieval???) for Selected Patients with Acute Ischemic Stroke. *J Emerg Med*. 2017;52(2):255–61.
5. **Yang M-H, Lin H-Y, Fu J, Roodrajeetsing G, Shi S-L, Xiao S-W**. Decompressive hemicraniectomy in patients with malignant middle cerebral artery infarction: A systematic review and meta-analysis. *Surg*. 2015;13(4):230–40.
6. **Stroke Unit Trialists' Collaboration**. Organised inpatient (stroke unit) care for stroke. *Cochrane Database Sys Rev*. 2007;4(9):CD000197.
7. **Stroke I, Collaborative T**. The International Stroke Trial (IST): a randomised trial of aspirin , subcutaneous heparin , both , or neither among 19 435 patients with acute ischaemic stroke. 1997;349:1569–81.
8. **Chen Z-M**. CAST: randomised placebo-controlled trial of early aspirin use in 20 000 patients with acute ischaemic stroke. *Lancet*. 1997;349(9066):1641–9.
9. **Hsu JE, Jones TA**. Time-sensitive enhancement of motor learning with the less-affected forelimb after unilateral sensorimotor cortex lesions in rats. *Eur J Neurosci*. 2005;22(8):2069–80.
10. **Carmichael ST, Kathirvelu B, Schweppe CA, Nie EH**. Molecular, cellular and functional events in axonal sprouting after stroke. *Exp Neurol*. 2017;287:384–94.
11. **Dharmasaroja P**. Bone marrow-derived mesenchymal stem cells for the treatment of ischemic stroke. *J Clin Neurosci*. 2009;16(1):12–20.
12. **Lees JS, Sena ES, Egan KJ, Antonic A, Koblar SA, Howells DW, et al.** Stem cell-based therapy for experimental stroke: A systematic review and meta-analysis. *Int J Stroke*. 2012;7(7):582–8.
13. **Shen LH, Li Y, Chen J, Zacharek A, Gao Q, Kapke A, et al.** Therapeutic benefit of bone marrow stromal cells administered 1 month after stroke. *J Cereb Blood Flow Metab*. 2007;27(1):6–13.
14. **Rosenblum S, Wang N, Smith TN, Pendharkar A V, Chua JY, Birk H, et al.** Timing of intra-arterial neural stem cell transplantation after hypoxia-ischemia influences cell engraftment, survival, and differentiation. *Stroke*. 2012;43(6):1624–31.
15. **Leong WK, Henshall TL, Arthur A, Kremer KL, Lewis MD, Helps SC, et al.** Human Adult Dental Pulp Stem Cells Enhance Poststroke Functional Recovery Through Non-Neural Replacement Mechanisms.

Stem Cells Transl Med. 2012;1:177–87.

16. **Soleman S, Yip PK, Duricki D a, Moon LDF**. Delayed treatment with chondroitinase ABC promotes sensorimotor recovery and plasticity after stroke in aged rats. *Brain*. 2012;135(Pt 4):1210–23.
17. **Carmichael ST**. Targets for neural repair therapies after stroke. *Stroke*. 2010;41(10 Suppl):S124-6.
18. **Lee J-K, Kim J-E, Sivula M, Strittmatter SM**. Nogo receptor antagonism promotes stroke recovery by enhancing axonal plasticity. *J Neurosci*. 2004;24(27):6209–17.
19. **Tsai SY, Markus TM, Andrews EM, Cheatwood JL, Emerick AJ, Mir AK, et al.** Intrathecal treatment with anti-Nogo-A antibody improves functional recovery in adult rats after stroke. *Exp Brain Res*. 2007;182(2):261–6.
20. **Gillani RL, Tsai SY, Wallace DG, O'Brien TE, Arhebamen E, Tole M, et al.** Cognitive recovery in the aged rat after stroke and anti-Nogo-A immunotherapy. *Behav Brain Res*. 2010;208(2):415–24.
21. **Aspey BS, Cohen S, Patel Y, Terruli M, Harrison MJ**. Middle cerebral artery occlusion in the rat: consistent protocol for a model of stroke. *Neuropathol Appl Neurobiol*. 1998;24(6):487–97.
22. **McLeod DD, Beard DJ, Parsons MW, Levi CR, Calford MB, Spratt NJ**. Inadvertent Occlusion of the Anterior Choroidal Artery Explains Infarct Variability in the Middle Cerebral Artery Thread Occlusion Stroke Model. *PLoS One*. 2013;8(9):1–5.
23. **Tsuchiya D, Hong S, Kayama T, Panter SS, Weinstein PR**. Effect of suture size and carotid clip application upon blood flow and infarct volume after permanent and temporary middle cerebral artery occlusion in mice. *Brain Res*. 2003;970(1–2):131–9.
24. **Dittmar M, Spruss T, Schuierer G, Horn M**. External carotid artery territory ischemia impairs outcome in the endovascular filament model of middle cerebral artery occlusion in rats. *Stroke*. 2003;34(9):2252–7.
25. **Abeysinghe HCS, Bokhari L, Dusting GJ, Roulston CL**. Brain Remodelling following Endothelin-1 Induced Stroke in Conscious Rats. *PLoS One*. 2014;9(5):1–14.
26. **Windle V, Szymanska A, Granter-Button S, White C, Buist R, Peeling J, et al.** An analysis of four different methods of producing focal cerebral ischemia with endothelin-1 in the rat. *Exp Neurol*. 2006;201(2):324–34.
27. **Hughes PM, Anthony DC, Ruddin M, Botham MS, Rankine EL, Sablone M, et al.** Focal lesions in the rat central nervous system induced by endothelin-1. *J Neuropathol Exp Neurol*. 2003;62(12):1276–86.
28. **Naidoo V, Naidoo S, Mahabeer R, Raidoo DM**. Cellular distribution of the endothelin system in the human brain. *J Chem Neuroanat*. 2004;27(2):87–98.
29. **Carmichael ST**. Rodent models of focal stroke: size, mechanism, and purpose. *NeuroRx*. 2005;2(3):396–409.
30. **Nakagomi S, Kiryu-Seo S, Kiyama H**. Endothelin-converting enzymes and endothelin receptor B messenger RNAs are expressed in different neural cell species and these messenger RNAs are

coordinately induced in neurons and astrocytes respectively following nerve injury. *Neuroscience*. 2000;101(2):441–9.

31. **Miyake K, Takeo S, Kaijihara H**. Sustained decrease in brain regional blood flow after microsphere embolism in rats. *Stroke*. 1993;24(3):415–20.

32. **Mayzel-Oreg O, Omae T, Kazemi M, Li F, Fisher M, Cohen Y, et al.** Microsphere-induced embolic stroke: An MRI study. *Magn Reson Med*. 2004;51(6):1232–8.

33. **Gerriets T, Li F, Silva MD, Meng X, Brevard M, Sotak CH, et al.** The macrosphere model: Evaluation of a new stroke model for permanent middle cerebral artery occlusion in rats. *J Neurosci Methods*. 2003;122(2):201–11.

34. **Zhang L, Zhang RL, Jiang Q, Ding G, Chopp M, Zhang ZG**. Focal embolic cerebral ischemia in the rat. *Nat Protoc*. 2015;10(4):539–47.

35. **Gralla J, Schroth G, Remonda L, Fleischmann a, Fandino J, Slotboom J, et al.** A dedicated animal model for mechanical thrombectomy in acute stroke. *AJNR Am J Neuroradiol*. 2006;27(6):1357–61.

36. **Watson BD, Dietrich WD, Busto R, Wachtel MS, Ginsberg MD**. Induction of reproducible brain infarction by photochemically initiated thrombosis. *Ann Neurol*. 1985;17(5):497–504.

37. **Labat-gest V, Tomasi S**. Photothrombotic Ischemia: A Minimally Invasive and Reproducible Photochemical Cortical Lesion Model for Mouse Stroke Studies. *J Vis Exp*. 2013;(76):3–8.

38. **Fluri F, Schuhmann MK, Kleinschnitz C**. Animal models of ischemic stroke and their application in clinical research. *Drug Des Devel Ther*. 2015;9:3445–54.

39. **MacRae I**. Preclinical stroke research - Advantages and disadvantages of the most common rodent models of focal ischaemia. *Br J Pharmacol*. 2011;164(4):1062–78.

40. **Wester P, Watson BD, Prado R, Dietrich WD**. A photothrombotic “ring” model of rat stroke-in-evolution displaying putative penumbral inversion. *Stroke*. 1995;26(3):444–50.

41. **Qian C, Li PC, Jiao Y, Yao HH, Chen YC, Yang J, et al.** Precise characterization of the penumbra revealed by MRI: A modified photothrombotic stroke model study. *PLoS One*. 2016;11(4):1–13.

42. **Jackson SJ, Andrews N, Ball D, Bellantuono I, Gray J, Hachoumi L, et al.** Does age matter? The impact of rodent age on study outcomes. *Lab Anim*. 2017;51(2):160–9.

43. **Casals JB, Pieri NCG, Feitosa MLT, Ercolin ACM, Roballo KCS, Barreto RSN, et al.** The use of animal models for stroke research: A review. *Comp Med*. 2011;61(4):305–13.

44. **Dutta S, Sengupta P**. Men and mice: Relating their ages. *Life Sci*. 2016;152:244–8.

45. **Lindner MD, Gribkoff VK, Donlan N a, Jones TA**. Long-lasting functional disabilities in middle-aged rats with small cerebral infarcts. *J Neurosci*. 2003;23(34):10913–22.

46. **Rewell SSJ, Fernandez JA, Cox SF, Spratt NJ, Hogan L, Aleksoska E, et al.** Inducing stroke in aged, hypertensive, diabetic rats. *J Cereb Blood Flow Metab*. 2010;30(4):729–33.

47. **Metz GA, Whishaw IQ**. The Ladder Rung Walking Task: A Scoring System and its Practical Application. *jove*. 2009;3–5.

48. **Whishaw IQ, Pellis SM**. The structure of skilled forelimb reaching in the rat: A proximally driven movement with a single distal rotatory component. *Behav Brain Res*. 1990;41(1):49–59.
49. **Yushkevich PA, Piven J, Hazlett HC, Smith RG, Ho S, Gee JC, et al.** User-guided 3D active contour segmentation of anatomical structures: Significantly improved efficiency and reliability. *Neuroimage*. 2006;31(3):1116–28.
50. **Karetko-Sysa M, Skangiel-Kramska J, Nowicka D**. Disturbance of perineuronal nets in the perilesional area after photothrombosis is not associated with neuronal death. *Exp Neurol*. 2011;231(1):113–26.
51. **Lee JK, Park MS, Kim YS, Moon KS, Joo SP, Kim TS, et al.** Photochemically induced cerebral ischemia in a mouse model. *Surg Neurol*. 2007;67(6):620–5.
52. **Piao MS, Lee J-K, Jang J-W, Kim S-H, Kim H-S**. A mouse model of photochemically induced spinal cord injury. *J Korean Neurosurg Soc*. 2009;46(5):479–83.
53. **Tsiminis G, Klarić TS, Schartner EP, Warren-Smith SC, Lewis MD, Koblar SA, et al.** Generating and measuring photochemical changes inside the brain using optical fibers: exploring stroke. *Biomed Opt Express*. 2014;5(11):3975.
54. **Shih-Yen T, Papadopoulos CM, Schwab ME, Kartje GL**. Delayed Anti-Nogo-A Therapy Improves Function After Chronic Stroke. 2010;119(Pt 24):5124–36.
55. **Madinier A, Quattromani MJ, Sjölund C, Ruscher K, Wieloch T**. Enriched housing enhances recovery of limb placement ability and reduces aggrecan-containing perineuronal nets in the rat somatosensory cortex after experimental stroke. *PLoS One*. 2014;9(3).
56. **Wiersma AM, Fouad K, Winship IR**. Enhancing spinal plasticity amplifies the benefits of rehabilitative training and improves recovery from stroke. *J Neurosci*. 2017;37(45):0770-17.
57. **Alaverdashvili M, Moon SK, Beckman CD, Virag A, Whishaw IQ**. Acute but not chronic differences in skilled reaching for food following motor cortex devascularization vs. photothrombotic stroke in the rat. *Neuroscience*. 2008;157(2):297–308.
58. **Clarkson AN, López-Valdés HE, Overman JJ, Charles AC, Brennan KC, Thomas Carmichael S**. Multimodal examination of structural and functional remapping in the mouse photothrombotic stroke model. *J Cereb Blood Flow Metab*. 2013;33(5):716–23.
59. **Farr TD, Whishaw IQ**. Quantitative and Qualitative Impairments in Skilled Reaching in the Mouse (Mus musculus) After a Focal Motor Cortex Stroke. *Stroke*. 2002;33(7):1869–75.
60. **Lee VM, Burdett NG, Carpenter TA, Hall LD, Pambakian PS, Patel S, et al.** Evolution of photochemically induced focal cerebral ischemia in the rat - Magnetic resonance imaging and histology. *Stroke*. 1996;27(11):2110–8.
61. **van Bruggen N, Cullen BM, King MD, Doran M, Williams SR, Gadian DG, et al.** T2- and diffusion-weighted magnetic resonance imaging of a focal ischemic lesion in rat brain. *Stroke*. 1992;23(4):576–83.

62. **Imielinska C, Rosiene J, Jin Y, Liu X, Udupa J, Zacharia B, et al.** Ground truth for evaluation of ischemic stroke hybrid segmentation in a rat model of temporary middle cerebral artery occlusion. *Int Congr Ser*. 2005;1281:74–9.

63. **Allen LM, Hasso AN, Handwerker J, Farid H**. Sequence-specific MR Imaging Findings That Are Useful in Dating Ischemic Stroke. *RadioGraphics*. 2012;32(5):1285–97.

64. **Leiva-Salinas C, Wintermark M**. Imaging of Ischemic Stroke. *Contin Lifelong Learn Neurol*. 2016;22(5):1399–423.

65. **Clark RK, Lee E V, Fish CJ, White RF, Price WJ, Jonak ZL, et al.** Development of tissue damage, inflammation and resolution following stroke: an immunohistochemical and quantitative planimetric study. *Brain Res Bull*. 1993;31(5):565–72.

Chapter 6: Concluding remarks

6.1: Project Significance

The unifying concept behind this thesis is the need for new treatments for stroke to extend the therapeutic window and enhance long-term recovery. This need arises because current strategies for managing stroke increase survival, but fall short of reversing the chronic neurological disability that often results from stroke. As a result, many stroke victims live with permanent and severe disability, at a great cost to the individual and to the community[1]. Therefore, this thesis addressed aims relating to two overlapping paradigms of potential stroke treatment: stem cell transplantation and interruption of perineuronal nets (PNNs).

The first results chapter (Chapter 2; published manuscript) tested the ability of adult human dental pulp stem cells (DPSC) to enhance permeability across an *in vitro* model of the blood-brain barrier (BBB). Dental pulp stem cell conditioned media were able to increase the permeability of an endothelial and astrocyte co-culture model BBB. This effect was found to be due to the expression of vascular endothelial growth factor-a (VEGF-a). This cytokine was expressed in DPSC populations and blockade of its receptor inhibited the ability of DPSC to induce BBB permeability. The rationale for this study lay in the concept of stem cell transplantation as a treatment for ischaemic stroke. Both direct intracerebral transplantation[2] and intravascular[3,4] stem cell transplantation have shown efficacy in pre-clinical stroke studies. Critically, it has been demonstrated that stem cells transplanted via an intravascular route can enter the brain parenchyma[3]. This is important because intravascular administration is much less invasive than direct intracerebral transplantation and is less likely to result in complications. The results outlined in Chapter 2 of this thesis elucidate the likely mechanism by which stem cells may enter the brain parenchyma following intravascular transplantation.

Another goal of research in cell-based stroke therapy is to elucidate the mechanisms of action that underlie its efficacy. This was addressed by the second results chapter (Chapter 3; manuscript in preparation), which explored the ability of DPSC to degrade PNNs. Conditioned media samples from DPSC were shown to attenuate staining of PNNs in a cell monolayer and in brain slice sections. Conditioned media were subsequently interrogated for the presence of enzymes known to digest PNNs. It was found that DPSC express matrix metalloproteinase-2 (MMP-2) in its active form. This enzyme is known to digest aggrecan, one of the main PNN components. This study was undertaken to elucidate the mechanism of action of cell-based therapy in stroke. Despite showing efficacy in numerous pre-clinical studies[2,3,5], these mechanisms have still not been fully characterised. These results demonstrate that DPSC are capable of digesting PNNs through the expression of MMP-2. This is noteworthy because PNNs are potent inhibitors of neuroplasticity in the adult central nervous system and removal of PNNs creates a period of enhanced neuroplasticity[6–8]. Therefore, a likely hypothesis is that transplanted stem cells improve outcomes after stroke by enhancing neuroplasticity. This will help to inform the optimisation of cell-based therapies in future.

Given that digestion of PNNs is a hypothetical mechanism of action for cell-based stroke therapy, it is important to understand the endogenous regulation of PNNs following stroke. This was investigated in the third results chapter (Chapter 4; manuscript in preparation). To the best of our knowledge, this study provides the most complete coverage of PNN components by immunohistochemistry in the cortex of mice following photochemical infarction to date. The critical outcomes of this study were that cartilage link protein-1, aggrecan and WFA-binding glycans were significantly downregulated in the region contralateral to the infarct. This may underlie a period of enhanced neuroplasticity that has been observed during recovery from ischaemic stroke[9–11]. There was also an enrichment of 4-O-sulfated chondroitin in the infarct border zone, which may underlie some of the inhibitory function of the glial scar. Understanding the endogenous regulation of the mechanisms responsible for inhibiting neuroplasticity in adults will contribute to the development of new treatments for ischaemic stroke, with adult neuroplasticity as the target. Post-stroke neuroplasticity may be further enhanced by disrupting PNNs artificially, either through cell-based therapy as we have shown, or through enzymatic digestion.

The development of new treatments aimed at the chronic sequelae of stroke, such as those described above, requires an *in vivo* model of chronic stroke. In the fourth results chapter (Chapter 5; manuscript in preparation), a photochemical method was used to induce focal infarction in the motor cortices of aged mice. Acute, but not chronic deficits were detected by the ladder rung behaviour test and no deficit was detected by the skilled reach behaviour test. Infarcts were detected by T1 MRI at one week post-stroke, but not at later time points. Brain tissue from mice euthanised at regular time points up to nine weeks post-stroke was analysed by histology. These results demonstrated that infarcts generated by this photochemical method underwent a similar evolution to other stroke models[12]. This study was undertaken to fill the need for a standardised model of chronic stroke. The limitations of this study will be used to inform the future development of a chronic stroke model. This would provide a valuable preclinical model in which to evaluate the efficacy of potential treatments aimed at enhancing recovery in the chronic phase of stroke. Such therapies will include those targeted at enhancing neuroplasticity, such as stem cell transplantation and PNN disruption.

This thesis clarified aspects of the mechanisms of action underlying the efficacy of cell-based therapy for stroke. In particular, it described the interactions between DPSC and brain microstructures – the BBB and PNNs. Chapter 2 provided evidence towards a hypothetical mechanism by which stem cells transplanted by an intravascular route may gain access to their target in the brain parenchyma. Once at the site of action, transplanted stem cells are hypothesised to elicit a therapeutic effect through bystander effects. Results presented in Chapter 3 suggest that one of these mechanisms of action may be the enzymatic degradation of PNNs, which would therefore permit enhanced neuroplasticity. This concept was explored further in Chapter 4, which revealed a temporary downregulation of PNNs following stroke that was more significant in the contralateral hemisphere. These findings may underlie a period of enhanced neuroplasticity that follows ischaemic stroke and artificial extension of post-stroke PNN downregulation is therefore a promising therapeutic target. Finally, the future development of these treatment options for victims of chronic stroke requires an appropriate *in vivo* model of chronic stroke. Chapter 5 presented a preliminary study towards the development of such a model.

6.2: Future Directions

Chapter 5 outlines a preliminary study towards the development of a chronic model of photochemical infarction in mice. These negative results and the limitations of the study should inform the future development of a chronic stroke model. A study should be conducted comparing the effects of different illumination times and aperture sizes on infarction size and long-term outcomes of behaviour tests. Based on the discussion in Chapter 5, appropriate parameters would be aperture sizes between 2mm and 5mm, and illumination times between 5 and 20minutes. Additionally, a larger battery of behaviour tests should be used, though the skilled reach test should not be included as it appears that it is not appropriate for detecting chronic disability[13,14]. Sample size should be powered to detect smaller functional deficits; at least 29 animals should be used per group. T2- and diffusion-weighted MRI should be used to confirm infarct consistency at one week post-stroke and histological changes should be analysed post mortem.

Stem cells have been shown to be capable of migrating across the BBB following intravascular transplantation[3]. Chapter 2 suggests that a likely mechanism for this is that stem cells enhance BBB permeability through the paracrine expression of VEGF-a. However, we do not provide direct evidence for this hypothesis. To do this, it will be necessary to replicate the study using an *in vivo* model. Stem cells should be transplanted via an intravascular route into an animal model of chronic stroke. It is important that this take place in the chronic phase of stroke for two reasons 1) This would mimic the clinical situation of humans receiving stem cell transplantation for stroke and 2) the acute and subacute phases of stroke recovery include innate periods of increased BBB permeability[15,16], which would influence results. VEGF-a would then be blocked through regular administration of cediranib or bevacizumab. To control for the effects of endogenous VEGF-a, DPSC deficient in this cytokine should also be generated and used. If DPSC-derived VEGF-a is partly responsible for BBB transmigration, then blockade of VEGF-a signalling and use of VEGF-a deficient DPSC would reduce entry of the DPSC into the brain parenchyma and may attenuate the therapeutic capacity of intravascular stem cell transplantation.

Building on the results described in Chapter 3, it will be important to evaluate the relative importance of MMP-2 expression and PNN degradation in cell-based stroke therapy. This study would comprise two main components. Firstly, a population of MMP-2 deficient DPSC would need to be developed, which could be achieved relatively easily through CRISPR-Cas9 genome editing.

A chronic stroke model would then be treated by stem cell transplantation with DPSC or MMP-2 deficient DPSC. The functional and neuroanatomic correlates of neuroplasticity would then be measured for the two groups. This could be achieved using behaviour testing along with fMRI to detect function reallocation, followed by BDA injection and fibre tracing from the contralateral hemisphere to count midline-crossing corticospinal tract fibres. Another measure of neuroanatomic plasticity to consider would be to measure cortical dendrite length and dendritic tree complexity in both the ipsi- and contralateral hemispheres. The contribution of MMP-2-mediated PNN disruption to therapeutic efficacy would be determined by comparing the functional outcomes and measures of neuroanatomic plasticity between these two groups.

Several concepts remain to be investigated with regards to the post-stroke regulation of PNNs and other inhibitory ECM components. Chapter 4 identified a temporary downregulation of aggrecan and PNN-associated glycans contralateral to a cortical photochemical infarction in mice. We hypothesised that this might be one of the mechanisms behind the phenomenon of function relocation, where the activities normally carried out by an infarcted cortical region are relocated to the homotopic contralateral region following ischaemic stroke. This is a difficult hypothesis to test as it would require a negative control in which endogenous downregulation of PNNs after stroke is blocked, and the mechanism by which post-stroke PNN modulation occurs is not yet known. One way to begin examining this problem would be to use retrograde axonal tracing to label midline-crossing primary corticospinal neurons projecting to the deafferented spinal cord. Co-staining for aggrecan and WFA-binding glycans in the contralateral cortex would then be conducted to determine whether these midline-crossing neurons originate in regions where PNNs are downregulated.

Work produced by the Fawcett[8] and Schwab[17] groups has demonstrated the critical importance of timing in combination therapies involving rehabilitation and enhancement of neuroplasticity through disruption of PNNs and inhibition of Nogo signalling respectively. Both suggest that the optimum treatment schedule is that rehabilitation occurs after enhancement of neuroplasticity, rather than concurrently. It would be interesting to determine whether this phenomenon exists in other potential treatment modalities. The paper produced by the Fawcett group only tested the combination of PNN disruption and rehabilitation on a rodent model of spinal cord injury. It would therefore be useful to replicate this study using a model of chronic stroke. From there, it would also be useful to determine whether stem cell therapy in a chronic stroke model could be optimised through the timing of adjunct task-specific rehabilitation.

6.3: References

1. **Norrving B, Kissela B**. The global burden of stroke and need for a continuum of care. *Neurology*. 2013;80(Issue 3, Supplement 2):S5–12.

2. **Leong WK, Henshall TL, Arthur A, Kremer KL, Lewis MD, Helps SC, et al.** Human Adult Dental Pulp Stem Cells Enhance Poststroke Functional Recovery Through Non-Neural Replacement Mechanisms. *Stem Cells Transl Med*. 2012;1:177–87.

3. **Rosenblum S, Wang N, Smith TN, Pendharkar A V, Chua JY, Birk H, et al.** Timing of intra-arterial neural stem cell transplantation after hypoxia-ischemia influences cell engraftment, survival, and differentiation. *Stroke*. 2012;43(6):1624–31.

4. **Shen LH, Li Y, Chen J, Zacharek A, Gao Q, Kapke A, et al.** Therapeutic benefit of bone marrow stromal cells administered 1 month after stroke. *J Cereb Blood Flow Metab*. 2007;27(1):6–13.

5. **Lees JS, Sena ES, Egan KJ, Antonic A, Koblar SA, Howells DW, et al.** Stem cell-based therapy for experimental stroke: A systematic review and meta-analysis. *Int J Stroke*. 2012;7(7):582–8.

6. **Pizzorusso T, Medini P, Berardi N, Chierzi S, Fawcett JW, Maffei L**. Reactivation of Ocular Dominance Plasticity in the Adult Visual Cortex. *Science (80-)*. 2002;298(5596):1248–51.

7. **Pizzorusso T, Medini P, Landi S, Baldini S, Berardi N, Maffei L**. Structural and functional recovery from early monocular deprivation in adult rats. *Proc Natl Acad Sci U S A*. 2006;103(22):8517–22.

8. **García-Alías G, Barkhuysen S, Buckle M, Fawcett JW**. Chondroitinase ABC treatment opens a window of opportunity for task-specific rehabilitation. *Nat Neurosci*. 2009;12(9):1145–51.

9. **Wolf SL, Thompson PA, Winstein CJ, Miller JP, Blanton SR, Nichols-Larsen DS, et al.** The EXCITE Stroke Trial: Comparing Early and Delayed Constraint-Induced Movement Therapy. *Stroke*. 2010;41(10):2309–15.

10. **Dimyan M a, Cohen LG**. Neuroplasticity in the context of motor rehabilitation after stroke. *Nat Rev Neurol*. 2011;7(2):76–85.

11. **Bonita R, Beaglehole R**. Recovery of motor function after stroke. *Stroke*. 1988;19(12):1497–500.

12. **Clark RK, Lee E V, Fish CJ, White RF, Price WJ, Jonak ZL, et al.** Development of tissue damage,

inflammation and resolution following stroke: an immunohistochemical and quantitative planimetric study. *Brain Res Bull*. 1993;31(5):565–72.

13. **Clarkson AN, López-Valdés HE, Overman JJ, Charles AC, Brennan KC, Thomas Carmichael S**. Multimodal examination of structural and functional remapping in the mouse photothrombotic stroke model. *J Cereb Blood Flow Metab*. 2013;33(5):716–23.

14. **Alaverdashvili M, Moon SK, Beckman CD, Virag A, Whishaw IQ**. Acute but not chronic differences in skilled reaching for food following motor cortex devascularization vs. photothrombotic stroke in the rat. *Neuroscience*. 2008;157(2):297–308.

15. **Khatri R, McKinney A, Swenson B, Janardhan V**. Blood–brain barrier, reperfusion injury, and hemorrhagic transformation in acute ischemic stroke. *Neurology*. 2012;

16. **Sandoval KE, Witt KA**. Blood-brain barrier tight junction permeability and ischemic stroke. *Neurobiol Dis*. 2008;32(2):200–19.

17. **Wahl AS, Omlor W, Rubio JC, Chen JL, Zheng H, Schroter A, et al.** Asynchronous therapy restores motor control by rewiring of the rat corticospinal tract after stroke. *Science (80-)*. 2014;344(6189):1250–5.